MOLECULAR AND CELLULAR STUDY OF LIVER DISEASES: *FOCUSING ON THE BIOLOGY OF TOLL-LIKE RECEPTORS IN LIVER TUMOURS*

Thesis submitted for the degree of Doctor of Philosophy (PhD)

Fatma El Zahraa Ammar Saleh Mohamed

University College London

2013

Declaration

I, Fatma El Zahraa Ammar Saleh Mohamed confirm that the work presented in this thesis is my own.

Abstract

Background. Liver cancer is the 3rd commonest cause of cancer death worldwide. Understanding the mechanisms of hepatocarcinogenesis is vital for developing more effective treatments. Chronic liver disease is a predisposing factor for development of hepatocellular carcinoma (HCC) and increased translocation of gut bacteria is believed to exacerbate this inflammatory condition. Toll-like receptors (TLRs) play a crucial role in immunity against microbial pathogens and recent evidence suggests they may be important in pathogenesis of chronic liver disease. The aim of this thesis was to explore the role of TLRs in the pathogenesis of HCC.

Materials & Methods: Tissue microarrays obtained from patients with cirrhosis, viral hepatitis and HCC were stained with for TLR4, TLR7 and TLR9 and the data were validated in actual patient samples. The role of gut translocation was explored in an animal model of HCC using diethylnitrosamine (DEN) and nitrosomorpholine (NMOR) after treatment with Norfloxacin. Proliferation of HCC cell lines were studied after stimulation (Imiquimod and CpG-ODN) and inhibition of TLR7 and TLR9 (IRS 954) and chloroquine. The effect of these interventions was confirmed in the DEN and NMOR and, a xenograft model. The studies were extended to determine their effect in cholangiocarcinoma.

Results: TLR7 and TLR9 but not TLR4 were up regulated in HCC tissue and gut decontamination with Norfloxacin did not prevent HCC development but reduced liver fibrosis. TLR7 stimulation increased cell proliferation of HuH7 cells significantly and inhibition of TLR7 and TLR9 using IRS or chloroquine resulted in significant inhibition. TLR7 and TLR9 inhibition using IRS 954 and chloroquine reduced tumour growth in xenograft models and, chloroquine also decreased liver fibrosis and tumour growth in the DEN and NMOR model. These beneficial effects were also observed in cholangiocarcinoma.

Conclusion: In conclusion, these data suggest that inhibiting TLR7 and TLR9 and, using chloroquine could be potential novel therapeutic strategies for the prevention and the progression of primary liver cancers in susceptible patients.

Table of contents

List of figures

List of Tables

List of abbreviations

1. ADH: Alcohol dehydrogenase
2. ALD: Alcoholic liver disease.
3. APC: Adnometous polyposis coli
4. BCG: Bacillus Calmette-Guérin
5. BCL-XL: B-cell lymphoma-extra large
6. BMI: Body mass index
7. BRACA1, 2 : Breast cancer type 1 or 2 susceptibility protein
8. CC: Cholangiocarcinoma
9. CD14: Cluster of differentiation 14
10. CpG Cytosine-phosphate-Guanine
11. CQ: Chloroquine
12. DAB: Diaminobenzidine
13. DAMPs: Damage associated molecular patterns
14. DEN: Diethylnitrosamine
15. DNA: Deoxyribonucleic acid
16. EDTA: Ethylenediaminetetraacetic acid
17. EMT: Epithelial mesenchymal transition
18. ERK: Extracellular signal-regulated kinases
19. FOX03: Forkhead box O3
20. GSD1: Glycogen storage disease type 1
21. GSK3: Glycogen synthase kinase 3
22. H&E: Haematoxylin and Eosin stain
23. HBV: Hepatitis B Virus
24. HCC: Hepatocellular carcinoma
25. HCV: Hepatitis C Virus
26. IKK: Inhibitor of NF-κB kinase
27. IMOs: Immunomodulatory oligonucleotides
28. IMQ: Imiquimod
29. IRS: Immunoregulatory DNA sequence
30. JNK: c-jun N-terminal kinase
31. LAL: Limulus Amebocyte Lysate
32. LBP: Lipopolysaccrhide binding protein
33. LC3B: light chain 3B protein.

34. LPS: Lipopolysaccrhide
35. MAPK: Mitogen-activated protein kinases
36. MEOS: Microsomal ethanol oxidizing system
37. MMP13: Matrix metallopeptidase 13
38. M-PER: Mammalian protein extraction reagent
39. BSA: Bovine serum albumin
40. mRNA: Messenger Ribonucleic acid
41. MyD88: Myeloid differentiation primary response protein 88
42. NAD: Nicotinamide adenine dinucleotide
43. NAFLD: Non- alcoholic fatty liver disease
44. NASH: Non-Alcoholic steatohepatitis
45. NF-κB: Nuclear factor Kappa-light-chain of activated B cells
46. NMOR: Nitrosomorpholine
47. NOD-SCID: Non Obese Diabetic severe combined immunodeficiency
48. NS: Non-structural protein
49. pAkt: Phosphorylated Akt
50. PAMPs: Pathogen-associated molecular patterns
51. PBS: Phosphate buffer saline
52. PI3K: Phosphatidylinositide 3-kinases
53. RB: Retinoblastoma
54. RNA: Ribonucleic acid
55. ROS: Reactive oxygen species
56. SLE: Systemic lupus erythematosus
57. MTS: [3-(4, 5-dimethylthiazol-2-yl)-5-(3-carboxymethoxyphenyl)-2-(4-sulfophenyl)-2H-tetrazolium, inner salt)
58. TAK1: Transforming growth factor –β-activated protein kinase1
59. TIR: Toll/Interleukin-1 receptor
60. TLR4: Toll like receptor 4
61. TLR7: Toll-like receptor 7
62. TLR9: Toll-like receptor 9
63. TLRs: Toll Like Receptors
64. TMA: Tissue microarray
65. TNF-α: Tumour necrosis factor-α
66. TRAF6: Tumour necrosis factor receptor-associated factor 6

67. TRIF: TIR-domain-containing adapter-inducing interferon-β
68. VEGF: Vascular endothelial growth factor
69. α1-ATD: α1- Antitrypsin deficiency

Acknowledgments

I would like to thank my primary supervisor Prof Rajiv Jalan for his kind supervision and guidance throughout this project as well as my secondary supervisor Dr Steven Olde Damink and my tertiary supervisor, Dr Shane Minogue.

I would also like to thank Dr Tu Vinh Loung and Dr Alison Winstanley for their kind analysis of all the histopathological and immunohistochemical data from my study.

I would like to thank Dr Nathan Davies for the technical help to implant the xenografts and Abeba Habtesion to help look after the animals.

I would like to thank Dr Shane Minogue for help with the confocal microscopy analysis and Dr Fausto Andreola for help and advice with the proliferation assays , Pamela leckie for help with the endotoxin assay analysis and Dr Manil Chouhan for performing the MRI analysis.

I would like to thank Dr Banwari Agarwal, Dr Dipok Dhar and all the other colleagues who provided scientific advice. This thesis would not have been possible without the help of my good friend Dr Rajai Al-Jehani who provided valuable scientific advice and spent many hours carefully proof-read the thesis.

Last but not least I would like to thank my husband Ali and my daughters Nada and Yasmina for all their patience, love and support throughout my PhD and to whom I will be eternally grateful.

I thankfully acknowledge the Egyptian government and Minia University for funding my scholarship and this research.

To my parents

Introduction

1. Introduction

1.1 Epidemiology and global distribution of HCC

Liver cancer is the fifth most common cancer in the world and the third commonest cause of cancer death (Parkin et al., 2001 and Chen et al., 2006). About 85-90% of all primary liver cancer cases are diagnosed as hepatocellular carcinoma (HCC) (El Serag, 2011). Nearly one million new cases of HCC are diagnosed annually accounting for approximately 500,000-600,000 deaths (Sherman, 2008, Feo et al., 2009 and Schutte et al., 2009). The prognosis of HCC is poor with a median survival of less than one year (El Serag and Rudolph, 2007) and an actual 1-year survival rate of 3-5% (Schutte et al., 2009).

HCC is more common in men than women (Sherman, 2008), the mean male to female ratio being 2-4:1. HCC is the fifth most common cancer in men and seventh in women (El Serag, 2011). It has also been noted that the peak HCC incidence in female patients occurs around 5 years later than in males (Schutte et al., 2009). The high incidence of HCC in the male population is probably due to the higher exposure to risk factors such as sex hormones (Schutte et al., 2009). It has been shown that orchidectomy reduces the effect of chemical carcinogens in male rats (Leong and Leong, 2005).

In the high incidence areas, HCC is common in younger patients, whereas in the low incidence areas it is predominantly a disease of the elderly (Leong and Leong, 2005). The age-specific patterns are related to the differences in the distribution of dominant hepatitis virus in the population, the age at which viral infection occurs, and co-existence of other risk factors. Of note, most Hepatitis C virus (HCV) carriers become infected in adulthood while most Hepatitis B virus (HBV) carriers acquire infection at a very young age (El Serag and Rudolph, 2007).

There is a geographic variability in the distribution of HCC cases, highest incidence reported in south-east Asia and sub-Saharan Africa (Leong and Leong, 2005 and El Serag and Rudolph, 2007). China alone accounts for more than 50% of the cases (El Serag and Rudolph, 2007). European countries,

historically, have a low incidence of HCC, but over the past 20-years the incidence rate in Europe has been on the rise. Similarly, although North and South America have a lower incidence of HCC (El Serag and Rudolph, 2007), the incidence of HCC has more than tripled in the United States of America in the last two decades (El Serag, 2011).

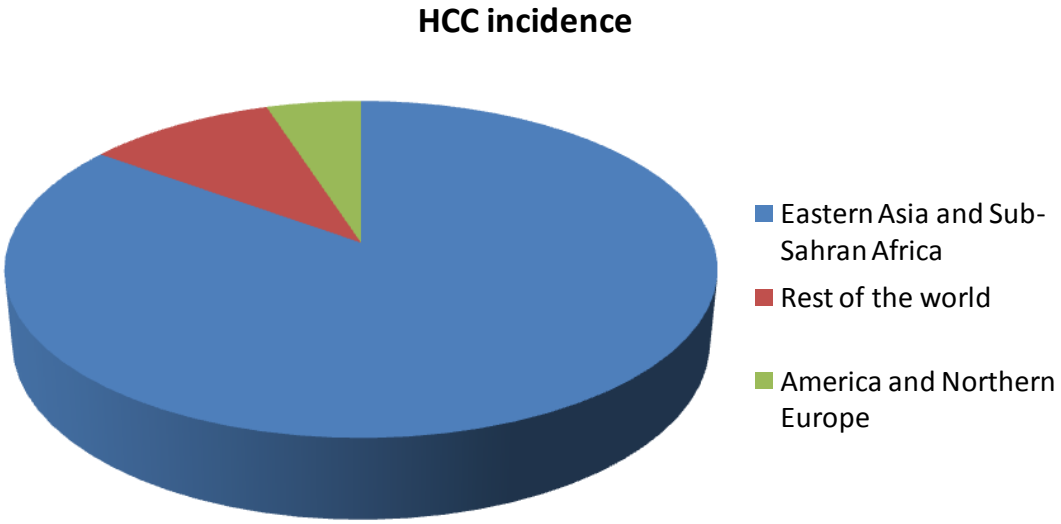

Figure 1: Incidence of HCC worldwide.

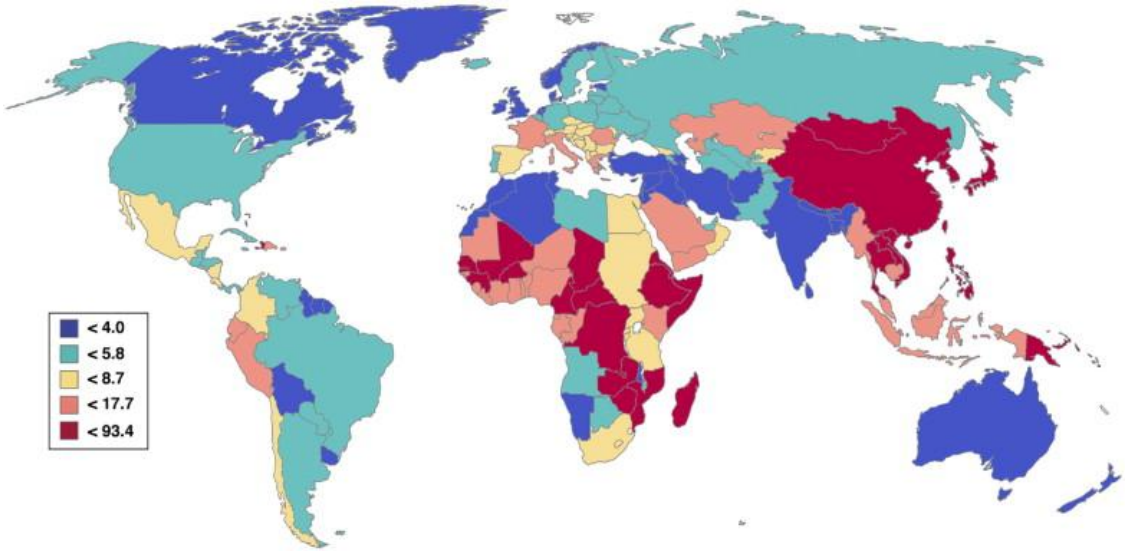

Figure 2: Regional variations in the mortality rates of HCC. The rates are reported per 100, 000 persons (Adapted from El Serag and Rudolph, 2007).

1.2 Risk factors for development of HCC

The aetio-pathogenesis of HCC involves a process characterised by an increased hepatocyte turnover following chronic liver injury and regeneration, triggered by a variety of insults (Fung et al., 2009). Around 70%-90% of HCC cases are observed in patients with liver cirrhosis and long standing hepatic inflammation (Schutte et al., 2009). The risk factors (described below) induce tumour formation and proliferation through a number of distinct and complex biochemical pathways. However, nearly all of them seem to have an inflammatory basis.

1.2.1 Viral hepatitis

One of the most important risk factors for HCC development is chronic hepatitis B and C (Dragani, 2010). HBV, and less commonly HCV, can cause HCC due to the oncogenic properties of the viruses themselves (Fung et al., 2009). HCV and HBV increase the risk of developing HCC by 20- fold (Schutte et al., 2009), and are responsible for more than 80% of all cases of HCC globally.

HBV can cause HCC directly by increasing inflammation and regeneration. This process leads to accumulation of potential mutations in the hepatocyte genome resulting in HCC (Fung et al., 2009). HCC can also be induced directly through integration of HBV DNA into the host genome (Rocken and Carl-McGrath, 2001). This direct pathway does not occur in HCC induced by HCV because this is an RNA virus and does not contain the reverse transcriptase enzyme. Therefore HCV can only cause HCC through indirect pathways (Fung et al., 2009). In hepatitis C, the structural proteins (Core, E1, E2 and p7) and the non-structural proteins (NS2, NS3, NS4A, NS4B, NS5A and NS5B) are the main carcinogenic agents and host- viral protein interactions the main pathway behind hepatocarcinogenesis (Kim et al., 2007). For example, the NS5B affects the cell cycle and leads to arrest at the G2 Phase (Baek et al., 2006). NS5A alters intracellular calcium levels, reactive oxygen species (Gong et al., 2001) and inhibits apoptosis (Baek et al., 2006).

Since the discovery of the HBV vaccine, there has been a decline in the HBV-related HCC (Schutte et al., 2009). On the other hand, the incidence of HCV-

related HCC has continued to increase due to higher rates of intravenous drug abuse and contaminated blood supply (Armstrong et al., 2000). Hepatitis A and E have no carcinogenic effects as neither virus leads to chronic hepatitis. Hepatitis D virus infects the liver only in patients with hepatitis B thus making it difficult to evaluate its direct role in hepatocarcinogensis. It has been suggested however that hepatitis D places additional load on the damaged liver contributing to the risk of HCC (Leong and Leong, 2005).

1.2.2 Life style; Alcohol, Obesity and Non-Alcoholic steatohepatitis

a) Alcohol

Heavy alcohol consumption is a major risk factor for HCC in developed countries (Schutte et al., 2009). Heavy alcohol intake is defined as long-term ingestion of more than 50-70g/day for an average of 10 years (El Serag and Rudolph, 2007).

Chronic alcohol consumption is associated with a variety of liver diseases ranging from steatosis, steatohepatitis, cirrhosis, and finally to HCC (Mandrekar and Szabo, 2009). There is evidence of a direct carcinogenic effect of alcohol on the liver; however, there are several mechanisms implicated in the initiation of HCC (Schutte et al., 2009).

Ethanol is primarily metabolised in the hepatocytes through alcohol dehydrogenase (ADH) in the cytosol, microsomal ethanol oxidizing system (MEOS) in endoplasmic reticulum which also contain inducible cytochrome P450 2E1, and catalase which is located in the peroxisomes (McKillop and Schrum, 2005). ADH dependent ethanol metabolism induces nicotinamide adenine dinucleotide (NADH) which results in an increase in the synthesis of reactive oxygen species (ROS). These substances cause peroxidation damage to DNA (McKillop et al., 2006). In alcohol induced liver injury, the innate immune response is activated in the liver, macrophages and the Kupffer cells playing a crucial role in the early stages of pathogenesis (Hines and Wheeler, 2004).

The effect of alcohol on the liver is evident in many cells including the innate immune cells, liver parenchymal cells and the hepatocytes. Innate immune

cells, including the macrophages (Kupffer cells), recognise the endotoxin/lipopolysaccharide in the portal circulation during the early stages of alcohol-induced liver injury. Alcohol induces oxidative stress with production of inflammatory cytokines such as tumour necrosis factor-α (TNF-α) in the macrophages resulting in alcoholic liver disease (ALD). Furthermore, alcohol also sensitises hepatocytes to apoptosis through TNF-α (Mandrekar and Szabo, 2009).

b) Obesity and Diabetes

In a prospective cohort study conducted in the United States, it was reported that liver cancer mortality rates were 5 times higher amongst men with high baseline body mass (Calle and Rodriguez, 2003). The risk of developing HCC is higher in patients whose body mass index (BMI) exceeds 30kg/m^2 (Chen et al., 2008 and Polesel et al., 2009). Obesity, especially central obesity, is associated with hepatic steatosis (Ratziu et al., 2000 and Ratziu et al., 2004).
The effect of obesity on liver is called the non- alcoholic fatty liver disease (NAFLD) the features of which ranges from fatty liver (steatosis), steatohepatitis to cirrhosis. Increased hepatic steatosis is often associated with severe necro-inflammatory activity and fibrosis (El Serag and Rudolph, 2007).

Several studies found a significant association between diabetes and HCC (El Serag and Rudolph, 2007). Insulin resistance is another such factor associated with hepatic steatosis (Ratziu et al., 2000 and Ratziu et al., 2004). Diabetes has been reported to be a risk factor for NAFLD and NASH, the latter shown to have a causative link with HCC (Schutte et al., 2009).

1.2.3 Other factors

a) Toxins

A potent hepatocarcinogenic toxin is the mycotoxin aflatoxin B_1, which has been classified as a carcinogen by the International Agency for Research on Cancer (Schutte et al., 2009). It is produced by fungi of the Aspergillus family such as Aspergillus Flavis and Aspergillus Parasitans. They grow mainly on cereal grains stored in humid regions (Leong and Leong, 2005). The role of Aflatoxin in hepatocarcinogensis is due to its ability to induce a high degree of

chromosomal instability (Pineau et al., 2008). Simultaneous infection by viral hepatitis B potentiates the carcinogenic effects of these toxins (Schutte et al., 2009). Aflatoxin is also one of the most potent genotoxic agents. It induces multiple chromosomal alterations and unscheduled DNA synthesis (Wang and Groopman, 1999).

b) Haemochromatosis

Haemochromatosis results from the excessive accumulation of iron in the liver due to hereditary or acquired causes. It leads to chronic inflammation with subsequent fibrosis and can lead to cirrhosis (Schutte et al., 2009). HCC in haemochromatosis patients with or without cirrhosis suggests a direct hepatocarcinogenic effect of iron (Kowdley, 2004 and Kew, 2009). A Swedish study has reported that hereditary haemochromatosis increases the risk of HCC by 1.7 fold (El Serag and Rudolph, 2007).

c) Autoimmune hepatitis

Autoimmune hepatitis is a chronic and progressive autoimmune disease associated with inflammation and hepatocellular necrosis. It is more common in females and around 70% of all cases are detected in women between the ages of 15 and 40 years. Diagnosis is based on clinical (jaundice, fever and right upper quadrant pain), laboratory (increase ALT and AST, serum gamma globulin concentrations more than twice the normal levels, and sometimes the presence of antinuclear antibodies and/or anti-smooth muscle antibodies (Krawitt, 1996) and histological features. Autoimmune hepatitis can progress to cirrhosis, often leading to HCC with an annual incidence rate of 1.1% (Yeoman et al., 2008).

d) α1- Antitrypsin deficiency (α1-ATD)

α1- Antitrypsin deficiency is an inherited metabolic disorder which prevents α1-Antitrypsin being exported from hepatocytes as a consequence of mutations in the coding sequence of the serine protease inhibitor. The abnormal accumulation of glycoprotein α1- Antitrypsin in the hepatocytes results in apoptosis, hepatitis, fibrosis and cirrhosis (Fairbanks and Tavill, 2008). Homozygous patients become symptomatic about 15 years earlier than those

who are heterozygous (Schutte et al., 2009). In α-1 antitrypsin deficiency, older cells with accumulated mutant glycoprotein stimulate newly formed cells to proliferate (Rudnick and Perlmutter, 2005). As a result of accumulation of genetic mutations, hepatocellular adenoma and carcinoma develop on a background of chronic inflammation (Fairbanks and Tavill, 2008).

e) Glycogen storage disease type 1 (Von Gierke's disease, GSD1)

Von Gierke's disease is caused by a deficiency of glucose-6-phosphatase (G6Pase), which leads to accumulation of glycogen in the liver (Dragani, 2010). There are two distinct types of this disease, the type 1a (complete absence of G6Pase) and type 1b (deficiency of glucose-6-phosphate translocase at the endoplasmic reticulum membrane) (Janecke et al., 2001). Most cases of GSD1 present with hepatocellular adenoma in the second and third decades of life. HCC may develop as an adenoma-carcinoma sequence (Franco et al., 2005).

f) Miscellaneous

Several other factors are implicated as potential risk factors for HCC. These risk factors include biological conditions such as hepatic porphyrias, Tyrosinemia type 1 and hypothyroidism (Dragani, 2010), chemical factors such as nitrites, hydrocarbons, solvents, pesticides and processed food (Leong and Leong, 2005) and radiation. Both internal α and β radiation are carcinogenic (Leong and Leong, 2005).

1.3 Histopathological changes from normal to HCC

As a result of chronic hepatic injury, hepatic necrosis results and this is followed by proliferation. **Chronic hepatitis** is characterized by infiltration of inflammatory cells, mainly lymphocytic infiltration, with much less lobular involvement. Piecemeal necrosis and fibrosis may also be present. Depending on the presence or absence of piecemeal necrosis; chronic hepatitis may be divided into chronic active hepatitis and chronic persistent hepatitis (Chadwick et al., 1979).

Repeated cycles of destruction and regeneration in chronic liver disease lead to liver cirrhosis. Histologically, **cirrhosis** is characterised by the presence of abnormal liver nodules surrounded by collagen deposition. Within these nodules, hyperplastic nodules may be formed which develop into dysplasia leading subsequently to HCC (Farazi and DePinho, 2006).
Severity of fibrosis can be staged according to Ishak scoring criteria:

Table 1: Ishak criteria for fibrosis scoring (Ishak et al., 1995 and table adopted from Standish et al., 2006).

Ishak Score	Ishak description
0	No fibrosis (normal)
1	Fibrous expansion of some portal areas± short fibrous septa
2	Fibrous expansion of most portal areas± short fibrous septa
3	Fibrous expansion of most portal areas with occasional portal to portal bridging
4	Fibrous expansion of portal areas with marked bridging portal to portal as well as portal to central
5	Marked bridging with occasional nodules (incomplete cirrhosis)
6	Cirrhosis

Dysplastic nodules are pre-cancerous, also known as adenomatous hyperplasia, hepatocellular pseudotumour, adenomatous regeneration and borderline nodule (Leong and Leong, 2005 and Wong and Ng, 2008).

Classification is divided into high and low dysplastic nodule based on cytological features and the degree of histologic abnormality (Wong and Ng, 2008). With increasing grade of dysplasia, hepatocytes become preneoplastic, which find a suitable environment for growth and proliferation to progress into malignant cells (Hussain et al., 2007). Malignant foci may be found in some of these nodules. This is known as nodule-in-nodule (Teoh, 2009). Hepatocytes progress from being benign to preneoplastic and then malignant. This takes place on a background of inflammatory conditions, which lead to cirrhosis.

Hepatocellular carcinoma: The gross picture (macroscopically) of HCC may constitute single or multicentric nodules, which may be well demarcated from surrounding liver tissue or have infiltrative growth (Kalinski and Roessner, 2009). The cross-section of these nodules may show areas of haemorrhage and necrosis. The most important criteria of current tumour classification of Union Internationale contre Le Cancer (UICC) is vascular invasion of portal or hepatic veins.

Microscopically, depending on the degree of differentiation, HCCs can resemble normal hepatic tissue. HCC cells may take on different patterns, trabecular pattern enclosing sinusoid-like blood spaces, pseudoglandular or acinar pattern and compact or scirrhous pattern (Kalinski and Roessner, 2009). The hepatocytes show high nucleo-cytoplasmic ratio, abundant finely granular eosinophilic cytoplasm, and prominent nucleoli. There are cytologic variations in the form of clear cell type, pleomorphic type with giant cells and the sarcomatoid type (Drebber and Dienes, 2006).

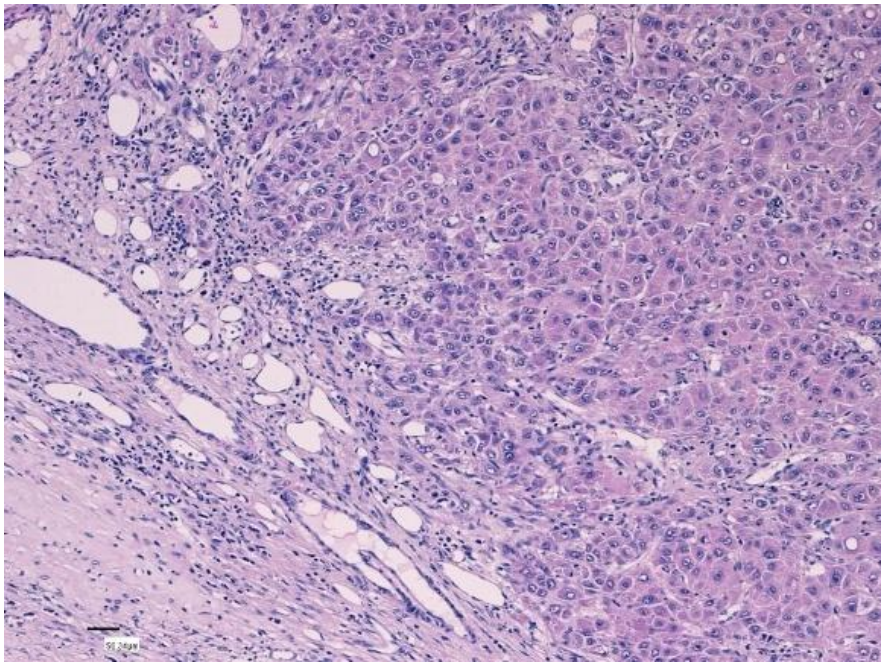

Figure 3: Microscopic picture of HCC showing polygonal cells with increased nucleocytoplasmic ratio and prominent nuclei.

1.4 Molecular pathogenesis of Hepatocellular carcinoma

Carcinogenesis is the end result of accumulation of chromosomal abnormalities which can lead to cellular dysfunction. These abnormalities may be genetic or epigenetic (Wong and Ng, 2008). Accumulation of genetic alterations causes abnormal growth, malignant transformation followed by vascular invasion and metastasis (Teoh, 2009).

For instance, genetic alterations include chromosomal deletions, gene amplifications, aneuploidy, rearrangement, mutations and epigenetic alterations including modulation of DNA methylation (Tada and Omata, 2009). Both genetic and epigenetic alterations activate mediators that enhance cellular proliferation (such as cellular proto-oncogenes) and inactivate mediators that inhibit cell proliferation (tumour suppressor genes) (Pang et al., 2006). Mutations in human cancer have been found in many genes such as p53, adenomatous polyposis coli (APC), cancer breast 1(BRAC1) and (BRAC2), retinoblastoma (RB), Ras and β-catenin. These genes are responsible for cell proliferation, cell cycle progression, apoptosis and metastasis. In HCC, it was found that p53 and β-catenin are the most frequently mutated genes (Wong and

Ng, 2008). As an example of the most frequent chromosomal deletions in HCC; deletions on chromosomal arms 17p, 8p, 16q, 16p, 13q, 1p, 4q, and 9p, and addition onto chromosomal arms 1q, 6p, 8q, 17q and 20q (Leong and Leong, 2005 and Pang et al., 2006).

Genetic alterations may be inherited mutations or acquired. Acquired genetic alterations are due to a combination of chemical, physical or biological carcinogens attacking cells (Leong and Leong, 2005). Carcinogenesis occurs due to either direct DNA damage followed by abnormal regeneration or secondary to chronic inflammation followed by cirrhosis. It is important to note that, 90% of HCC cases have a background of chronic inflammation and fibrosis (or cirrhosis) irrespective of the cause of liver disease (Elsharkawy and Mann, 2007). Free radicals resulting from inflammation can damage DNA and proteins directly (Hussain et al., 2007). As detailed above, the high incidence of developing HCC on a background of chronic inflammation makes the inflammation–cancer relationship a target for further study and investigation.

1.5 Inflammation- cancer relationship in liver diseases

Rudolf Virchow in 1863 noticed that cancer often occurred at sites of chronic inflammation suggesting that inflammation may play a pivotal role in tumourigenesis (Balkwill and Mantovani, 2001).

The important role of inflammation and infection have also been shown to be integral in the pathogenesis of liver, colon, oesophagus, stomach, cervical, and nasopharyngeal cancer by causing cell damage and creating a microenvironment rich in cytokines that can enhance cell replication, angiogenesis and tissue repair (Palapattu et al., 2009). In addition to these cancer types, a previous study highlighted that hepatocarcinogensis is strongly linked to chronic liver damage as it rarely exists in non diseased livers (El Serag and Rudolph, 2007). The pathway from chronic liver inflammation to HCC is a multi-stage process involving progression from mild to severe liver inflammation followed by hepatic fibrosis, cirrhosis and finally hepato-carcinogenesis. Liver inflammation is initiated by inflammatory cells either resident or recruited to the liver in response to signals released from damaged hepatocytes as a result of exposure to toxins, infection or auto-immune causes. These inflammatory cells produce pro-inflammatory cytokines such as Interleukin 1B, Interferon-Gamma and Tumour necrosis factor α, which contribute to the creation of a pro-inflammatory microenvironment leading to further hepatocellular damage.

This ultimately leads to hepatocellular regeneration and restoration of liver integrity (Ramadori et al., 2008). The inflammation and cell proliferation subside after the noxious agent is removed and the repair is complete. However, when the assaulting agent is unable to be removed, the persistent infiltration of inflammatory cells and continuous damage to the parenchyma leads to activation of a wound-healing response characterized by the appearance of myfibroblast-like cells. Activated myofibroblasts are responsible for hepatic fibrosis. These activated myofibroblasts may either be derived from quiescent hepatic stellate cell, bone marrow precursor or by epithelial to mesenchymal transition (EMT) (Brenner, 2009). Oxidative stress resulting from increased production of free radicals (ROS and reactive nitrogen species (RNS)) and peroxides is another important factor contributing to tissue damage and fibrogenesis. According to Parola and Pinzani (2009) these three events; (1)

chronic activation of the wound-healing reaction; (2) oxidative stress and reactive intermediates and; (3) derangement of epithelial-mesenchymal interactions are the key mechanisms underlying the initiation and maintenance of liver fibrogenesis (Parola and Pinzani, 2009). .

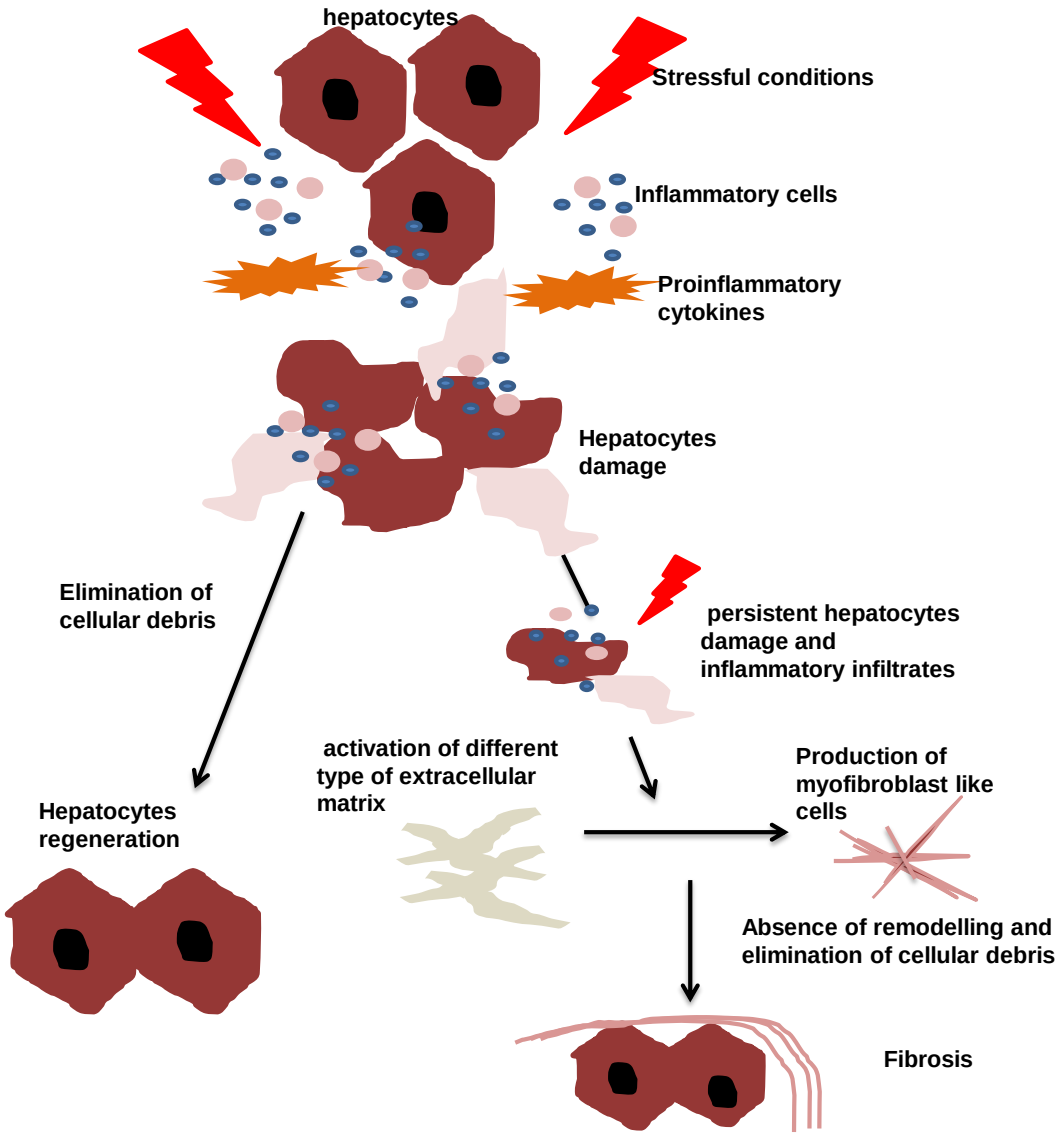

Figure 4: Mechanism of liver inflammation and fibrosis. The process of inflammation initiated with inflammatory cells, which produce pro-inflammatory cytokines which in turn lead to damage of stressed cells. This is followed by elimination of cellular debris and regeneration of hepatocytes. However with persistent of these stressfull conditions, there is absence of hepatocytes regeneration and an activation of wound healing proceeds and lead to fibrosis.

Cirrhosis is the most advanced stage of liver fibrosis and is characterized by irreversible changes in the normal tissue architecture whereby hepatocytes lose their normal two-cell plate-like arrangement and regenerative nodules are formed surrounded and separated by fibrotic septae. Distortion of the liver parenchyma leads to a reduction in the blood flow to parts of the liver resulting in tissue hypoxia, portal hypertension and increased risk of liver failure. At the same time the cirrhotic environment promotes the accumulation of genetic and epigentic mutations in pre-neoplastic hepatocytes or liver stem cells. These genetic alterations activate positive signals of cellular proliferation (including proto-oncogenes) and inactivate inhibitory signals of cell proliferation (including tumour suppressor genes) resulting in cells with autonomous growth potential. The altered cells develop into dysplastic foci and form nodules which finally undergo malignant transformation to HCC

Chronic inflammation also leads to stimulation of apoptosis and increase of oxidative stress which may lead to DNA damage (Schutte et al., 2009). This is due to the toxic metabolites such as acetaldehyde which have the capability to bind to DNA (Inoue et al., 2001) leading to genomic alterations. The alterations become severe with inhibition of DNA-repair enzymes (Homann et al., 2006) and therefore lead to accumulation of abnormal DNA and end up with neoplastic transformation of the cells.

Up regulation of toll like receptors (TLRs) signalling pathway has been reported in chronic liver diseases previously. LPS, the potent TLR4 stimulant is elevated in the systemic circulation and the portal vein of cirrhotic patients (Pradere et al., 2010). Moreover, TLR4 was identified as one of seven genes associated with development of cirrhosis in patients with chronic hepatitis C (Huang et al., 2007). There is evidence suggesting the implication of TLRs in chronic liver disease and cirrhosis, which can serve as a background for HCC. Thus, in order to understand the mechanism of liver inflammation, we were interested in the role of TLRs.

1.6 Toll like receptors

The Toll protein was discovered in Drosophila. It was shown to be essential during embryogenesis for determining the dorsal–ventral patterning (Anderson et al., 1985 and Morisato et al., 1995). It also has a role in the early formation of the innate immune system (Lemaitre et al., 1996 and Cherry and Silverman, 2006) and it was also found that mutation of TLR in Drosophila increases susceptibility to fungal infection (Kawai and Akira, 2006). TLRs are well known to play an important role in innate immune responses (Kawai and Akira, 2006).

To date, 13 subtypes of TLRs have been discovered (Park et al., 2009). The human TLR family includes 10 members (Kawai and Akira, 2006 and Mencin et al., 2009). These TLRs are stimulated by pathogen-associated molecular patterns (PAMPs). PAMPs are structural motifs expressed by bacteria, viruses and fungi (Janeway and Medzhitov 2002, Akira et al., 2006). Recently, danger-associated molecular patterns (DAMPs) have been reported to be a potent stimulant of TLRs and are derived from injured host and necrotic cancer cells (Sato et al., 2009). TLRs are divided into different families according to the phylogenetic properties (Roach et al., 2005). Each family is made up of TLR members, which respond to a general class of PAMPs. A specific ligand (DAMPs or PAMPs) has the ability to stimulate one particular member of the TLR family (table 2).

Table 2: TLRs and their corresponding PAMPs

Members of TLRs family	Corresponding stimulators (PAMPs)
TLR2, TLR1, TLR6 and TLR10	bacterial (lipopeptides, lipoteichoic acid, and peptidoglycan), fungal (Zymosan) and Viral (viral core proteins)
TLR3	recognizes the double-strand RNA and synthetic RNA derivatives (polyinosilic-polycytidylic acid)
TLR4	Lipopolysaccharide (LPS)
TLR5	Bacterial flagella
TLR7, TLR8 and TaLR9	TLR7 and TLR8 respond to nucleic acid structures such as guanosine- or uridinerich single-stranded RNA (ssRNA), from viruses TLR9 recognizes unmethylated CpG DNA motifs from DNA bacteria

The TLR2 family includes TLR2 with TLR1, TLR6 and TLR10. They respond to molecular patterns which include bacterial (lipopeptides, lipoteichoic acid, and peptidoglycan), fungal (Zymosan) and viral (viral core proteins) pathogens (Takeuchi and Akira, 2001 and Takeuchi et al., 2002). TLR3 recognizes the double-strand RNA and synthetic RNA derivatives (polyinosilic-polycytidylic acid) (Alexopoulo et al., 2001 and Matsukura et al., 2006).

TLR4 has receptors for lipopolysaccharide (LPS) (Yang et al., 2002) which forms a complex with LPS-binding protein (LBP), the membrane CD14 molecule and the MD-2 glycoprotein. These attach to the extracellular domain of TLR4 (Rallabhandi et al., 2006). TLR5 recognizes bacterial flagella through its monomeric constituent (Hayashi et al., 2001).

TLR7, TLR8 and TLR9 are in one family. TLR7 and TLR8 respond to nucleic acid structures such as guanosine- or uridine-rich single-stranded RNA (ssRNA) from viruses (Heil et al., 2004). TLR9 recognizes unmethylated CpG DNA motifs from DNA bacteria (Hemmi et al., 2000) and also unmethylated CpG in viral genome which is not common in vertebrate genome and if present, this

CpG dinucleotide is highly methylated (Krieg, 2007). However, recently it was found that TLR9 can be stimulated by either host or pathogen derived DNA (Basith et al., 2012). TLR1, TLR2, TLR4, TLR5 and TLR6 are expressed on the cell surface while TLR3, TLR7, TLR8 and TLR9 are present on the endosome lysosome membrane (Seki and Brenner, 2008).

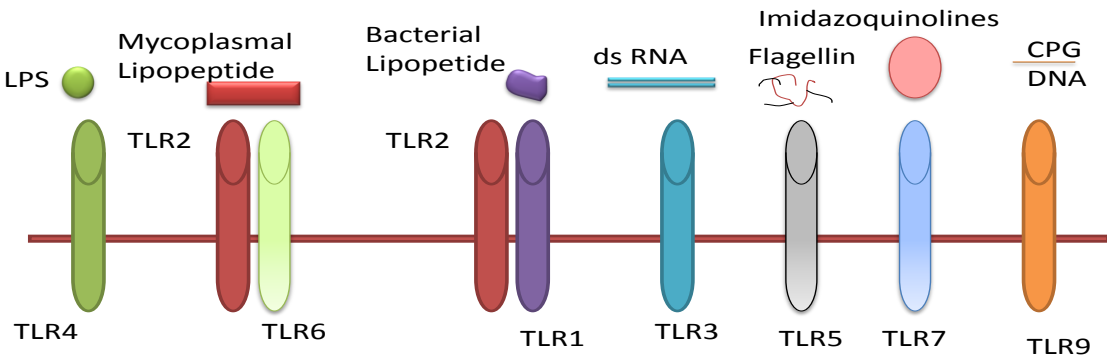

Figure 5: TLRs Receptors and their ligands (Adapted from Akira, 2004).

1.6.1 TLR pathway

There are two pathways for TLR members to be stimulated, MyD88- dependent (all TLRs except TLR3) and MyD88 independent (TLR3 and TLR4) pathways. MyD88-dependent pathways play a role in the activation of p38, c-jun N-terminal kinase (JNK) and inhibition of NF-κB kinase (IKK)/NF-κB (Seki and Brenner, 2008). Once stimulated, MyD88 activates IRAK through phosphorylation, the cascade leading to activation of TRAF6, which then activates JNK and NF-κB (Takeda and Akira, 2004). There are four members of IRAK that stimulate or inhibit TLR pathways. IRAK1 and IRAK4 interact with MyD88 through its N-terminal, which possesses an aspartate residue in the kinase domain leading to a stimulatory cascade. IRAK-2 and IRAK-M do not have this residue, and are therefore inactive catalytically (inhibitory stimulus) (Janssens and Beyaert, 2003).

Upon stimulation, IRAK4 and IRAK1 activate tumour necrosis factor receptor-associated factor 6 (TRAF6). TRAF6 activates transforming growth factor–β-activated protein kinase1 (TAK1) which activates the inhibitor of kappa β kinase (IKK) complex (Kawai and Akira, 2006).

TLR3 and TLR4 use the TIR-domain containing the adapter-inducing interferon-β (TRIF) or TRIF-dependant pathway (the MyD88-independent pathway), which utilizes TRAM for its activation. TRAM is an adapter protein, which links TLR4 and TLR3 to TRIF (Kawai and Akira, 2006). TRIF stimulation leads to the activation of the transcription factor IRF-3 inducing INF-β (Takeda and Akira, 2004). The end result of the MyD88 dependent and non dependent TLR activation is the stimulation of the transcription factor nuclear factor-kappa B (NF-κB).

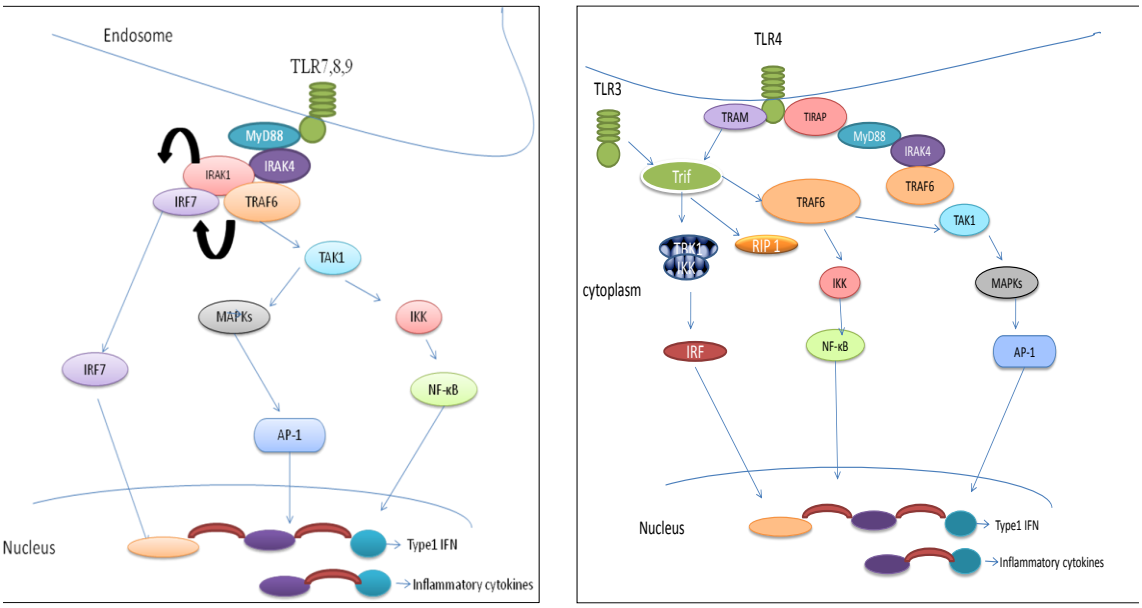

A) TLRs MyD88 dependent pathway

B) TLRs MyD88 -independent pathway and dependant pathway

Figure 6: MyD88-dependent and independent pathways. (A) MyD88-dependent: MyD88 stimulation leads to activation of IRAK by phosphorylation which in turn leads to activation of TRAF6 and NF-κB. (B)MyD88- independent pathway; stimulation of TRIF leads to activation of the transcription factor IRF-3 followed by INF-B (adapted from Kawai & Akira, 2006).

1.6.2 Role of Toll like receptors in liver inflammation-cancer progression

Due to the anatomical relationship between the liver and the intestine, and increased gut permeability associated with chronic liver disease, the liver is exposed to gut-derived pathogens and pathogenic molecules. This stimulates TLRs, releasing multiple cytokines and inflammatory mediators including activation of NF-κB, which is one of the most potent inflammatory mediators. NF-κB activation produces an inflammatory state in the liver through up regulation in the expression of cytokines, chemokines, growths factors, adhesion molecules, matrix metalloproteinase and anti-apoptotic proteins (Shishodia and Agarwal, 2002 and Pikarsky et al., 2004), thus inducing chemoresistance in cancer cells (Nakanishi and Toi, 2005) and hepatocyte death (Elsharkawy and Mann, 2007). In addition to NF-κB pathway, TLRs also act as potent activators of gene transcription and translation (Wolska et al., 2009), causing chemoresistance and cancer progression (Chen et al., 2008).

Not only TLR4 is linked to liver disease but also elevated bacterial DNA levels in blood and ascites of liver cirrhosis patients (Guarner et al., 2006 and Frances et al., 2008) suggesting a strong causative link between infection and liver inflammation. The bacterial unmethylated CpG-containing DNA stimulates TLR9 (Yang and Seki, 2012), leading to further inflammation, liver fibrosis, and malignancy. Indeed, an increased expression of TLR9 is observed in many malignant human cell lines such as lung cancer cells (Droemann et al., 2005), human gastric carcinoma cells (Schmausser et al., 2005) and human prostate cancer (Ilvesaro et al., 2007). Moreover, TLR9 modulates cytotoxicity by enhancing the NK cell cytokine response to antibody-coated tumour cells (Wysocka et al., 2004, Roda et al., 2005 and Ren et al., 2008).

1.6.3 TLR effects in cancers

The idea that TLRs are restricted to immune cells has changed, with a number of recent studies confirming expression of functional TLRs in cancer cells as well (Basith et al., 2012).

a) TLRs in cancer immunology, cytotoxicity

In any immune response, regulatory T cells (Treg) mediate antigen-specific immune attenuation and therefore can assist the tumour progression. The function of Tregs is to inhibit exaggerated immunological reactions (Coussens and Werb, 2002, Fisson et al., 2003 and Sakaguchi, 2004) including autoimmune, antimicrobial and antitumour immune responses by inhibiting T cell, B cells and NK cells (Yang et al., 2009).

It was found that Treg cells produce mRNA for TLR4, TLR 5, TLR 7 and TLR 8 and TLR4 stimulation with LPS activates the suppressive function of Treg on cytotoxic T lymphocytes (Caramalho et al., 2003) which inhibit antitumour immune response and lead to tumour progression. On the other side, stimulation of TLR9 modulates cytotoxicity of tumour cells by enhancing the NK cell cytokine response to antibody-coated tumour cells (Wysocka et al., 2004, Roda et al., 2005 and Ren et al., 2008).

Although TLRs recruit more immune cells to the tumour microenvironment, the tumour cells secrete pro-angiogenetic and growth factors, which make the tumour more resistant and can escape the cytotoxic lymphocytes.

Recently, some TLR agonists have been used as a vaccine for induction of anti-tumour immunity and the use of TLR agonists have shown promising results as anticancer agents. Therefore Basith and colleagues described the role of TLRs in cancer as double edged sword (Basith et al., 2012).

b) TLR effect on proliferation

Cancer develops as a result of increase of the cell proliferation to cell-death ratio (Hanahan and Weinberg, 2000). NF-κB has been reported to have a role as a hepatocyte survival factor (Elsharkawy and Mann, 2007). NF-κB signalling produces more cytokines, chemokines and antiapoptotic proteins, which contribute to increase in tumour proliferation (Basith et al., 2012). It was found that TLR stimulation leads to the activation of phosphoinositide3-kinase (PI3K) and Akt which may have a role in regulation of glycogen synthase kinase 3 (GSK3) (Monick et al., 2001 and Martin et al., 2005) and β-catenin (Monick et al., 2001 and Thiele et al., 2001). It also activates MAP kinase, JNK, p38 and ERK (Rakoff-Nahom and Medzhitov, 2008).

Previous studies reported that TLR ligands augment tumour growth (Harmey et al., 2002, Luo et al., 2004, Sfondrini et al., 2006 and Huang et al., 2007). It has been reported that TLR4 with TLR3 play a role in tumour proliferation (Jego et al., 2006, Chochi et al., 2008, Kundu et al., 2008 and Pries et al., 2008).

c) TLR effect on Apoptosis

NF-κB which is produced from stimulation of TLRs activates pro-apoptotic factors. In addition, NF-κB up regulates TNF-α which inhibits apoptosis (Salaun et al., 2006). TLR4 was found in the human lung cancer cell line and thought to play a role in protecting lung cancer cells through the induction of immunosuppressive cytokines and resistance to apoptosis (He et al., 2007). In some studies, TLR9, TLR3, TLR4 and TLR7 trigger apoptosis (Jahrsdorfer et al., 2002, Jahrsdorfer et al., 2005, Smits et al., 2007, Lehner et al., 2007 and

Paone et al., 2008). However, Jego and colleagues found that in myeloma cells triggering TLR7 and TLR9 prevents chemotherapy-induced apoptosis and induces cell growth (Jego et al., 2006). Another study suggested that the anti-apoptotic effect of TLR9 was through involvement of HSP90β. Lim et al., suggested the mechanism of anti-apoptotic effect mediated by stimulation of TLR9 depended on the Akt-FoxO3a signaling pathway (Lim et al., 2010).

d) TLR effect on Angiogenesis

It has been demonstrated that both TLR2 and TLR9 act as pro-angiogenic factors (Chang et al., 2005). TLR4 also enhances chemoresistance (Kelly et al., 2006). Although TLR9 is a pro-angiogenic factor it can also act as an anti-angiogenic factor together with TLR7 (Li et al., 2005, Majewski et al., 2005 and Damiano et al., 2006). NF-κB was also found to promote angiogenesis (Muccioli et al., 2012).

e) TLR effect on Metastasis

TLR-derived signals regulate the function of cyclooxygenases, chemokines, VEGF and matrix metalloproteinase (Rakoff-Nahoum et al., 2004, Pull et al., 2005 and Fukata et al., 2006). They have been known activate mesenchymal stem cells (Pevsner- Fisher et al., 2007). It was noticed that injecting 4T1 murine mammary carcinoma cells into the tail vein of mice resulted in increased lung metastasis after LPS (TLR4 agonist) injection (Harmey et al., 2002). In two different studies, stimulation of TLR9 was associated with increased cancer invasion and this was attributable to the activity of matrix metallopeptidase-13 (MMP13) (Ilvesaro et al., 2007 and Ilvesaro et al., 2008).

f) TLR effect on autophagy

Autophagy is a process of intracellular compartment degradation in stressful conditions and this process is thought to be related to cell survival, cell death and antigen presentation (Munz, 2009, Dalby et al., 2010 and Levine et al., 2011). Autophagy is primarily a cell survival mechanism. However, excessive autophagy can cause programmed cell death, which can be through apoptotic or non-apoptotic pathways (Gozuacik and Kimchi, 2004). In addition to this, autophagy enhances the process of presentation of tumour antigen via MHC

class II (Dengjel et al., 2005, Schmid and Munz, 2007 and Bertin and Pierrefite-carle, 2008). This suggests that autophagy can have an anti-tumoural effect by increasing immune surveillance (Bertin and Pierrefite-carle, 2008). However, in solid tumours which express MHC class II the tumour antigen presentation could enhance tumour growth as a result of induction of tolerance (Dengjel et al., 2006 and Bertin and Pierrefite-carle, 2008).

TLR signaling was suggested to link the autophagy pathway to phagocytosis (Sanjuan et al., 2007). Two subsequent studies demonstrated that TLR ligands have the ability to stimulate autophagy (Xu et al., 2007 and Delgado et al., 2008). A previous study showed that CpG (TLR9 ligand) not only induced autophagy in different tumour cell lines such as colon, breast and prostate cancer, but also that TLR9 itself was required for autophagy (Bertin and Pierrefite-carle, 2008). Light chain B (LC3B) is continuously degraded during the process of autophagy and more LC3B is needed to replenish the LC3B pool (Mammucari et al., 2008). For autophagy, the fusion of autophagosome with lysosomes is a mandatory step. Chloroquine has been reported to inhibit the fusion of autophagosome, thereby inhibits autophagy (Boya et al., 2005 and Ramser et al., 2009).

g) TLR effect on cytotoxicity and tumour management

Interestingly, it was noted that chemotherapy can induce initial inhibition of tumour growth, which is then followed by recurrence of more aggressive tumour phenotypes. This may be explained by the stimulation of TLRs by partial induction of cell death after chemotherapy, which stimulates inflammatory cells in a process known as sterile inflammatory response (Chen et al., 2008).

Inhibition of endosomal TLRs has a potential therapeutic in autoimmune diseases treatment. Chloroquine, the antimalrial drug has been used to treat immune-mediated inflammatory disorders such as SLE, rheumatoid arthritis and Sjogren's syndrome (Sun et al., 2007). It also inhibits CpG DNA-driven cellular activation (Macfarlane and Manzel, 1998) and this inhibition occurs as a consequence of alkalinisation as acidification of endosome is essential for TLR

activation (Macfarlane and Manzel, 1998, Hacker et al., 1998 and Yi and Krieg, 1998).

1.6.4 Clinical application of TLRs agonist and antagonist

a) Clinical application of TLRs agonist

- TLR2 agonist SMP-105 consists of mycolic acids and peptidoglycan derived from Mycobacterium Bovis. It has been used to treat bladder cancer (Simons et al., 2008).
- TLR3 was found to be a promising candidate for cancer treatment and clinical trials have reported that darn (TLR3 agonist) is linked to survival in cancer patient particularly breast cancer, primary and metastatic clear cell renal cancer (Salaam et al., 2006).
- TLR4 agonist, monophosphoryl lipid A (MPLA) is less toxic than the well-known agonist LPS. This has been approved as a part of the improved hepatitis B vaccine (Basith et al., 2012).
- TLR5 agonist (Flagellin) is under investigation with another component for the treatment of viral infection and as a vaccine against influenza (Huleatt et al., 2008).
- TLR7 agonist (imiquimod) has been approved as a topical treatment of cancer skin and cutaneous metastasis (Schon and Schon, 2008).
- TLR9 agonist unmethylated CpG (cytosine-phosphate-guanine) has been studied in targeting many cancers (Basith et al., 2012). However, immunomodulatory oligonuclutides (IMOs), which are also TLR9 stimulants are in clinical development for chronic HCV treatment. IMO-2055 has an anticancer effect and it is under clinical trial for the treatment of non-small lung cancer and in colorectal cancer (Krieg, 2008).

b) Clinical application of TLRs antagonist

TLRs antagonists have also been used in the treatment of different diseases.

- TLR2 inhibitor is being investigated for the treatment of inflammatory diseases including cardiac and kidney ischemia/reperfusion injuries and sepsis (Arslan et al., 2008).

- TLR4 antagonist, Chaperon 10 had been tested in patients with multiple sclerosis, for the treatment of sepsis and septic shock, rheumatoid arthritis and psoriasis (Vanags et al., 2006 and Broadley and Hartl, 2009).
- TLR7 and TLR9 antagonists, IMO-3100 have been developed for the treatment of autoimmune diseases. Dynavax produced an oligonucleotide-based compound, which inhibits endosomal TLRs, called immunoregulatory sequences (IRS 954). IRS 954 inhibits both TLR7 and TLR9 and has been tested in animal models for the treatment of systemic lupus erythematosis and also under investigation for the treatment of HIV infection (Pawar et al., 2007).

Another inhibitor of TLR7 and TLR9 is the antimalarial drug, chloroquine. It has been used as an endosomal TLR inhibitor. It is a weak base and it incorporates into the acidic vesicle within the endosome and interferes with its acidification as the acidic pH is mandatory for the endosomal TLR activation (Macfarlane and Manzel, 1998, Yi and Krieg, 1998 and Kuznik et al., 2011). It has been reported also that chloroquine inhibit the CpG-TLR9 interaction and can be used as TLR9 antagonist and endosomal acidification inhibitor at the same time (Rutz et al., 2004).

Aims

2. Aims of the study

This thesis was designed to explore the role of toll like receptors in the pathogenesis of HCC and evaluate their role as a potential therapeutic target. Specifically I aimed to

1. Establish 2 animal models of primary liver cancer; a chemically-induced and a xenograft model.
2. Determine whether gut decontamination with Norfloxacin could prevent HCC.
3. Determine whether the expressions of TLR4, TLR7and TLR9 were increased in primary liver cancer in patient.
4. Evaluate the expression of these TLRs in primary liver cancer cell-lines and the effect of stimulation or inhibition on cell proliferation.
5. Determine the effect of inhibiting TLR7 and 9 using specific antagonists or non-specific inhibitor (chloroquine) in animal models.

Materials and Methods

3 Materials & Methods

- **Animal models are explained in details in chapter (4.1).**
- **All the reagents that had been used in this research are reported in the appendix section.**

3.1 Animal tissues collection

Rats and mice were anaesthetized in an induction chamber supplied with isoflurane from a vaporizer (5% and O_2 1L/min) until the rodent was anaesthetised then anaesthesia was maintained using isoflurane (2%). The liver was surgically removed and pictures of each liver were taken. In the case of rats the dimensions of the whole rat liver and any obvious tumour(s) was measured using a ruler. Half of the liver was then placed in 10% formalin and the other half was snap frozen in liquid nitrogen. The formalin-fixed tissue contained representative areas of tumour and tumour-free tissue. The snap-frozen liver samples were divided into liver tissue macroscopically free from tumour and tumour nodules.

In the case of mice only the tumours were measured. The tumour was excised and snap-frozen in liquid nitrogen. A corresponding tumour free area of liver tissue was also snap-frozen in a separate tube. In other cases the whole of the mouse liver was fixed in formalin. Blood was collected in heparinised tubes which were placed directly on ice and then centrifuged for 10 minutes, 13000 rpm, 4°C.

3.2 Processing of tissue for histological examination

Freshly harvested livers from rats and mice were cut into thin slices using a scalpel and placed in an embedding cassette for processing in a Benchtop Tissue Processor (Leica TP1020). The processor automatically fixes the tissue in formalin, dehydrates it in alcohol and infiltrates it with paraffin wax (Ficher Scientific, UK). Once the tissue processing was complete, 4 µm sections were cut from the paraffin embedded tissue blocks using a microtone (Leica, UK). The sections were then mounted from warm water (40C) onto adhesive poly- L-Lysine coated glass slides ready for immunohistochemical staining and analysis.

3.3 Haematoxylin and Eosin (H&E) staining

Paraffin-embedded tissue sections were stained with H&E using conventional methods. The sections were first de-paraffinised by immersing in two tanks of xylene, 2 x 5 minutes each and rehydrated by submerging in descending grades of ethanol; 100%, 95% and 75% ethanol, 5 minutes each. The sections were then washed in distilled water for 5 mins, stained with Mayer/s Haematoxylin (Dako, UK), 3 mins, rinsed in tap water for 15 minutes, stained with Eosin (Sigma, UK) for 1 min and washed in a few changes of distilled water before dehydrating with ascending grades of ethanol; 75%, 95% and 100% ethanol, 3 minutes each. Finally, the slides were cleared in 2 separate tanks of xylene, 5 minutes each, and mounted as follows: a drop of DPX mounting medium (Sigma, UK) was placed in the middle of a coverslip making sure to avoid any air bubbles. The slide to be mounted was tapped to remove excess xylene and gently lowered on top of the coverslip so that the tissue section was sandwiched between the slide and coverslip. The slide was then turned over and the DPX allowed to fully spreading under the coverslip. The slides were left to harden in a fume hood overnight before being examined under microscope.

3.4 Reticulin staining

The silver stain has the ability to bind to collagen and fibrous tissue.

- **Methods**

The sections were first de-paraffinised by immersing in two tanks of xylene, 2 x 5 minutes each and rehydrated by submerging in descending grades of ethanol; 100%, 95% and 75% ethanol, 5 minutes each. The sections were washed in distilled water. The slides were treated with acidified potassium permanganate for 10 minutes then washed well with distilled water. Oxalic acid was added to cover the slides for 1 minute until the colour acquired by potassium permanganate disappeared; the slides were then washed with water. Ammonium sulphate was added to slides for 10 minutes then washed with water. The slides were treated with ammonical sliver solution for 5-20 seconds then washed and 10% formalin was added for 1 minute. Then the slides were washed in water and dehydrated with ascending grades of ethanol; 75%, 95% and 100% ethanol, 3 minutes each. Finally, the slides were cleaned in 2

separate tanks of xylene, 5 minutes each, and mounted as described in in the previous section (3.3).

3.5 Picro-Sirius red staining

This stains the collagen and fibrous tissue with red colour.

- **Method**

The sections were first de-paraffiinised by immersing in two tanks of xylene, 2 x 5 minutes each and rehydrated by submerging in descending grades of ethanol; 100%, 95% and 75% ethanol, 5 minutes each. The sections were washed in distilled water. Then sections were treated with picro-Sirius mixture for 15 minutes then 100% ethanol for 5 minutes. The slides were dehydrated with ascending grades of ethanol; 75%, 95% and 100% ethanol, 3 minutes each. Finally the slides were cleared in 2 separate tanks of xylene, 5 minutes each, and mounted as described in section (3.3).

3.6 Measuring Liver enzymes and bilirubin

Plasma samples were analyzed for ALT, AST and bilirubin (Cobas Integra 400, Roche Diagnostics, Burgess Hill, West Sussex, UK).

Using a specific tube for Cobas (Roche Diagnostics Ltd, UK), 200µl of rat's plasma was added. The corresponding cartridges for the enzymes and bilirubin were placed in the Cobas machine. The machine was run according to manufacturer's instructions.

3.7 Endotoxin kinetic LAL assay measurement

- **Method**

1. The samples (rat's plasma) were diluted 1:10 LAL reagent water to prevent protein interference (50µL sample + 450µL LAL) then heated in a boiling water bath for 10 minutes.
2. The Standard Reconstituted Endotoxin was diluted to obtain a 50EU/ml concentration (220µL for the standard curve plus 20uL/sample).
3. Plate reader was switched on, Endotoxin test was selected, and temperature adjusted to 37ºC.

4. 5-point standard curve (50EU to 0.005EU) was made, in duplicate with the following dilutions :

a) 111µL of the 50EU standard in the first well A of the 1st 2 rows

b) 100µL of LAL water in the wells B, C, D, E, F first 2 rows

c) 11µL from the well A into the well B, from B to C and so on. Down to E, 11µL was discarded from well E. Well F was the blank sample.

5. 100µL of each sample was transferred aseptically in quadruplicate (4 wells in the plate). In the last two wells, 10µL of 50EU standard endotoxin was added as spike well.

6. The plate was then placed in plate reader for 5 minutes to warm up.

7. The LAL reagent was prepared as the following (each bottle was diluted with 3.2ml of LAL reagent water) then vortexed for 20 seconds. 100µL of LAL regent was added to each well to start the reaction. Then the plate was read at 350 – 650nm (on scan mode).

3.8 Western blot

3.8.1 Protein extraction from liver tissue

The liver tissue was disrupted using a pre-cleaned, autoclaved pestle and mortar which had been pre-cooled by placing in a -20ºC freezer for an hour or more. A small piece of liver tissue, 100 mg, was dissected from the frozen tissue stock, and weighed by placing it inside an eppendorf safe-lock tube (Eppendorf UK Limited) on ice. After weighing, the tissue was then placed in the cold mortar and 300µl of lysis buffer added per 100 mg of tissue. The pestle was used to macerate the tissue to a pulp and the grinding continued until a homogenous liquid was produced. The tissue extract was poured into a sterile 1.5ml eppendorf safe-lock tube and then centrifuged for 5 minutes, 13000 rpm, 4°C. The supernatant was then aliquoted into a fresh eppendorf tube and the protein concentration in the liver tissue lysate determined using a biuret assay.

3.8.2 Determination of Protein Concentration

- **Biuret Protein Assay**

The protein concentration in the liver tissue extract was determined using the biuret protein assay. This is a colorimetric assay used to determine the the protein concentration. It is used for detecting the presence of peptide bonds. It depends on the reduction of copper (II) ions to copper (I), the latter forms a complex with the nitrogen of the peptide bonds in an alkaline solution. A violet colour indicates the presence of proteins.

- **Preparation of albumin standard curve**

A set of protein standards was prepared from a 2 mg/ml albumin (Zenalb) stock solution with the following concentration: 40µg/ml, 20µg/ml, 10µg/ml, 5µg/ml and 2.5µg/ml.

- **Biuret assay**

200µl of Biuret solution was added per well in 96 wells. Standard serial dilution of albumin was prepared from albumin. 10µl from each standard and from each sample was placed into the biuret solution in the 96-well plate in duplicate for 2 hours at 37°C then read in a plate reader for 562nm wave length. After the reading, the amount of protein in each well was calculated.

3.8.3 Addition of loading buffer to protein extract

The loading buffer (LB) (Life technologies, UK) contains SDS which is a detergent that denatures the proteins and applies a negative charge which allows the proteins to migrate through a gel based on their length. The LB also contains a dye, bromophenol blue, which helps to track the movement of proteins through the gel and glycerol, which adds viscosity to the mix making it easier to load the samples on a gel. The samples were prepared by mixing 20 ug of protein in given volume, made up to 15µl in de-ionised water, with 1/4th volume of 4 x LB and 1/10th volume of reducing agent (Life technologies, UK). The samples were then heated to 95-100°C for 5 minutes to denature the proteins and help SDS to bind. The samples were then spun briefly for a few seconds in microcentrifuge to bring all the droplets to the bottom of the tube.

The samples were then ready to load onto an SDS polyacrylamide gel for electrophoresis.

3.8.4 Gel electrophoresis

Electrophoresis of proteins was carried out using pre-cast 4-12% Bis-Tris Nupage gels (Life Technologies, UK). The gel cassette was removed from its casing and placed inside a Nupage gel tank according to the manufacturer's instructions. The gel tank was then filled with 1 x SDS running buffer (Life Technologies, UK). The gel comb was gently removed and a Pasteur pipette was used to gently wash the wells. The protein samples were then loaded onto the gel along with a protein molecular weight marker (See Blue ladder, Life technologies) loaded onto one of the wells. The lid was then put in place on the gel tank, which was then connected to an electrical power supply. Electrophoresis was then carried out at 200V for 45 minutes or until the blue dye was around 1cm from the bottom of the gel.

3.8.5 Western blot transfer

a) Transfer buffer

25ml of 20X transfer buffer (Life Technologies, UK) was added to 375 ml deionised water then 100 ml of methanol was added. Prior to transfer Four sponges and 2 filter papers were soaked in the transfer buffer for around 30 min. The PVDF was first activated by soaking it in ice cold methanol for 15 seconds followed by ice cold transfer buffer for 5 minutes.

b) Transfer of proteins from gel to membrane

When gel electrophoresis of proteins was complete, the proteins were transferred from the gel onto a membrane made of polyvinylidene difluoride (PVDF, Life technologies, UK) by electroblotting. During this process, the proteins move from within the gel onto the membrane whilst maintaining the organization they had within the gel. As a result of this blotting process, the proteins are exposed on a thin surface layer for detection. The transfer sandwich was then assembled as seen in (Fig. 7) in a transfer cassette XCell II™ Blot Module CE Mark (Life Technologies, UK).

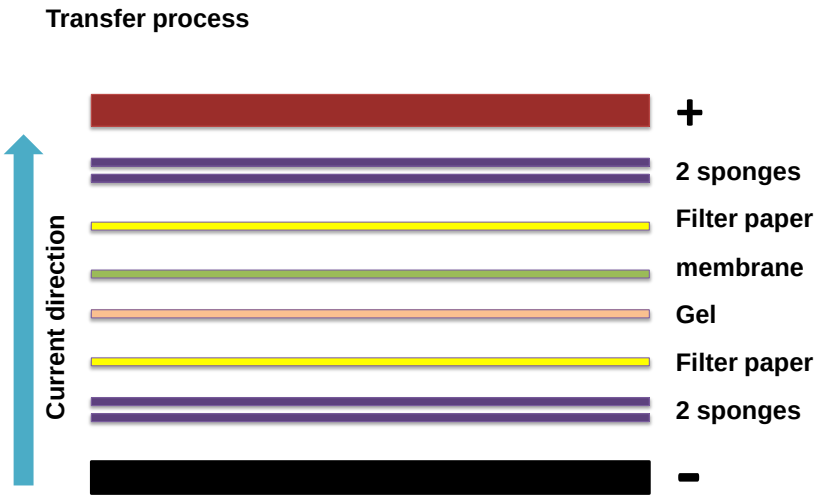

Figure 7: Transfer process. The diagram showing the arrangement of the sponge, paper, membrane and gel in the transfer cassette. The current flow runs from cathode to anode.

Any air bubbles were removed from between the layers by using a designated roller which was rolled over the different layers after they were put in place. Once the stack was complete, the sandwich unit was closed and placed in the blotting apparatus following manufacturer's instructions. Ice cold transfer buffer was then poured on top of the sandwich until its contents were entirely immersed. The compartment outside the sandwich unit was filled with distilled water. The lid was then placed on the blotting apparatus which was then connected to an electrical power supply. Protein transfer was carried out at 30 V for 1 hour.

c) Checking protein transfer

After western blotting was complete, protein transfer to the PVDF membrane was checked by staining with Ponceau S solution (Sigma, UK). The membrane was removed from the blotting sandwich and immediately immersed in a sufficient volume of Ponceau S to cover the membrane. Five minutes later the Ponceau S (Sigma , UK) was poured off and the membrane was rinsed in several changes of deionised water until the background membrane staining disappeared and the pink protein bands were clearly visible. Once protein transfer was verified, the stain was completely removed from the proteins by continued washing with Tris-Buffered Saline and Tween 20 (TBST) buffer for 20 minutes. The membrane was then blocked and probed with antibody as described in the next section.

3.8.6 Probing membrane with antibody

Probing of Western blot membranes with antibody involves several steps. SNAP i.d. Protein Detection System (Millipore, UK) was used. It is a device that has place to accommodate particular cassettes; the cassettes are opened and the membrane inside was hydrated with de-ionised water then the Polyvinylidene difluoride (PVDF) membrane after which was put in specific order, the membrane face which was contact with gel during the transfer was put directly to face the cassette's membrane then the cassette closed and put in the device. The nonspecific binding was blocked with block solution (Millipore, UK). This block reduces the background and eliminates false positives for an hour. Following the blocking step, the blocking solution was removed by suction and the membrane was incubated with the following primary antibodies: mouse monoclonal NF-κB (1/500, Millipore, UK), rabbit polyclonal Akt (1:1000, cell signalling, UK), rabbit monoclonal pAkt (Ser473) (1:1000, cell signalling, UK), rabbit polyclonal LC3B (1:1000, cell signalling, UK) and rabbit polyclonal VEGF (1:500, Abcam, UK). For checking the loading, protein amount, rabbit polyclonal β-actin (1:500, Abcam, UK) and mouse monoclonal α-tubulin (1:1000, Millipore, UK) the antibodies were diluted in blocking solution for 10 minutes. Then the antibody was removed by suction and after three washes with TBST 5 ml each and suction was turned on to remove the washing buffer. The membrane in the cassette was incubated with the secondary antibody diluted in blocking buffer for 10 minutes. The secondary antibody is directed at a species-specific portion of the primary antibody (hence it is referred to as anti-mouse (1:5000, Abcam, UK), anti-rabbit (1:5000 cell signalling). The secondary antibodies were horseradish peroxidase-conjugated. The secondary antibody was removed by suction and the 5ml of TBST was put in the cassette to wash the membrane 3 times then the wash buffer was removed by suction and the cassettes removed from the snap id device.

3.8.7 Visualizing antibodies on Western Blots by ECL

The enhanced chemiluminescence (ECL) Western Blotting substrate for visualizing bound antibodies on membrane blots was used as recommended by the manufacturer (GE healthcare life sciences, UK). One ml of each of the detection reagents, Reagents 1 and 2, was mixed and added to the membrane. After 1 minute the membrane was drained, covered in cling film and exposed to photographic film (Thermoscientific, UK) up to 2 minutes inside an intensifying film cassette. The exposed film was then removed and placed in a film developer to visualize the antibody signals. If necessary, a second sheet of photographic film was exposed to the membrane for a longer or shorter period of time (from a few seconds to 10 minutes) in order to get a stronger or weaker signal.

3.9 TNF-α measurement by ELISA

Measuring rat TNF-α was performed by ELISA (BD Bioscences, UK) on liver tissue lysate. Liver tissue was homogenised and protein was measured as in section 3.8.1 and 3.8.2. 96-well plate was used and the plate was read on wave length 650nm as specified in the protocol and the results presented as the amount of TNF-α per amount of protein added (known from protein measurement).

- **Method**
  a) 96-well plate was coated with the capture antibody. Capture antibody was diluted 1 in 250 in coating buffer and then 100µl was added per well. The plate was sealed and incubated overnight in 4°C.
  b) On the second day the plate was washed with 300µL per well (5 times). This was blocked by adding 250µL of assay diluents to each well and incubated for 1 hour. Then this was washed 5 times as described before.
  c) Sample or standard was added per well (in duplicate) as follow. 50µL of assay diluent in each well, then 50µL of sample or standard. The samples used were tissue lysates.
  d) A seven point standard curve was achieved using serial dilutions. Then the plate was covered and incubated for 2 hours. After 2 hours the plate

was washed 5 times as before with washing buffer. Then, the detection antibody was added.

e) The detection antibody was diluted 1 in 250 in assay diluents and 100µL of the diluted detection antibody was added to each well. The plate was covered and incubated for 1 hour then washed as before. 100µL of Streptavidin-HRP was added to each well after dilution (1 in 250 with assay diluents) and plate covered and incubated for 30 minutes. The plate was then washed 7 times with 300µl per well each time. 100µL substrate solution was added per well and incubated for 20 minutes at room temperature in a dark place.

f) After 20 minutes, 50µl of stop solution was added per well. The plate was taped to mix gently and the plate was placed in the plate reader and read at a wavelength of 450nm.

3.10 Immunohistochemistry

3.10.1 Materials

a) Human Tissue Microarrays

Human tissue microarrays (TMA) were purchased from Vbiolabs, Cambridge (UK). Custom made slides were prepared containing 4µm parallel sections from 111 paraffin embedded human liver tissues of different histologies. The samples were originally derived from 78 males and 33 females of a similar age group. 96 of cases were associated with hepatitis virus infection; 53 with HBV and 33 with HCV. Details of the tissue samples along with the relevant clinical data are given in (Table 3).

Table 3: Details of the Tissue Microarrays

Histology	Total No.	Males No.	Females No.	Median Age (range)		No. with hepatitis virus	
				Males	Females	B	C
Normal	9	6	3	42 (34-58)	41 (30-41)	0	0
Hepatitis	26	19	7	55 (26-68)	57 (52-72)	18	8
Cirrhosis	24	23	1	55 (33-69)	47 (47)	16	8
Hepatocellular carcinoma	41	24	17	54.5 (29-68)	53 (41-72)	19	18
Cholangio carcinoma	9	2	7	54.5 (34-63)	61 (27-69)	0	0

b) Archival Liver Tissue (Validation Set)

Paraffin embedded liver tissue samples from patients who were admitted to the Royal Free Hospital between 1993 & 2004 were retrieved from the hospital pathology department. The histology of these samples and other relevant data are given in Table 2. All the cases of HCC were on a background of cirrhotic liver. 4 micron sections were cut from each paraffin-embedded tissue block using a microtome. The sections were placed on poly-L Lysine coated slides (VWR, UK).

Table 4: Details of the archival liver tissue samples (Validation Set)

Histology	Total No.	Males No.	Females No.	Age Range		No. with Hepatitis virus	
				Males	Females	B	C
Normal	2	-	-	-	-	-	-
cirrhosis	5	-	-	-	-	-	-
HCC	19	16	3	43 - 68	31 - 51	3	9

3.10.2 Immunohistochemistry procedure

Immunohistochemistry was carried out on the human tissue specimens (TMA and validation set). Paraffin was removed (from the sections) by heating at 60˚C for 20 minutes before processing. Tissue section on glass slides were first de-paraffiinised by immersing in 3 changes of xylene, 5 mins each and rehydrated by submerging in descending grades of ethanol; 100%, 90%, 80 %, and 70% ethanol, 5 mins each. Following a 5 minute wash in phosphate buffered saline (PBS) the slides were immersed in target retrieval solution, citrate pH 6 (Dako UK Ltd) and placed in a microwave oven for 10 minutes at 700 watt power. The slides were allowed to cool for approximately 30 mins approximately and then washed in PBS, 3 x 2 mins. The excess liquid was removed by gently tapping the slides on a piece of tissue before applying 10% hydrogen peroxide for 30 mins to block the endogenous peroxidase activity. This was followed by another wash in PBS, 3 x 2 min. The PBS was carefully removed again before incubating the slides with serum blocking reagent (Life Technologies, UK) for 30 mins. The blocking reagent was tapped off the slides and the excess liquid was wiped away from around the tissue. Each tissue section was then covered with diluted primary antibody or negative control (without primary antibody) and left to incubate overnight at 4 C in a closed chamber. The slides were removed from the incubation chamber and washed in PBST, 3x2 minutes. The excess liquid was then wiped away and each section was covered with secondary antibody for 45 minutes. The slides were next washed in PBST, 3x2 mins and covered in freshly prepared Diaminobenzidine (DAB) chromogenic/substrate solution for 2-3 minutes

(Envision Kit, Dako UK Ltd). Following by a 5 min rinse in tap water the slides were counterstained with Haematoxylin (Dako UK Ltd), 3 mins, followed by another wash in tap water for 20 mins. Finally, the coverslips mounted with aqueous mounting medium (Life Technologies, UK). The slides then placed in an oven for 30 min to harden.

3.10.3 Scoring of the immunohistochemistry data

The immunohistochemically stained slides were examined by two independent pathologists. Smooth muscle actin staining was scored by the presence or absence of the stain. For TLR4, TLR7 and TLR9 the scoring system was depend on the intensity and extent. The total score was calculated as the following.

- **The staining intensity was scored as follows:**

(0) No staining

(+) Faint staining

(++) Moderate staining

(+++) Intense staining

- **The staining extent was scored as follows:**

< 1/3 of the cells stained

> 1/3 and <2/3 of cells stained

> 2/3 of the cells stained.

- **Then total score was calculated as the following:**

Table 5: Scoring system of immunohistochemistry

staining Score	description
0	Negative or + staining in less than 1/3 of the cells
1	(+) intensity in more than 1/3 of the cells or ++ in less than 1/3
2	(++) or (+++) intensity of staining in more than2/3 of the cells

Ki-67 index: A proliferation index was calculated by counting 1000 tumour cells and using a cell counter to count the number of Ki-67-positive nuclei among the 1000 nuclei in highly expressed selected fields (el-Sader et al., 1996) and the index was presented as percentage.

3.11 Cell cultures

3.11.1 Cell Lines

Human hepatocellular carcinoma cell line HepG2 was purchased from the American Type Culture Collection (ATCC) (as frozen vial). The human hepatocellular carcinoma cell line HuH7 was purchased from SIGMA (as a growing cells). HuCCT1 cell line was provided by another Laboratory (Riken BioResource centre, Japan).

3.11.2 Cell Culture Medium

Cells were grown in T75 culture flasks angled neck filter sterile (VWR) containing 15 ml of Dulbecco's minimal essential medium (DMEM) for HepG2 and HuH7 or Roswell Park Memorial Institute (RPMI) for HUCCT1 both media supplied with 2mM glutamine purchased from (Gibco) supplemented 10% fetal bovine serum (FBS) heated inactivated, from (Gibco), and 10000 U penicillin streptomycin (Life Technologies, UK). The culture flasks were placed at 37°C in a 5% CO2 incubator. The culture medium was changed twice a week until the cells were 70-80% confluent after which the cultures were subdivided by trypsinization.

3.11.3 Trypsinization of cell cultures

Cell lines were subcultured by trypsinization. The culture medium was discarded from the flask and the cells were rinsed with 10 ml PBS (Life Technologies, UK). The PBS was poured off and 1ml of 0.25% Trypsin-EDTA (Life Technologies, UK) was added to the flask. The flask was then incubated at 37C for 2-3 minutes to allow the cells to detach from the flask. The trypsin was then neutralized by adding 5 ml of DMEM containing 10% FBS. The trypsinised cells where divided equally between five T75 flasks each containing 10ml of DMEM supplemented with 10% FBS, 2mM glutamine and 10 000 U of penicillin/ streptomycin.

3.11.4 Cell Counting by Trypan Blue Staining

Freshly trypsinised cells were counted using a haemocytometer as follows: 10µl of Trypan blue (Sigma, UK) were mixed with an equal volume of a well-mixed cell suspension. The haemocytometer was cleaned by rinsing in distilled water followed by 70% ethanol. The haemocytometer coverslip was cleaned in the same way then carefully placed in position on the counting chamber. 10 µl of the typan blue cell suspension were applied to the edge of the coverslip using a Gilson pipette and allowed to run under the coverslip. When the counting chamber was completely filled with sample the cell numbers were determined by direct counting under a light microscopy at 20 X objective. Live cells appear colourless whilst dead cells stain blue.

The number of live cells in one of the large corner squares was counted in each of the 4 large corner squares and an average was taken. The average was then multiplied by the dilution factor (in this case 2) and by 10^4, i.e. the average was multiplied by 20 000.

3.11.5 Cell Viability and proliferation Assay

- **Principle of the assay**

The assay is composed of tetrazolium compound [3-(4, 5-dimethylthiazol-2-yl)-5-(3-carboxymethoxyphenyl)-2-(4-sulfophenyl)-2H-tetrazolium, inner salt; MTS]. MTS is reduced by living cells into coloured product that is soluble in tissue culture medium. The assay was performed by adding the reagent directly to the culture wells and it was incubated for 2 hours and then recording the absorbance at 490nm with a 96-well plate reader (Data sheet of the MTS assay, Promega).

The cells were grown in 96-well plate (Nunc) 10^4 cells were seeded separately into 3 wells each and the number of cells was estimated after 24, 48, 72 and 98 hours to detect the growth behaviour of the cells. Before the reading, the media which was added to the cells was discarded and 100µl of fresh media added to each well. Then 20µl of the proliferation assay solution was added to the media (as described by the manufacture protocol). The plate was incubated (37ºC and 5% $CO_{2)}$ for 2 hours. The plate was placed in the plate reader and read at a wavelength of 490 nm.

- **Cell response to treatment**

10^4 HuH7 or HuCCT1 cells per well were plated in a 96-well plate. A time-course (24, 48 and 72-hours) of the proliferation of the cells was determined following treatment with CpG-ODN 5μM (TLR9 agonist, Invivogen, UK), Imiquimod 5ug/ml (TLR7 agonist, Invivogen, UK), chloroquine 15uM (Invivogen, UK) and IRS- 954 (Dynavax, USA) 20ug/ml [IRS-954 is an immunoregulatory DNA sequence which is a specific TLR7 and TLR9 antagonist and is being developed as a potential treatment of systemic lupus erythematosis (Barrat el al., 2005). The proliferation assay was performed to detect any effect of treatment on proliferation.

3.11.6 Neutral red uptake test

- **Principle of the test**

This test is based on the ability of viable cells to uptake the supravital dye Neutral Red (NR). NR is weak cation which, through non-inionic passive diffusion penetrates cell membrane and accumulates in the lysosomes (Repetto et al., 2008).

- **NR dye preparation**

Under sterile conditions, neutral red stock solution was prepared by dissolving 40 mg neutral red dye (Sigma, UK) in 10ml PBS in a falcon tube then protected the tube from light by foil. The neutral red stock solution was diluted 1:100 in DMEM media and kept overnight in the incubator.

HuH7 cells were trypsinised and seeded 10^4 cells per well for 48 hours and treated with the dosage as in cell response to treatment section. DMEM media was discarded and 100μl of the diluted NR solution was added per well. The plate was incubated for 2 hours. Then the plate was examined under light microscopy to observe the red stain inside the cells.

3.11.7 Immunofluorescence staining

HuH7 cells and HuCCT1 cells were stained using the immunofluorescence technique. From each cell line, $5x10^3$ cells were grown on 13mm glass coverslips (treated with 1 molar HCL then rinsed in 70% ethanol and finally washed with PBS). Coverslips with cells were placed in 24-well plate for 24 hours incubation to allow the cells to settle down.

Then coverslips with cells were treated in duplicate with one of the following treatments: Imiqumoid (IMQ), CpG, chloroquine and IRS and one group without any treatment as a control. The dosage of treatment mentioned in cell response to treatment section. After 24 hours the media was discarded and cells fixed with methanol as describe before (Minogue et al., 2006). Then the cells were washed with PBS and 70% cold methanol was added to each well. Then the plate was placed in -20ºC freezer for no longer than 3 minutes this was then washed with PBS tree times then blocked with 3% bovine serum albumin (BSA)(Sigma, UK) for 20 minutes. After blocking the following antibodies were added after dilution in 0.3% BSA as an antibody diluent. Mouse monoclonal TLR9 (1/50, Abcam, UK), mouse monoclonal lamp-1 (1/100Abcam, UK), rabbit polyclonal TLR7 (1/100, Abcam, UK) and Rabbit polyclonal calnexin (1/100, cell signaling). The matching secondary antibody was diluted in the same antibody diluents, antimouse Alex fluor 543 (1/500, Life Technologies, UK) and anti rabbit Alex fluor 488 (1/500, Life Technologies, UK) with hoechst 33342 (1/5000, Life Technologies, UK) for nuclear counterstaining. Cells were mounted using prolong gold antifade reagent (Life Technologies, UK) and observed under an LSM 510 Meta laser-scanning confocal microscope, (Carl Zeiss Ltd). All images were obtained with a Zeiss 63× 1.4 NA oil-immersion objective with pinholes set to one Airey unit. 12-bit fluorescence images were collected to peak.

3.11.8 Western Blot Analysis for cells

The expression of specific proteins in the cell cultures was examined by Western blot analysis. The method involves the following steps which are described in more in sections 3.8

1. Extraction of proteins from cells
2. Measurement of protein concentration in the cell.

3. Separation of proteins by electrophoresis on a nupage gel.

4. Transfer of proteins from the gel to membrane

5. Staining of the protein with antibodies

6. Visualization of antibody signal by ECL reagent (steps 3, 4, 5 and 6 were described before in section 3.8

- **Protein extraction from cell cultures**

Cells were grown in T75 flasks until they were about 80% confluent. The culture medium was then discarded and the cells were rinsed in 10 ml of PBS. The PBS was discarded and 500µl of mammalian protein extraction reagent M-PER (Thermo Fisher Scientific, UK) was added to the flask. The cells were then scraped off the flask using a cell scraper (Fischer scientific, UK) and collected in a 1.5 ml eppendorf tube then placed on ice and sonicated for 1 min. The tube was spun for 5 min, 13000 rmp, 4°C to pellet the debris. The supernatant was collected and then aliquoted into a fresh tube and the protein concentration determined using a Bicinchoninic Acid (BCA) Protein Assay Kit (Thermo Fischer Scientific, UK).

- **Protein estimation by micro BCA Assay Kit**

The Bicinchoninic acid (BCA) assay was used to determine protein concentration in the cell culture lysates. The principle of the assay is the reduction of Cu II to Cu I by proteins in an alkaline medium then detection of the Cu I ions by BCA reagent. BCA is a chromogenic reagent that reacts with Cu I ions producing a purple complex with strong absorbance at 562nm. The intensity of the colour produced is directly proportional to the concentration of protein in the sample. The protein concentration is determined by measuring the colour intensity in the sample against a protein standard curve. The standard curve is prepared using a series of bovine serum albumin (BSA) dilutions, at known concentration, which are assayed alongside the unknown(s) (Data sheet of the assay).

- **Method**

A serial dilution of the protein extracted from cells, 1/75, 1/100 and 1/150 had been prepared in distilled water and had been put in triplicates and standard serial dilution of albumin 40mg/ml, 20mg/ml, 10mg/ml, 5mg/ml and 2.5mg/ml was prepared. In 96-well plate the dilution of standard was put in total volume 150µl in descending order in duplicate with one with only water then the reagents had been mixed as a kit instruction and incubated with the proteins from the cells for 2 hours in 37°C then read in a plate reader for 562nm wave length. After the reading, the amount of protein in each well was determined after the linear regression correction and the accuracy of standard was calculated.

- **Albumin Standard**

BSA (2mg/ml) in 0.9% saline a set of protein standards was prepared from a 2 mg/ml BSA stock solution with the following concentration: 40µg/ml, 20µg/ml, 10µg/ml, 5µg/ml and 2.5µg/ml.

3.12 Statistical analysis

Continuous variables were analysed with t-test or ANOVA. For inter-group comparison, Mann-Whitney-U-test or Kruskal-Walllis test were used for the nonparametric analyses. For correlation spearman test was used. Statistical significance was taken as $P< 0.05$. All statistical analyses were performed using Prism software Version 4 (GraphPad).

Results

4.1 Establishment of HCC animal models

4.1.1 Introduction

Animal models of HCC were established to determine the role of TLRs in HCC. Types of HCC animal models that have been used are as follows:

a) Chemical-induced models of HCC

Many chemical carcinogens have been used to develop HCC models including: Carbon tetrachloride, diethynitrosamine, acetylaminoflurane and nitrosomorpholine. Natural substances such as aflatoxin, pyrrolizide and safrole have also been used **(**Heindryckx et al., 2009). These substances have been administered orally by mixing with food or drinking water or via intraperitoneal injection.

b) Viral-induced Models of HCC

Previous studies have used HBV, HCV and Woodchuck hepatitis virus to produce HCC related to viral infection. The viral models have been used to test chemoprevention of HCC and evaluation of gene therapy. However, these models take more than 2 years to develop and are associated with considerable expense. Both factors ruled out the possibility of these models for our study (Wu et al., 2009).

c) Transplantable models of HCC & Cholangiocarcinoma

There are two common transplantable models of HCC, syngeneic models and xenograft models. Syngeneic models are created by implantation of rodent cancer cell lines into inbred animal to produce tumours. In these models the immune system is intact. The xenograft models are created by implanting human cancer cells taken directly from a patient (or cultured cell line) into immunodeficient mice (mainly nude mice). The xenograft models have the advantage of perhaps making the model mimic the human tumour behaviour more closely, but the major disadvantage is the absence of the immunologic interaction, which occurs normally between the host and the tumour (Wu et al., 2009).

d) Genetically engineered models of HCC

Genetically engineered models of HCC are highly sophisticated using transgenic mouse technology. These models use immunocompetent animals and have been shown to demonstrate similar pathophysiological features to human cancers. However, they are expensive and substantial time is required for successful tumour development (Heindryckx et al., 2009).

4.1.2 Choice of animal models for exploring our aim

From the above models we decided to develop

a) chemically induced model of HCC for the following reasons:

i. A relatively short period of time is required for tumour induction: typically three months.
ii. Technically simple requiring oral or intraperitoneal administration of an agent.
iii. Relatively inexpensive.

b) Xenograft model

Human cells can be used in this model and therefore the behaviour of any resulting tumours is more likely to be representative of the situation in humans.

Two different models of HCC were established in an attempt to ensure the results obtained from our studies were not model specific. For our purposes, a small animal (such as rats and mice) model was preferable for ease of handling. All experiments were conducted in accordance with local ethical approval and subjected to the complied with the UK's animals' (Scientific Procedures) Act 1986.

4.1.3 DEN & NMOR- induced rat model of HCC

a) Method of establishment

Fischer rats were chosen as the first model as they are well-known for their ability to develop HCC (Yoshino et al., 2005). Thirteen, 5-weeks old male rats were divided into two groups: 1) the carcinogen group (n=7) and 2) the naive group (n=6). All rats were acclimatised for one week before beginning the experiment (standard housing conditions 29-32°C, humidity 60%-65%). From the start of the study, animals were health checked on alternate days including

body weight and drinking water intake to ensure that the carcinogen treated rats were not unduly affected by the administration of the substances.

Rats were injected with diethylnitrosamine (DEN) (100mg/kg) intraperitoneal (IP) on day zero and given nitrosomorpholine (NMOR) 80 PPM in drinking water for a period of 14 weeks. All rats (from carcinogen treated group) underwent an MRI scan at week 10 and week 14. For the MRI, rats were transported to the UCL animal radiology unit and anesthetised with isoflurane. They were then allowed to recover, and after a period of observation they were then returned to their ordinary cages. MRI scanning was conducted using a 9.4 Tesla scanner with a horizontal bore system (Agilent, Varian). MRI settings used were: fast, multi-slice, spin echo with a 1mm slice thickness. Thirty slices were obtained per rat in the coronal orientation. Images were analysed using Amira software 5.3.1. Total liver volume and volume of each nodule were calculated.

One carcinogen group rat was culled at week 10 and the other rats were culled at week 16. Animals were terminated under terminal anaesthesia by isoflurane (inhalation). Livers were collected and fixed in 10%formalin. Four µm liver sections were cut and stained with H&E, reticulin and Sirius red for histopathological evaluation. Smooth muscle actin immunohistochemistry staining was also carried out. (Further details of histology technique are provided in section materials and methods).

b) Results of DEN & NMOR rat model

At the beginning of the experiment, the average weight of the rats was 229.3±10.5 g for carcinogen group and 221-249g in the naive group. At the end of experiment the carcinogenic group weighted 328-353g and the control group 430-478g ($P < 0.01$). In both groups there was an increase body weight, although this was reduced in the carcinogen treated group.

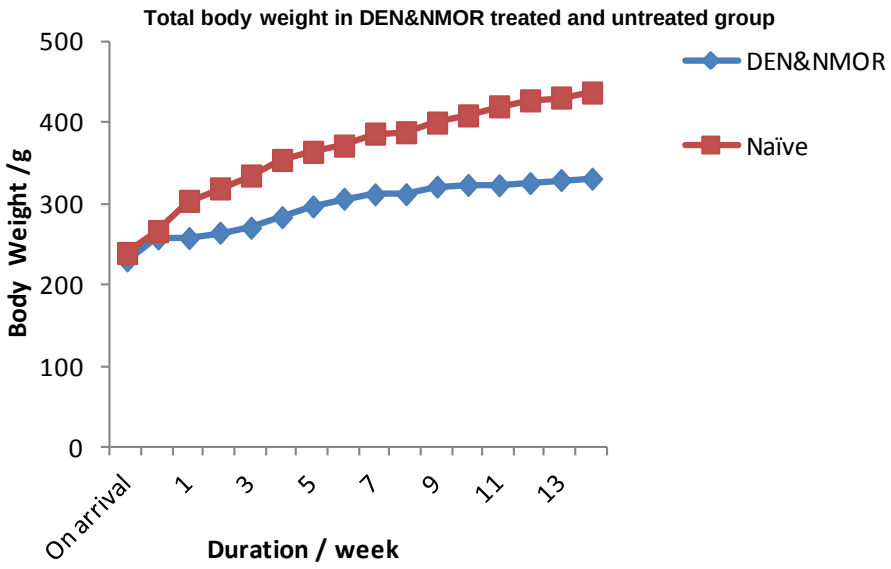

Figure 8: Graph showing increase in the body weight of rats in both groups treated or untreated with DEN and NMOR. The weight of rats treated with DEN and NMOR was lower compared to the naïve untreated rats.

I. Rat liver MRI scans

At week 10, there were small pinhead sized lesions that could not be conclusively classified as tumours. At week 14 multiple nodules of variable sizes (Fig. 9), suggestive of tumour, were identified in all rats in the carcinogen group.

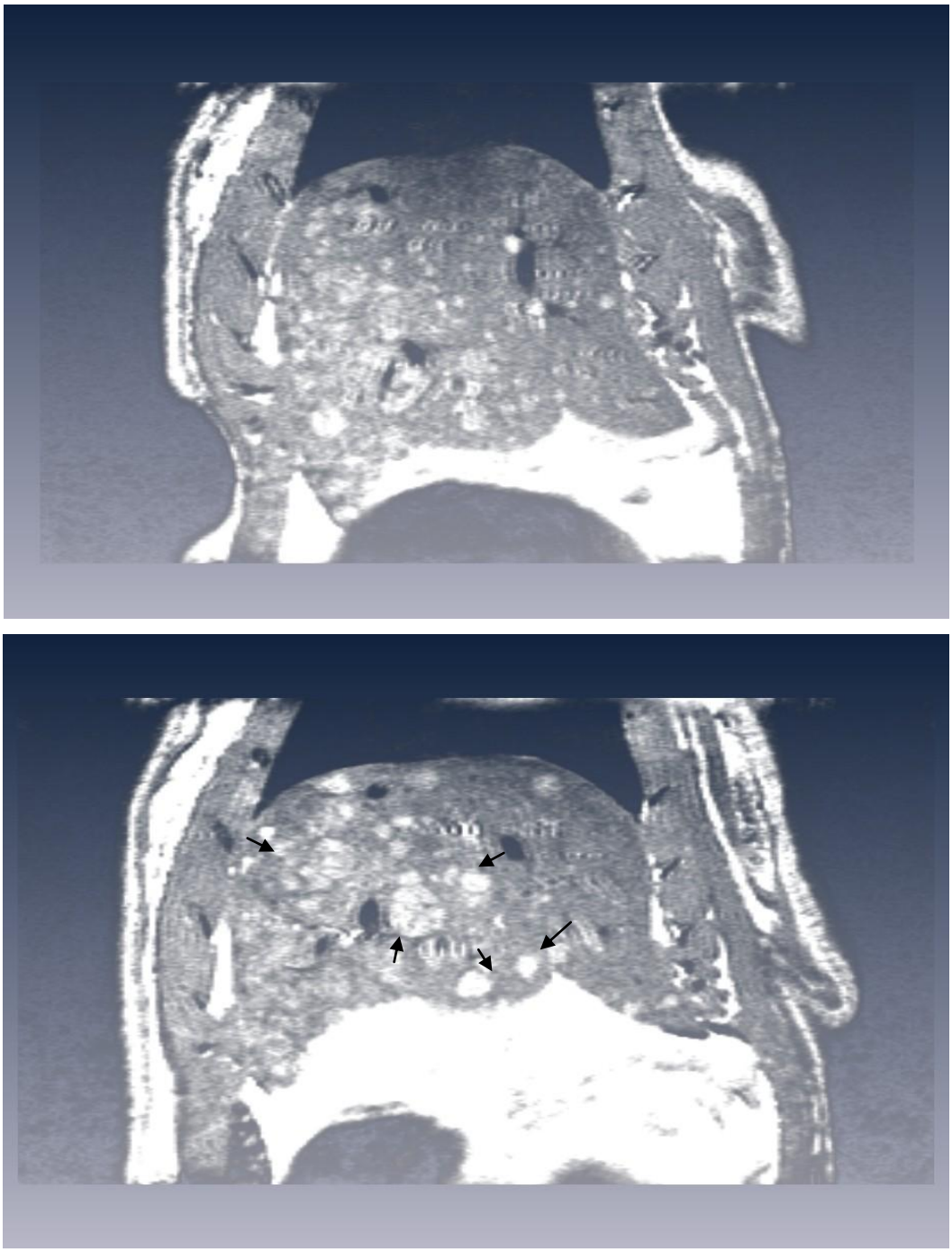

Figure 9: MRI scanning showing liver lesion after 14 weeks treatment with DEN and NMOR. The arrows point to the lesions.

By using Amira software, the total liver volume and total nodule volume were calculated and the percentage of nodule volume relative to total liver volume was estimated as listed in the table (6).

Table 6: Liver lesion volume in rats treated with DEN and NMOR. MRI scan results of DEN and NMOR treated rats showing the total volume of lesion compared to liver volume per rat.

	Liver volume/pixels	Lesion volume/pixels	%
Rat 1	15462.36133	2616.24585	16.92009
Rat 2	12224.68652	1799.691772	14.72178
Rat 3	14481.61719	1471.139038	10.15867
Rat 4	14390.74316	820.014832	5.69821
Rat 5	12694.27246	1324.208862	10.43155
Rat 6	13924.06055	2082.059082	14.95296

II. Histopathology of DEN & NMOR rat livers

Macroscopic appearance rat livers

The livers of rats in carcinogen group were found to be pale in colour and larger in volume (average of 5x4x3 cm), compared to the control group (average of 3.5x3x2 cm). The livers in the carcinogen group were nodular with an irregular surface, and on cut sections showed multiple pale nodules (Fig. 10). In the control group, all the animals had normal livers; a bright red glossy colour with a smooth outer surface, cut section shows homogenous liver tissue without any nodules (Fig. 10).

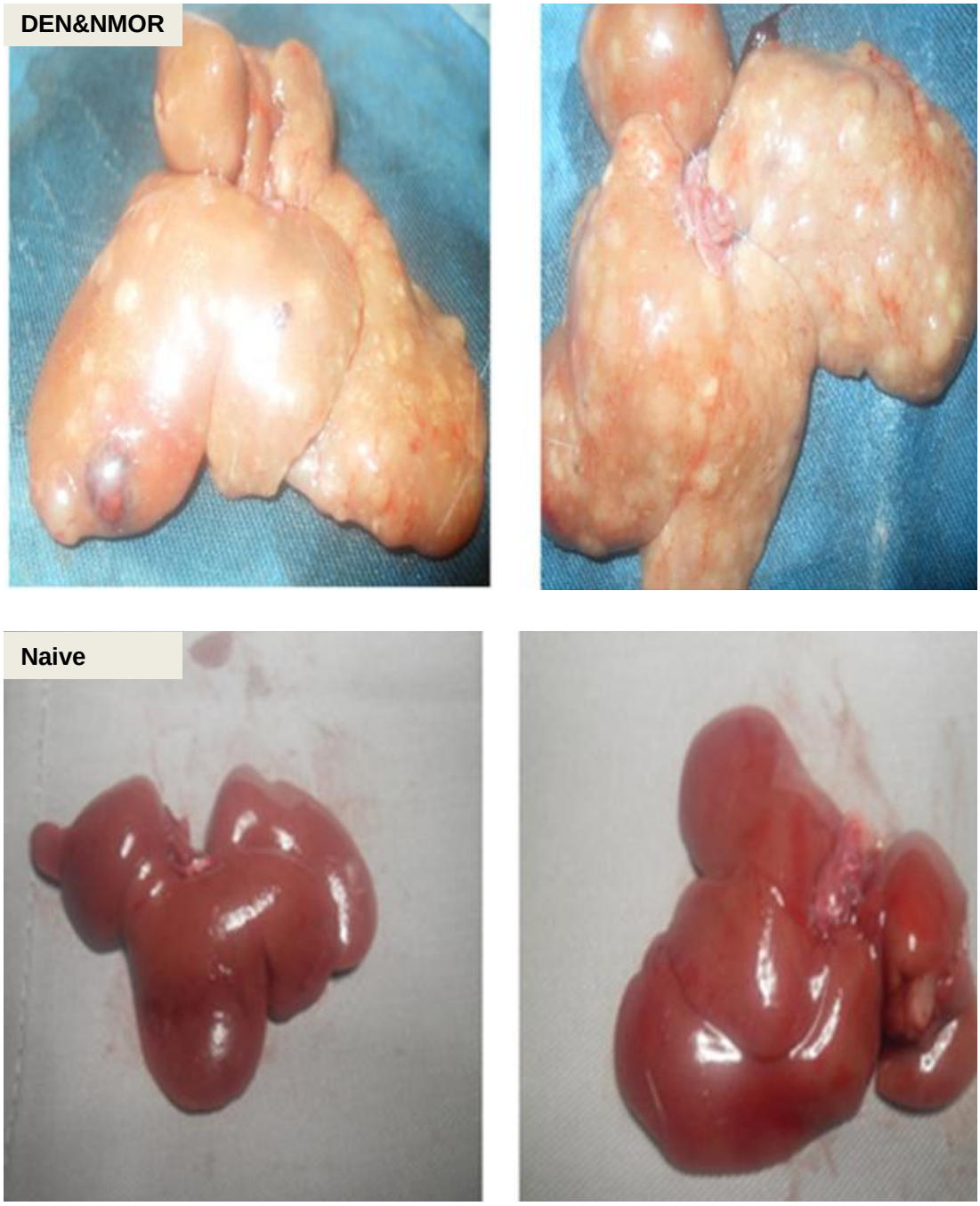

Figure 10: Macroscopic picture of livers obtained from DEN and NMOR treated and untreated rats. Livers of treated rats demonstrate multinodular irregular outer surface and pale colour, while livers from naive group demonstrate bright red smooth outer surface.

Microscopic appearance of rat livers

- **Haematoxylin & Eosin staining**

Two independent pathologists assessed and graded slides from the livers of all rats. Liver from one animal that was culled at week ten demonstrated high-grade dysplasia (atypical polygonal large cells with large nucleus and prominent nucleoli). The non-tumourous background showed an inflammatory cell infiltrate, with bridging necrosis and fibrosis. In addition, there were small foci indicative of HCC showing small compact cells with hyperchromatic nuclei (Fig. 11).

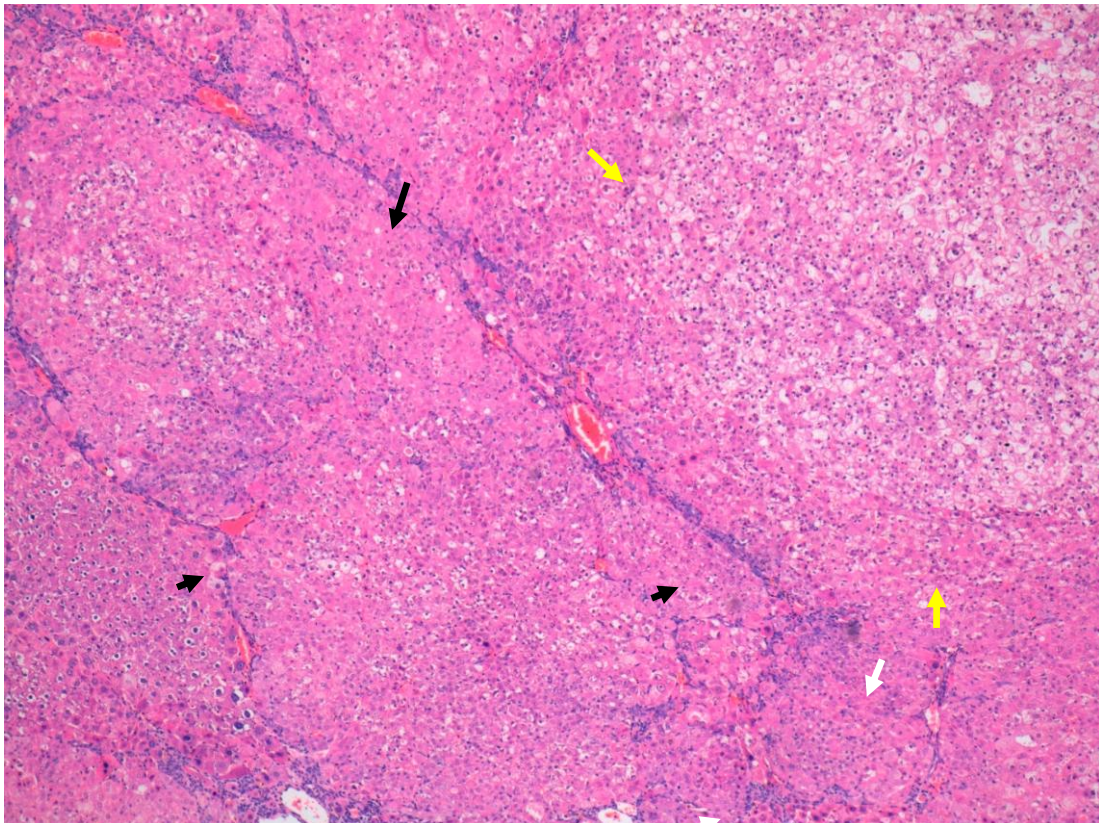

Figure 11: Histopathologic changes in rat liver treated with DEN and NMOR for 10 weeks showing dysplasia and inflammation. Areas of severe inflammation (black arrows) and high-grade dysplasia (yellow arrows) with foci suspicious of HCC (white arrow).

After 16 weeks, all the livers of rats treated with DEN and NMOR developed severe inflammation, necro-inflammatory foci, bridging necrosis (moderate to severe) and multiple scattered dysplastic nodules, which together formed the background for multiple foci of HCC. The hepatocytes inside these foci showed

frequent abnormal mitosis, increased nucleo-cytoplasmic ratio and irregular nuclear membranes which provided further support that these represented HCC foci. The tumour grade ranged from well differentiated to poorly differentiated HCC. Five out of six developed moderate to poorly differentiated HCC and severe inflammation. One animal developed well-differentiated HCC. All the animals developed fibrosis, which was confirmed with reticulin staining.

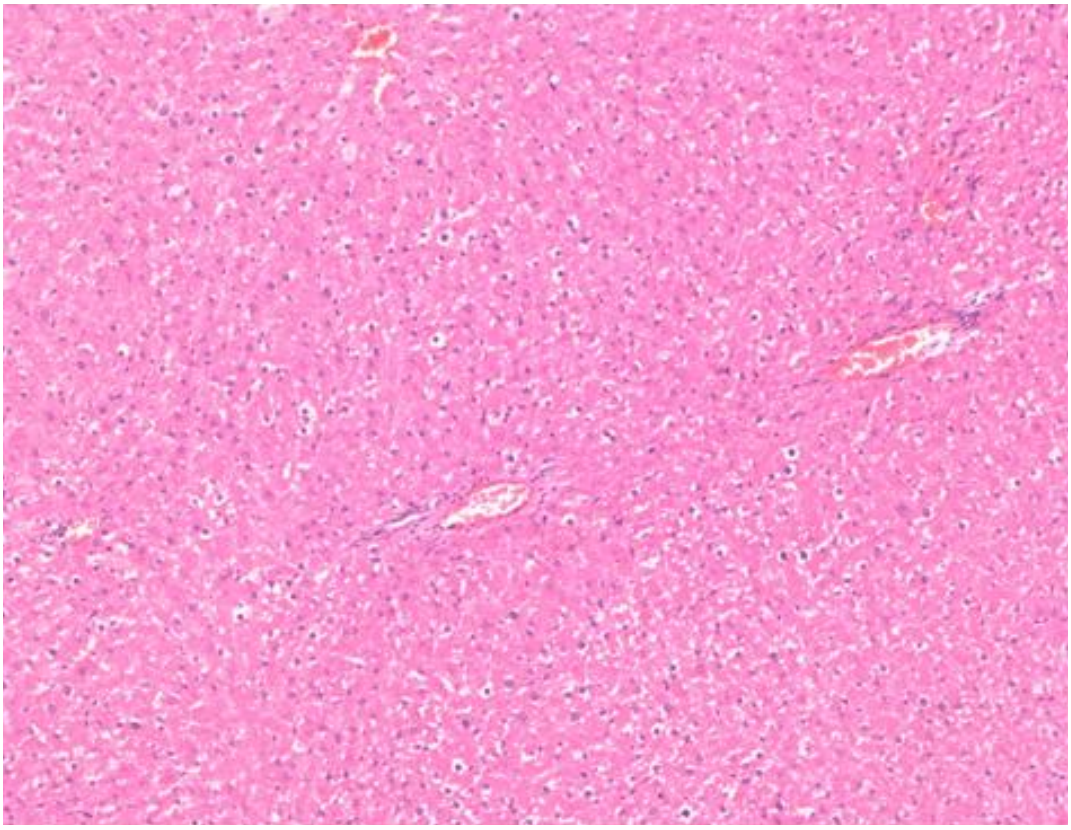

Figure 12: Microscopic picture of normal rat liver showing the central vein and hepatocytes radiating around with no inflammation or atypical cells.

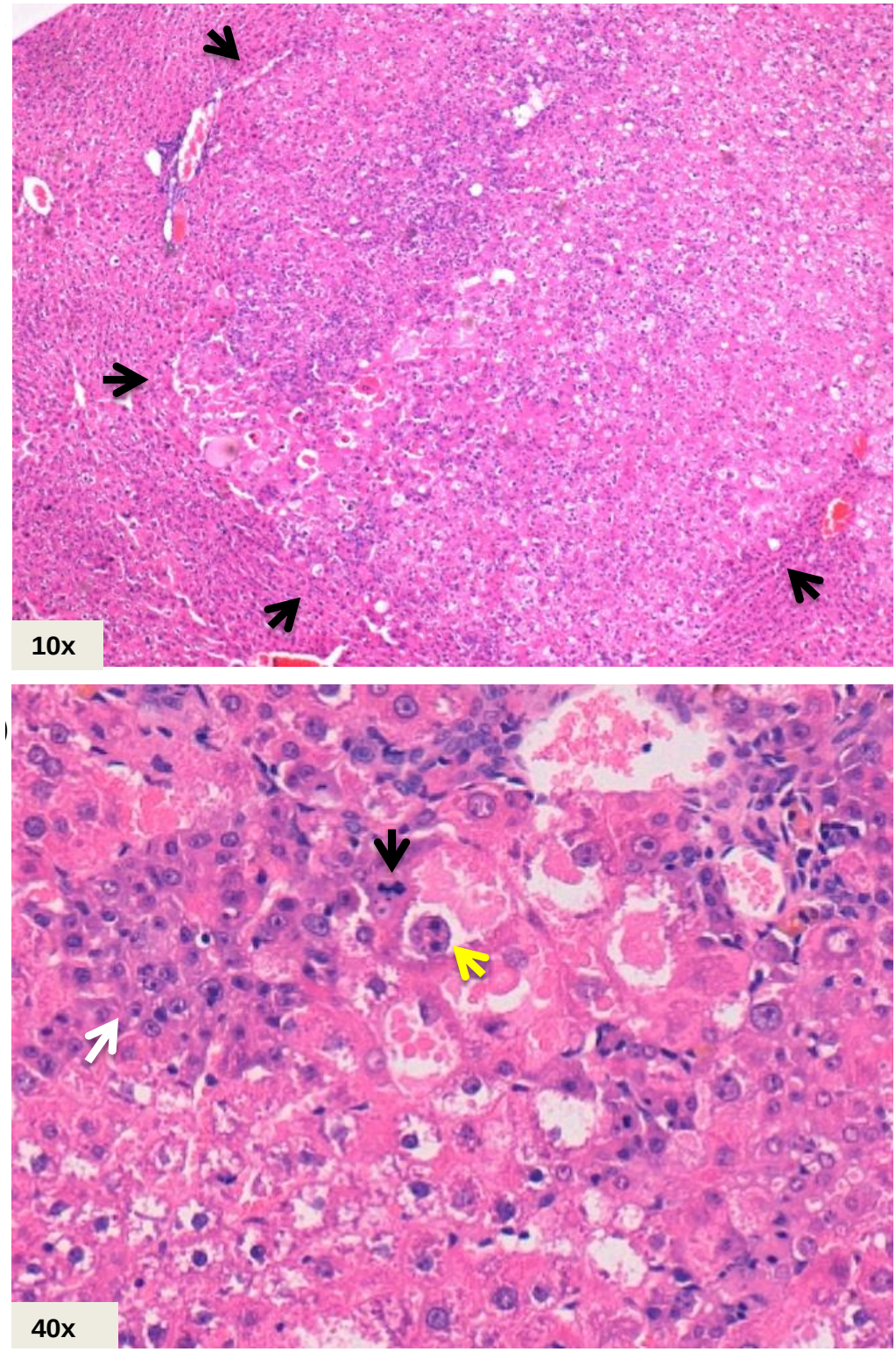

Figure 13: Microscopic picture of liver section derived from DEN and NMOR treated rats for 14 weeks: 10x magnification showed nodules of atypical cells, the black arrows point to the nodules. 40x magnification showed atypical cells within the nodules. There was small cell dysplasia (white arrow), pleomorphism of the cells with prominent nucleoli and other cells had two nucleoli (yellow arrow). There were also abnormal mitoses (black arrow) suggesting that this is a malignant nodule (HCC).

- **Smooth muscle actin staining (SMA)**

Immunohistochemical analysis of liver sections stained with SMA antibody (shown in brown colour) in all blood vessel walls. It was also found also within the foci identified as HCC providing additional confirmation of tumourigenesis as it stained the newly formed blood vessles within the tumour (Fig. 14).

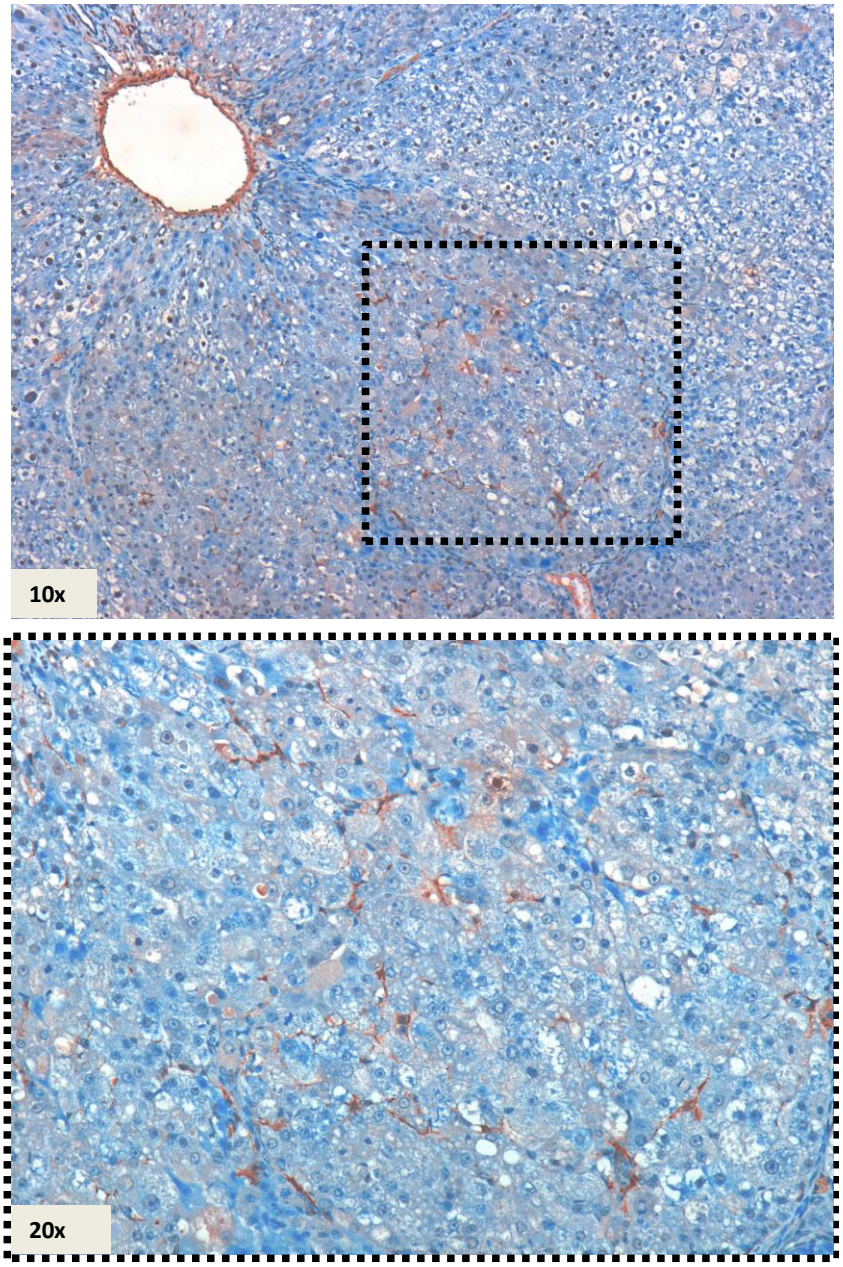

Figure 14: immunohistochemistry of smooth muscle actin (SMA) 10x magnification showed brown staining in the smooth muscle in the wall of blood vessels and the smooth muscle in the new blood vessels in the tumour mass. 20x showing the SMA staining in the tumour.

- **Reticulin & Sirius red staining**

The DEN and NMOR treated rats developed liver fibrosis which was detected by silver stain (black colour) with reticulin or Sirius red. The fibrosis varied from 3/6-5/6 grade depending on Ishak criteria listed page (28). The fibrosis in the carcinogen treated group varied from bridging fibrosis, portal to portal and in some cases it was found to be portal to central. Bridging fibrosis reached the level of incomplete cirrhosis where the fibrous bands formed incomplete nodules (Fig. 15). However, the livers in the control group did not show any evidence of fibrosis.

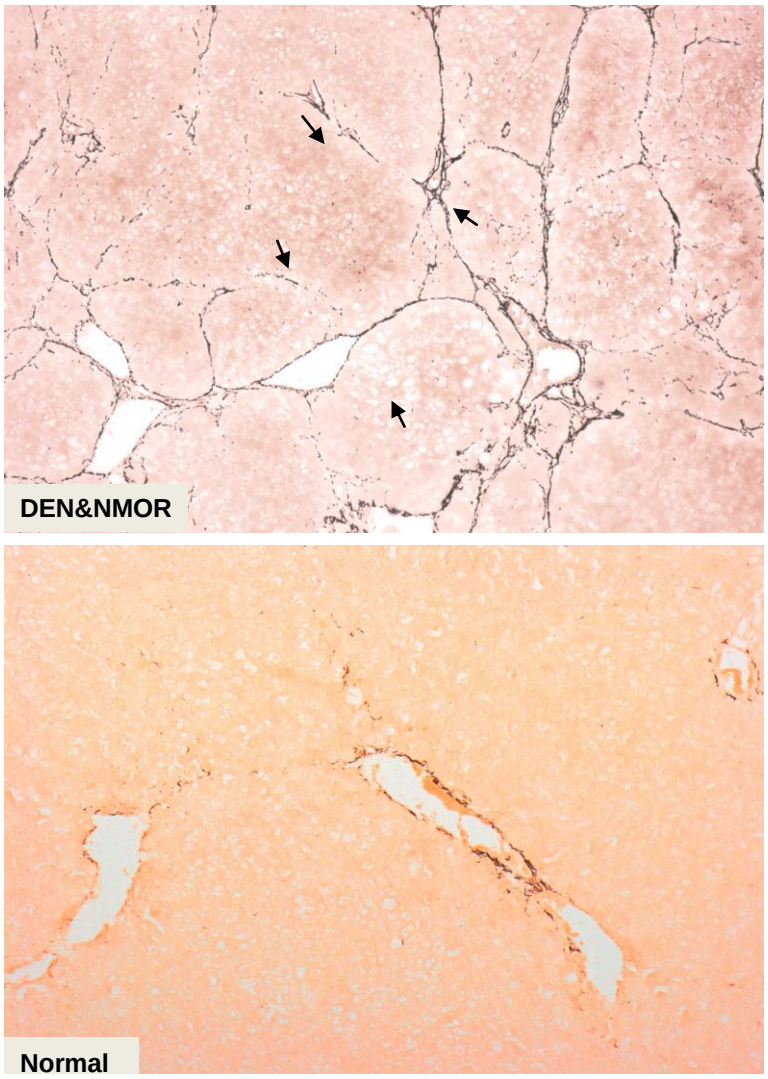

Figure 15: Reticulin staining of liver section obtained from naïve (normal) and DEN & NMOR treated rat showing silver staining around blood vessels and fibrous band of pre-cirrhotic stage of liver with incomplete nodules and in normal liver the silver staining is around the blood vessels only.

Sirius red staining also confirmed fibrosis. Livers obtained from the carcinogen group showed evidence of severe fibrosis (Fig. 16).

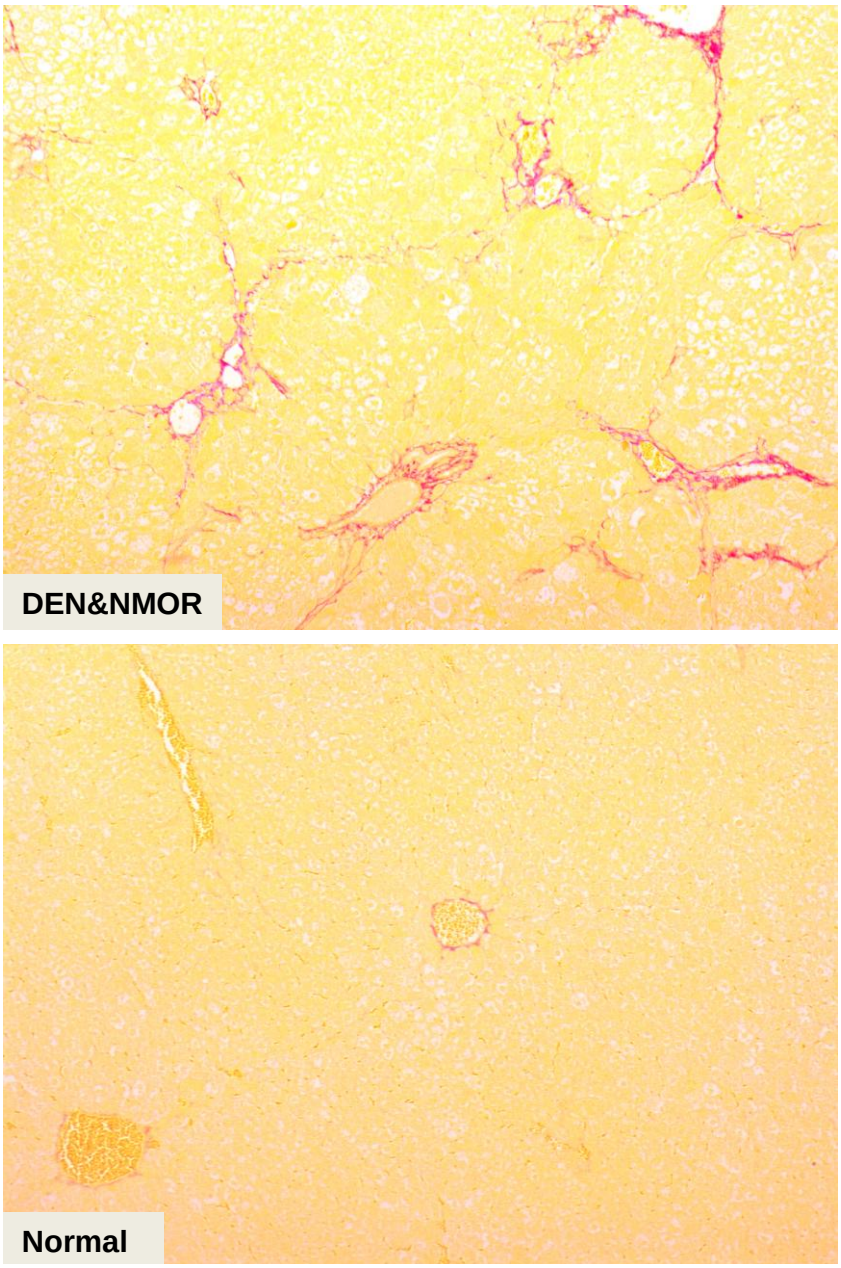

Figure 16: Sirius red staining of liver section obtained from Naive (normal) and DEN & NMOR treated rats. It stained the collagen in the wall of blood vessels and fibrous tissue red. Liver section obtained from normal and DEN&NMOR treated rats showed multiple red stained fibrous septa, which tended to form nodules with DEN&NMOR treatment and only red staining around blood vessels in normal liver.

4.1.4 Xenograft mouse model of HCC

a) Method of Establishment

Scatton and colleagues established the xenograft model in seven to eight week old male NOD-SCID mice (Scatton et al., 2008). The value of choosing this type of mouse is that they have severe combined immunodeficiency and therefore the injected cells in the liver are not exposed to repeat cycles of inflammation which can lead to cell rejection. The human cell lines used (HuH7, HepG2 and HuCCT1) were injected intrahepatically following visualisation via a small laparotomy with five million cells in 100µl of saline of either HuH7 or HepG2 (hepatocellular carcinoma cell lines) HuCCT1 (cholangiocarcinoma cell-line) underneath the Glisson's capsule. The procedure was performed under general anaesthesia using sterile conditions, with the laparotomy closed using absorbable suture (Vicryl, Johnsosn and Johnson). The animals were allowed to recover, before being returned to the housing rooms in independently ventilated cages for the duration of the study. Blood and tissue samples were collected under terminal anaesthesia.

Mice were injected intrahepatically with either HuH7 (n=7) or HepG2 (n=5) or HuCCT1 (n=7). For HepG2 and HuCCT1 cells it took about approximately 60 days (study protocol duration) to develop a tumour nodule, while proliferation with HuH7 was noticeably faster and at 60 days these animals often developed a massive tumour that would lead to the animal having impairment in its movement with some mice dying before the protocol study period was complete. In consideration of this the end-point for the HuH7 injected mice was revised to 35 days. With the HCC cell lines, it was found that there was a tumour in the liver and another mass was usually found outside the liver attached to the muscle wall over the site of cell injection, which could be explained as leakage from the injection site. With HuCCT1 cells, even though the cells were injected intrahepatically, there was no tumour found inside the liver but instead the tumour nodule found was outside the liver attached to the muscle of the abdominal wall. The tumour size was calculated by multiplying the three dimensions of the mass.

b) Results of mouse xenograft models

I. HuH7 derived tumour characteristics

The HuH7 cells derived tumour characterised by its rapid proliferation and the masses formed inside and outside the liver. The masses developed inside the liver were lobulated outer surface and the cut sections showed areas of necrosis and haemorrhage, which increased proportionally with the tumour volume. The average volume of these tumours varied from 0.2 cm^3 to 3 cm^3 (Table 3). However, there were two cases in which the tumour developed outside the liver and there was no lesion within the liver. These masses were similar macroscopically and microscopically to the tumour cells inside the liver (Fig. 17). The volume of these tumours varied from a mean of 2.3±0.5 cm^3 and only one animal developed tumour within the liver only without any extra-hepatic masses.

Table 7: 3 HuH7 derived tumour volumes in NOD-SCID mice

HuH7 derived tumour volume (cm^3)		
Intra-hepatic mass	**Extra-hepatic mass**	**Total mass volume**
0.62	0.6	1.22
0.5	3.6	4.1
0.26	1.26	1.52
0	0.5	0.5
3	0.05	3.05
2.4	0	2.4
0	3.38	3.38

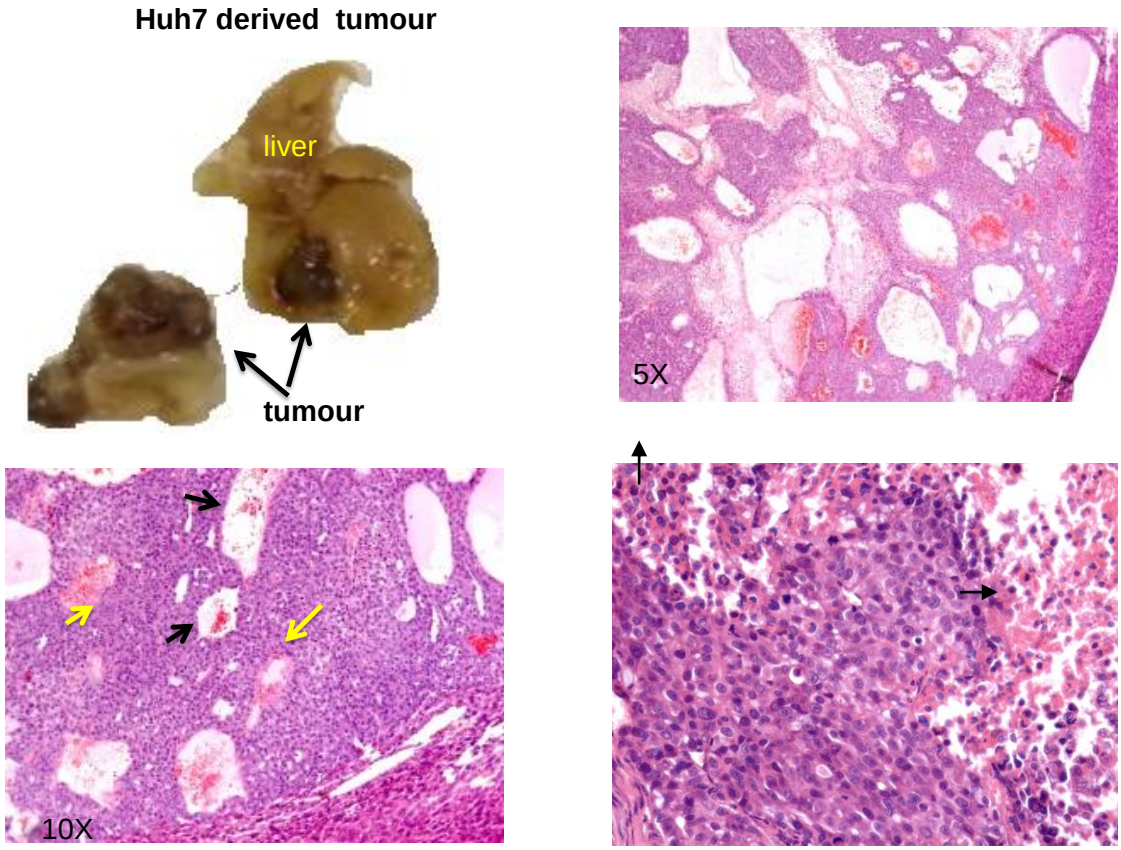

Figure 17: Macroscopic and microscopic picture of HuH7 derived tumour. The tumour was formed inside and outside the liver. The microscopic picture 5x shows the tumour (blue lesion). 10x shows areas of haemorrhage (black arrows) and areas of necrosis (yellow arrows). 40x shows HCC cells and areas of necrosis (black arrows).

II. HepG2 derived tumour characteristics

HepG2 cells derived tumours also formed inside and outside the liver. It was characterised by its slower rate in progression compared to HuH7. The masses that developed inside the liver were distinct from the surrounding tissue and the cut sections showed areas of necrosis and haemorrhage. The tumour volume of these tumours varied from a mean of 2.0±0.7 cm^3 (Table 4). The extra-hepatic masses were similar macroscopically and microscopically to the tumour cells inside the liver (Fig. 18) and they attached to the muscle of the anterior abdominal wall. The volume of these tumours varied from 0.1 cm^3 to 2.4 cm^3.

Table 8: HepG2 derived tumour volumes in NOD-SCID mice

HepG2 derived tumour volume (cm^3)		
Intra-hepatic masses	**Extra-hepatic masses**	**total masses volume**
0.69	0.675	1.365
1.4	0.18	1.58
0.125	0.375	0.5
1.152	2.4	3.552
1.575	2.4	3.975

HepG2 derived tumour

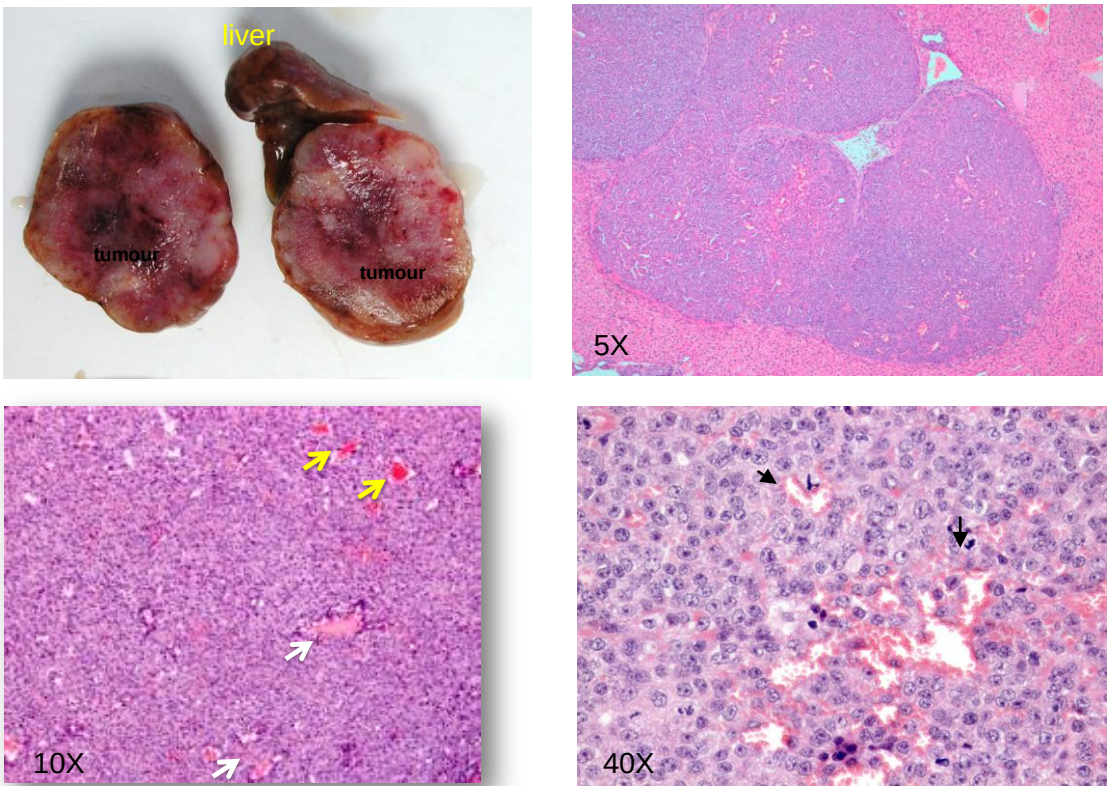

Figure 18: Macroscopic and microscopic picture of HepG2 derived tumour. The mass was formed inside the liver and compressed the surrounding liver tissue. The microscopic picture 5x magnification revealed dark blue cells surrounded by normal liver. 10x showed area of haemorrhage (yellow arrows) and areas of necrosis (white arrows). 40x showed malignant cells with prominent nuclei and frequent abnormal mitosis (black arrows).

III. HuCCT1 derived tumour characteristics

The main aim of developing this type of tumour was to study cholangiocarcinoma, which is a primary liver cancer. This tumour was different from the previous type of HCC cells induced tumour. All the tumour masses were formed outside the liver and nothing was found within the liver tissue. This tumour had different phenotype macroscopically to the other models. This tumour was white in colour, rounded and had a smooth outer surface. The cut section did not show any haemorrhage or necrosis (Fig. 19). HuCCT1 derived tumour was attached to the anterior abdominal wall muscle as well. The volume of this tumour varied from 1 cm^3 to 1.95 cm^3 (Table 9).

Table 9: HuCCT1 derived tumour volumes in NOD-SCID mice

HuCCT1 derived tumour volume (cm^3)
1.44
1.95
1.10
1.44
1.44
1.00
1.10

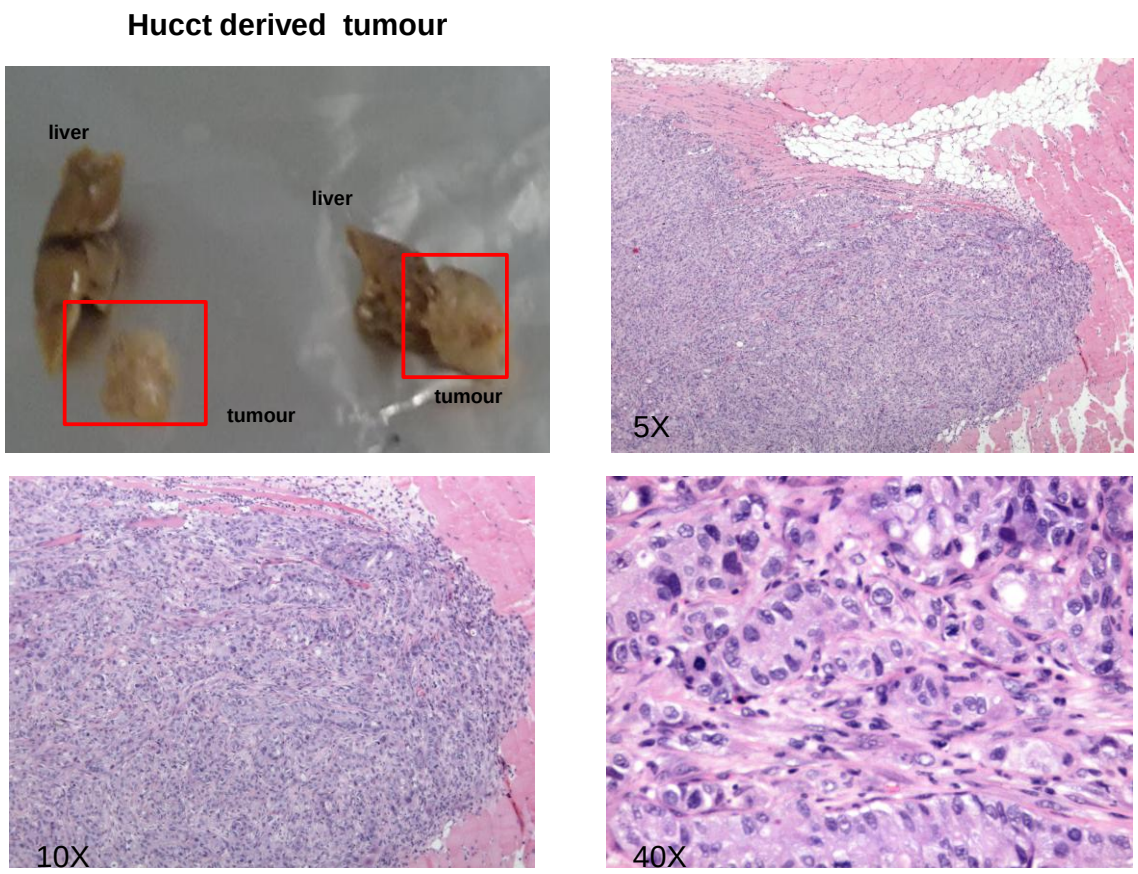

Figure 19: Macroscopic and microscopic picture of HuCCT1 cell derived tumour. The tumours found outside the liver, the red box surrounded the mass. 5x showed the invasion of the tumour to the abdominal muscle wall.10x magnification showed the acinar pattern formation by the cells. 40x magnification revealed malignant epithelial cells with nuclear pleomorphism and prominent nuclei surrounded by stroma consistent with cholangiocarcinoma.

4.1.5 Discussion

There are different types of HCC models, chemical-induced, transplantable, viral and genetically engineered models. The last two types are more expensive and time consuming to develop. In this study, the chemical and transplantable-induced models were established, as they are relatively easy, cheap and quick to develop – approximately 2 to 3 months. In our chemical-induced model, DEN and NMOR treatment was used to induce HCC on a background of fibrosis and inflammation in Fischer rats. Yoshino and colleagues originally developed the use of DEN and NMOR to induce HCC in rats (Yoshino et al., 2005). Following treatment with these drugs the animals were weighed twice weekly for 16 weeks as a means of checking their development and relative health. Their weight was found to increase over time although the rate of weight gain was less than in the control untreated rats. Other than this, the rats appeared normal with no obvious abnormalities. This was taken as an indication that the chemical-induced HCC model was a stable and suitable model for our study.

After 10 weeks of DEN and NMOR treatment the rats were scanned by MRI to look for any tumours in their livers. At this time point only a few pinhead size lesions could be seen in some of the rat livers. After 14 weeks of treatment multiple masses were detectable in all the treated rat livers. The size of these lesions was measured using the Amira software program. The average size of these masses varied from 5 to 16% of the total liver volume. The treatment with DEN and NMOR was stopped after 14 weeks and the rats were culled two weeks later. The livers were harvested from the DEN and NMOR treated rats as well as the control group. The livers of the treated rats were noticeably paler in colour with multiple nodules visible on the outer surface as well as the inner surfaces of the cut liver. There were also areas of haemorrhage within some of the nodules suggesting that these were malignant lesions.

When the H&E stained liver sections from the carcinogen treated rats were examined under a microscope they revealed foci and nodules with cellular atypia, hyperchromatism, increased nucleo-cytoplasmic ratio, prominent nucleoli and abnormal mitotic figures suggestive of HCC. Other changes in the

form of large and small cell dysplasia were also observed in the background liver of the treated animals. In addition, the background liver was severely inflamed.

Histological examination of the liver sections by reticulin and Sirius red staining (of the fibrous bands and collagen) revealed the livers from the treated rats were also fibrotic. According to the Ishak criteria (Ishak et al., 1995) the stage of fibrosis varied from stage 3 (fibrous expansion of most portal areas with occasional portal to portal bridging) to stage 5 (incomplete cirrhosis).

Immunohistochemical analysis of the liver sections with smooth muscle actin (SMA), which stains the blood vessel smooth muscle cells, was used to identify newly formed blood vessels within the liver nodules. SMA staining was therefore useful for distinguishing malignant nodules from nodules formed as a result of incomplete cirrhosis and which contained dysplastic cells.

Successful establishment of the chemically induced HCC model above provided the opportunity to examine the effects of liver inflammation on HCC growth and development. The model was also useful for targeting various molecular pathways, which could play an important role in HCC pathogenesis.

One obvious disadvantage of this chemically-induced HCC model is that it may not be representative of the way that HCC develops in humans. For this reason a second tumour model using human liver cancer cell xenografts was established with the view that these may be more representative of primary liver cancer behaviour in humans. In this case HCC (HuH7 or HepG2) or CC (HuCCT1) cells from established cultures were injected into the sub-capsular area of the right liver lobe of NOD-SCID mice. These mice are immuno-compromised thus reducing the possibility of rejection of the injected cells. The xenografts were initially allowed to establish for 60 days. However, by this time some of the animals injected with the HuH7 died and others developed abdominal masses, which were large enough to prevent the mice from walking. As a result, the experiment with the HuH7 cells was repeated using a fresh

group of NOD-SCID mice but in this case the xenografts were allowed to develop for only 35 days in total.

At the end of the 60 day period the animals injected with HepG2 and HuCCT1 were culled and their livers harvested. In the case of the HuCCT1 injected animals no tumours were detected in the liver but instead tumours were observed attached to the anterior abdominal wall. This unexpected result could be due to the fact that these cells derived from bile duct cancer cells, which may prefer to grow outside the liver. Fava and colleagues developed a xenograft cholangiocarcinoma mice model outside the liver. However, they used different types of cells such as SV40-transformed normal human cholangiocytes and Mz-ChA-1cell lines (Fava et al., 2009).

In the case of mice injected with HCC lines, Huh 7 or HepG2, the cancer cells formed intra-hepatic tumours and in some cases small nodules were found outside the liver attached to the muscle of the anterior abdominal wall. Their exact location was in the midline with some shifting toward the right hypochondrium. The extra-hepatic masses may have arisen as a result of leakage from the site of cell injection or as a result of tumour invasion. The mean volume of the HuH7, HepG2 and HuCCT1 derived tumours was found to be 2.3 ± 0.5cm^3, 2.0 ± 0.7 cm^3 and 1.45 ±0.5 cm^3 respectively. H&E analysis of tumour sections derived from the HepG2 and HuH7 injected animals revealed the tumour histology had the criteria of HCC i.e. polygonal cells, hyperchromatic nuclei, prominent nucleoli and abnormal mitotic figures. In addition, there were areas of haemorrhage and necrosis. Histological analysis of the HuCCT1 derived tumours had all the hallmarks of cholangiocarcinoma; sheets of cuboidal cells within a stromal background, the cuboidal cells showing increased nucleo-cytoplasmic ratio and nuclear hyperchromatism with lots of abnormal mitotic figures scattered within the tumour.

As well as being more representative of the situation in humans, establishment of the tumour xenograft models enabled us to study the effects of inhibiting particular cell receptors, which were up regulated in primary human liver cancers.

One of the disadvantages of the xenograft model was the complicated surgical procedure needed to inject the cancer cells into the livers and the high rates of animal mortality incurred during or shortly after surgery. Another disadvantage with this model is that the tumour environment in an immunocompromised animal is very different from that of a normal animal. It is well established that tumourigenesis is an integrated process whereby the interactions between tumour and immune system can have a significant effect on tumour behaviour (Igney and Krammer, 2002).

Challenges of establishing xenograft models and lessons learnt:

One of the biggest hurdles in establishing the xenograft models was trying to avoid the high mortality rate associated with the NOD-SCID mice. These animals are extremely fragile and many died either during or shortly after the surgical interventions. Some expired in response to administration of anaesthetic only whilst others arrested a few seconds following intra-hepatic injection of cells. In order to reduce the number of deaths occurring during surgery the latter was carried out by one individual who was highly skilled with operating on mice. The surgical procedures were conducted in a highly sterile environment,: The anaesthetic chamber and surgical table were all thoroughly cleaned by spraying with 70% ethanol and wiping with clean tissue prior to any surgery; the floor and walls in the area surrounding the surgical table were also cleaned with 70 % ethanol and all surgical instruments were cleaned and sterilized by autoclaving prior to use. The high mortality rate associated with the NOD-SCID mice often meant that the number of viable animals at the end of some experiments was smaller than initially planned. As a precaution any experiment involving NOD-SCID mice should begin with a larger number of animals than is actually required in order to take such losses into account.

4.2 Effect of gut decontamination on HCC pathogenesis

4.2.1 Introduction

Several studies have suggested that increased gut permeability in the presence of chronic liver disease maintain a state of enhanced and continuous exposure of the liver to pathogen associated molecular patterns (PAMPs) (Mencin et al., 2009). This may form the basis for the persistent activation of TLR-MyD88-TRAF6- NF-κB system, which in turn leads to chronic liver inflammation and development of HCC. NF-κB was linked to inflammation-fibrosis-carcinoma sequence (ElSharkawy and Mann, 2007). Particularly, TLR4 has been a target for therapy in chronic liver disease and fibrosis (Soares et al., 2010). As inflammation and fibrosis was found to be a hallmark in the development of HCC and gut sterilization inhibited the development of liver fibrosis (Rakoff-Nahoum et al., 2004 and Seki et al., 2007), I decided to study the effect of gut decontamination on chronic inflammation and development of HCC in DEN&NMOR rodent model of HCC. The aims of this study were to reduce bacterial translocation using the antibiotic Norfloxacin and monitor the effect on HCC development.

4.2.2 Gut decontamination using Norfloxacin in rat model of HCC

I. Method

Three groups of 6 rats each were used for this experiment:

i. The first group of rats were treated with the carcinogens DEN&NMOR for 14 weeks in order to induce HCC as previously described in chapter 4.1.

ii. A second group DEN & NMOR treated rats were also given Norfloxacin treatment by gavage at a dose of 20mg/kg/day in two divided doses for 14 weeks.

iii. A third group of naïve rats were used as controls.

II. Results of Gut Decontamination

Histopathology of livers from Norfloxacin treated rats

a) Macroscopic appearance of rat livers

The animals in each group were terminated at the end of experiment under terminal anaesthesia. The livers of rats treated with DEN&NMOR were pale in colour, bigger in size (around 5x4x3 cm), and nodular in character with irregular surfaces, and on cut section showed multiple nodules, which were even paler than the surrounding tissue. In the group treated with Norfloxacin in additon to DEN&NMOR the livers were much brighter and red in colour with smoother outer surfaces, and measured smaller (around 4x3.5x2 cm). The cut section of the liver in both groups showed nodules, which were paler than the surrounding tissue. In the naive group, all animals had normal bright red glossy livers with smooth outer surfaces and around 3.5x3x2 cm, cut section showing homogenous liver parenchyma devoid of nodules.

Figure 20: Macroscopic appearance of livers from DEN & NMOR rat models of HCC in the presence or absence of Norfloxacin treatment. The liver from the rat without Norfloxacin treatment is pale with an irregular outer surface and multiple nodules. The liver from the Norfloxacin-treated rat is brighter and less nodular in appearance.

b) Microscopic appearance of rat livers

- **Haematoxylin & Eosin staining**

Following Haematoxylin and Eosin staining, two independent pathologists examined the slides under light microscopy.

All animals in the DEN&NMOR group; developed severe inflammation, apoptosis, bridging necrosis (moderate to severe) and multiple scattered dysplastic nodules with multiple foci of HCC. The presence of HCC was confirmed by the presence in these foci of frequent abnormal mitosis, increase in the nucleo-cytoplasmic ratio and irregular nuclear membrane. The tumour grade ranged from well differentiated to poorly differentiated HCC, and in addition, all the animals developed severe fibrotic changes, which were confirmed with reticulin staining.

In the Norfloxacin, treated group the liver tissue showed less inflammation and only the severity of fibrosis was mild to moderate. HCC in all the animals were well-differentiated except in one rat in this group where there was only evidence of a very early grade of HCC, considered high-grade dysplasia.

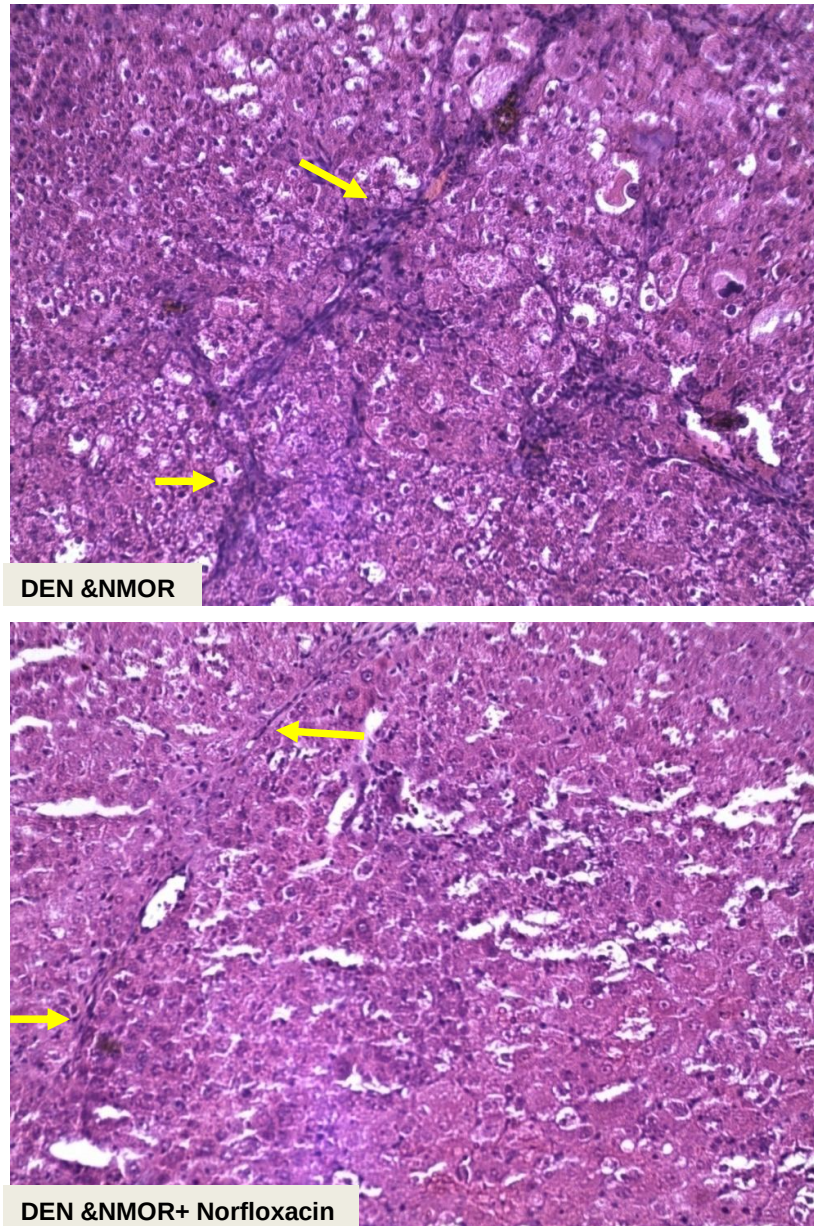

Figure 21: H&E stained liver sections from DEN&NMOR rat models of HCC in the presence or absence of Norfloxacin treatment. Yellow arrows point to areas of inflammation. Without Norfloxacin treatment, the liver inflammation is severe. With Norfloxacin treatment, the liver inflammation is minimal.

- **Evaluation of liver inflammation & fibrosis with Norfloxacin treatment using reticulin staining**

In DEN and NMOR group all the rats developed inflammation and liver fibrosis ranging from grade 3/6 and 5/6 according to Ishak criteria, while in the Norfloxacin treated group there was minimal inflammation in the liver. The degree of fibrosis varied from 0/6 to 2/6, and did not exceed 2, suggesting a significant reduction in the development of fibrosis with Norfloxacin treatment ($P < 0.04$).

Table 10: Pathological differences in fibrosis and tumour development between rats treated with DEN&NMOR±Norfloxacin

Rat No	DEN&NMOR	DEN&NMOR+Norfloxacin
1	Incomplete cirrhosis, 5/6 fibrosis, multifocal poorly differentiated HCC	Fibrosis grade 1/6, well differentiated HCC
2	Fibrosis 4/6 , Foci of HCC	Fibrosis 2/6, haemorrhagic HCC
3	Fibrosis 5/6, 2 foci of HCC moderately differentiated	Fibrosis 1-2/6, with some dysplastic Changes suggestive of early HCC
4	Fibrosis 4/6, one focal HCC moderately differentiated, and 2 foci well differentiated	Fibrosis 0/6, moderately differentiated HCC
5	Fibrosis 3/6 and moderately differentiated HCC	Fibrosis 0/6, well differentiated HCC
6	Fibrosis 4/6, well differentiated HCC	Fibrosis 1/6, well differentiated HCC

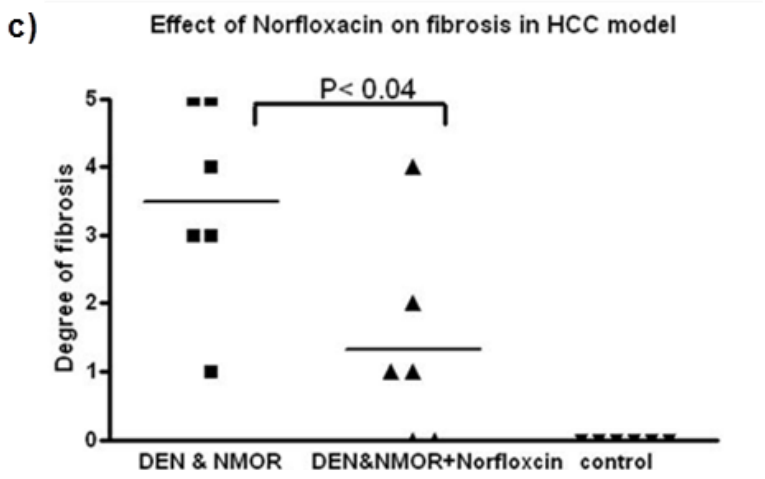

Figure 22: Graph demonstrating degree of liver fibrosis in DEN & NMOR rat models of HCC in the presence or absence of Norfloxacin treatment and in naive rats. The degree of liver fibrosis is significantly lower in the Norfloxacin treated rats compared to that in the livers from the DEN & NMOR only treated rats.

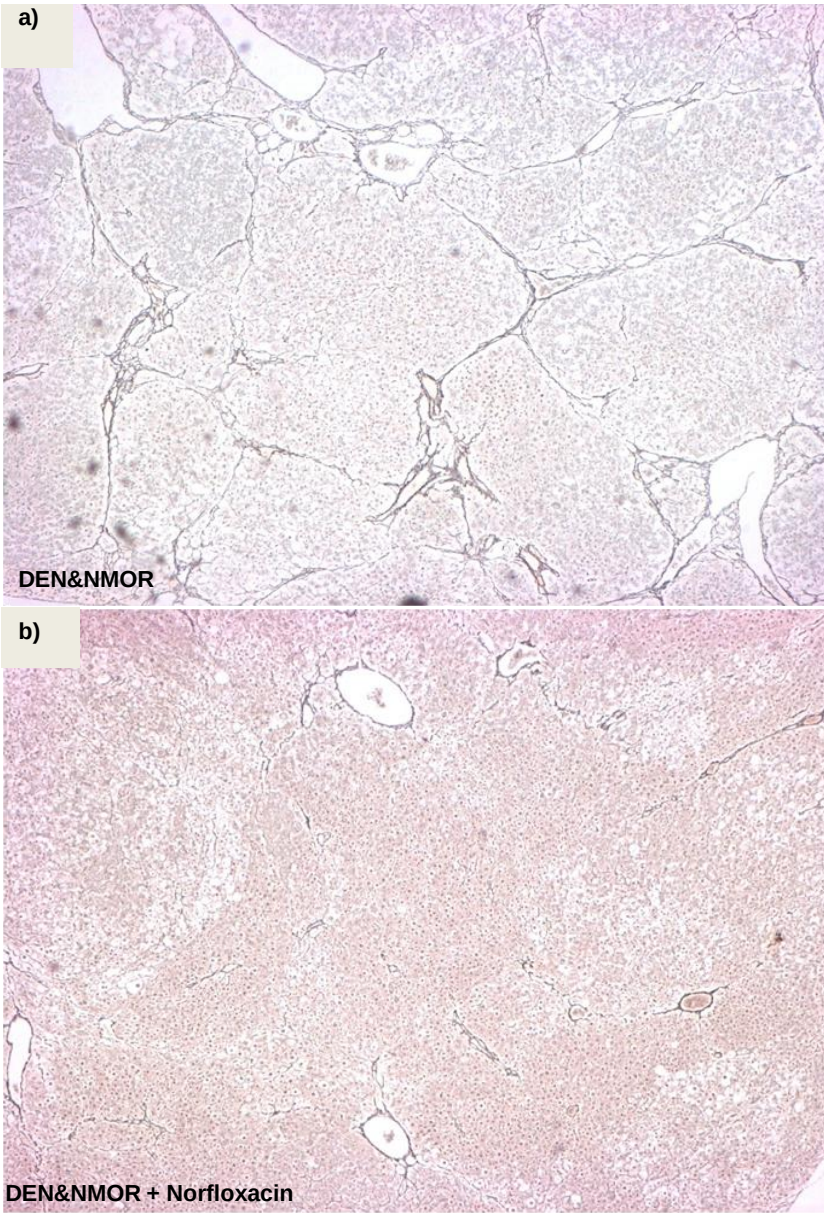

Figure 23: Reticulin staining in livers from DEN&NMOR rat models of HCC in the presence or absence of Norfloxacin treatment. Multiple fibrous bands are visible in the liver of the DEN&NMOR only treated rat. The degree of fibrosis is minimal in the liver of the Norfloxacin treated rat.

4.2.3 Improvement of liver enzymes with Norfloxacin treatment

Serum transaminases, AST and ALT, were measured in all animals (Cobas Integra 400, Roche Diagnostics, Burgess Hill, West Sussex, UK).

ALT and AST (mean ±SE) levels were significantly lower the group treated with Norfloxacin ($P < 0.05$, and $P < 0.01$ respectively)

Table 11: Reduced levels of ALT and AST with Norfloxacin treatment in DEN & NMOR rat models of HCC ($P < 0.05$ for ALT & $P < 0.01$ for AST).

Test	DEN&NMOR U/L	DEN&NMOR+Norfloxacin U/L	Control U/L
ALT	143.4 ±5.1	120.2±4.0	68.4±4.8
AST	142.3±3.17	118.0±1.3	77.1±9.4

4.2.4 Decreased endotoxin levels in response to Norfloxacin treatment

In order to prove a possible connection between the protective effect of Norfloxacin on liver inflammation through its effect on gut decontamination and subsequent reduction in endotoxin (LPS) production, an endotoxin assay was carried out. The plasma levels of endotoxin were measured as (EU/ml). There was a significant reduction in the endotoxin level (P =0.02) with Norfloxacin treatment. No endotoxin was detected in the control group.

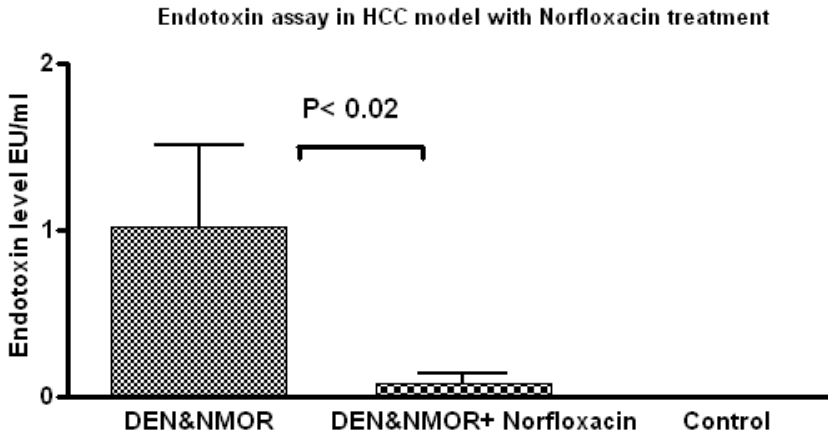

Figure 24: Graph showing endotoxin levels in the DEN & NMOR rat model of HCC in the presence or absence of Norfloxacin treatment. Gut decontamination using Norfloxacin treatment resulted in a significant reduction of endotoxin levels in the DEN&NMOR rat models.

4.2.5 TLR4 expression decreased in rat livers with Norfloxacin treatment.

To determine whether gut decontamination has an effect on the expression of TLR4, immunohistochemistry using TLR4 antibody was performed on liver tissue derived from DEN&NMOR treated rats with and without Norfloxacin treatment. TLR4 was negative in the malignant hepatocytes and was only found positive in the background of HCC. TLR4 expression was strongly positive (Score 2) in the cytoplasm of non-malignant hepatocytes which formed the background in the non-Norfloxacin treated group. In the Norfloxacin treated group, TLR4 expression varied from mild to moderate (Score 1) suggesting down-regulation of TLR4 in the liver following Norfloxacin treatment (Fig. 26).

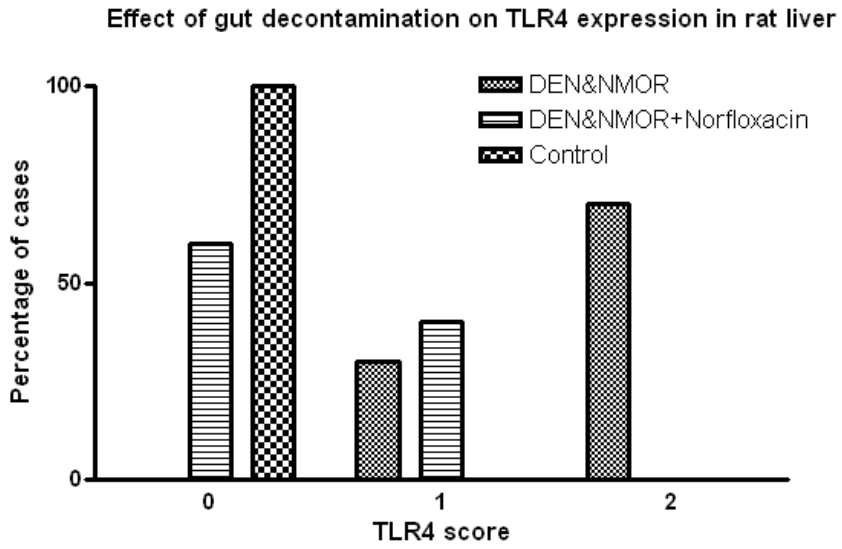

Figure 25: Graph demonstrating reduced TLR4 expression with Norfloxacin treatment in livers from DEN&NMOR rat models of HCC. The TLR4 scores are from non-tumour regions of the liver.

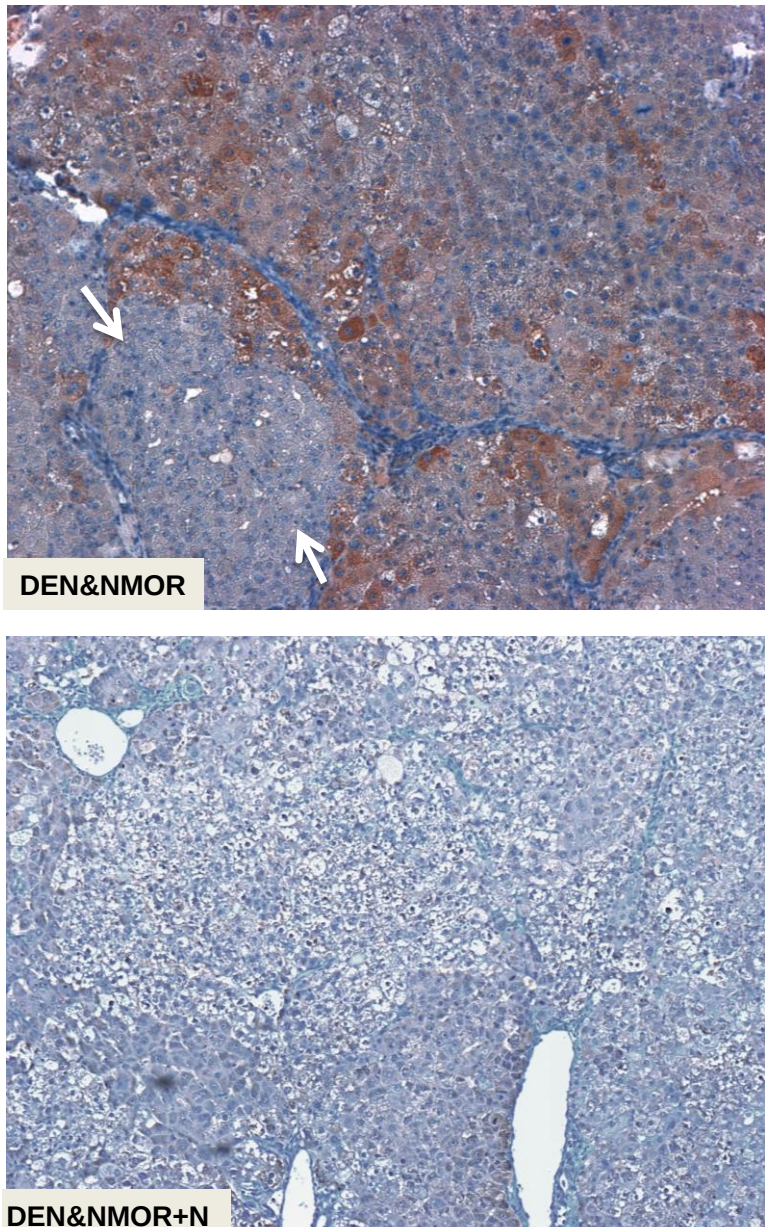

Figure 26: Immunohistochemical analysis of TLR4 expression in livers from DEN & NMOR rat models of HCC in the presence and absence of Norfloxacin treatment. TLR4 is not expressed in malignant hepatocytes (white arrow) but highly expressed in the surrounding background tissue from the liver of the DEN & NMOR treated rat. Very weak expression of TLR4 is seen in the liver of the Norfloxacin treated rat.

4.2.6 NF-κB expression decreased in rat livers with Norfloxacin treatment

Using western blot, an up regulation of NF-κB protein was observed in the liver tissue lysate obtained from the DEN&NMOR induced HCC group without Norfloxacin treatment, which was significantly reduced in the Norfloxacin treated group, (P <0.02).

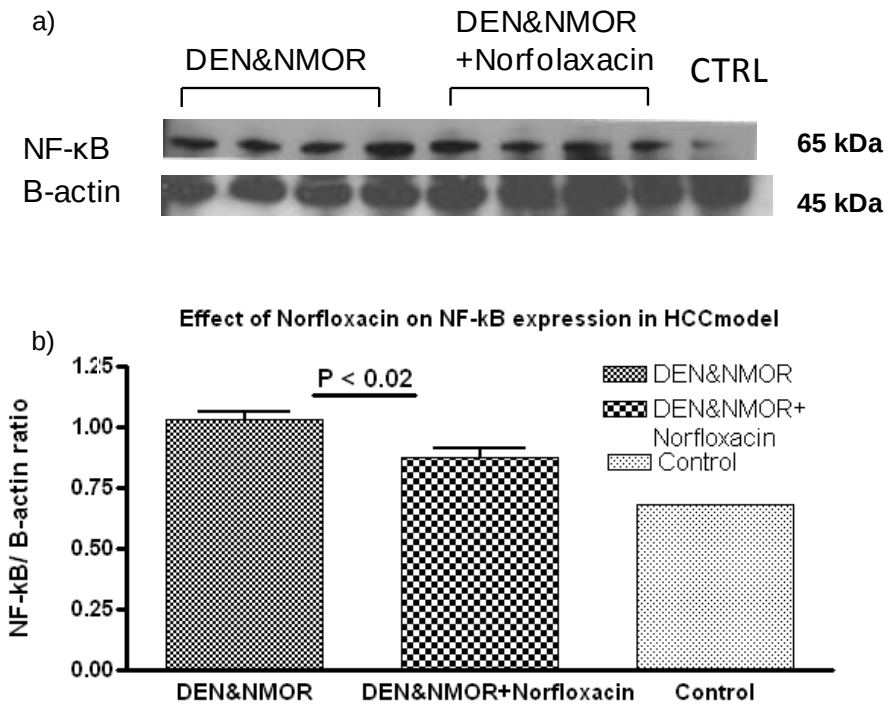

Figure 27: Western blot analysis showing reduced expression of NF-κB with Norfloxacin treatment in livers of DEN & NMOR rat models of HCC. (a) The expression of NF-κB was up regulated in the liver of DEN & NMOR treated rats compared to normal untreated rat liver. However, the levels of NF-κB expression were significantly reduced in the livers of Norfloxacin treated rats compared to those without Norfloxacin treatment (P <0.02). (b) The graph shows the densitometry results from the Western blot expressed as the ratio of NF-κB relative to β-actin signal.

4.2.7 TNF-α expression is not significantly altered in rat livers with Norfloxacin treatment

TNF-α level was measured using ELISA in liver tissue lysate obtained from rats treated with DEN&NMOR ± Norfloxacin. The results were divided by the amount of protein per sample. In DEN and NMOR animals TNF-α level was 193±149.3 pg/1µg protein of liver tissue lysate, which showed slight, statistically non-significant, reduction with Norfloxacin co-treatment; 111.5±63.8 (P =0.783). TNF-α level in the liver of Naïve rat as control was 32.8±7.5.

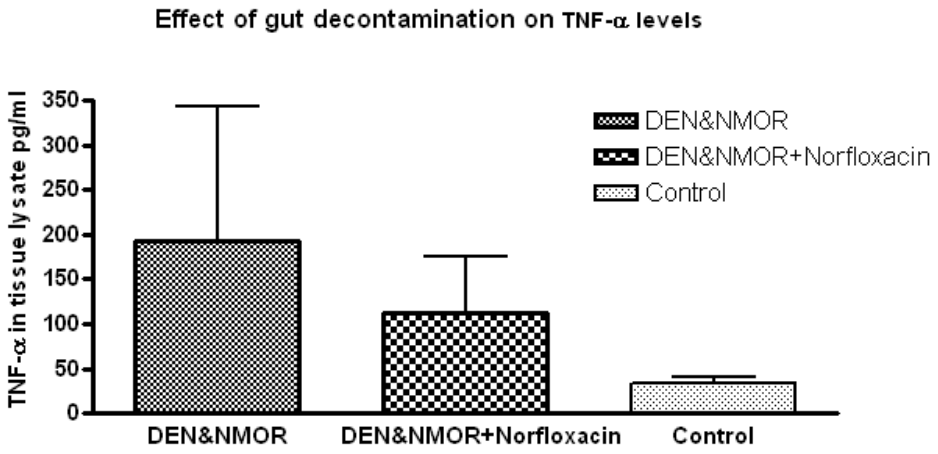

Figure 28: Graph showing levels of hepatic TNF-α in livers of DEN & NMOR rat models of HCC with and without Norfloxacin treatment. TNF-α levels were increased in the livers of DEN & NMOR-treated rats compared to the livers from naïve rats. There was no significant reduction in levels of TNF-α expression in response to Norfloxacin treatment.

4.2.8 Discussion

The idea that a relationship exists between chronic inflammation and cancer was first suggested by Virchow in 1863. Persistent inflammation in chronic liver disease is believed to be the predisposing factor in HCC development (Chen et al., 2008). Persistent inflammation of the liver in these patients is thought to arise from an increased exposure of the liver to pathogens associated molecular patterns (PAMPs) derived from the gut. The translocation of these pathogens from the gut to the liver is a consequence of the increased gut permeability frequently found in patients with chronic liver disease (Bauer et al., 2002). Particularly, the levels of circulating bacterial lipopolysaccharides (LPS) have been reported to be increased in patients with liver cirrhosis (Lin et al., 1995, Chan et al., 1997 and Pinzone et al., 2012). LPS is known to be a stimulator of TLR4 (Fitzgerald et al., 2003). Toll like receptor 4 has been reported to play an important role in liver fibrosis (Seki et al., 2007) and promotion of HCC (Dapito et al., 2012).

Several studies on patients with cirrhosis and in animal models of cirrhosis have shown that decontamination of the gut using antibiotics such as Norfloxacin can lead to a decrease in bacterial translocation from the gut to the liver (Gines et al., 1990, Llovet et al., 1996 and Rabiller et al., 2002). Further studies in humans also demonstrated a reduction in bacterial translocation in response to Norfloxacin treatment (Francés et al., 2008). In addition to these findings a reduction in liver inflammation was also reported with Norfloxacin treatment in rodent models of liver fibrosis (Zhang et al., 2010). However, the effects that gut decontamination might have on HCC development had not been reported prior to our study. I therefore set out to examine the effect of gut decontamination using antibiotics in rat model of HCC. The HCC rat model used in this study had previously been developed in our laboratory (Chapter 4.1). For this particular experiment one group of rats was treated with the antibiotic Norfloxacin for 14 weeks in addition to treatment with the carcinogens DEN and NMOR. A second group of rats was treated with DEN and NMOR only. A third group of control rats which was not given either carcinogens or antibiotics was also included in the study.

The experiment was terminated 16 weeks later as previously described and the livers were immediately removed for examination. There were some obvious differences in the macroscopic appearance of the livers in all 3 groups. The livers from the Norfloxacin and carcinogen treated rats were paler and the surface of the liver was more irregular than livers from the control untreated group of rats. The livers from the rats treated with DEN and NMOR were even paler and more irregular than those from either the control or Norfloxacin with carcinogen treated groups. All rats treated with DEN and NMOR developed multiple tumours regardless Norfloxacin treatment. There were no obvious differences in the number and size of tumours between the two groups macroscopically. However, closer inspection of the tumours histologically revealed some differences in tumour grade between the two different groups. The tumours from the Norfloxacin treated rats were found to be mild to moderately differentiated whilst 5/6 livers from the rats treated with DEN and NMOR also included tumours with poor differentiation. A similar study on the effect of gut sterilization on HCC development was recently reported by Dapito and colleagues. A number of antibiotics (ampicillin, neomycin, metronidazole and vancomycin) were used for gut sterilization in a CCL4-induced mouse model of chronic liver injury and HCC (Dapito et al., 2012). The outcome of this study was a reduction in the number and size of tumours, by 90% and 70% respectively, in the antibiotic treated group of mice. Moreover, TLR4 mutant mice demonstrated less HCC number and size. The authors concluded that the intestinal microbiota could promote HCC progression in chronically injured liver through stimulation of the TLR4 pathway by LPS derived from translocated bacteria.

The results from our study on gut decontamination and development of HCC were not as dramatic as those of Dapito but the lack of poorly differentiated tumours in the Norfloxacin plus carcinogen treated rats in our study and their appearance in the group of rats without gut decontamination could lend support to the idea that gut bacterial translocation could influence tumour development and/or behaviour although the number of animals used in our study is too small to confirm this. The differences in results between our study and that of Dapito et al. may in part be explained by the fact that only one type of antibiotic,

Norfloxacin, was used in our study whereas a combination of 4 different antibiotics which targeted a variety of pathogens other than gram negative bacteria were used for gut decontamination in the study by (Dapito et al., 2012) No data was given regarding liver fibrosis in their study.

Although the effect of selective gut decontamination on HCC development was marginal in our study, the impact on liver fibrosis was more remarkable. The degree of fibrosis in the rat livers was assessed histologically by staining the liver sections with reticulin and examining them microscopically. The degree of liver fibrosis as scored by the Ishak criteria was found to be 3/6 - 5/6 for rats treated with carcinogens alone and 0/6 - 2/6 for rat livers treated with carcinogens plus Norfloxacin. Selective gut decontamination with Norfloxacin, therefore, significantly reduced fibrosis in the livers of rats treated to gut decontamination compared to those without gut decontamination ($P < 0.04$).

In addition to reducing liver fibrosis, the treatment of rats with Norfloxacin also resulted in an improvement of the level of the liver enzymes ALT ($P < 0.05$) and AST ($P < 0.01$). An improvement of liver function with Norloxacin treatment was previously demonstrated in two separate models of liver cirrhosis using CCL4 and BDL treated rats (Zhang et al., 2010 and Shah et al., 2012). These findings are all compatible with the hypothesis that bacterial translocation from the gut into the systemic circulation could play a role in liver inflammation and fibrosis.

In order to confirm that gut decontamination by Norfloxacin treatment was successful in our experimental rats the levels of plasma endotoxin in these animals were measured using an endotoxin assay. As expected, the levels of plasma endotoxin were significantly reduced in the Norfloxacin treated group of animals as compared with the Norfloxacin untreated group ($P < 0.02$). In the naïve control group of rats no endotoxin was detectable. Since the endotoxin plasma levels are a reflection of the levels of circulating LPS the results from the assay confirmed that there was reduction with Norfloxacin treatment. A reduction in plasma endotoxin levels and bacterial translocation from the gut in response to Norfloxacin treatment have also recently been reported (Zhang et al., 2010 and Corradi et al., 2012)

It is known that bacterial LPS acts as ligands and stimulators of TLR4 so I decided to examine the levels of TLR4 expression in the livers of our experimental rats to see if Norfloxacin treatment also had any effect on these. The levels of TLR4 expression, as measured by immunohistochemical analysis of the rat liver sections using a TLR4-specific antibody, were very low in the naïve group of animals but high in the rats treated with DEN and NMOR alone (Score 2) in the liver background and not in HCC. In the group of rats treated with Norfloxacin with carcinogens TLR4 expression in liver background was higher (Score 1) than normal but significantly lower than in the non-Norfloxacin treated group ($P < 0.01$). This findings are compatible with TLR4 being stimulated by bacterial LPS and suggests that selective gut decontamination reduces inflammation and fibrosis via the TLR4 pathway. Although Testro and colleagues reported that Norfloxacin increased the expression of TLR4 in cirrhosis, their study investigated the expression of TLR4 in mononuclear cells and not hepatocytes (Testro et al., 2010). This suggests that different location of TLR4 could have several effects on the pathogenesis of liver disease.

Since NF-κB and TNF-α are known to be stimulated by TLR4 (as well as other TLRs) I decided to also look at their expression in the rat livers. The expression of NF-kB was measured by Western blot analysis and demonstrated low levels in the liver from the naïve rats but was highly expressed in both groups of carcinogen treated rats. However, in the Norfloxacin treated animals the levels of NF-kB were significantly lower than in the untreated animals ($P < 0.02$). The levels of TNF-α were measured by ELISA assays on rat liver tissue lysates that were macroscopically free from any visible tumour. The TNF-α levels were found to be low in the naïve rat livers but high in the livers of the all the carcinogen treated animals. The levels of TNF-α expression were lower in the Norfloxacin treated rats as compared with the non-Norfloxacin treated rats but this difference was not significant ($P = 0.7$). A similar study on the effects of gut decontamination using Norfloxacin in a cirrhosis model using BDL rats was previously carried out by Shah et al. In this particular case. the effects of gut decontamination on the kidneys was studied. The endotoxin levels were found to be reduced in the plasma of the Norfloxacin treated rats as compared with

the non-Norfloxacin treated rats. Levels of TLR4, NF-kB b and TNF-α expression were also downregulated in the kidneys of the Norfloxacin treated rats compared with non-Norfloxacin treated rats (Shah et al., 2012).

In summary my findings support the hypothesis that bacterial translocation from the gut to the systemic circulation may play a role in liver inflammation and fibrosis and this action may be brought about through induction of the TLR4 / NF-kB pathway. Selective gut decontamination with Norfloxacin does not however, appear to have a dramatic effect on HCC development and / or progression despite that fact that Norfloxacin can bring about a reduction in TLR4 and NF-kB b expression. Norfloxacin is a poorly absorbed antibiotic, which acts mainly on gram-negative bacteria so the possibility that other types of pathogens may still play a role in HCC development via translocation from the gut still exists. The pathways used by these pathogens may circumvent the TNF-α pathway. TNF-α is known to be stimulated by other TLRs and pathways. Many studies revealed that LPS and unmethylated CpG, which is derived from bacterial translocation, are involved in the pathogenesis of chronic liver disease (Takeuchi and Akira, 2010 and Frasinariu et al., 2012). In addition, several lines of investigation in humans indicate that TLR9 is up regulated in chronic liver disease and promotes the development of non-alcoholic steatohepatitis and hepatic fibrosis (Gäbele et al., 2008, Stadlbauer et al., 2008 and Henao-Mejia et al., 2012). Increased bacterial DNA is a feature of cirrhosis due to bacterial translocation (Seki and Schnabl, 2012) and the unmethylated CpG sequences in bacterial DNA are potent stimulators of TLR9 (Yamamoto and Takeda, 2010). An examination of TLR9 and TLR4 expression in human livers will be presented in the next chapter.

4.3 TLR Expression in human liver tissue

As gut decontamination with Norfloxacin was not linked to great effect on HCC development, I decided to study the expression of the TLR4, TLR7 and TLR9 in HCC and a variety of human liver diseases. These TLRs were correlated to chronic liver diseases in many studies (Gabele et al., 2008, Mencin et al., 2009, Starkel et al., 2010, Jing et al., 2012 and Xu et al., 2012). Expression of TLR4, TLR7 and TLR9 in human liver was examined by immunohistochemistry on custom made tissue arrays containing a variety of human liver samples and a validation set as described in materials and methods.

4.3.1 Results of TLR expression in tissue microarrays

a) TLR4 expression in liver tissue microarrays

- **Normal Liver:** TLR4 expression was negative in normal liver hepatocytes but strongly positive (Score 2) in the cytoplasm of all the bile duct epithelium in all 9 cases.
- **Hepatitis:** TLR4 expression was negative in the hepatocytes but strongly positive in the bile duct epithelium and inflammatory cells in all 26 hepatitis cases.
- **Cirrhosis:** Weak cytoplasmic staining (Score 1) of hepatocytes was observed in 3/24 cases of cirrhosis. The remaining 21 cases were all negative for TLR4 expression in the hepatocytes. However, the bile ducts, inflammatory cells and fibroblasts in all 24 cases were strongly positive for TLR4 expression.
- **HCC:** TLR4 expression was negative in the hepatocytes but strongly positive in the bile ducts, inflammatory cells and fibroblasts in 41 cases of HCC.

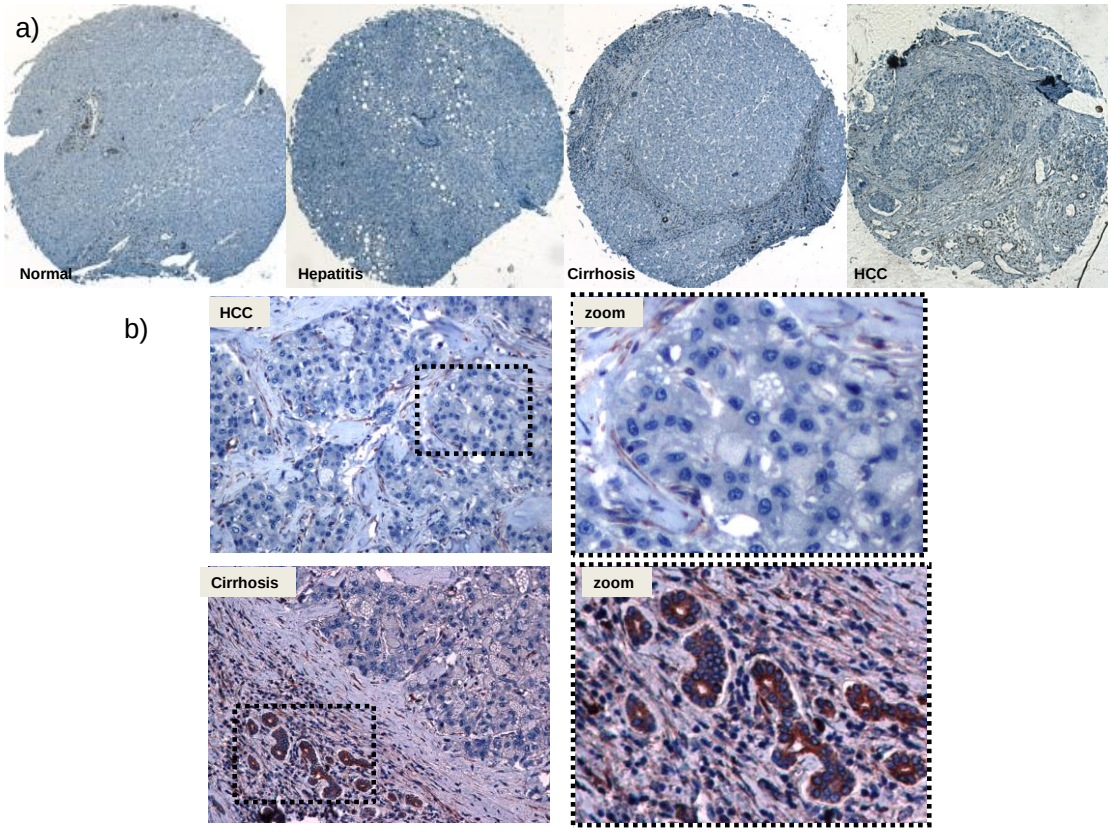

Figure 29: TLR4 expression in liver tissue arrays (a) TLR4 expression is absent in the hepatocytes of normal liver. The hepatitis liver demonstrates TLR4 expression in the bile duct epithelium and inflammatory cells. In the cirrhotic liver TLR4 expression is absent in the hepatocytes but strongly expressed in the bile duct epithelium, inflammatory cells and fibrous tissue. In HCC, TLR4 expression is absent in the hepatocytes but visible in the inflammatory cells and bile ducts. b) The HCC and cirrhotic tissue shown at higher magnifications.

a) TLR7 expression in liver tissue microarrays

- **Normal liver:** TLR7 was detected as dark brown staining around hepatocyte nuclei in 2/9 normal livers. However, the expression involved less than 1/3 of the hepatocyte in each case (Score 1). Faint brown cytoplasmic staining was detected in 2 cases in less than 1/3 of the hepatocyte in each case.
- **Hepatitis:** Perinuclear TLR7 was detected in 9/26 cases of hepatitis. However, less than 1/3 of the hepatocyte nuclei were stained in 8 cases (Score 1). One case showed perinuclear TLR7 in more than 1/3 of the hepatocytes (Score 2). Cytoplasmic TLR7 was observed in 5 cases of hepatitis in less than 1/3 of the hepatocytes and considered as (0).

- **Cirrhosis:** TLR7 was expressed in 6/24 cases of cirrhosis. In 3 cases less than one third of the hepatocyte nuclei stained positive for TLR7 (Score 1) and in 2 cases more than two thirds of the hepatocyte showed cytoplasmic TLR7 (Score 1) (Fig. 30). Perinuclear TLR7 was detected in more than two third of the hepatocytes in one case (Score 2).
- **HCC:** TLR7 was expressed in 37/41 HCCs. The expression involved over two thirds of the hepatocyte nuclei (Score 2) in 27 cases (Fig. 30) and less than one third of the hepatocyte nuclei (Score 1) in 9 cases and one case showed cytoplasmic TLR7 in more than two third of the hepatocytes (Score 2). 4 HCCs were negative for TLR7.

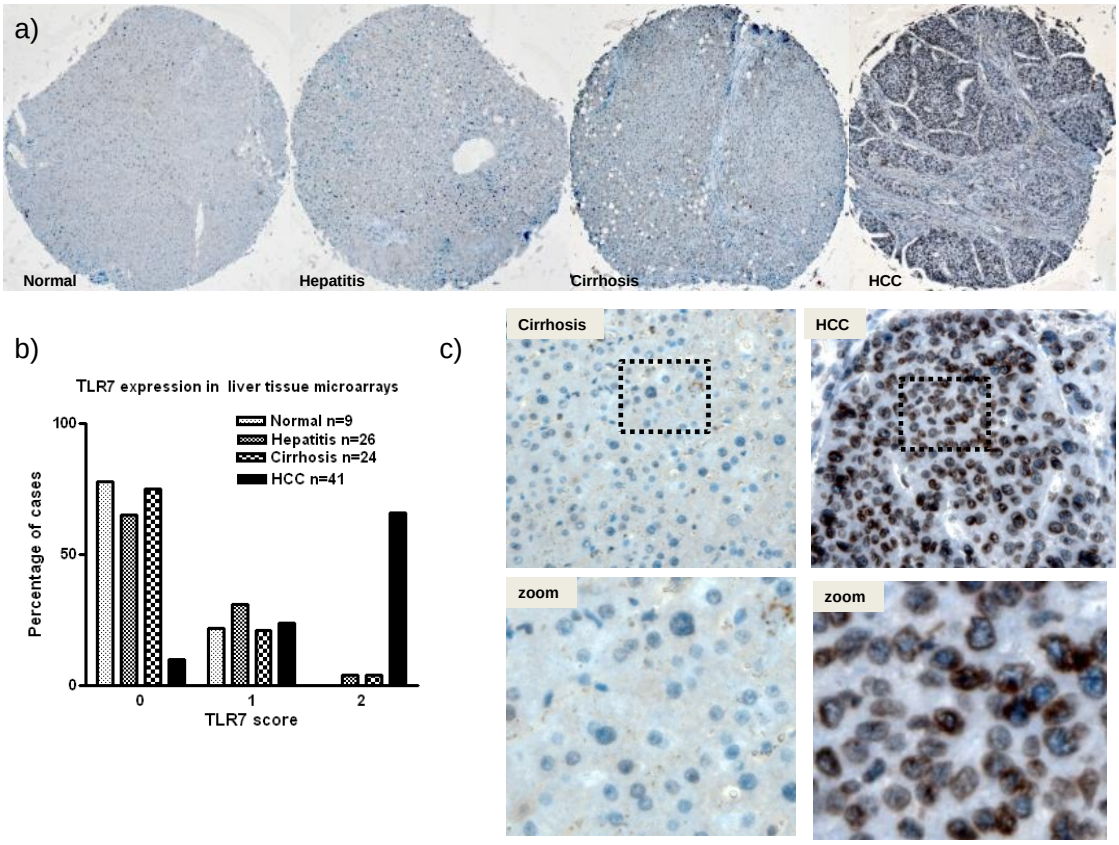

Figure 30: TLR7 expression in liver tissue arrays. a) TLR7 is absent in the normal, hepatitis and cirrhosis tissues. Perinuclear expression of TLR7 is seen in the HCC section. b) Graph demonstrating the percentage of normal, hepatitis, cirrhosis and HCC cases in the liver tissue arrays expressing TLR7 at different levels; 0 = no expression, 1 = weak and 2 = high expression. c) 40 x magnification of the cirrhosis and HCC tissue. The dark brown staining of TLR7 is seen more clearly in the nuclei of HCC cells. The zooming box shows some cytoplasmic staining of TLR7 in the cirrhosis tissue.

b) TLR9 expression in liver tissue microarrays

- **Normal liver:** TLR9 expression was visible on the cell membranes in 2/9 cases. No cytoplasmic staining was detected in 8/9 cases of the normal livers and (Score1) TLR9 was found in 1/9 case.
- **Hepatitis:** Membranous staining was detected in 12 cases of hepatitis. Cytoplasmic TLR9 was absent in 21/26 of hepatitis cases and faintly cytoplasmic in more than two third of hepatocytes (Score 1) in the other 5 cases.
- **Cirrhosis:** Membranous staining of TLR9 was observed in the hepatocytes of 13/24 of cirrhosis cases. Cytoplasmic TLR9 was not detected in 23/24 cases and was visible in 1 case (Score1).
- **HCC:** Cytoplasmic staining of TLR9 was observed in 29/41 HCCs and absent in 12 cases. TLR9 score was (Score 1) in 11 cases and high (Score 2) in the remaining 18. No cytoplasmic staining was observed in 12 HCCs.

Membranous staining of TLR9 was seen in 13/41 HCCs. The membranous staining was associated with weak cytoplasmic staining of TLR9 in 9 cases (Score 1) and with high cytoplasmic staining (Score 2) in the remaining 4 cases.

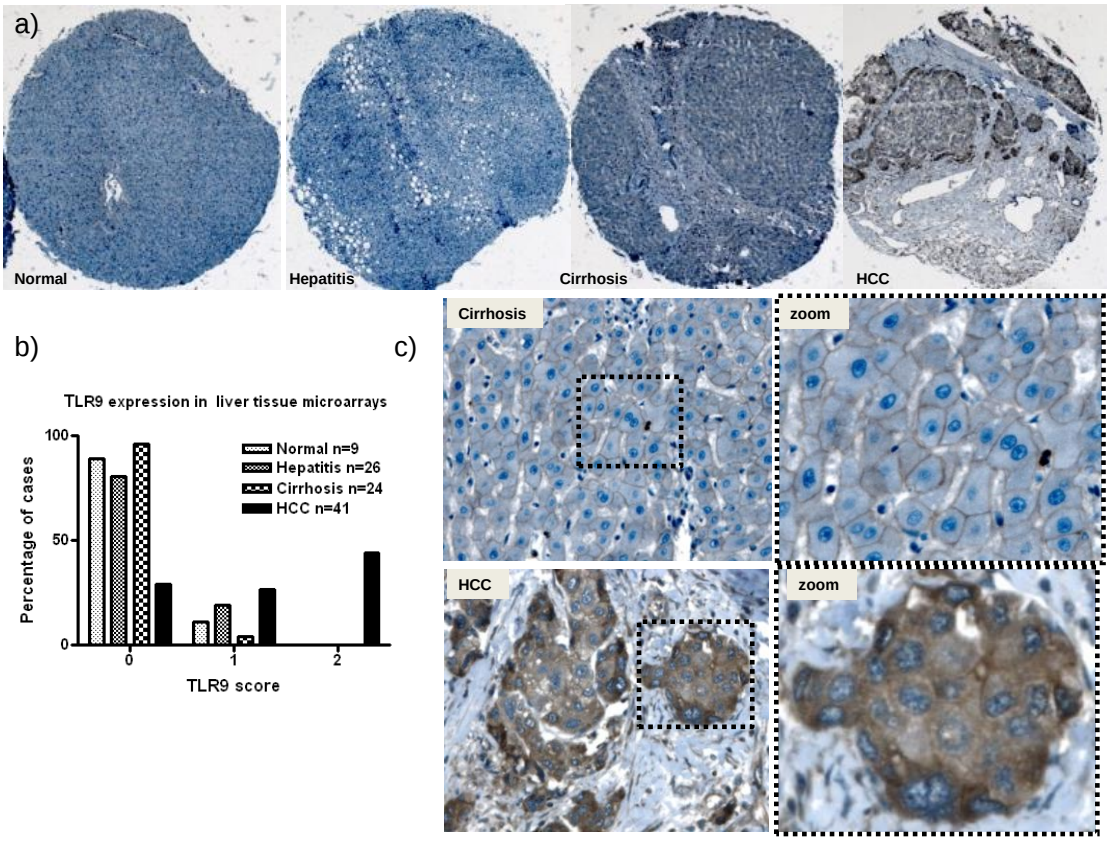

Figure 31: TLR9 expression in the liver tissue arrays. (a) TLR9 is absent in normal and hepatitis tissue. Weak cytoplasmic expression of TLR9 is visible in the cirrhosis section. In HCC, TLR9 is highly expressed in the cytoplasm of malignant hepatocytes. b) Graph demonstrating the percentage of normal, hepatitis, cirrhosis and HCC cases in the tissue array expressing cytoplasmic TLR9 at different levels; 0 =no expression, 1 =weak expression or 2 =high expression. c) 40 x magnification of the cirrhosis and HCC sections with zooming boxes showing more clearly the membranous expression of TLR9 in the cirrhosis sample and its expression in the cytoplasm of malignant hepatocytes in the HCC section.

4.3.2 Results of TLR expression in human liver tissue validation set

a) TLR4 expression in human liver tissue validation set

TLR4 expression was absent in malignant hepatocytes but positive in the normal bile ducts, inflammatory cells and fibroblasts of the cirrhotic liver. These findings are similar to those observed in the liver tissue arrays.

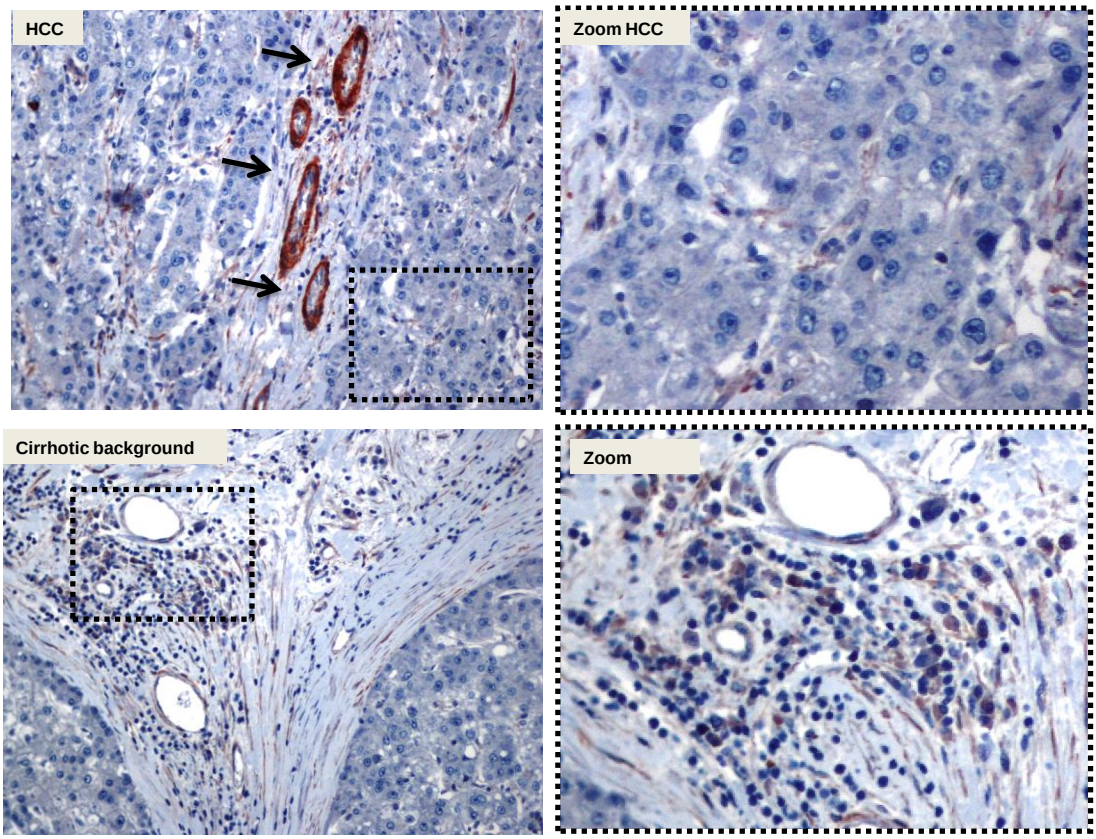

Figure 32: TLR4 expression in HCC and cirrhotic background. The top left image shows absence of TLR4 expression in the malignant hepatocytes but high TLR4 expression in the bile duct epithelium (black arrows). Top right is a magnified image of the TLR4 negative hepatocytes. The lower left image shows high expression of TLR4 in the inflammatory cells of the cirrhotic background, seen more clearly in the magnified image to the lower right.

b) TLR7 expression in human liver tissue validation set

- **Normal liver:** TLR7 was not detected in the cytoplasm or the nuclei of 2/2cases.
- **Cirrhosis:** TLR7 was found in hepatocytes perinuclear in 1/5th of the cases. However the expression was found in less than 1/3 of the hepatocytes (Score 1). The other 4 cases were all negative.

- **Cirrhotic background**: 6/19 cases were positive for TLR7. 5 cases exhibited perinuclear TLR7 in less than 1/3 of the hepatocytes (Score 1) and 1 exhibited cytoplasmic TLR7 in more than 2/3 of the hepatocytes (Score 1). The remaining 13 were all negative for TLR7.
- **HCC:** TLR7 was expressed in 16/19 cases. The expression was found perinuclear in less than 1/3 of the malignant hepatocytes (Score 1) in 4 cases and perinuclear in more than 2/3 of the malignant hepatocytes (Score 2) in 12 cases. The remaining 3 cases were all negative for TLR7.

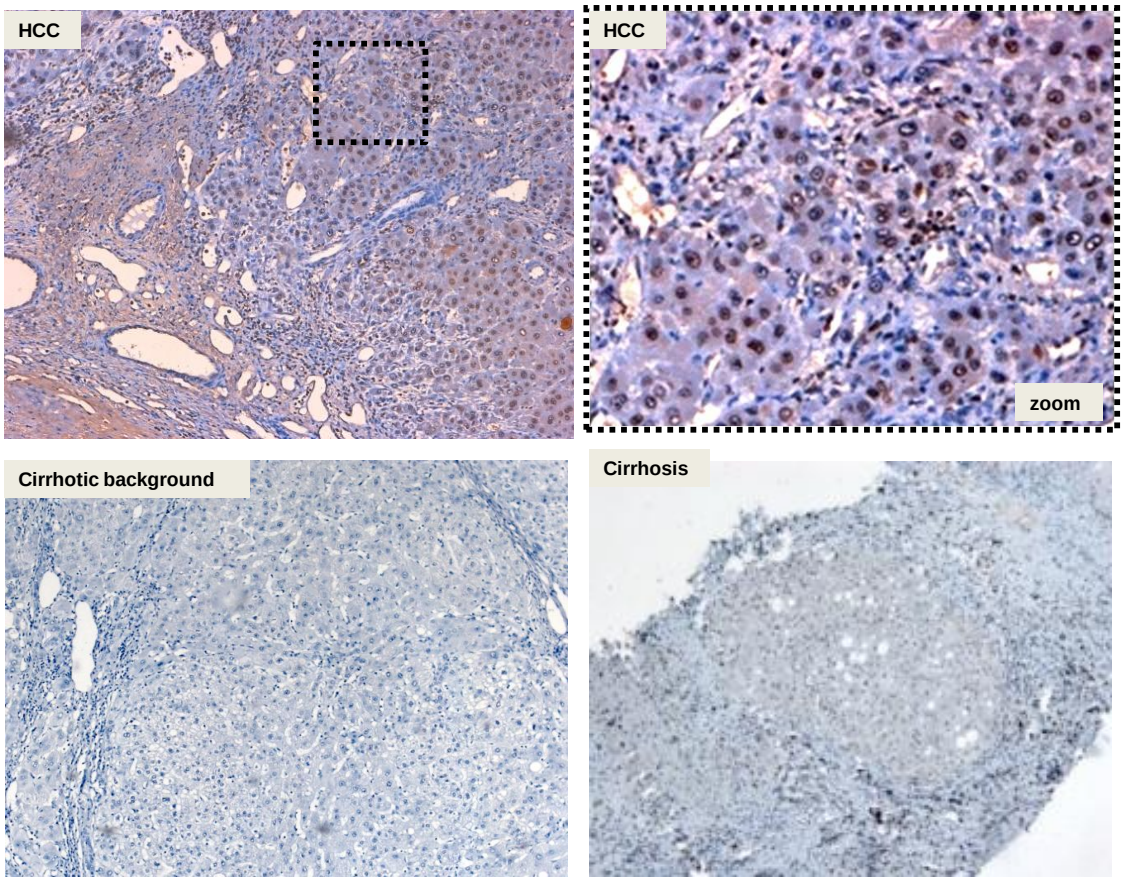

Figure 33: TLR7 expression in the validation set confirms the findings in the tissue microarrays. Peri-nuclear expression of TLR7 is visible in more than two thirds of malignant hepatocytes in the HCC section (top left and top right images). TLR7 was weakly expressed in the cirrhotic background and cirrhotic tissue (lower left and lower right)

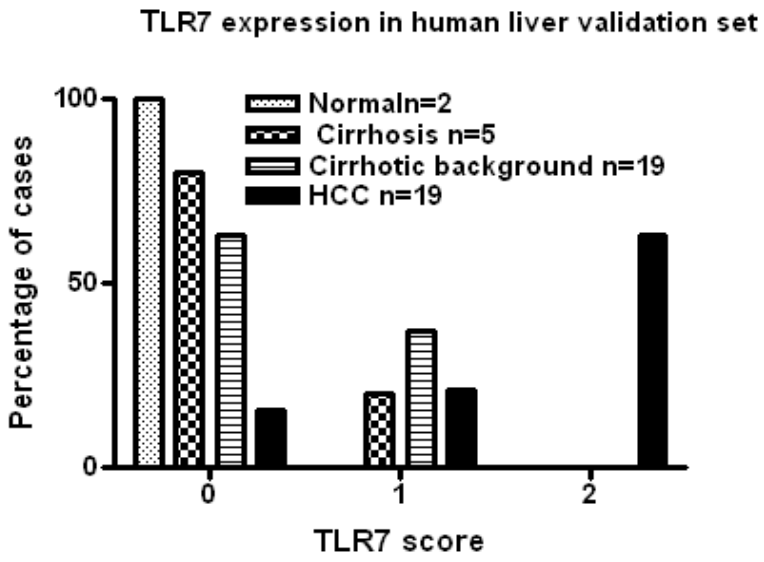

Figure 34: Graph showing distribution of TLR7 expression among normal, cirrhosis, cirrhotic background and HCC tissues from the validation set expressed as the percentage of cases demonstrating no (0), weak (1), or high (2) expression of TLR7. TLR7 was not expressed in normal liver but a large proportion of HCCs demonstrated high expression of TLR7. Its expression was largely weak or absent in the cirrhotic background and cirrhosis cases.

c) TLR9 expression in human liver tissue validation set

- **Normal liver:** The 2 normal livers were both negative for TLR9 expression.
- **Cirrhosis:** 2/5 cases demonstrated weak (Score 1) cytoplasmic TLR9 expression. The other 3 were TLR9 negative.
- **Cirrhotic background:** 7/19 cases expressed cytoplasmic TLR9. The expression was low (Score 1) in 6 cases and high (Score 2) in 1 case. The remaining 12 cases were TLR9 negative.
- **HCC:** 14/19 cases were positive for TLR9. The expression was weak (Score 1) in 8 cases, high (Score 2) in 6 cases. The remaining 5 cases were all negative for TLR9 expression (Fig. 35).

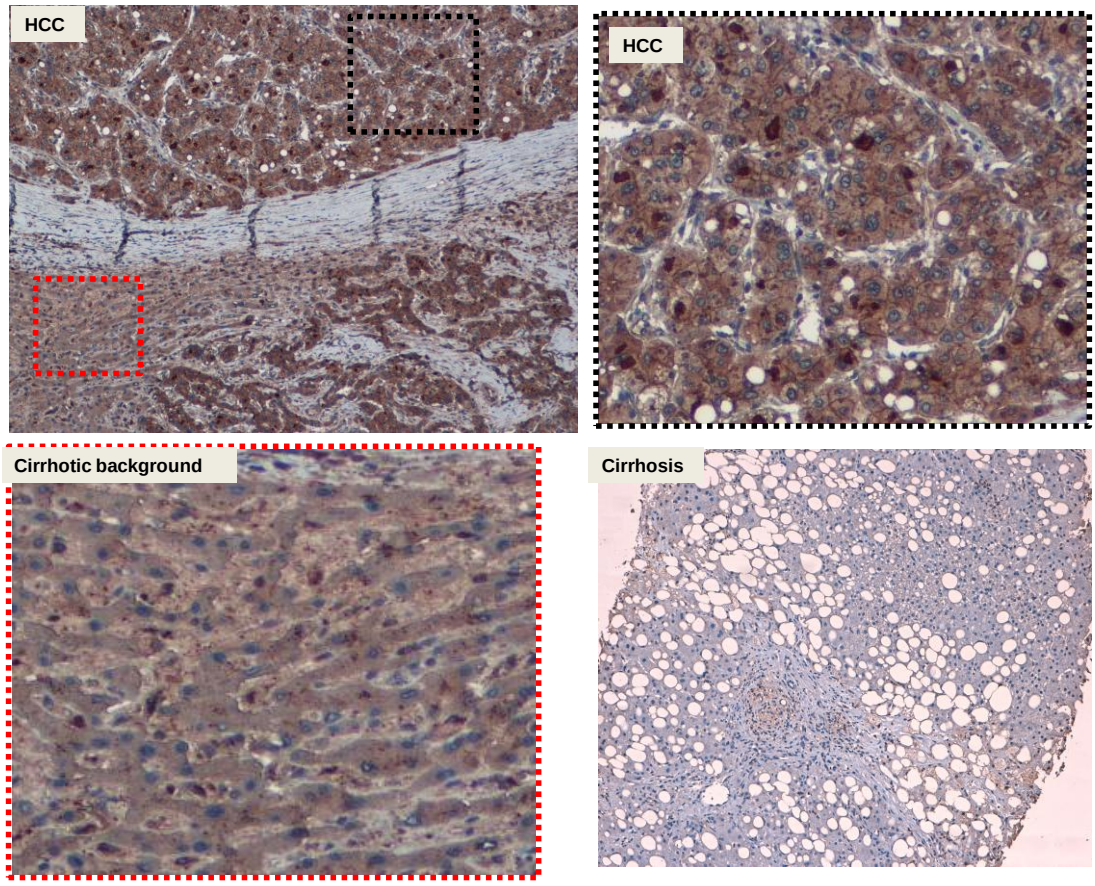

Figure 35: TLR9 expression in the validation set of liver samples confirms the findings in the tissue microarrays. The top left image shows intense brown cytoplasmic staining of TLR9 in more than two thirds of the malignant hepatocytes - seen more clearly at higher magnification in the top right image. A magnified image of the cirrhotic background within the red zooming box can be seen to the lower left and demonstrates less intense cytoplasmic staining of TLR9. The image to the lower right demonstrates weak cytoplasmic expression of TLR9 in the liver cirrhosis section.

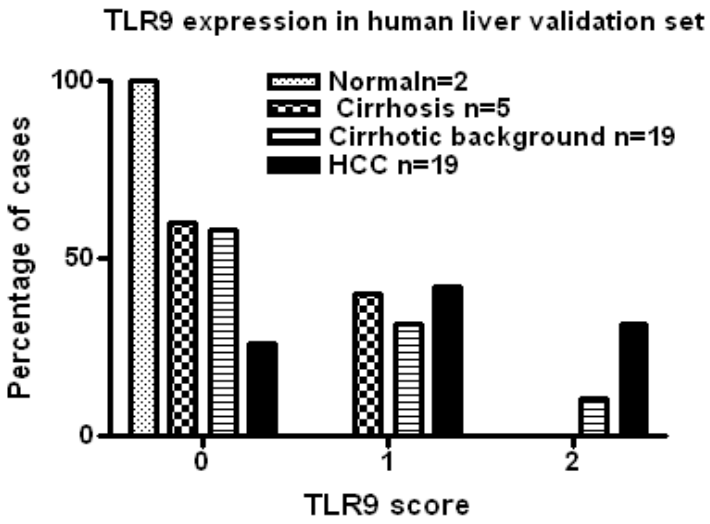

Figure 36: Graph showing distribution of TLR9 expression among normal, cirrhosis, cirrhotic background and HCC tissue from the validation set expressed as the percentage of cases demonstrating no (0), weak (1), or high (2) expression of TLR9. TLR9 was not expressed in normal liver but high expression was demonstrated in HCCs and cirrhotic background.

4.3.3 Increased TLR7 & TLR9 expression correlates with high Ki-67 proliferation index.

Ki-67 index was estimated as percentage of positivity of hepatocytes nuclei stained with Ki-67. By examination all HCC cores in tissue microarray and validation set, It was found that cases showed high expression of TLR7 (Score 2) had high Ki-67 index. There were a significant correlation between increased TLR7 expression and increased the Ki-67 index r= 0.3 and ($P < 0.05$). By investigating the correlation between Ki-67 index and TLR9 staining, I found that the highest proliferation index was associated with high expression of TLR9 in HCC. There were also close correlation between increased TLR9 expression in HCC cases and proliferation index r=0.5 and ($P < 0.0001$).

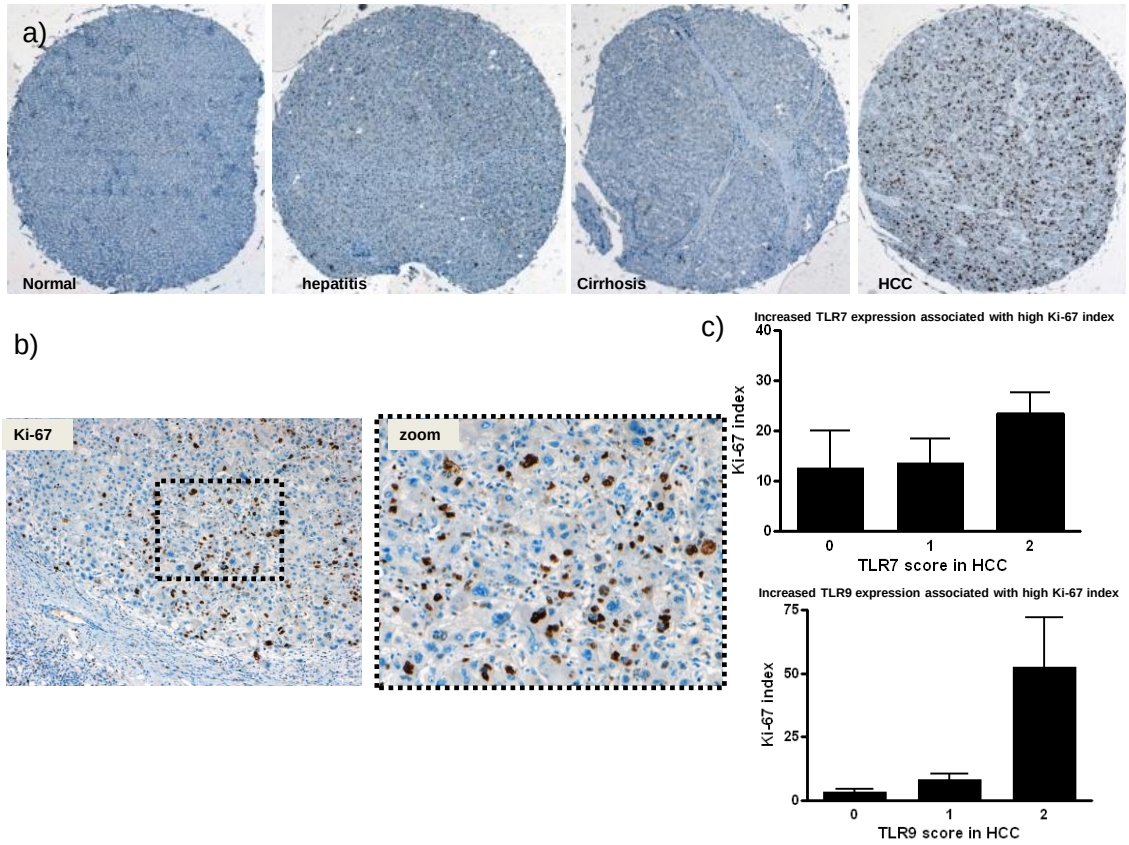

Figure 37: High Ki-67 index was associated with high TLR7 and TLR9 expression of a) Cores represented different cases from TMA stained with immunohistochemistry technique and Ki-67 antibody showing the difference in Ki-67 expression. There were no Ki-67 expression in normal, hepatitis and cirrhosis whereas there was high expression of Ki-67 in HCC core. b) HCC section from the validation set showing the high expression of Ki-67 index and zooming box showing the Ki-67 in the nuclei of malignant hepatocytes. c) Graph demonstrates the correlation between the high expression of TLR7 and TLR9 with high proliferation index estimated with Ki-67.

4.3.4 Summary of TLR & Ki-67 data in human liver tissue arrays & validation set

- TLR4 is not expressed in HCC cells but highly expressed in inflammatory cells and fibroblasts.
- TLR7 is highly expressed perinuclear in HCC cells. The expression is weak in hepatitis and cirrhosis.
- TLR9 is expressed on the hepatocyte cell membranes in hepatitis and cirrhosis. There is a shift in expression from cell membranes to the cytoplasm in malignant hepatocytes where it is expressed at high levels.
- There is a positive correlation between Ki-67 proliferation index and expression of TLR7 and TLR9. This suggests there may be a link between over-expression of these TLRs and proliferation of the tumour cells in HCC.

4.3.5 Discussion

There is much evidence in the literature to suggest that increased expression of TLR4 and TLR9 play important roles in development of chronic liver disease and fibrosis (Dolganiuc et al., 2006, Seki et al., 2007 Gäbele et al., 2008, Stadlbauer et al., 2008, Aoyama et al., 2010 and Henao-Mejia et al., 2012). However, prior to the beginning of our research little if anything was known about the roles of TLR4, TLR7 and TLR9 in HCC pathogenesis and progression. I therefore set out to determine if any relationship existed between these TLRs and the development of HCC in human liver. For this purpose two sets of liver tissue were examined by immunohistochemistry (1) a custom made liver tissue microarray containing formalin fixed paraffin embedded (FFPE) liver samples from normal, hepatitis, cirrhosis and HCC tissue and (2) a set of liver samples, dubbed the validation set, consisting of FFPE tissue samples from normal, cirrhosis and HCC on a background of cirrhosis obtained from the Pathology department of the Royal Free Hospital, London.

The immunohistochemistry data from the TMA samples and validation set revealed a very similar pattern of TLR 4 expression; TLR4 was not expressed in the hepatocytes from normal livers, hepatitis or HCC cases. Only weak staining of hepatocytes was observed in a few cases of cirrhosis (3/24 from the TMA). In contrast, however strong expression of TLR4 was visible in the fibroblasts, inflammatory cells and bile duct epithelium in the different types of liver tissue from both the TMA and validation set. Our findings are in agreement with those of Vespasiani-Gentilucci, et al., 2012 who reported that the parenchymal elements responsible for the highest level of TLR4 expression were the hepatic progenitor cells and biliary epithelial cells of interlobular bile ducts in HCV related liver disease. Furthermore, they found a significant correlation between TLR4 positivity and stage of liver disease and grade of inflammation. It was concluded that TLR4 expression by hepatic progenitor cells and biliary epithelial cells contributes to the progression of liver damage in the course of chronic HCV-related infection.

Unlike our findings, however, Wei et al., 2008 demonstrated that TLR4 is expressed in the cytoplasm and cell membranes of hepatocytes in normal and

chronic hepatitis livers. A similar finding was reported by Benias who showed increased TLR4 and TLR9 expression in hepatocytes of chronic Hepatitis C liver (Benias et al., 2012) TLR4 expression has also been reported in focal hepatocytes and inflammatory cells of paediatric hepatitis C (Mozer-Lisewska et al., 2005). These findings suggest some role for TLR4 in the pathogenesis of chronic hepatitis both in adults and children.

Only one other study has so far been reported on TLR4 expression in HCC. (Jing et al., 2012). However, in contrast to our findings they found that TLR4 was expressed in the vast majority (86%) of HCCs examined. Furthermore, high expression of TLR4 in the primary HCCs was shown to significantly correlate with HCC metastasis and recurrence. It was therefore suggested that TLR4 could potentially be used as a novel prognostic marker and therapeutic target for HCC. The differences in TLR4 data from our study and that of Jing et al. may be partly explained by differences in the sample population or differences in HCC aetiology. However, the lack of TLR4 expression in our HCCs and its presence in inflammatory cells within or surrounding the HCC tissue is a finding that I previously observed in our rat animal models of HCC (discussed in Chapter 4.2). It may be the case in our HCC samples that expression of TLR4 is not necessary for HCC pathogenesis, but this doesn't rule out the possibility that TLR4 expression in the surrounding tumour environment might still have an immunomodulatory influence on tumour behaviour since inflammatory cells are known to produce signals which promote vital processes in tumour development, such as angiogenesis, tumour growth and invasion (reviewed by Hanahan and Weinberg, 2011 and Oblak and Jerala, 2011).

TLR7 expression in the normal liver tissues was weakly detectable in only 2/11 cases (9 cases TMA and 2 cases validation set). The staining was perinuclear but occurred in less than 1/3 of hepatocytes. In the cirrhotic liver TLR7 was weakly expressed in 20% of cases (6/24 from the TMA set and 1/5 from the validation set) only one case showed strong expression (from the TMA). In the hepatitis tissues, the TLR7 expression was also weak and involved only 30% of cases (8/26 in the TMA). Only one case of hepatitis tissue exhibited strong

expression of TLR7. As in the case of normal livers the pattern of TLR7 expression was also perinuclear in the cirrhotic and hepatitis tissues.
Unlike TLR4, the expression of TLR7 was found to be up regulated in the majority (85%) of HCC samples (35/41 HCCs from the TMA and 16/19 HCCs from the validation set). The level of TLR7 expression was strong in 61% of HCCs (37/60 HCCs) and weak to moderate in 23% of all positive cases (14/60 HCCs). The expression was also confined to the perinuclear region of hepatocytes in all of 51 positive cases of HCC. The same pattern of perinuclear staining was previously reported in lung adenocarcinoma and bronchial epithelium (Cherfils-Vicini et al., 2010).

The up regulated expression of TLR7 in HCC suggests that TLR7 may play an important role in HCC development and/or progression. This is supported by TLR7 expression studies in other cancers e.g. in oesophageal carcinoma TLR7 expression was found to be high and a strong correlation was found between the levels TLR7 of expression and tumour grade (Sheyhidin et al., 2011). Similarly in cervical cancer a strong correlation was reported between levels TLR7 expression and tumour differentiation (Hasimu et al., 2011). In another study using cell lines derived from lung cancer increased TLR7 expression was shown to promote cell survival and tumour progression (Cherfils-Vicini et al., 2010). In addition, TLR7 has also been reported to promote pancreatic cancer growth (Ochi et al., 2012).

Although few investigations have been conducted on the expression of TLR7 protein in human liver, there has been some mRNA expression studies reported on ALD and HCV (Starkel et al., 2010 and Tarantino et al., 2013). However, in contrast to the TLR7 immunohistochemistry findings Lin and colleagues reported TLR7 mRNA was significantly down regulated in neoplastic hepatocytes (Lin et al., 2013). It is difficult to make direct comparisons between these findings and our immunohistochemistry data. Furthermore, little is known about the expression of TLR7 in the liver and other human tissues and these will need to be determined more precisely in future before any definitive conclusions can be reached.

An examination of TLR9 in the normal livers demonstrated expression in only 18% of cases (2/9 TMA and 0/2 from the validation set). The expression was confined to the membrane of the hepatocytes in both cases. In the hepatitis tissues, expression of TLR9 was seen in a total of 46% of cases (17/26 TMA). The staining was membranous in 12/26 cases and low cytoplasmic expression (Score 1) was found in 5/26. In the cirrhotic tissues, TLR9 was expressed in 55% of cases (14/24 TMA and 2/5 validation set). The expression was membranous in 54% of TMA cases and weak cytoplasmic (Score 1) in 10% of all cases (1/24 TMA and 2/5 of validation set cases). In the HCC tissues TLR9 expression was more widespread with 71% (29/41 TMA and 14/19) demonstrating positivity for TLR9. The staining was strong in 40% of cases (18/41 TMA and 6/19 validation set cases) and weak in the remaining 31%. However, the expression was mainly cytoplasmic in the HCCs although some membranous co-staining of TLR9 was observed in 13 / 60 (21%) of cases (9 were associated with weak cytoplasmic staining of TLR9 and 4 cases were associated with strong cytoplasmic expression).

During the course of my investigation, another study on TLR9 expression in HCC was reported. Similar to our findings, a high percentage of HCCs (87%) was shown to express TLR9 (87%) (Tanaka et al., 2010). However, unlike our findings the pattern of TLR9 expression was largely membranous. The up regulated expression of TLR9 in our samples and those of Tanaka suggests that TLR9 might have a role to play in hepatocarcinogenesis. This is supported by immunohistochemistry studies in other cancers, which have demonstrated high levels of TLR9 expression in oesophageal, prostatic and cervical cancer (Takala et al., 2011, Kauppila et al., 2011, González-Reyes et al., 2011 and Hasimu et al., 2011). In addition, the up regulation of TLR9 was also found to be associated with poor differentiation in oesophageal adenocarcinoma (Kauppila et al., 2011) and lymph node metastasis in cervical carcinoma (Hasimu et al., 2011). Furthermore, the addition of a TLR9 agonist to a HCC cell line was found to increase survival of the HCC cells when treated with the anti-cancer drug Adriamycin (Tanaka et al., 2010).

In order to determine whether there was any relationship between the expression of TLR7 or TLR9 and proliferation of HCC I also looked at the

pattern of Ki-67 staining in all HCCs from the TMA and validation set. I found a significant correlation between high proliferation index and high expression of TLR7 r=0.3 (P <0.05) and TLR9 r=0.5 (P <0.0001) in both sets of samples. These findings further strengthen the idea that TLR7 & and TLR9 are involved in HCC proliferation. Further support is provided by the findings in other studies, For instance, Min et al., 2011 reported that high expression of TLR9 in human oral squamous cell carcinoma tissue was significantly associated with high ki-67 index. A correlation between increased TLR7 expression and increased tumour proliferation has also been described in pancreatic cancer (Ochi et al., 2012).

In conclusion, my immunohistochemistry data has demonstrated that expression of TLR7 and TLR9 is up regulated in human HCC. In addition, there is a strong association between high expression of these TLRs and high proliferation index. The results suggest TLR7 and TLR9 may have an important role to play in HCC pathogenesis. A role for TLR4 cannot be ruled out at this stage. However, additional studies are needed to more precisely determine the pattern of TLR4, TLR7 & TLR9 expression in normal liver as well as diseased liver and HCC before I can fully appreciate their role in these different conditions.

4.4 Expression of TLR7 & TLR9 in HuH7 human HCC cell line

4.4.1 Introduction

Over expression of TLR7 and TLR9 in human HCC has been described in the previous chapter. A correlation between the high expression of these TLRs and high proliferation index was found suggesting that TLR7 and TLR9 may have a role in HCC pathogenesis. It is well-known that both TLR7 and TLR9 localise to endosomal compartments in many cells (Ewald et al., 2008) and contribute to signal transduction in the nucleus (Platta and Stenmark, 2011). The subcellular distribution of TLR9 has previously been shown to be linked to its activation status (Latz et al., 2004). For example, in dendritic cells, TLR9 under resting conditions is located in the endoplasmic reticulum and upon stimulation, it translocates to the lysosomes (Latz et al., 2004). Chloroquine is known to inhibit TLR7 and TLR9 signaling by altering the endosomal pH (Macfarlane and Manzel, 1998, Yi et al., 1998 and Kuznik et al., 2011)

4.4.2 Aims

1. Determine whether TLR7 and TLR9 expressed in HCC cell lines such as HuH7 and study their distribution.
2. Determine whether TLR7 and TLR9 stimulation by using specific agonists such as imiquimod (IMQ) and CpG-ODN respectively or TLR7 and TLR9 inhibition using specific antagonists (IRS 954) or signalling inhibitor (chloroquine) is associated with change of their subcellular localisation.
3. Determine whether TLR7 and TLR9 stimulation and inhibition influence the proliferation of HuH7 cell line.
4. Study the effect of TLR7 and TLR9 stimulation or inhibition on protein expression of some of the well-known pathways in HCC such as Akt and LC3B.

These proteins expression were investigated for the following reasons:

- Akt pathway has been implicated in HCC carcinogenesis and its role was linked to cell survival and proliferation in HCC in previous studies and (Chen et al., 2011 and Zhou et al., 2011) and chloroquine treatment has a potential effect on Akt and phosphorylated Akt (pAkt) (Loehberg, et al., 2012).

- Chloroquine was known previously by its effect on autophagy which is a one of the pivotal pathways in tumourigenesis (Ding et al., 2011) and particularly HCC (Shimizu et al., 2012).

4.4.3 Results of TLR7 & TLR9 Expression Studies in HuH7 Cells

a) <u>TLR7 & TLR9 distribution in untreated HuH7 cells</u>

Immunofluorescence staining with TLR7 or TLR9 antibodies demonstrated that TLR7 and TLR9 are both expressed in HCC. TLR7 was localised mainly in the nucleus and for some extent in the cytoplasm of HuH7 cells whereas TLR9 was detected in the cytoplasm as shown in (Fig. 38).

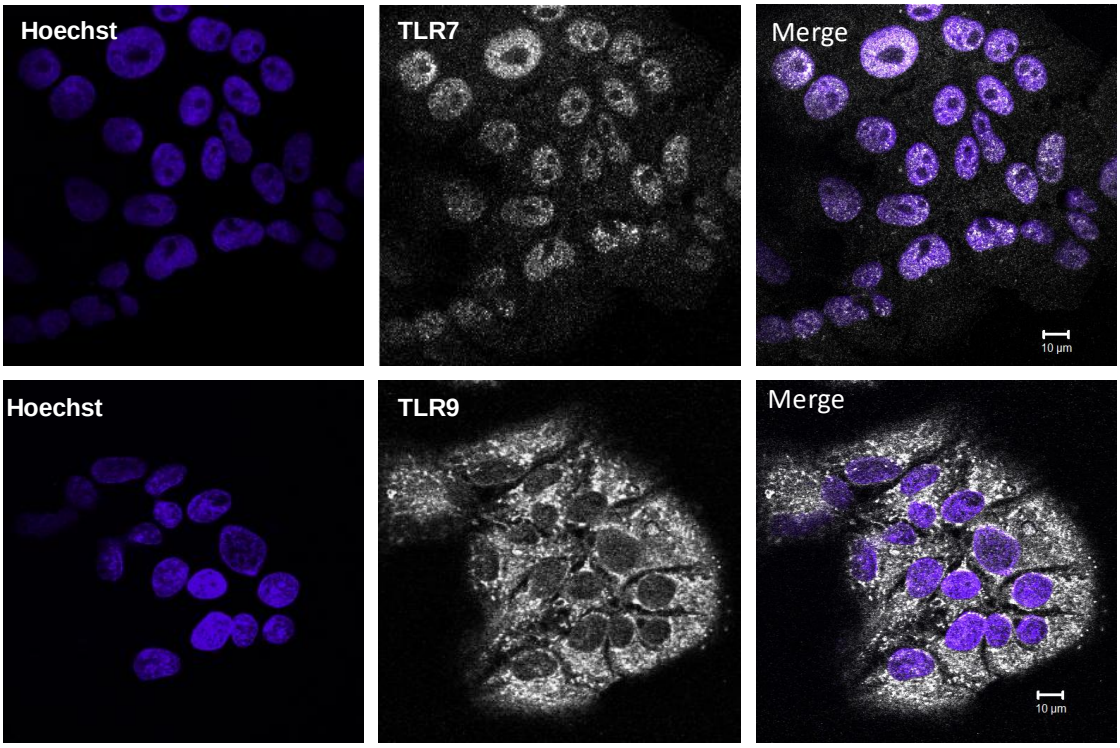

Figure 38: TLR7 and TLR9 expression in HuH7 cells and differences in their subcellular distribution. In HuH7 cells fixed with methanol, TLR7 was found mainly in the nucleus as shown in the TLR7 (white channel0. The merged channel shows the TLR7 in white and the nuclear Hoechst 33342 stain in blue. TLR9 was highly expressed in the cytoplasm (white channel) and the location clearly appeared in merge channel with TLR9 staining and Hoechst 33342.

This experiment confirmed the presence of TLR7 and TLR9 in HuH7 cells and raised an important question: does the localisation of TLR7 or TLR9 impact HCC progression?

b) <u>TLR7 subcellular localisation unchanged with IMQ, chloroquine or IRS treatment of HuH7 cells</u>

Having demonstrated that the intra-cellular distribution of TLR9 is altered upon stimulation in previous study, I investigated whether the localisation of TLR7 in HuH7 cells may also alter in response to treatment with IMQ (TLR7 stimulant), chloroquine and IRS (TLR7 inhibitors). However, no detectable changes in TLR7 distribution were found with any of the above treatments (Fig. 39).

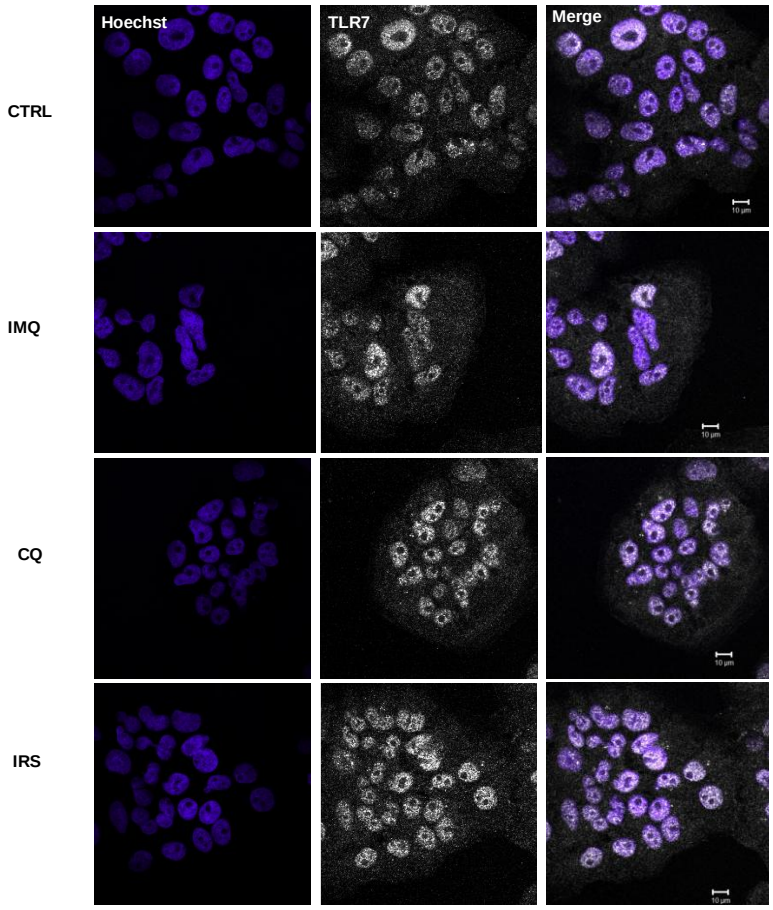

Figure 39: TLR7 localisation in HuH7 cells did not change with IMQ, CQ or IRS treatment. In methanol fixed HuH7, TLR7 was detected in the nucleus of HuH7 cells (white channel). The blue channel is Hoechst 33342. The merge channel showed both TLR7 and Hoechst 33342. There were no changes observed in the localisation of TLR7 with IMQ (TLR7 agonist) or with chloroquine or IRS (TLR7 and TLR9 inhibitor) treatment (scale bar=10µm).

c) TLR9 expression shifts towards nucleus with CpG-ODN treatment of HuH7 Cells

Subcellular distribution of TLR9 was affected by CpG-ODN treatment. In untreated HuH7 cells, TLR9 was found homogenously distributed in the cytoplasm. Upon treatment with CpG-ODN (TLR9 stimulant), TLR9 stained vesicles shifted from the cytoplasm to accumulate around the nucleus. This phenomenon was not observed with chloroquine or IRS treatment (Fig. 40).

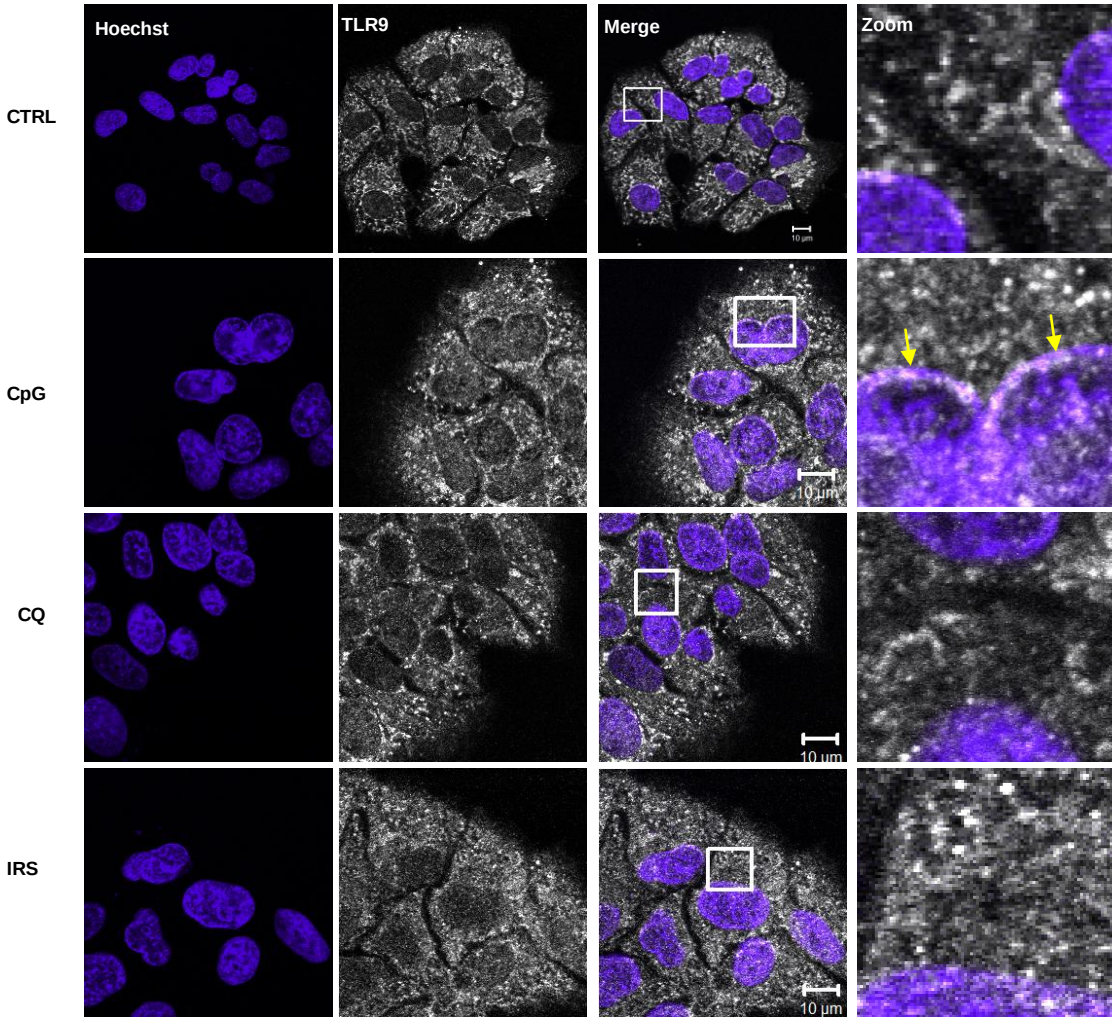

Figure 40: Shifting of TLR9 stained vesicles from the cytoplasm to accumulate around the nucleus with CpG-ODN treatment. Methanol fixed HuH7 cells and immunofluorescent staining with TLR9 antibody and Hoechst 33342 showed TLR9 in untreated HuH7 was found homogenously distributed in the cytoplasm whereas with CpG treatment there was more aggregation of TLR9 stained vesicles around the nucleus in the zooming box (yellow arrows). With chloroquine, treatment or IRS, TLR9 was in the cytoplasm and there was no accumulation around the nucleus. Scale bar =10µm).

4.4.4 TLR9 does not localise to the endoplasmic reticulum in HuH7 cells

TLR9 has previously been reported to translocate between the endoplasmic reticulum (ER) and endolysosomal system in response to stimulation and inhibition. I therefore investigated whether the subcellular localisation of TLR9 in HuH7 cells is altered upon treatment with CpG-ODN, chloroquine and IRS. Co-immunofluorescence staining of HuH7 cells with TLR9 and organelle markers in which TLR9 was predicted to co-localise, such as the ER marker calnexin and the lysosomal marker lamp-1, was performed. In HuH7 cells either treated with CpG-ODN, chloroquine, IRS or untreated, there was no clear evidence supporting that TLR9 co-localised with the endoplasmic reticulum (ER) marker calnexin (Fig. 41).

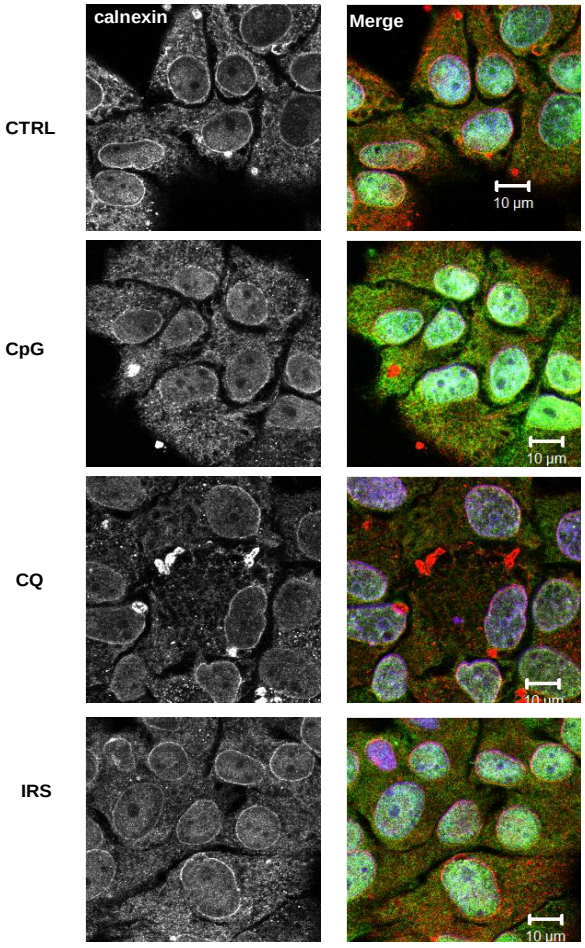

Figure 41: Co-localisation between TLR9 and calnexin was not observed in untreated or treated HuH7 cells. In the merge panel TLR9 green colour, calnexin (red colour) and (blue colour) Hoechst 33342 there was no co-localisation observed in untreated HuH7 or with CpG, CQ and IRS treatment.

4.4.5 Limited co-localisation of TLR9 and lamp-1 in HuH7 cells

In untreated HuH7 cells, limited co-localisation of TLR9 and the lysosomal marker lamp-1 was found. This limited co-localisation did not change upon CpG-ODN, chloroquine or IRS treatment (Fig. 42).

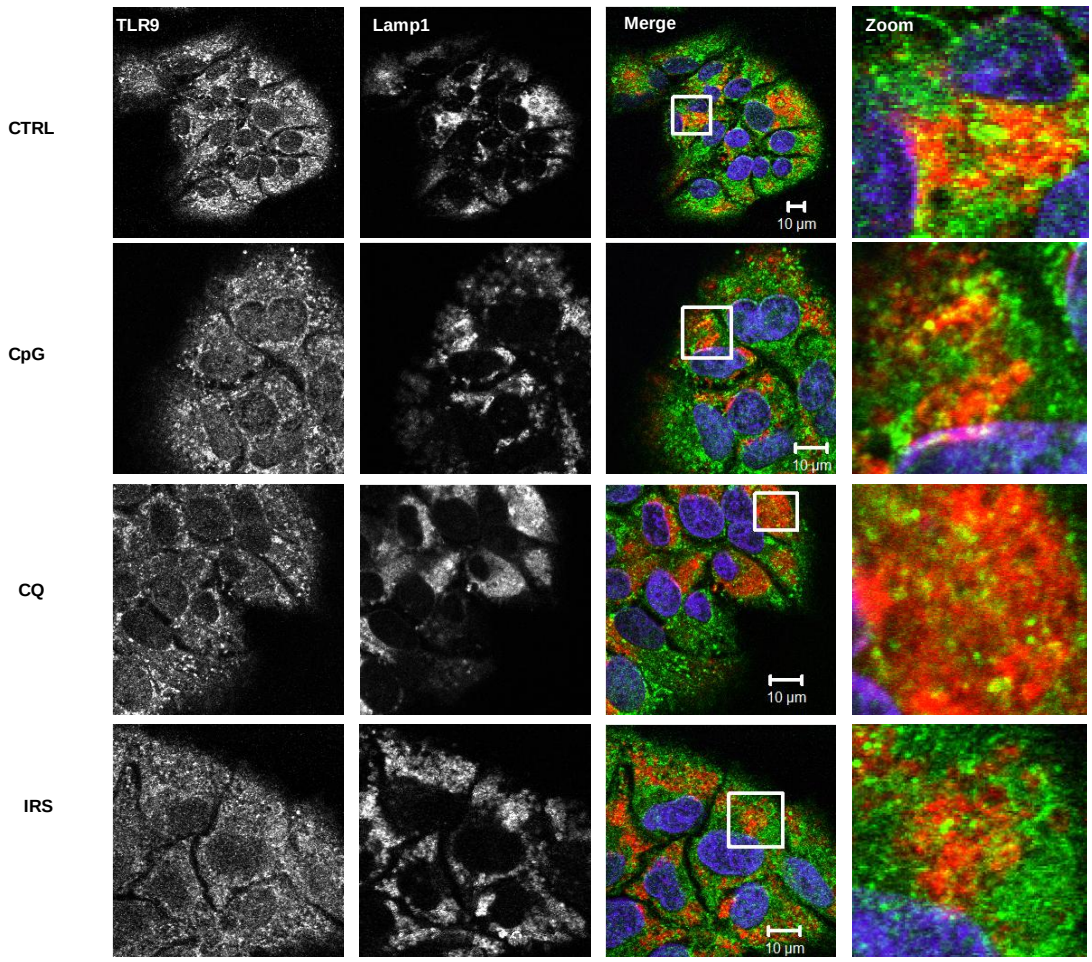

Figure 42: Limited co-localisation of TLR9 and lysosomal marker (lamp-1) found in HuH7 cells. In methanol fixed HuH7 and double immunofluorescence staining with TLR9 and lamp-1 antibodies, limited co-localisation was found between TLR9 and lysosomal marker lamp-1 (appeared yellow in colour in the merge channel). There were no changes detected for the TLR9 and lamp-1 co-localisation associated with CpG, chloroquine, or IRS treatment the merge panel showing TLR9 (green colour), lamp-1 (red colour) and Hoechst 33342 in nucleus (blue colour).

4.4.6 Swelling of lysosomes in response to chloroquine treatment of HuH7 cells

As it was expected from the known effect of chloroquine on lysosome, chloroquine treatment was associated with ballooning or swelling of the lysosome, which was detected with the lamp-1 staining (Fig. 43). This effect was not observed with CpG-ODN, IRS treatment and control untreated cells.

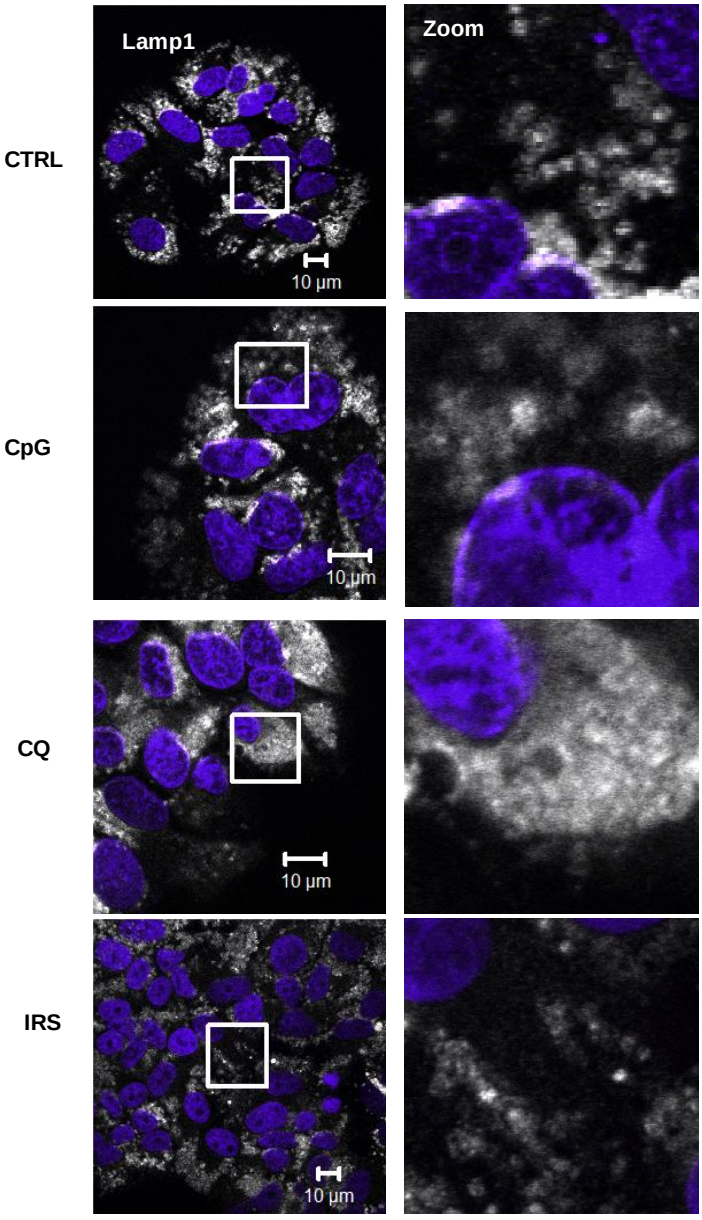

Figure 43: Lysosomal swelling associated with chloroquine treatment. Methanol fixed HuH7 stained with lamp-1 the late endosomal marker showing swelling of the lysosome with chloroquine treatment. Zoom box showing clearly the difference between lysosome labelled with lamp-1 with chloroquine treatment compared to the control, CpG and IRS treatment.

4.4.7 Results of TLR7 & TLR9 proliferation studies in HuH7 cells

Cell proliferation was assessed by seeding 10,000 cells per well (96-well plate) in triplicate for each condition. Cell viability was measured by adding 3-(4, 5-dimethylthiazol-2-yl)-5-(3-carboxymethoxyphenyl)-2(4-sulfophenyl)-2H-tetrazolium MTS reagent (Promega) treatment details and dosages are reported in materials and methods section.

a) <u>TLR7 stimulation with IMQ increased proliferation of HuH7 cells</u>

Treatment of HuH7 cells with IMQ for 48 hours resulted in a significantly higher rate of cell proliferation when compared to that of untreated control cells ($P < 0.04$) (t-test n=3).

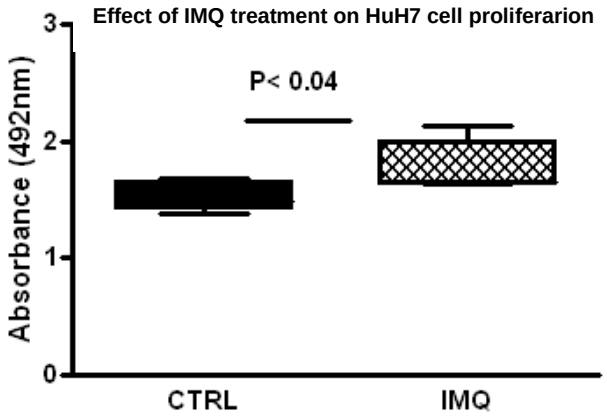

Figure 44: Increased HuH7 cell proliferation with IMQ treatment. After 48 hours incubation of 10^4 HuH7 cells in triplicate in 96-well plate, cell proliferation was measured using MTS proliferation assay. There was a significant increase in absorbance reading in the wells treated with 5µg/ml IMQ treatment (TLR7 agonist) compared to the untreated cells (P <0.04).

b) <u>HuH7 cell proliferation unchanged in response to TLR9 stimulation with CpG-ODN</u>

On the other hand, treatment of HuH7 cells with TLR9 ligand CpG for 48 hours did not show significant influence on HuH7 cell proliferation measured with the MTS assay.

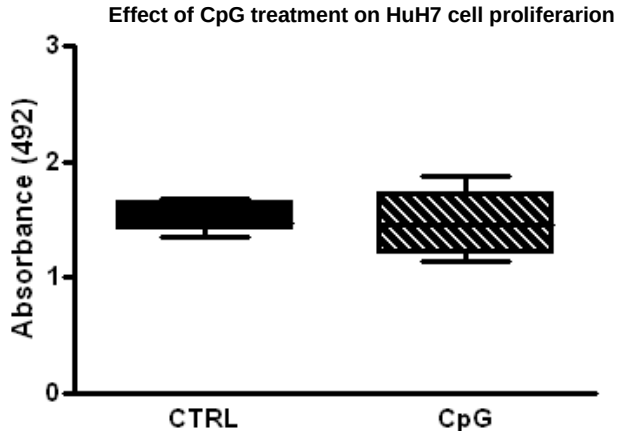

Figure 45: Graph demonstrating CpG-ODN treatment does not increase proliferation of HuH7 cells. The cells were incubated with 5 µM CpG (TLR9 agonist) for 48 hours and their proliferation rate was then measured using the MTS assay. There was no significant increase of absorbance in the CpG-ODN treated cells compared to untreated HuH7 control cells (CTRL). The experiment was conducted in triplicate

c) <u>Reduction of HuH7 Cell proliferation in response to chloroquine or IRS treatment</u>

Chloroquine treatment for 48 hours inhibited the proliferation of HuH7 cells. The level of absorbance measured showed significant reduction with chloroquine treatment compared to untreated cells ($P < 0.003$) (t test, n=3).

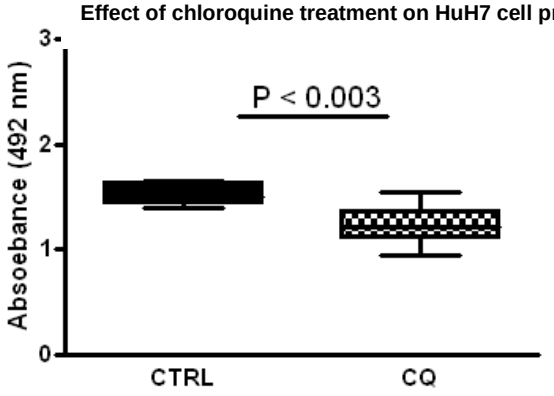

Figure 46: Graph demonstrating chloroquine treatment inhibited HuH7 cell proliferation. HuH7 cells were treated with 15 µM chloroquine for 48 hours and their proliferation rates were then measured by MTS assay. There was significant reduction of absorbance readings in the chloroquine treated cells compared with untreated control HuH7 cells (P <0.003). The experiment was conducted in triplicate.

Using MTS assay, it was found that IRS treatment for 48hours inhibited HuH7 cell proliferation. The inhibition of HuH7 cells proliferation with IRS treatment compared to the control untreated cells was significant (P <0.001) (t test, n=3).

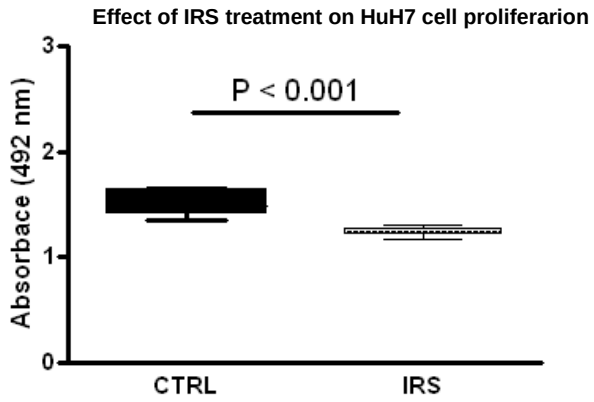

Figure 47: Graph demonstrating IRS treatment inhibited HuH7 cell proliferation. HuH7 cells were incubated with 20 µg/ml of IRS for 48 hours and their proliferation rate was then measured by MTS assay. There was a significant reduction of absorbance readings in the IRS treated cells compared with untreated control HuH7 cells (P <0.001). The experiment was conducted in triplicate.

d) <u>Inhibitory effects of chloroquine & IRS on HuH7 cell proliferation are not due to cytotoxicity</u>

The inhibition of HuH7 cell proliferation associated with chloroquine and IRS treatment raised the question whether the effect of chloroquine and IRS treatments treatment was inhibitory or due to cell cytotoxicity? To address this question a neutral red (NR) uptake test was performed (details in materials and methods section). The principle of NR test based on the binding of cationic supravital dye to anionic sites in the lysosomes of viable cells; the dead and the injured cells did not retain the dye.

Examination of HuH7 cells by light microscopy revealed the following:

Treated cells with chloroquine or IRS and also untreated cells picked up and retained the red stain (NR) inside all the cells (Fig. 48) the red dye inside all HuH7 cells could be proof that all cells alive and the treatment had not a cytotoxic effect suggesting that chloroquine and IRS effect could be inhibitory.

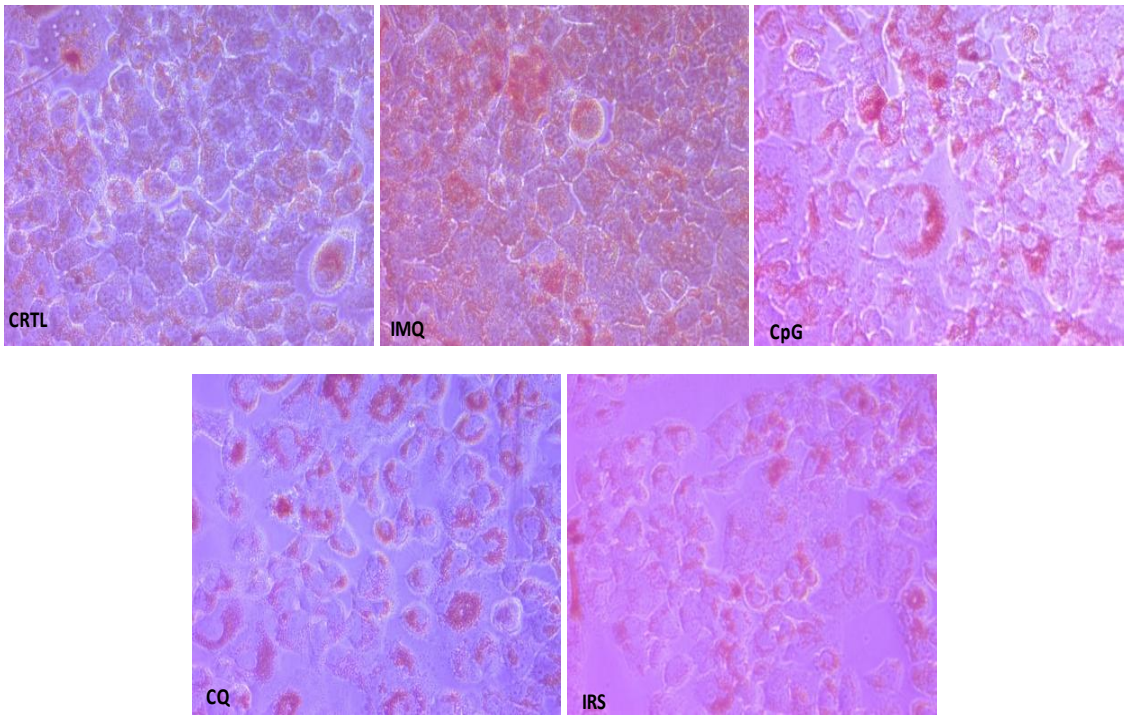

Figure 48: Chloroquine and IRS treatment had an inhibitory but not cytotoxic effect on HuH7 cell proliferation. Images shown are of HuH7 cells treated with IMQ, CpG-ODN, chloroquine (CQ), IRS or untreated control cells (CTRL) stained with neutral red. Uptake of the red dye can be seen in all cells from the different treatments indicating that they are viable. However, the density of cells treated with chloroquine or IRS is visibly less than that of control, IMQ or CpG treated HuH7 cells.

4.4.8 pAkt expression increased with IMQ but decreased with chloroquine & IRS treatment of HuH7 cells

After 48 hours of treatment, an increase in phosphorylated Akt (Ser 473) (pAkt) protein expression was observed with IMQ treatment but this was clearly reduced with chloroquine and IRS treatment compared to control (Fig. 49). There was no clear difference found with CpG treatment. These data suggest that inhibiting TLR7 and TLR9 may reduce cell proliferation through its effect of Akt pathway.

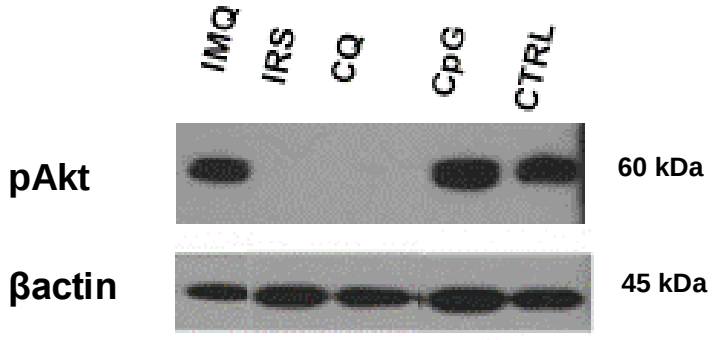

Figure 49: Western blot showing increased expression of pAkt protein in HuH7 cells after treatment with IMQ for 48 hours and decreased expression of pAkt protein in response to chloroquine (CQ) and IRS treatment.

4.4.9 Expression of LC3B autophagy marker increased with chloroquine treatment of HuH7 cells

The expression of LC3B protein increased with chloroquine treatment (Fig. 50) and this can be explained by the fact that chloroquine is known to inhibit autophagic degradation by preventing the fusion of lysosomes with autophagosomes, this lead to accumulation of LC3B protein without consuming and the net result is inhibition of autophagy despite the high level of LC3B expression. There was no expression of LC3B in control HuH7 cells suggesting that there is no role for autophagy in proliferation in these cells.

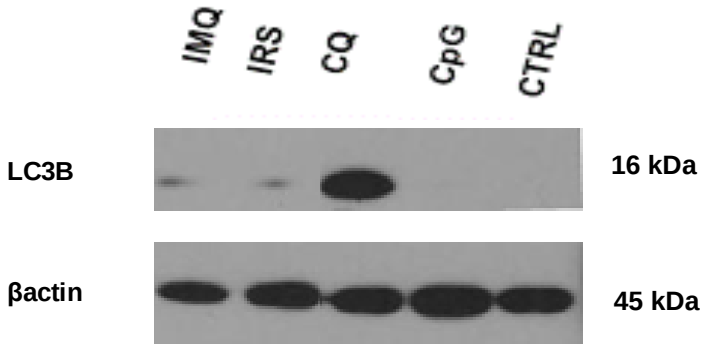

Figure 50: Western blot showing increased expression of LC3B protein in HuH7 cells after 48 hours of treatment with chloroquine. There was no expression of LC3B in the control untreated cells or in cells treated with CpG. The IMQ and IRS treated HuH7 cells expressed very low levels of LC3B.

4.4.9 Discussion

Following the immunohistochemistry data which showed up regulation of TLR7 and TLR9 in the HCC tissue samples in Chapter 4.3, this section was concerned with looking at expression of these two markers in the human carcinoma cell line HuH7. I was particularly interested in studying the effect of TLR7 and TLR9 agonists and antagonists on HuH7 proliferation and whether these treatments change their sub-cellular localisation.

The expression of TLR7 and TLR9 was initially examined using immunofluorescence staining with antibodies against each TLR. TLR7 was found to be expressed mainly in the nucleus whereas TLR9 expression was mainly cytoplasmic. There have been no reports of TLR7 studies in human hepatocellular carcinoma cell lines. A study by Tanaka and colleagues examined TLR9 expression in HCC cell lines, such as HuH7 and HepG2. They reported that membranous and cytoplasmic TLR9 expression was detected in HCC cell lines and may play an important role in tumourigenesis (Tanaka et al., 2010).

The sub-cellular localisation of TLR9 within cells has been shown alter in response to certain stimuli. Specifically, in dendritic cells TLR9 translocates from the ER to the endosomes upon stimulation with its CpG-ODN ligand. This translocation results in the activation and recruitment of the dendritic cells (Latz et al., 2004). As with TLR9, TLR7 is also known to localise within the endosomal compartments of many cells (Ewald et al., 2008) and contributes to signal transduction in the nucleus (Platta and Stenmark, 2011). For this reason, I decided to examine the effect of certain agonists and antagonists of TLR7 and TLR9 in the human HCC cell line HuH7 to see if these had any effect on the sub-cellular localisation of these TLRs. This was done by treating the HuH7 cell line with imiquimod (IMQ), TLR7 agonist, CpG (TLR9 agonist) chloroquine (Yasuda et al., 2008) and IRS (the latter are each inhibitors of TLR7 and TLR9) and comparing the sub-cellular distribution of each TLR in the treated and non-treated control cell lines by immune-fluorescence staining and laser-scanning confocal microscopy.

The distribution of TLR7 in the treated cells remained in the vicinity of the nucleus despite stimulation with IMQ or inhibition with chloroquine or IRS. The TLR7&TLR9 inhibitors chloroquine and IRS also had no effect on the cytoplasmic distribution of TLR9. However, the sub-cellular localisation of TLR9 was found to alter in response to CpG-ODN stimulation resulting in TLR9 staining vesicles accumulating around the Hoechst dyed nuclei. This change from a cytoplasmic to nuclear distribution of TLR9 has never been described in humans although it finding has been reported in equine lung **(**Schneberger et al., 2009).

TLR9 was shown in previous studies to be localised in the ER in macrophages and dendritic cells (Latz et al., 2004) and in Hela cells prior to TLR9 stimulation (Leifer et al., 2004). For my study the localisation of TLR9 within the cytoplasm in response to its stimulation (with CpG-ODN) with inhibition (using IRS and chloroquine) in HuH7 cells was examined to see if TLR9 co-localised with the endoplasmic reticulum marker calnexin under any of these different conditions. This was done by dual immunofluoresence staining using a TLR9 marker in addition to the endoplasmic reticulum marker calnexin. I found no evidence of co-localisation between TLR9 and calnexin in HuH7 cells in any of my experiments. The undetctable co-localisation between TLR9 and calnexin in the HuH7 cells might be explained by the fact that TLR9 can locate to different compartments within different cell types e.g. TLR9 is found translocate from the cell membranes to nuclei of equine lung tissue (Schneberger et al., 2009**)** whereas in human dendritic cells and macrophages it is found in the endoplasmic reticulum (Latz et al., 2004).

Another possibility may be that TLR9 is already maximally stimulated and located outside the endoplasmic reticulum in HuH7 cells. This is not an unreasonable prospect since it has previously been reported that DNA from damaged cells can also act as a stimulator of TLR9 (Basith et al., 2012).

In addition to the endoplasmic reticululm, subcellular localisation of TLR9 has also previously been reported in the endo-lysosomal system. For this reason I decided to look for any co-localisation of TLR9 with the lysosomal marker lamp-

1 within HuH7 cells under the different experimental conditions. I found limited co-localisation of TLR9 and lamp-1 markers regardless of stimulation or inhibition of TLR9 suggesting that TLR9 may reside in the lysosomes of HuH7 cells. The translocation of TLR9 from the ER to lysosomes in response to stimulation (de Jong et al., 2010) has previously been reported in human dendritic cells and macrophages (Latz et al., 2004). The co-localisation of TLR9 and lamp-1 in HuH7 cells is therefore consistent with the idea that TLR9 is already stimulated within these cells.

The effect of TLR7 and TLR9 stimulation or inhibition on proliferation of HuH7 cells was examined by treating these cells with IMQ, CpG-ODN, choroquinie or IRS over a time course of 72 hours and measuring cell proliferation at intervals of 24, 48 and 72 hours using the MTS assay. Using the TLR7 agonist IMQ, a significant increase in cell proliferation was found at 48 hours of treatment ($P < 0.04$) (Fig. 44). In vivo studies in a mouse model of pancreatic cancer has previously shown that stimulation of TLR7 vigorously accelerated tumour progression and induced the activation of a variety of oncogenes and loss of number tumour suppressor genes (Ochi et al., 2012). They concluded that TLR7 may be a useful target against which to develop a therapeutic treatment in pancreatic cancer. This may also hold true for HCC.

Treatment of HuH7 cells with the CpG-oligodeoxynucleotide (CpG-ODN), a TLR9 agonist did not result in a significant increase in cell proliferation at any of the measured time points. This is consistent with the findings of Tanaka et al. who also failed to detect any significant increase in proliferation of HCC cells in response to CpG-ODN treatment alone (Tanaka et al., 2010). However, they did find it that CpG-ODN treatment was able to reduce the cytotoxic effects of the anti-cancer drug Adriamycin on the HCC cells. This effect was achieved via the up regulation of various apoptosis inhibitors such as Survivin, Bcl-xL, XIAP and cFLIP (Tanaka et al., 2010). One possible explanation for the lack of increase in proliferation of HuH7 and other HCC lines in response to CpG-ODN stimulation of TLR9 by may be that TLR9 is already working at maximum capacity within these cells and is therefore unable to respond to any additional stimulatory signals.

Treatment of Huh 7 cells with the TLR7 and TLR9 inhibitors chloroquine or IRS resulted in a significant reduction in cell proliferation after 48 hours of treatment ($P < 0.003$ and $P < 0.001$ respectively). The effect of IRS treatment on cell proliferation in cancer has not previously been reported. However, the inhibitory effect of chloroquine treatment on cell proliferation has been demonstrated in other cancer cell lines derived from the lung and colon (Fan et al., 2006 and Zheng et al., 2009). These findings along with those from our present study strongly support a role for TLR7 and TLR9 in the promotion of HCC proliferation.

The process by which chloroquine and IRS bring about a reduction in HCC proliferation was examined more closely by conducting a viability assay using neutral red on HuH7 cells following 48 hours of treatment with chloroquine, or IRS. The uptake of neutral red was found to be retained in the lysosomes of all cells treated with choroquine or IRS and it was no different from that of untreated HuH7 cells or those treated with CpG-ODN or IMQ. In other words the inhibitory effect on proliferation of HuH7 cells following treatment with chloroquine or IRS was not due to cell death resulting from any cytotoxic effect of these drugs. A previous study on systemic lupus reported that using IRS 954 had no cytotoxic effect on cells (Guiducci et al., 2010).

In order to decipher more accurately the mechanisms by which IMQ, CpG, chloroquine, IRS exert their effects on cell proliferation I decided to look for signaling pathways through which they may operate. Akt has considered as one of the most activated proteins in many of human cancers and its activity in cancer cells could be explained by its ability to promote cell survival (Bhaskar and Hay 2007). Furthermore, chloroquine has been shown to be an effective chemosensitizer when used in combination with PI3K/Akt inhibitors (Loehberg et al., 2012). For this reason I decided that to examine the effects of chloroquine, IRS, CpG-ODN and IMQ treatment on the pAkt pathway in HuH7 cells. This was carried out by Western blot analysis using a pAkt antibody, which is the active form of Akt, on HuH7 cells from the different treatment groups. pAkt expression was markedly reduced in the HuH7 cells in response

to treatment with chloroquine or IRS for 48 hours. This suggests that inhibition of Huh 7 proliferation by chloroquine and IRS is brought about via their action on the Akt pathway. In comparison with untreated HuH7 cell the levels of pAkt expression in the IMQ-treated cells was found to be increased. However, no obvious difference was detected in the CpG-ODNs treated cells. Our Western blot data would suggest that proliferation of HuH7 cells involves TLR7 and TLR9 and that these exert their effects by acting via the Akt pathway. This concept is supported by other studies, Ochi and colleagues found markedly increased expression of pAkt in response to stimulation of TLR7 with ssRNA40 in K-ras transformed mouse pancreatic cells (Ochi et al., 2012). In a model of sepsis–induced cardiac dysfunction, CpG–ODN was found to significantly increase the level of pAkt in mouse cardiomyocytes (Gao et al., 2013). In vitro studies by the same group also demonstrated that CpG-ODN promoted the association of TLR9 with Ras and that this resulted in phosphorylation of Akt. In another study by Sester and colleagues, CpG DNA-induced survival of murine bone marrow-derived macrophages was shown to be completely dependent on TLR9. Furthermore, this survival effect was abrogated by the inhibition of PI3K/Akt pathway (Sester et al., 2006).

As well as being an inhibitor of TLR7 and TLR9, it is well established that chloroquine can act as an inhibitor of autophagy in cells. Many cancers rely on the processes of autophagy to promote their growth and survival under stressful conditions (Pivtoraiko et al., 2009 and Janku et al., 2011). The inhibitory effects of chloroquine on cell proliferation were therefore examined in relation to autophagy in the HuH7 cells. Using western blot analysis the expression of LC3B, which is a marker of autophagy, was examined in HuH7 cells under the different treatment conditions. The expression of LC3B was found to be low in untreated HuH7 cells and in HuH7 cells treated for with IRS, CpG-ODN or IMQ for 48 hours, which would suggest that these cells are not relying on autophagy for their proliferation. However, the expression of LC3B was up regulated in HuH7 cells in response to treatment with chloroquine. This result is not unusual since enhanced expression of LC3B and concomitant inhibition of autophagy has been reported by others (Boya et al., 2005, and Ramser et al., 2009). Our western blot data would suggest that the reduction in proliferation of HuH7 cells

in response to treatment with chloroquine is not associated with inhibition of autophagy. These results support the hypothesis that TLR7 and TLR9 play an important role in cell proliferation. However, these *in vitro* studies need to be confirmed *in vivo*.

4.5 Examination of TLR7&TLR9 in animal models of HCC

4.5.1 Introduction

Enhanced expression of TLR7 and TLR9 and their impact on tumour progression has been reported in hepatocellular carcinoma (HCC) and pancreatic cancer in previous studies (Tanaka et al., 2010 and Ochi et al., 2012). Inhibition of these receptors therefore can potentially retard the rate of growth of these tumours and delay progression. This effect has been observed in studies where adjunctive therapy with chloroquine, a non-specific inhibitor of TLR7 & 9, resulted in enhanced effect of traditional anticancer drug regime in the treatment of HCC (Ding et al., 2011 and Shi et al., 2011). Along with these studies, the effect of chloroquine and IRS (inhibitors for TLR7 and TLR9) on HCC cell line, HuH7, had been investigated in the previous chapter. We found that chloroquine or IRS treatment significantly reduced HuH7 cell proliferation after 48 hours compared to untreated cells. These observations led to the present set of experiments, which were aimed at studying the effect of chloroquine and IRS treatment on tumour growth *in vivo*. The effect of using TLR7- and TLR9-specific antagonists (IRS) or non-specific inhibitor (chloroquine) was studied in two animal models of HCC (xenograft model and chemical induced HCC).

4.5.2 Effect of chloroquine and IRS in mouse xenograft model of HCC

A xenograft model of HCC was used to clarify the effect of chloroquine and IRS treatment on tumour volume. Two HCC cell lines were used (HuH7 and HepG2).

a) <u>Method</u>

The material and method of surgery, injection of the cells and the tumour formed had been described in detail in chapter one. The animals divided into four groups. Each group contained 4-7 NOD-SCID mice:

- Group one (control): Intrahepatic injection of $5x10^6$ cells either HepG2 or HuH7 cells in mice with in 100µl of saline. These mice didn't receive any treatment. Mice injected intrahepatic with HepG2 n=5 and with HuH7 n=7
- Group two: The same as group one but received chloroquine in the form of 130 mg of chloroquine dissolved in one litre water and supplied as drinking

water. Mice injected intrahepatic with HepG2 n=5 for 60 days and with HuH7 n=6 for 35 days.

- Group three: the same as group one and injected with IRS-954 100μg (in 100μl) IP once per week. HepG2 n=4 for 60 days and with HuH7 n=7 for 35 days.

- **Measurement of tumour volume from mouse xenografts**

The tumour masses formed from cell injections were found:

- Inside the liver (intra-hepatic) and/or
- Attached to the muscle of the abdominal wall overlying the liver (extra-hepatic).

As described previously, the volume of each mass was measured separately by multiplying it three dimensions and the total volume was calculated by summation of the two volumes formed intrahepatic and extra-hepatic.
Results were presented as mean +/- SD. To compare between groups, unpaired t-test was used to compare one group of treatment to untreated control group.

b) <u>Results from the mouse xenograft models</u>

I. Histopathology of liver tumours derived from HepG2 and HuH7 injected mice

Histological assessment revealed that the masses formed inside and outside the liver formed of malignant cells with nuclear atypia, increased nucleo-cytoplasmic ratio and atypical mitotic figures. The microscopic features of the cells suggested features of malignant hepatocytes. Inside the tumours there were areas of haemorrhage and necrosis.

II. Volume of liver tumours from HepG2 injected mice

HepG2 injected mice developed both intra-hepatic and extra-hepatic tumours. The mean total tumour volume at the time of sacrifice was lower in both treated groups compared with the untreated group; control: 2.2±1.5; chloroquine: 0.4±0.3 and IRS: 0.6±0.3 cm^3 respectively.

Table 12: Volume of HepG2 derived tumours from mouse xenograft models of HCC in response to different treatments.

	Tumour volume (Mean±SD) cm^3			P value
	Intrahepatic	**Extrahepatic**	**Total**	
Control	0.99±0.6	1.2±1.1	2.2±1.5	
Chloroquine	0.2±0.3	0.3±0.35	0.4±0.3	0.03*
IRS	0.06±0.1	0.6±0.3	0.6±0.3	0.06

There was a significant reduction of total tumour volume (summation of intrahepatic and extrahepatic) with chloroquine treatment compared to control untreated mice (P <0.03) (Fig. 52). Although there was no significant reduction in total tumour volume between IRS treated group and control, the tumours formed intrahepatic in the group treated with IRS were the smallest volume between all the groups. It was noticed that even the largest tumour volume in the groups treated with either chloroquine or IRS showed marked necrosis compared to control.

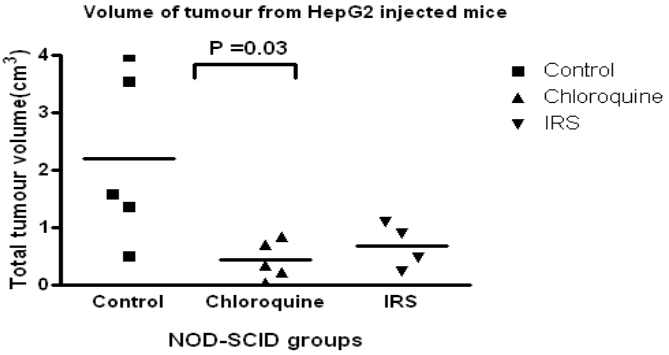

Figure 51: Graph demonstrating total volume of HepG2 derived tumours (both intra- and extra-hepatic) in the mouse xenograft models of HCC. There is a significant reduction of total tumour volume in the chloroquine treated mice compared to that of untreated control group (P =0.03).

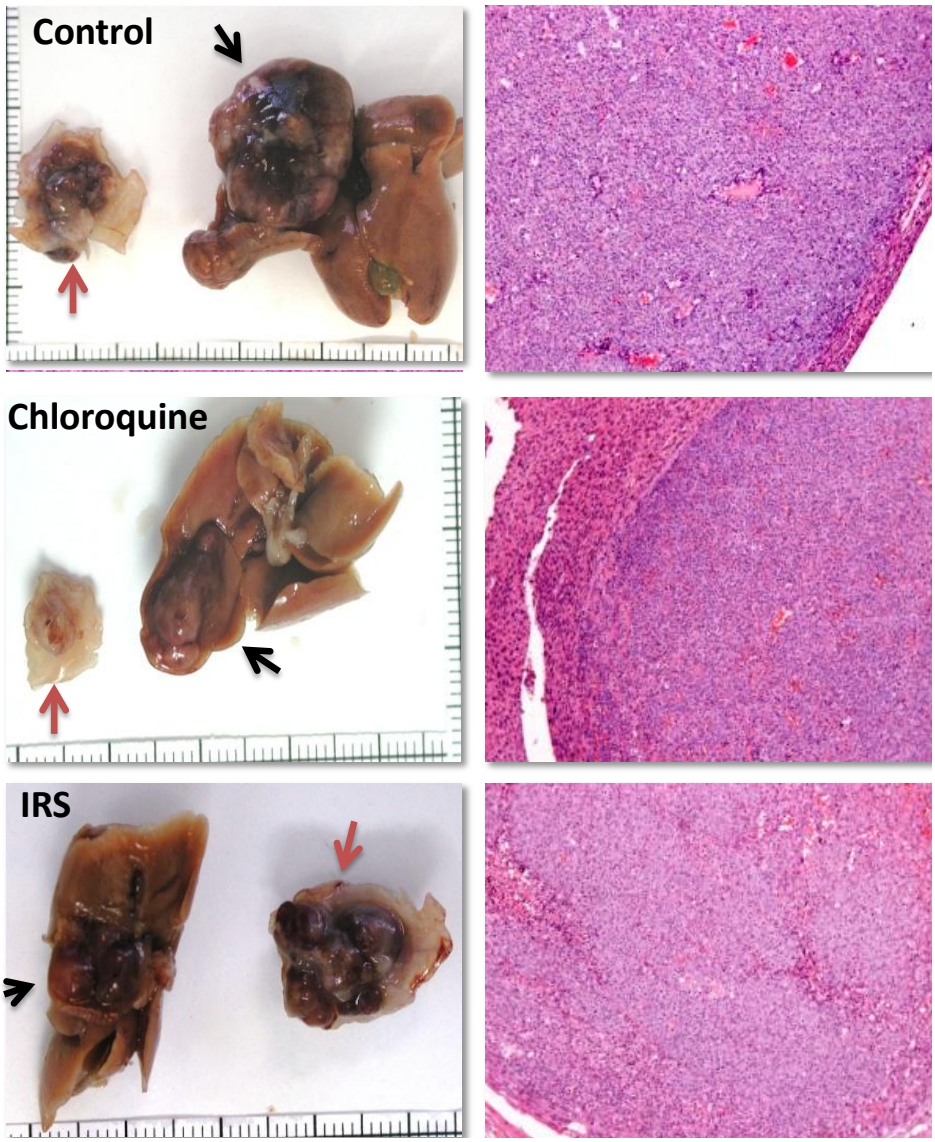

Figure 52: Tumour volume decreased in response to chloroquine and IRS treatment in the HepG2 derived mouse xenograft model of HCC. Black arrows point to intra-hepatic and red arrows point to extra-hepatic tumours. The intra-hepatic tumour is visibly larger in the liver of the untreated control mouse compared to that in chloroquine and IRS treated mouse. The H & E stained sections to the right show the histopathological features of the tumours.

III. Volume of liver tumours from HuH7 injected mice

HuH7 injected mice developed both intrahepatic and extrahepatic tumours (attached to the abdominal wall) in the animals with or without treatment. The mean tumour volume was lower in both the treated groups compared with the untreated group; control 2.3±1.3 cm^3, chloroquine 0.9±0.97cm^3.and IRS: 0.9 ± 0.7 cm^3

Table 13: Volume of HuH7 derived tumours from mouse xenograft models of HCC in response to different treatments.

	Tumour volume (Mean±SD) cm^3			P value
	Intrahepatic	**Extrahepatic**	**Total**	
Control	0.96±1.2	1.3±1.5	2.3±1.3	
Chloroquine	0.6±0.55	0.4±0.5	0.9±0.97	0.051
IRS	0.6±0.6	0.3±0.2	0.85±0.7	0.026*

The mice treated with chloroquine developed a borderline significant smaller tumour compared to untreated mice (P =0.05). However, a significant reduction of tumour volume was associated with IRS treated treatment (P <0.03) (Fig. 54). There was extensive necrosis with the treated groups either with chloroquine or IRS more than control in tumour with the largest tumour volume.

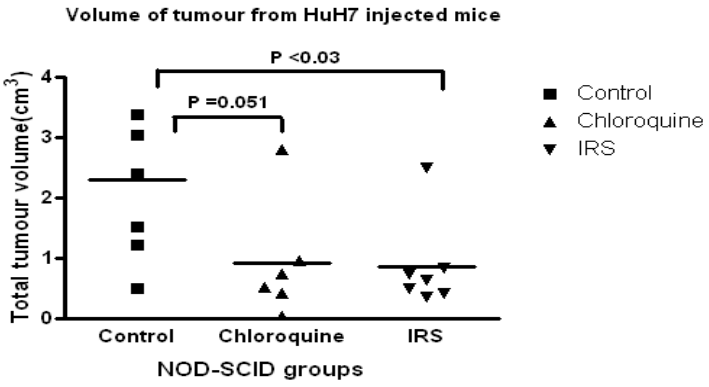

Figure 53: Graph demonstrating total volume of HuH7 derived tumours (both intra- and extra-hepatic) in mouse xenograft models of HCC. There is a significant reduction of total tumour volume in IRS treated mice compared to that of untreated controls group (P =0.03).

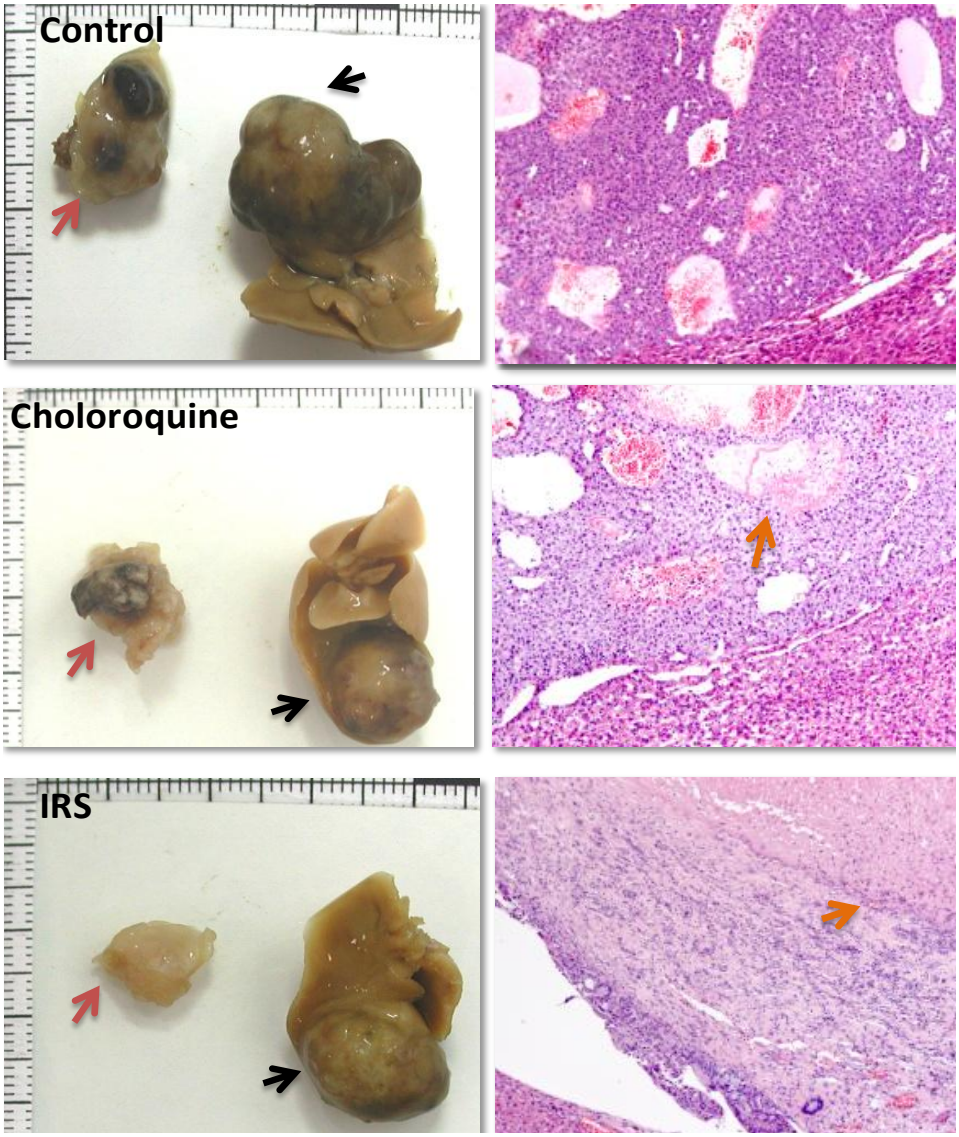

Figure 54: Tumour volume decreased in response to chloroquine and IRS treatment in the HuH7 derived mouse xenograft model of HCC. Black arrows point to intra-hepatic and red arrows point to extra-hepatic tumours. The intra-hepatic tumour is visibly larger in the liver of the untreated control mouse compared to that in chloroquine and IRS treated mice. The H&E stained sections on the right show the histopathological features of the tumours. There was necrosis in the tumour mainly the big one treated with chloroquine or IRS. Orange arrow points to the necrotic area.

4.5.3 Effect of chloroquine in a chemical-induced rat model of HCC

a) Method

Materials and steps of developing the model has been described in details in chapter one.

The animals divided into three groups of Fischer rats

- Group one: DEN and NMOR (carcinogens) treated rats (n=15).
- Group two: the same as group one but received chloroquine (Sigma, UK) 25mg/kg once a day by gavage for 14 weeks (n=20).
- Group three: naïve rat without treatment (n=4).

The development of HCC was assessed with macroscopic features and Haematoxylin and Eosin staining on liver rat. The assessment was performed on 8th, 10th and 12th and 16th weeks of treatment on selected rats from group one and group two.

b) Results from DEN & NMOR Rat Model of HCC

I. Histopathological assessment of rat livers

- **Macroscopic & Microscopic appearance of rat livers**
- Livers from rats treated with DEN&NMOR ± chloroquine were collected on 8, 10, 12 weeks after administration of DEN. After 16 weeks the rest of rats were culled. All rats were terminated under terminal anaesthesia. Livers from all groups were examined grossly and then liver sections were investigated under the light microscope.
- After 8 weeks of treatment with carcinogen (DEN&NMOR): liver section obtained from both groups treated with carcinogen with or without chloroquine did not show any evidence of HCC. However, liver sections from rats treated with carcinogen (n=3) had atypical cells in each liver with the following percentage 40%, 20% and 20%. The rats that received chloroquine (n=4) showed less atypical cells in 3 rats 5%, 5% and 20%.
- After 10 weeks of carcinogen treatment: two out of three of rats treated with carcinogen alone developed foci of HCC on a background of atypical cells. One out of three rats that received chloroquine showed one focus of dysplastic cells and not HCC on a background of atypical cells whereas the other two had normal liver**.**

- After 12 weeks of carcinogen treatment: all the rats of group one developed multiple nodules of HCC, which were seen macroscopically with variable sizes. Under the microscope there were multiple foci of HCC with a diameter of 2mm on a background of high-grade atypia in 90% of the cells and inflammation in the form of inflammatory cells infiltration with areas showing bridging necrosis and necroinflammatory foci scattered in the intralobular area. In chloroquine treated group, there was no evidence of malignancy. However, there were atypical cells which varied from 5% to 10%.
- At the end of the experiment after 16 weeks, all of the animals in group one developed multiple large nodules of HCC which were macroscopically visible (Fig. 55). Under the microscope there were multiple diffuse nodules up to 11 foci of HCC. The background liver was dysplastic and in some cases there were evidence of vascular invasion (Fig. 57). In group two, two out of seven animals developed small nodules of HCC (2 nodules each), the largest nodule did not exceed 1.4 mm. 5/7 had no evidence of HCC with normal hepatocytes and mild inflammation.

Figure 55: Livers from DEN&NMOR induced rat models of HCC demonstrating inhibition of tumour development in response to chloroquine treatment. a) The livers from DEN & NMOR only treated rats are pale in colour with nodules visible on the outer surface (white arrows) and in the cut section (black arrows). b) The livers from the chloroquine treated rats were brighter in colour with a smooth outer surface and no nodules visible in the cut section.

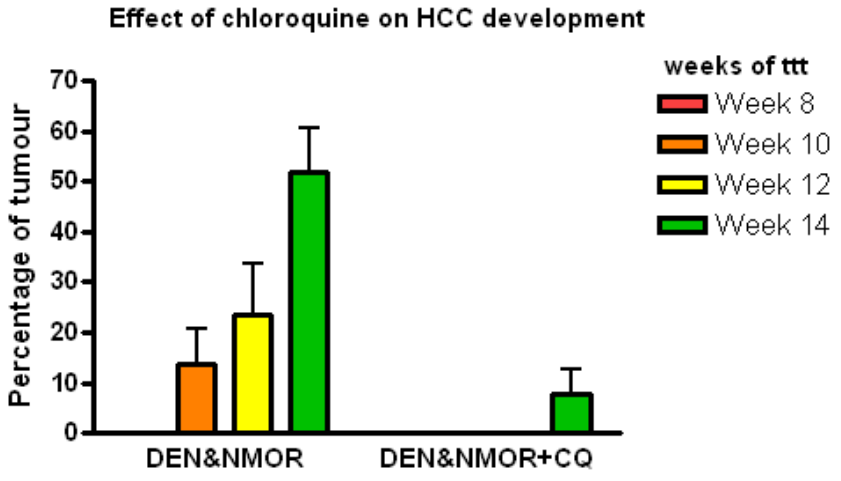

Figure 56: Graph showing the differences in the percentage of tumours developed in the livers of rats treated with DEN&NMOR±chloroquine. The percentage was calculated from the total size of HCC foci/ normal liver under microscopic examination of the slides from different time point of treatment (ttt: treatment).

Table 14: Data showing the difference in tumour development in the livers of rats treated with DEN&NMOR±chloroquine, (ttt: treatment)

	DEN&NMOR Mean±sd	**DEN&NMOR+CQ Mean±sd**	**P Value**
Percentage of tumour (tumour nodules sizes per tissue section/ size of tissue section *100)	12 weeks ttt 23.49±20.21 14 weeks ttt: 61.64±20.44	12 weeks ttt 0 14 weeks ttt: 4.540±8.1	 0.003**
Perentage of normal tissue in background tissue.	12 weeks ttt 7.50±5 14 weeks ttt 38.00±16.4	12 weeks ttt 80±33.7 14 weeks ttt: 85.71±7.87	0.008** 0.003**
Percentage of Atypical tissue in background tissue	12 weeks ttt 92.50±5 14 weeks ttt 62.00±16.4	12 weeks ttt 20.00±33.7 14 weeks ttt: 14.29±7.87	0.02* 0.003**

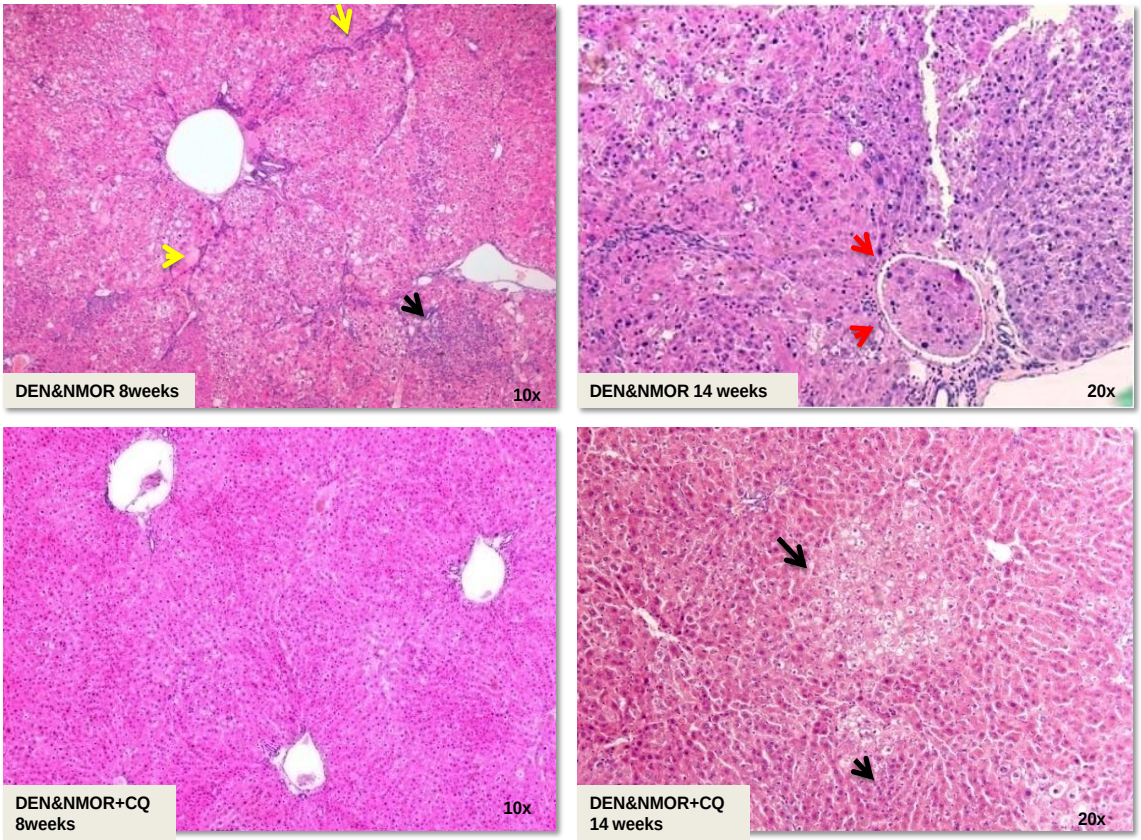

Figure 57: H&E stained liver sections from DEN&NMOR induced rat models of HCC at different stages of development. Foci of HCC (black arrows) are visible in the liver of the rat treated with DEN & NMOR for 8 weeks. After 14 weeks of treatment vascular invasion by malignant cells is observed (red arrows). The liver from a rat treated with DEN & NMOR plus chloroquine appears normal after 8 weeks of treatment. After 14 weeks of treatment small foci of HCC (black arrows) are visible in the rat liver

II. Assessment of liver fibrosis

Reticulin staining was performed on liver sections obtained from rats treated with DEN&NMOR±chloroquine.

- **<u>Reticulin staining in non-chloroquine treated rat livers</u>**
- On 8th week of treatment: Severe inflammation in the liver, in the form of portal tract expansion and bridging necrosis.
- On 12th week the inflammation progressed to fibrosis and formed incomplete septum.
- After 16 weeks: Severe fibrosis and incomplete cirrhosis (Fig. 58 and Fig. 59)

- **Reticulin staining chloroquine-treated Rat livers**
- After 8 weeks, liver sections showed histology varying from normal to mild inflammation (from 0 to 1).
- After 12 weeks of treatment, inflammation progressed to moderate inflammation up to 2.
- After 16 weeks the score of fibrosis found was 3/6-4/6.

DEN&NMOR 14 weeks

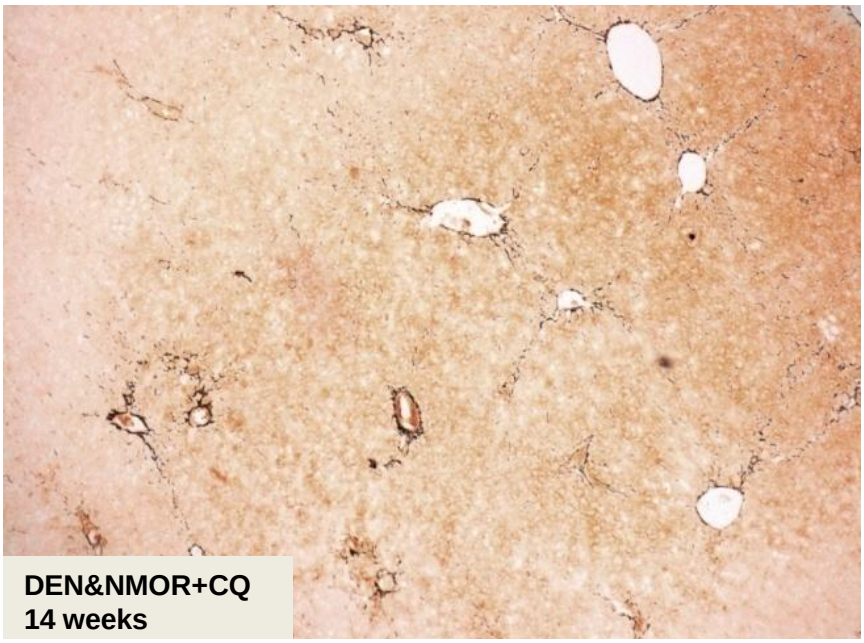

DEN&NMOR+CQ
14 weeks

Figure 58: Reticulin staining showing reduction in fibrosis with chloroquine treatment in chemical induced HCC model.

Table 15: The difference in the degree of liver inflammation and fibrosis between groups treated with DEN&NMOR±chloroquine. There was a significant reduction of fibrosis with chloroquine treatment

Weeks of treatment	DEN&NMOR	DEN&NMOR+ chloroquine
8	The degree of inflammation varied portal expansion to portal expansion with bridging fibrosis from (2/6 - 4/6)	There was no fibrosis there was portal expansion only in some cases and it was mild inflammation (0/6-1/6)
10	From bridging fibrosis portal to portal or portal to central and incomplete cirrhosis in one case (4/6-5/6)	The inflammation varied from no inflammation up to portal expansion with occasional bridging (0/6-3/6)
12	Incomplete cirrhosis marked bridging to occasional nodule (5/6)	From no inflammation to portal expansion with occasional bridging fibrosis (0/6- 3/6)
14	Incomplete cirrhosis (5/6)	Inflammation varied from portal expansion with occasional bridging fibrosis in some cases to marked bridging fibrosis with features or regressive (the bridging septa is incomplete) (from3/6-4/6)

- **Picro-Sirius Red staining in chloroquine & non-chloroquine rat livers**

Sirius red stain confirms the finding of reticulin stain. There was reduction of liver fibrosis score with chloroquine treatment. The fibrous tissue stained red in colour. There was bridging fibrosis after 10 weeks of treatment with DEN&NMOR, which progressed to incomplete nodule (pre-cirrhosis) after 14 weeks of treatment.

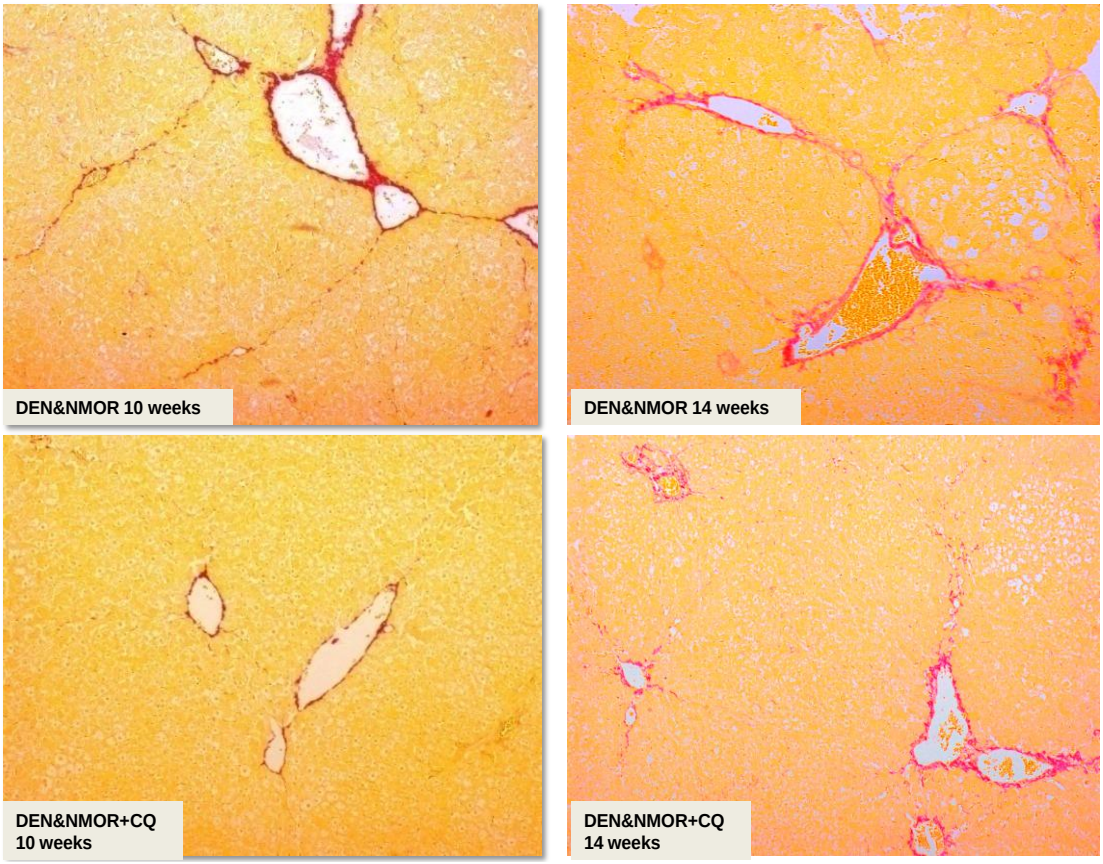

Figure 59: Sirius red staining showing levels of fibrosis in the liver of rats treated DEN&NMOR alone or with chloroquine. Rats treated with DEN&NMOR alone show evidence of liver fibrosis (red stain) after 10 weeks of treatment which progressed to pre-cirrhotic fibrosis after 14 weeks of treatment. The liver from the chloroquine treated rat showed no evidence of fibrosis after 10 weeks of treatment and the level of fibrosis was only moderate after 14 weeks.

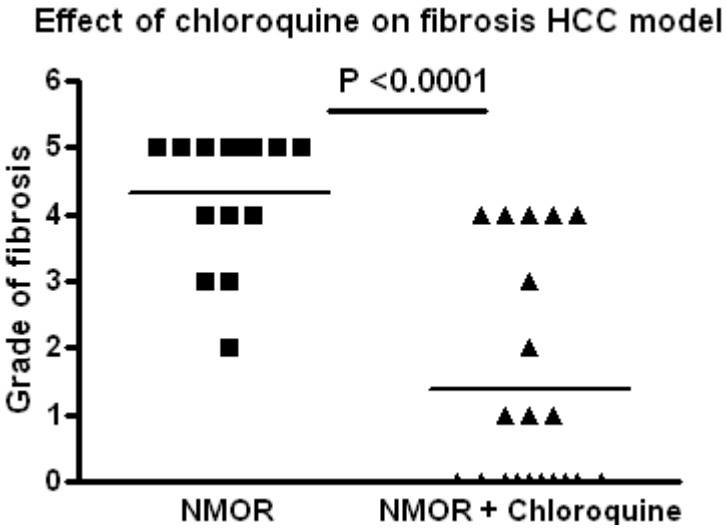

Figure 60: Graph showing the difference in liver fibrosis score between rats treated with DEN&NMOR±chloroquine. There was significant reduction of fibrosis with chloroquine treatment compared to the untreated group.

4.5.4 Improvement of rat liver enzymes in response chloroquine treatment

There was evidence of abnormal liver enzymes and bilirubin between the chloroquine treated and untreated groups. There was a significant reduction of alanine aminotransferase (ALT) (P <0.002), aspartate aminotransferase (AST) (P <0.001) and bilirubin (P <0.002) in group two that was treated with chloroquine compared to untreated group.

Table 16: Table showing improvement of liver enzymes and bilirubin with chloroquine treatment compared to the untreated group in HCC model. Results are presented as Mean±SE. ALT: alanine transaminase, AST: aspartate aminotransferase.

Test	Control	DEN&NMOR	DEN&NMOR +chloroquine
ALT	95.63±10.51	116±7.38	80±7.31
AST	98±5.63	109±3.47	90±2.072
Billirubin	1.2±0.06	1.6±0.089	1.2±0.05

4.5.5 TLR7 & TLR9 expression in livers of chloroquine and untreated rats

a) TLR7 expression in rat livers

TLR7 was found only perinucleir in malignant cells and juxtanuclear area.TLR7 was very high in intensity and distribution (Score 2) in liver sections obtained from chloroquine untreated group. With chloroquine treatment, TLR7 was found only in the areas with the small foci of HCC in 3 livers and with few cells (Score 1) and the rest livers from this group showed no staining of TLR7. Normal rat liver was negative for TLR7 (Fig. 61).

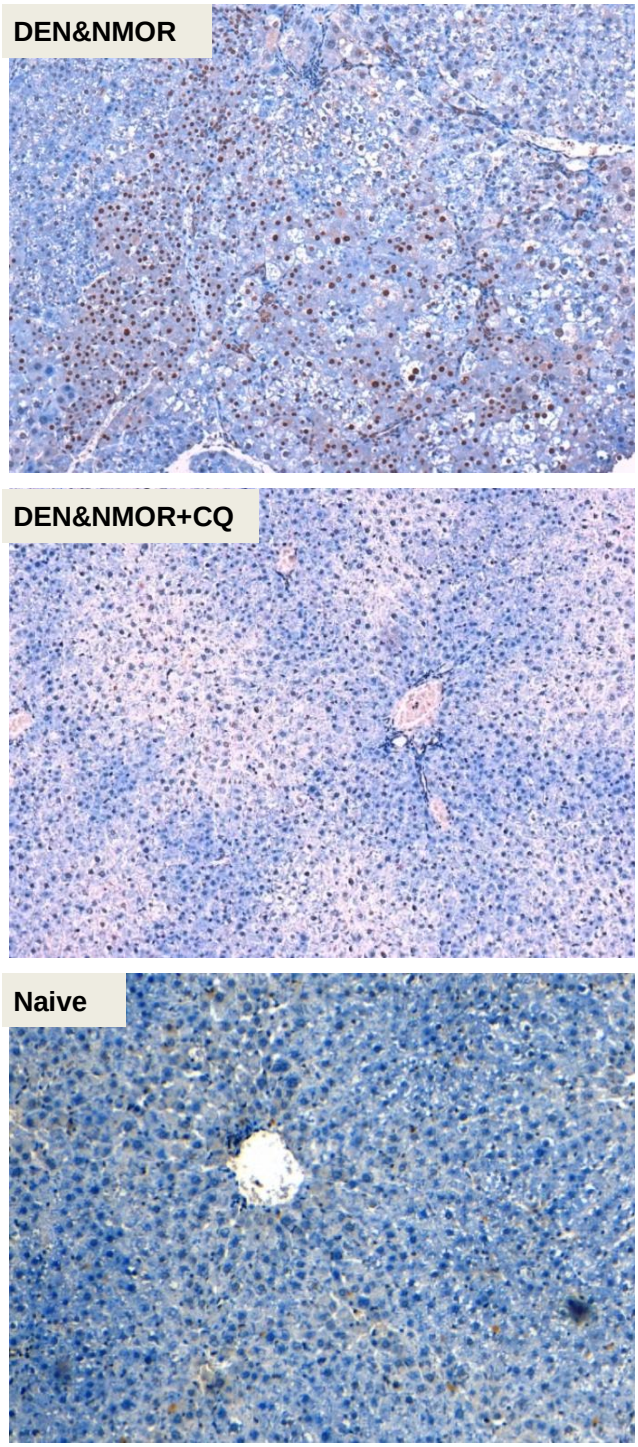

Figure 61: Immunohistochemistry staining of TLR7 in the DEN&NMOR HCC model. Liver section showing positive TLR7 in the nuclei of tumour areas induced with DEN and NMOR treatment (Score 2). With chloroquine treatment in addition to DEN&NMOR liver section revealed scattered cells stained with TLR7 in the nucleus of the cells less than 1/3 of the hepatocytes (Score 1). Liver section of naïve rat showing negative TLR7 staining.

b) TLR9 expression in rat livers

Hepatic localisation of TLR9 was different in each group. In the normal rat liver, TLR9 expression was very faint and located around the central vein only. With HCC development in the untreated group the distribution changed to surround the tumour nodules and was found in any zone of the liver including the portal area. The intensity of TLR9 staining varied from (++ - +++) and total Score was 2. Then with chloroquine treatment TLR9 was found around the central vein and the intensity was (++) and total Score was 1 (Fig. 62).

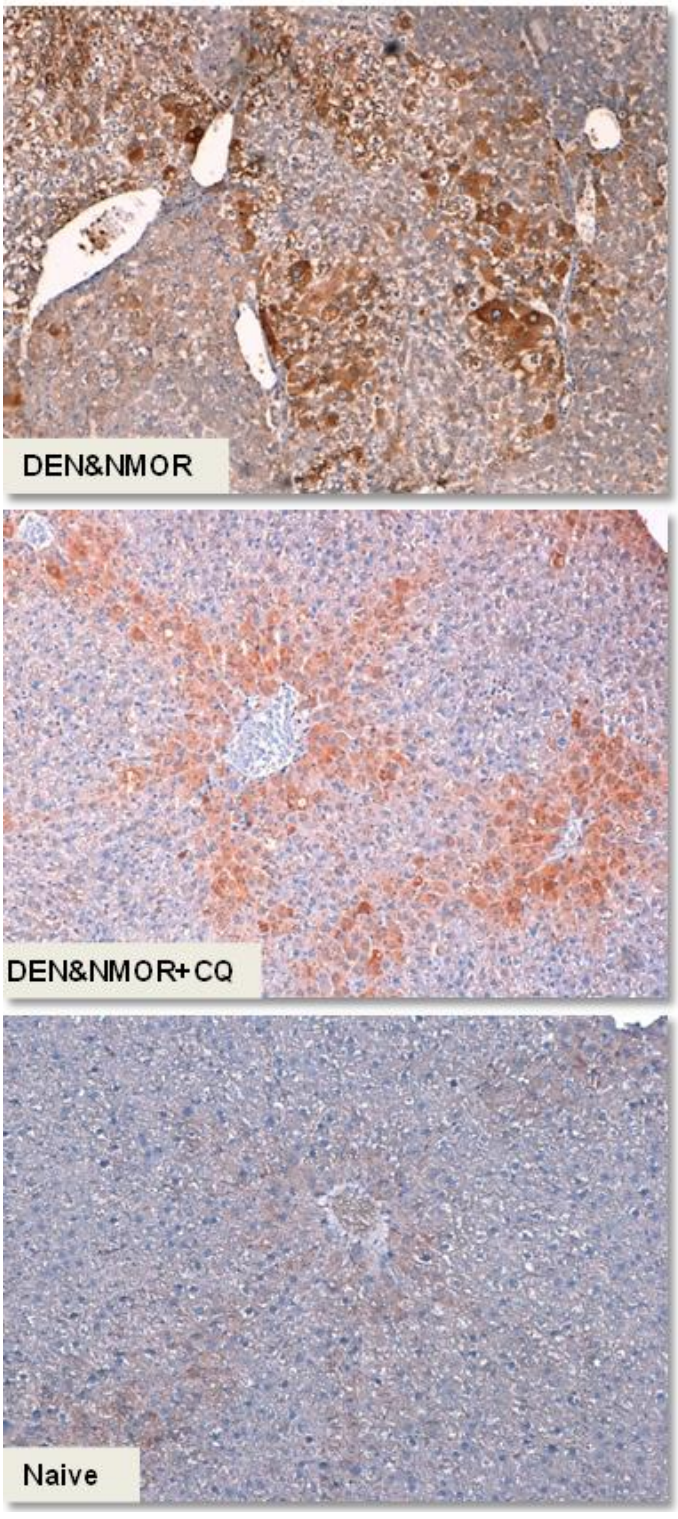

Figure 62: TLR9 expression in liver from DEN&NMOR induced rat models of HCC with or without chloroquine treatment and in normal untreated rat liver. TLR9 was highly expressed in the tumour and surrounding tissue of the liver from the DEN & NMOR treated rat. In the chloroquine treated rat, moderate expression of TLR9 was visible around the central vein only. Faint staining around the central vein was also be seen in the normal untreated rat liver.

4.5.6 Reduced expression of NF-κB in livers of rats treated with chloroquine

The expression of NF-κB, Akt and pAkt proteins were studied using western blot technique on liver lysate from DEN&NMOR treated rats, DEN&NMOR +chloroquine and Naïve animal. β-actin or α-tubulin was used as control for the loading proteins.

NF-κB protein expression was increased in liver lysate obtained from DEN and NMOR treated rats compared to naïve untreated animals. In liver lysates obtained from rats treated with chloroquine in addition to DEN and NMOR, NFκB expression was significantly reduced compared to DEN and NMOR only treated rats ($P < 0.05$)

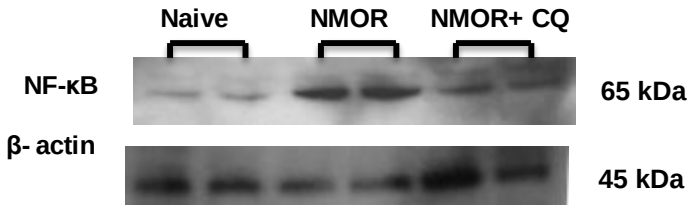

Figure 63: Western blot showing the effect of chloroquine on reduction of NF-κB in DEN and NMOR induced HCC compared to the untreated group.

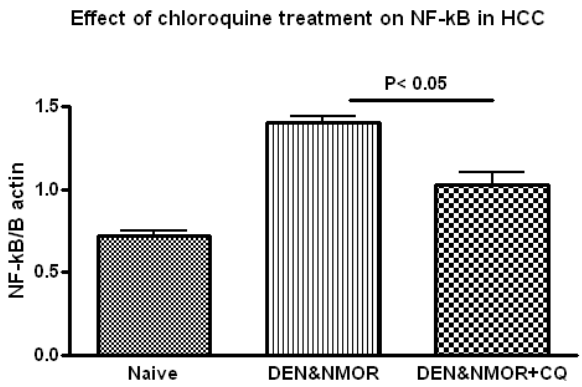

Figure 64: Densitometry results of the NF-κB Western blot from the DEN & NMOR induced rat model of HCC. Results are expressed as the ratio of NF-κB relative to β-actin signal. The graph demonstrates a significant reduction of NF-κB expression in response to chloroquine treatment in the DEN & NMOR rat model.

4.5.7 Reduced expression of Akt in livers of rats treated with chloroquine

Akt expression was increased with the progression of the tumour in HCC model as there was less in expression at 8 weeks compaired with of 14 weeks DEN and NMOR treatment. The effect of chloroquine in HCC model showed reduction of Akt expression compared with untreated animals at the same time points ($P < 0.001$). pAkt/Akt ratio did not change between DEN and NMOR with or without treatment. Although there was a reduction of pAkt this could be due to of a reduction of Akt expression.

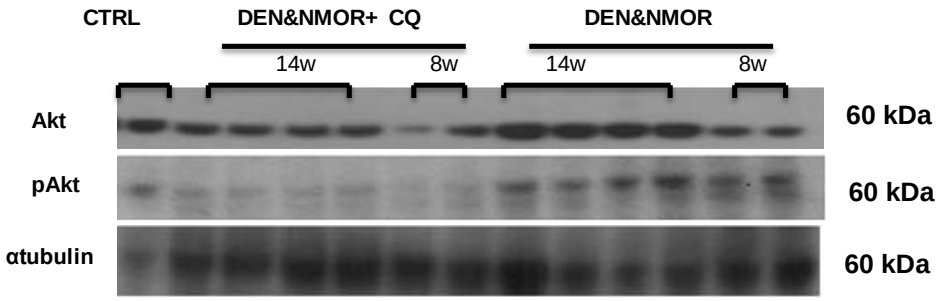

Figure 65: Decreased Akt expression in HCC model with chloroquine (CQ) treatment. Akt increased with tumour progression. 14 weeks treatment with DEN and NMOR showed increase in Akt expression compared with 8 weeks treatment. Chloroquine decreased the expression of Akt compared with untreated animals. There was reduction of pAkt with chloroquine treatment compared to DEN and NMOR without chloroquine.

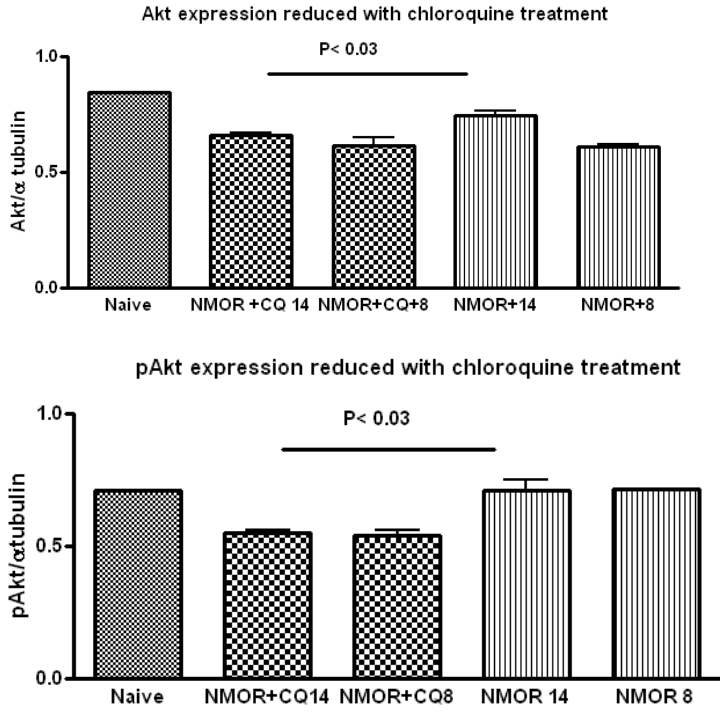

Figure 66: Chloroquine treatment reduced Akt and pAkt expression. Densitometric analysis of Akt/αtubulin and pAkt/αtubulin expression in HCC model, showing increased in the expression of Akt and pAkt in liver of DEN&NMOR treated rats and this high expression of Akt and pAkt significantly decreased with chloroquine treatment (P <0.03) and (P <0.03) respectively.

4.5.8 Discussion

The data from the immunohistochemical analysis of the human HCC tissue samples and the *in vitro* results from the HuH7 human HCC cell line experiments (Chapter 4.4) suggested that TLR7 and TLR9 may have an important role to play in HCC proliferation. The immunohistochemical data demonstrated increased expression of TLR7 and TLR9 in HCC. In addition, there was a good correlation between expression of these markers and the Ki-67 proliferation index. The results of the HuH7 cell culture studies demonstrated that the inhibition of TLR7 and TLR9 leads to suppression of cell proliferation. In order to confirm these findings *in vivo,* the effects TLR7 and TLR9 inhibition using chloroquine and IRS were investigated in the HCC mouse xenografts and chemically induced HCC rat models developed earlier in Chapter (4.1).

The mouse xenograft models consisted of two groups of NOD-SCID mice that had been injected with either HuH7 or HepG2 human HCC cells in their liver. The mice in each group were administered with either chloroquine in their drinking water or injected with IRS a day following the implantation of the HuH7 or HepG2 cells (described in Chapter 4.1). A control group of untreated HuH7 or HepG2 injected mice were also included in the study. At the end of the treatment period (35 days for the HuH7 mice and 60 days for the HepG2 mice) the animals were culled and their livers examined for tumours. Tumours were visible in the livers of all animals, both treated and untreated. In some mice, extra-hepatic tumours, attached to the abdominal wall were also observed. These are believed to have arisen as a result of leakage of tumour cells at the site of injection or direct tumour invasion. However, the mean tumour volume measured at the time of sacrifice was found to be lower in the animals administered either chloroquine or IRS when compared with the tumours from untreated mice.

The reduction in tumour volume was significant in the chloroquine-treated HepG2 injected mice ($P = 0.03$) but only reached borderline significance in the HuH7 derived tumours ($P = 0.05$). In the IRS treated mice the reduction in tumour volume was significant in the HuH7 derived tumours ($P = 0.02$) but not

significant in the HepG2 derived tumours (P =0.06). However, the number of animals in the latter group was very small (only 4 mice) due to the fact that some of the mice in this group died during the course of the study. The results from these *in vitro* experiments are consistent with the TLR7 and TLR9 data from the human HCC immunohistochemistry and HuH7 cell culture studies and provide additional support to the hypothesis that TLR7 and TLR9 play an important role in HCC proliferation. The inhibitory effect of chloroquine on HCC development has previously been demonstrated both *in vitro* and *in vivo* by Ding et al. and Shi et al. Specifically, the combined use of chloroquine with either oxaloplatin or sorafanib resulted in an enhancement of cell death in human HCC cultures and a more pronounced tumour suppression of HCC xenografts (Ding et al., 2011, Shi et al., 2011 and Shimizu et al., 2012).

Tumour xenograft models are a useful for examining human cancer behaviour *in vivo*. However, the need to establish them in immune-compromised animals means that any modulatory effect the immune system might have on tumour development is not accurately represented. Chemical-induced cancers in animal models provide an alternative means of studying tumour development within the environment of a fully functioning immune system. For this reason, the Fischer rat HCC model developed earlier, using DEN and NMOR, was also used to examine the effects of chloroquine on HCC development. DEN & NMOR rats were gavaged with chloroquine on a daily basis over a 14 week period then sacrificed at different time points (8, 10, 12, and 16 weeks) to examine their livers. A similar group of DEN & NMOR rats, which were not administered chloroquine, was also included in the study. Blood was taken from the animals prior to sacrifice to assess liver injury by measurement of the AST, ALT and bilirubin levels.

At 8 weeks from the start of the experiment no tumours were detected either macroscopically or histologically in any of the rat livers. In the chloroquine treated group 2 out of 4 rat livers were histologically normal but the other 2 showed signs of atypia involving 5 - 20% of hepatocytes. Mild inflammation of the liver was also seen in 2 cases. The liver inflammation was more severe and

the atypia more widespread involving 20 - 40% of hepatocytes in all 3 cases from the untreated group.

At 10 weeks multiple tumours were macroscopically visible in 2 of 3 livers from the untreated rats. Liver inflammation was severe and atypia more extensive involving 90-100% of rat hepatocytes in all 3 cases. However, no tumours were detected in any of the rat livers, either macroscopically or microscopically from the chloroquine treated group although some atypia and mild to moderate inflammation was visible in 3 of 4 cases. One liver was completely normal on examination.

At 12 and 16 weeks multiple tumours were macroscopically visible in all livers from the untreated rats and the cellular atypia was even more pronounced involving 50-90% of the background liver in all cases. This was accompanied by incomplete cirrhosis (5/6 according to the Ishak criteria) in all livers.
In the chloroquine treated group no tumours were visible at 12 weeks but atypia involving 5-10% of hepatocytes was seen in all 4 cases. At 16 weeks 2 of the 7 chloroquine treated rat livers developed tumours (2 nodules each) on a background cellular atypia involving 20-30% of hepatocytes.
The results from the rat HCC model above demonstrates that chloroquine treatment has a significant inhibitory effect on the development of inflammation or fibrosis ($P < 0.0001$) and HCC ($P < 0.0001$). The HCC *in vivo* data from the chemically induced rat model are similar to those from our mouse xenograft model and demonstrate that the inhibition of TLR7 and TLR9 leads to suppression of tumour growth regardless of an effective immune system. Furthermore, administration of chloroquine had a significantly beneficial effect on liver enzymes and bilirubin levels (all decreased to nearly normal levels) in the carcinogen treated rats suggesting that inhibition of TLR7 and TLR9 not only suppresses tumour growth (both frequency and size of tumours) but also has a protective effect on the liver from damage induced by carcinogens.
Overall the results from both the mouse xenograft and chemical-induced rat models of HCC further reinforce the concept that TLR7 and TLR9 play an important role in HCC growth. Furthermore, the data are a strong indicator that

the pathways to liver inflammation, fibrosis and hepatocarcinogenesis are closely linked to TLR7 and TLR9.
I demonstrated in previous section a significant effect of IRS 954 on inhibiting cell proliferation of HuH7 cells and this effect was translated into inhibitory effect on tumour masses in mice.

The effect of chloroquine on reducing liver fibrosis is demonstrated for the first time in this study. However, a previous study had shown that administration of chloroquine to chronic active hepatitis B patients returned AST and ALT values to normal levels (Kouroumalis and Koskinas et al., 1986). Another study in SLE patient diagnosed with autoimmune liver disease, chloroquine treatment was found to be effective in treatment of inflammatory conditions through its inhibitory effect on TLRs expressed on the dendritic cells (Efe et al., 2011) .
Several lines of investigation indicate that TLR9 is also up regulated in chronic liver diseases and promotes the development of non-alcoholic steatohepatitis and hepatic fibrosis (Gäbele et al., 2008, Stadlbauer et al., 2009 and Henao-Mejia et al., 2012). Increased circulating bacterial DNA is a hallmark of cirrhosis and the unmethylated CpG containing DNA serves as a potential ligand of TLR9 (Seki et al., 2012). Therefore, the inhibitory effect of chloroquine on fibrosis can be due to its inhibitory effect on TLR9.

In order to determine whether the action of chloroquine on the livers of the DEN&NMOR rat models of HCC was brought about through inhibition of TLR7 and TLR9 I also looked at the expression of these molecules by immmunohistochemisty. In normal naïve rats the expression of TLR9 was found to be extremely weak and confined to the central veins. However, in the DEN&NMOR treated rats expression of TLR9 was high (Score 2) and not confined to any particular region of the liver. In the rat livers which developed HCC, TLR9 was weakly detected within the tumours but its expression was high and heterogeneous in the surrounding liver tissue (Score 2). In the chloroquine treated rats, TLR9 staining was found to be weak (Score 1) but slightly higher than in the livers of normal naïve rats. It was also confined to the central veins. In the two chloroquine treated rats, which developed HCC, TLR9 was weakly present within the tumours but its expression was high in the immediate vicinity

of the tumour and in the hepatocytes around the central veins. Overall, it would appear that chloroquine treatment inhibits liver inflammation, fibrosis and tumourigenesis by inhibiting the expression of TLR9. However, its lack of expression within the rat tumours would suggest that TLR9 is not necessary for tumour growth. The results appear to contradict the data from the human HCCs and cell culture studies (Chapter 4.4) in which TLR9 is more highly expressed. One possible explanation for this discrepancy could be that TLR9 plays an important role during liver inflammation and initial stages of liver carcinogenesis in this rat model but its expression may not be necessary for tumour proliferation later on. Other TLRs or pathways could possibly take on more important roles during the later stages of tumour development and progression in these animals.

The expression of TLR7 was found to be completely absent in the livers of naïve rats. In the DEN & NMOR treated rats the expression of TLR7 in the early weeks was weak and involved less than one third of the hepatocyte nuclei (Score 1). However, TLR7 expression was higher in the tumours, which developed in later weeks (more than two thirds of malignant hepatocyte nuclei were positive for TLR7) (Score 2), although it remained low in the surrounding liver.

In the chloroquine treated group of rat livers, the expression of TLR7 was also absent in the early weeks of the experiment. As the weeks progressed, the expression of TLR7 increased slightly but still involved no more than one third of the hepatocyte nuclei (Score 1). In the livers and tumours, which developed in later weeks, the expression of TLR7 remained low (Score 1).

The TLR7 data in the carcinogen-induced rat model of HCC is more consistent than the TLR9 data with our findings in human HCC tissues and cell lines and provides further evidence that the inhibitory action of chloroquine on liver inflammation and tumour development is brought about through its inhibition of TLR7. Recent work that supports our findings comes from a study of pancreatic cancer in which TLR7 was shown to be highly expressed in the transformed epithelial cells as well as peritumoural inflammatory cells (Ochi et al., 2012). TLR7 expression was reported to be absent from the normal pancreas in

human and murine systems and furthermore, inhibition of TLR7 was shown to protect against development of pancreatic cancer. The authors concluded that TLR7 could be a potential target for treatment of pancreatic cancer in humans (Ochi et al., 2012). However, in contrast to the above, TLR7 activation has also been demonstrated to have antitumour properties and TLR7 agonists have been used as effective treatments for basal cell carcinoma (Tandon and Brodell, 2012) as well as melanoma (Adams et al., 2008). In order to explain these seemingly contradictory roles of TLR7, Ochi et al. proposed that in malignancies which are not associated with an inflammatory component TLR7 stimulation may elicit antitumour immune responses. However, malignancies that arise on a background of inflammation such as pancreatic cancer associated with chronic pancreatitis, TLR7 activation may have a pro-tumourigenic effect. Furthermore, TLR7 activation was found to stimulate tumour development in colon cancer and lung cancer by promoting inflammation as well as tumour cell survival (Grimm et al., 2010 and Cherfils-Vicini et al., 2010). The latter process seems also to apply to TLR7 and HCC.

The links between TLR9 and HCC have been discussed previously in Chapter 4.3 in light of Tanaka‘s study which reported that CpG-ODN promotes HCC proliferation and survival (Tanaka et al., 2010). In other cancer studies TLR9 activation was linked to promotion of cancer invasion in the prostate (Ilvesaro et al., 2007), breast (Merrell et al., 2006) in lung cancer cells, stimulation of the TLR9 pathway using CpG was recently shown to enhance tumour growth (Wang et al., 2012).

The mechanism of how TLR7 and TLR9 produce HCC is not completely clarified in this thesis. It is possible that the initial insults leading to liver inflammation leads to partial breakdown of the liver tissue which in turn leads to the release of ssRNA and unmethylated CpG DNA which act as stimulators of TLR7 and TLR9 respectively (Barrat et al., 2005). This in turn leads to the release of other pro-inflammatory cytokines and/or chemokines, which exacerbate the liver inflammation and increase the risk of developing of HCC. The inhibitory action of chloroquine on TLR7 and TLR9 may therefore help to

break this vicious circle by reducing the liver inflammation and thereby reduce the chances of developing HCC.

The expression of NF-kB protein in The DEN&NMOR rat model of liver inflammation and HCC was examined at the end of the experimental period, i.e. 16 weeks, in regions of liver tissue which were macroscopically free of tumour. Using Western blot analysis the expression of NF-kB in the liver of the DEN & NMOR only treated rats was seen to be higher than in the livers of naïve rats. However, this up regulated expression of NF-kB was diminished in the livers of the chloroquine treated rats. These findings are another confirmation that the reduced liver inflammation in response to chloroquine treatment occurs via a decrease in TLR7 and TLR9 stimulation leading to inactivation of the downstream NF-kB pathway. These results are consistent with the known action of TLRs in inflammatory pathways, which all culminate in the activation of NF-kB protein. The inhibition of TLR7 and TLR9 stimulation by chloroquine has previously been shown to significantly reduce the downstream activation of NF-kB in a human embryonic kidney cell line (HEK293) and human B cell line cell (Ramos) (lee et al., 2003). Furthermore, chloroquine has been shown to inhibit CpG-DNA–driven activation of NF-κB activation by acting as a TLR9 antagonist. Specifically, chloroquine inhibited binding of CpG to the TLR9 ectodomain (Kuznik et al., 2011). Our *in vivo* findings in the rat model of liver inflammation and HCC are consistent with the previous *in vitro* studies in the human cell lines and support the idea that NF-kB may act as a central link between hepatic injury, fibrosis and HCC as proposed by Luedde and Schwabe (2011).

One of the most frequently observed alterations in human cancer is the activation of the protein kinase Akt. This protein regulates a variety of cellular processes involved in cell survival and metabolism. The inhibition of Akt kinase previously has been shown to induce apoptosis and suppress the growth of human ovarian cancer cells *in vivo* and *in vitro* (Choi et al., 2008). In addition, chloroquine has been shown to reduce cell proliferation in a mouse colon carcinoma cell line and this effect was shown to be associated with a decreased level of pAkt (Zheng et al., 2009). Moreover, PI3k/Akt pathway inhibitors in combination with chloroquine have been shown to promote γ-irradiation-induced

cell death in primary stem-like glioma cells (Firat et al., 2011). Furthermore, CpG-ODN was shown to induce a protection against myocardial ischemic/reperfusion injury through activation of PI3K/Akt (Cao et al., 2013).

A link between Akt and TLR9 was demonstrated in the study by Guiducci et al., (2008) in which Akt phosphorylation was observed in human plasmacytoid predendritic cells following TLR9 stimulation with CpG. In light of the above information an investigation of Akt expression levels in our rat model was clearly warranted. The data from our study demonstrated a significant reduction in the levels of total Akt ($P = 0.03$) and pAkt ($P = 0.03$) in the livers of chloroquine treated rats when compared with the untreated rats. It is difficult to determine from our results whether the reduction in pAkt is just a reflection of the decreased total Akt levels or whether it is due to a direct reduction in Akt protein phosphorylation. Whichever the case, the findings are in keeping with the hypothesis that TLR7 and TLR9 up regulation play an important role in HCC by induction of Akt phosphorylation. Furthermore, the inhibition of these pathways could provide a novel approach to the treatment of HCC.

4.6 TLR expression in cholangiocarcinoma

4.6.1 Introduction

Hepatocellular carcinoma (HCC) and cholangiocarcinoma (CC) are primary liver cancers; CC is a malignant tumour that derives from cholangiocytes of either small intrahepatic bile ducts or ductules (intrahepatic cholangiocarcinoma; ICC), or of large extrahepatic bile ducts (extrahepatic cholangiocarcinoma; ECC). ICC and ECC differ in morphology, pathogenesis, risk factors, treatment and prognosis. However, some of the risk factors for ICC and HCC are the similar such as cirrhosis, chronic hepatitis B and C, alcohol use, diabetes, and obesity are major risk factors for ICC (Charbel and Al-Kawas, 2011). Moreover, there were recorded cases of mixed HCC and CC (Yano et al., 2003 and Chantajitr et al., 2006). This phenotypic overlap between HCC and CC is histopathologically an intermediate form between HCC and CC. In addition, there is a novel subtype of HCC was identified as cholangiocarcinoma like-HCC, which is believed to be derived from biliary lineage cells (Woo et al., 2010). These data suggest a common pathogenesis of primary intrahepatic epithelial cancers (HCC and ICC) (Palmer and Patel, 2012). I have shown previously that inhibition of TLR4 reduced liver fibrosis, which is one of the risk factors for developing HCC and ICC; also, I have shown that inhibition of TLR7 and TLR9 reduced the incidence and growth of HCC in animal models and *in vitro*. Unfortunately, there is not enough data supporting the role of toll-like receptors in CC development except in few studies on cholangiocarcinoma. These studies demonstrated that the carcinogenic effect of liver fluke Opisthorchis viverrini could be through chronic inflammation and stimulation of TLR2 or TLR4 (Pinlaor et al., 2005 and Ninlawan et al., 2010). Our aims in this chapter were to determine whether a) TLR4, TLR7 and TLR9 are up regulated in human CC. b) whether inhibition of the up regulated TLR signaling in CC reduced cell proliferation *in vitro* and tumour growth *in vivo*.

4.6.2 Results from human cholangiocarcinoma tissues

a) Results from tissue microarrays

By using immunohistochemistry technique and tissue microarray platform, ten cases of CC were compared with bile ducts in normal liver caes as control.

I. Decreased expression of TLR4 in cholangiocarcinoma

The normal bile duct epithelium was strongly positive (Score 2) for TLR4 in 80% and was moderately positive (Score 1) in 20% of cases. In CC, reduced TLR4 staining was observed compared to normal controls; 60% were negative and 10%-30% of cases stained for TLR4 (Score 2) (Score 1) respectively.

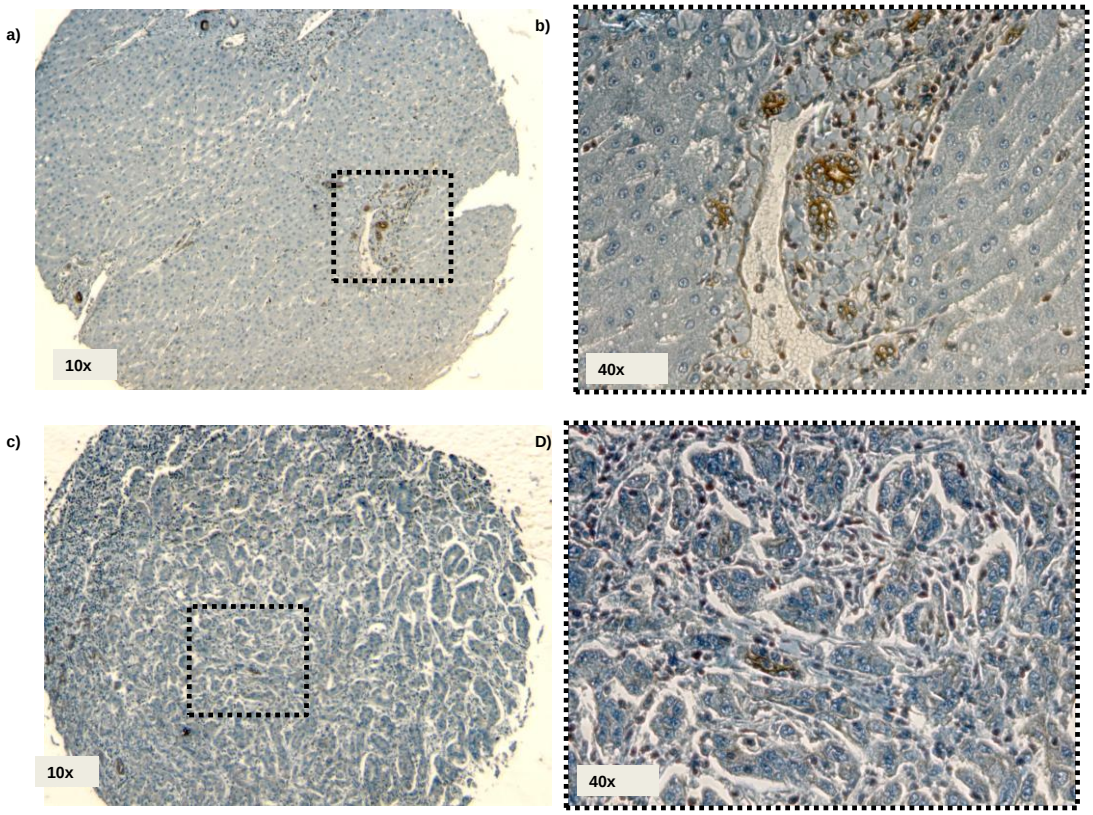

Figure 67: TLR4 expression analysis in normal liver and cholangiocarcinoma (CC). a) Normal liver section from the tissue microarray showing high expression of TLR4 in the bile duct epithelium but no expression in the hepatocytes. b) The area within the zooming box of image (a) is seen at higher (40x) magnification and shows more clearly the TLR4 expression in the bile ducts. c) CC section from the tissue microarray showing no expression of TLR4 in the malignant cells. d)At higher (40 x) magnification of the CC section, TLR4 expression is clearly visible in the inflammatory cells scattered within the tumour background.

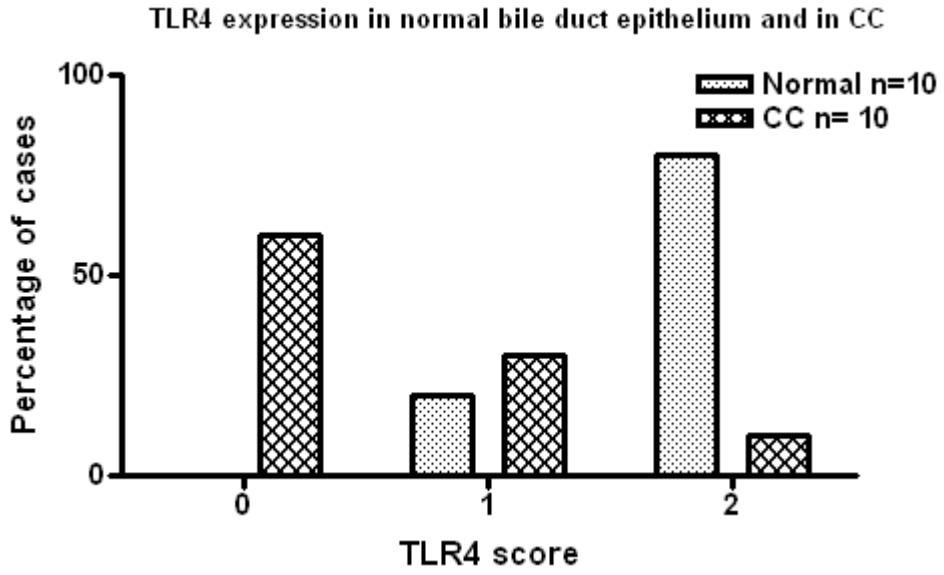

Figure 68: Graph showing the expression of TLR4 in normal bile duct and CC. There is up regulation of TLR4 in normal bile duct epithelium and down regulation in CC.

II. Increased expression of TLR7 in cholangiocarcinoma

All the normal bile duct epithelium were negative for TLR7 expression among the CC cases; 20% cases showed no staining of TLR7 while 30% cases had positive perinuclear staining of TLR7 in less than 1/3 of the tumour nuclei (Score 1) and 50% cases showed positive TLR7 in more than 2/3 of the CC nuclei (Score 2).

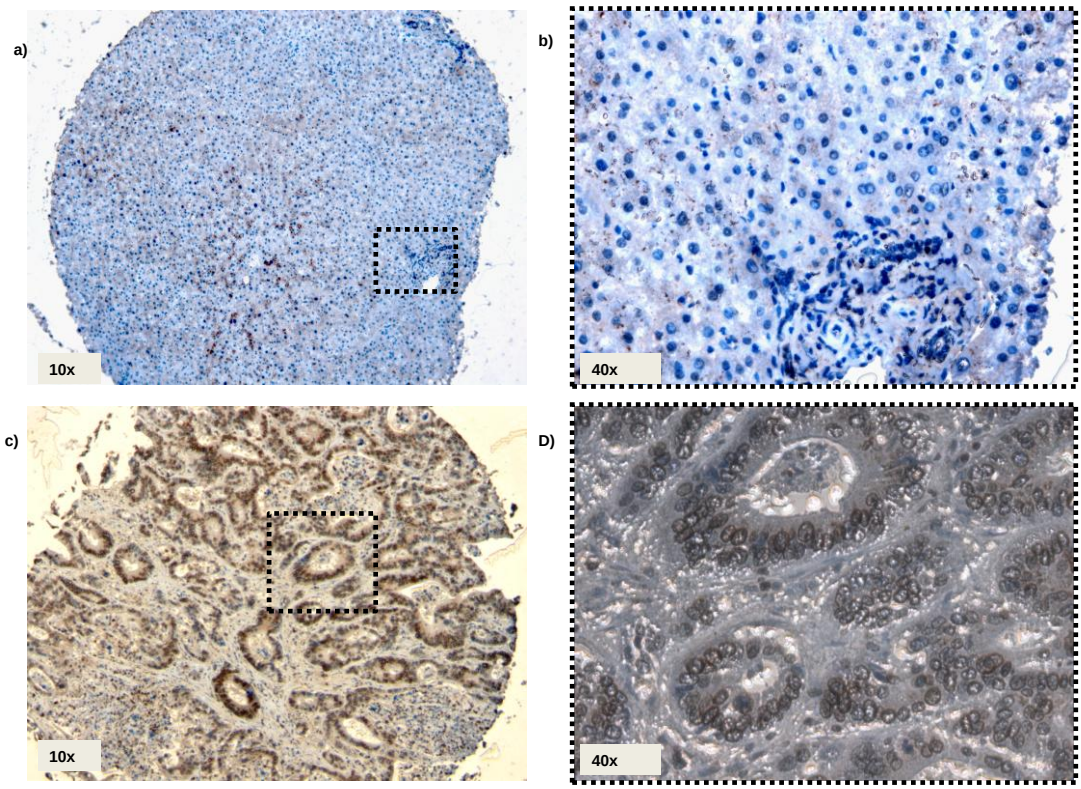

Figure 69: TLR7 expression in CC and normal bile duct epithelium: a) 10x core of tissue microarray of normal liver, showing negative TLR7 in bile duct epithelium, c) 10x of core of tissue microarray of CC, showing strongly positive TLR7 in nearly all acini. d) 40x of CC showing strongly positive of TLR7 in nuclear membrane of CC in 90% the malignant cells.

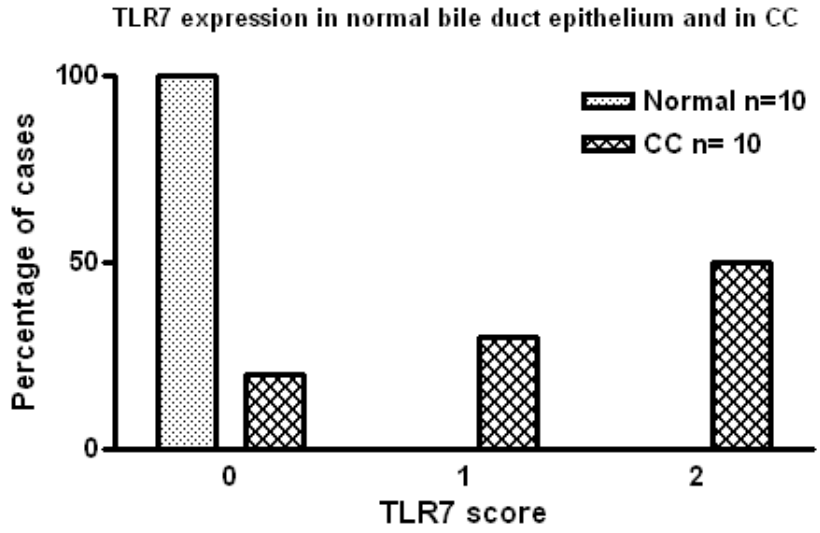

Figure 70: Distribution of TLR7 expression in normal bile duct and CC cases. There is significant up regulation of TLR7 in CC. Only 20% of cases were negative TLR7 staining. More than 50% of cases of CC had (Score 2) TLR7 and 30% of cases showed (Score 1). Normal bile duct epithelium was negative in all cases.

III. Increased expression of TLR9 in cholangiocarcinoma

The normal bile duct epithelium was mainly negative for TLR9 staining only one case (10%) stained with TLR9 (Score1), however, CC samples showed cytoplasmic TLR9 expression only 20% cases were negative, 30% were scored as Score 1 depending on the intensity and distribution of TLR9 staining. and 50% were scored as Score 2.

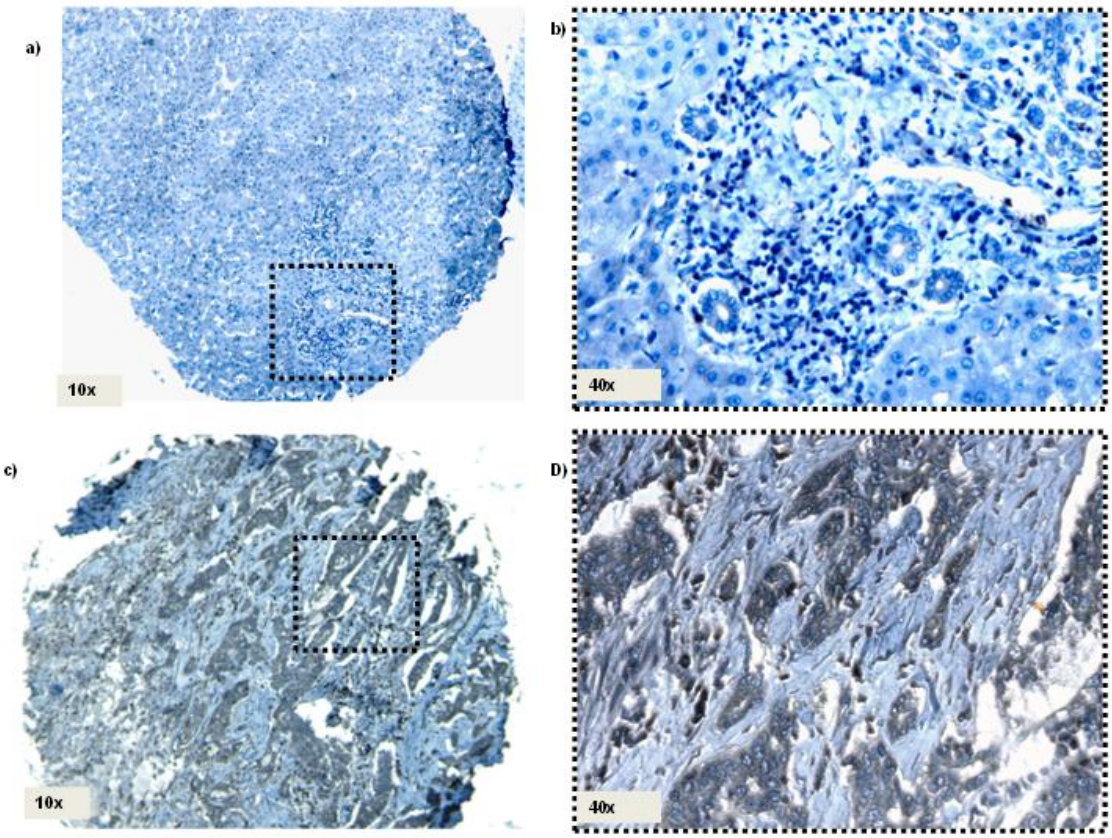

Figure 71: TLR9 expression in CC and normal bile duct epithelium: a) 10x core of tissue microarray of normal liver, showing negative TLR9 in bile duct epithelium, c) 10x core of tissue microarray of CC, showing strongly positive TLR9 in nearly all acini. d) 40x of CC showing strongly positive of TLR9 in the cytoplasm (Score 2) of CC in nearly all the malignant cells.

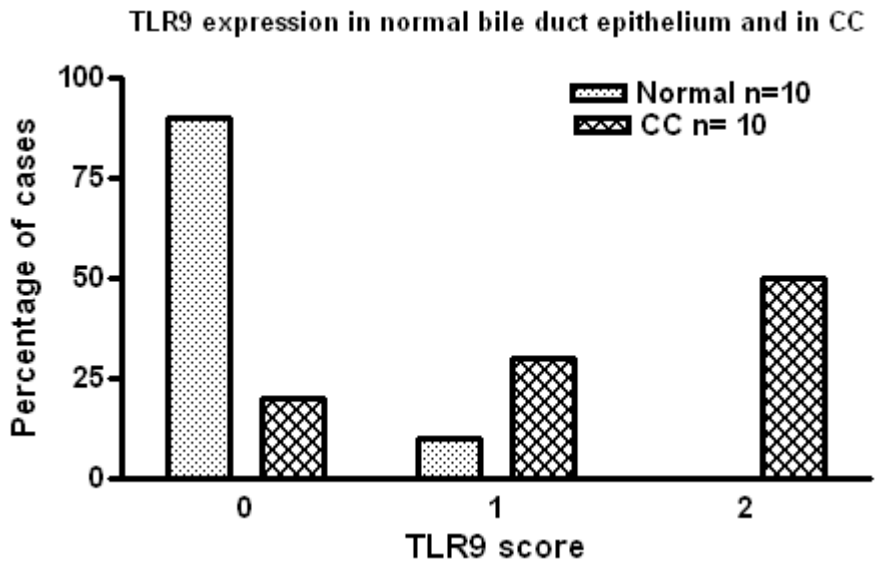

Figure 72: TLR9 expression in normal bile duct and CC samples. There is up regulation of TLR9 in CC.

4.6.3 TLR7 & TLR9 expression studies in the human HuCCT1 cholangiocarcinoma cell line

The observed overexpression of TLR7 and TLR9 in CC specimens led me to investigate their expression also in cholangiocarcinoma (HuCCT1 cell line). Similarly to what was found in the tissue sample by immunohistochemistry, confocal microscopy analysis in HuCCT1 showed a nuclear TLR7. On the other hand TLR9 was shown to be expressed in the plasma membrane, in the cytoplasm and in the nucleus (Fig. 73).

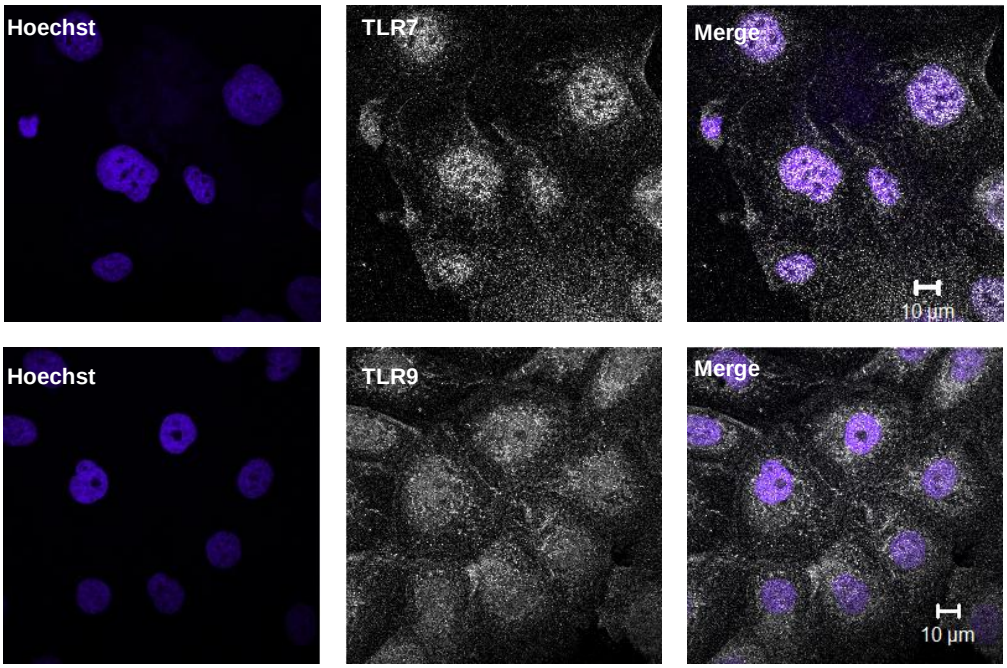

Figure 73: TLR7 and TLR9 were expressed in HuCCT1 cells. Immunofluorecense staining of TLR7 and TLR9 in methanol fixed HuCCT1. TLR7 was mainly expressed in the nucleus of HuCCT1 with residual expression in the cytoplasm. Merge of the staining of TLR7 (white) and nuclear staining Hoechst 33342 (blue). TLR9 (white) colour expressed in the plasma membrane, cytoplasm and nucleus. Merge channel of the TLR9 (white) and nuclear staining Hoechst 33342 (blue) (scale bar =10µm).

4.6.4 Subcellular localisation of TLR7 unchanged in response to IMQ, chloroquine or IRS treatment of HuCCT1 cells

HuCCT1 cells stained for TLR7 mainly in the nucleus and to some extent in the cytoplasm. No clear change in TLR7 localisation was observed with IMQ treatment (TLR7 stimulant), chloroquine or IRS treatment (TLR7 inhibitors) (Fig. 74).

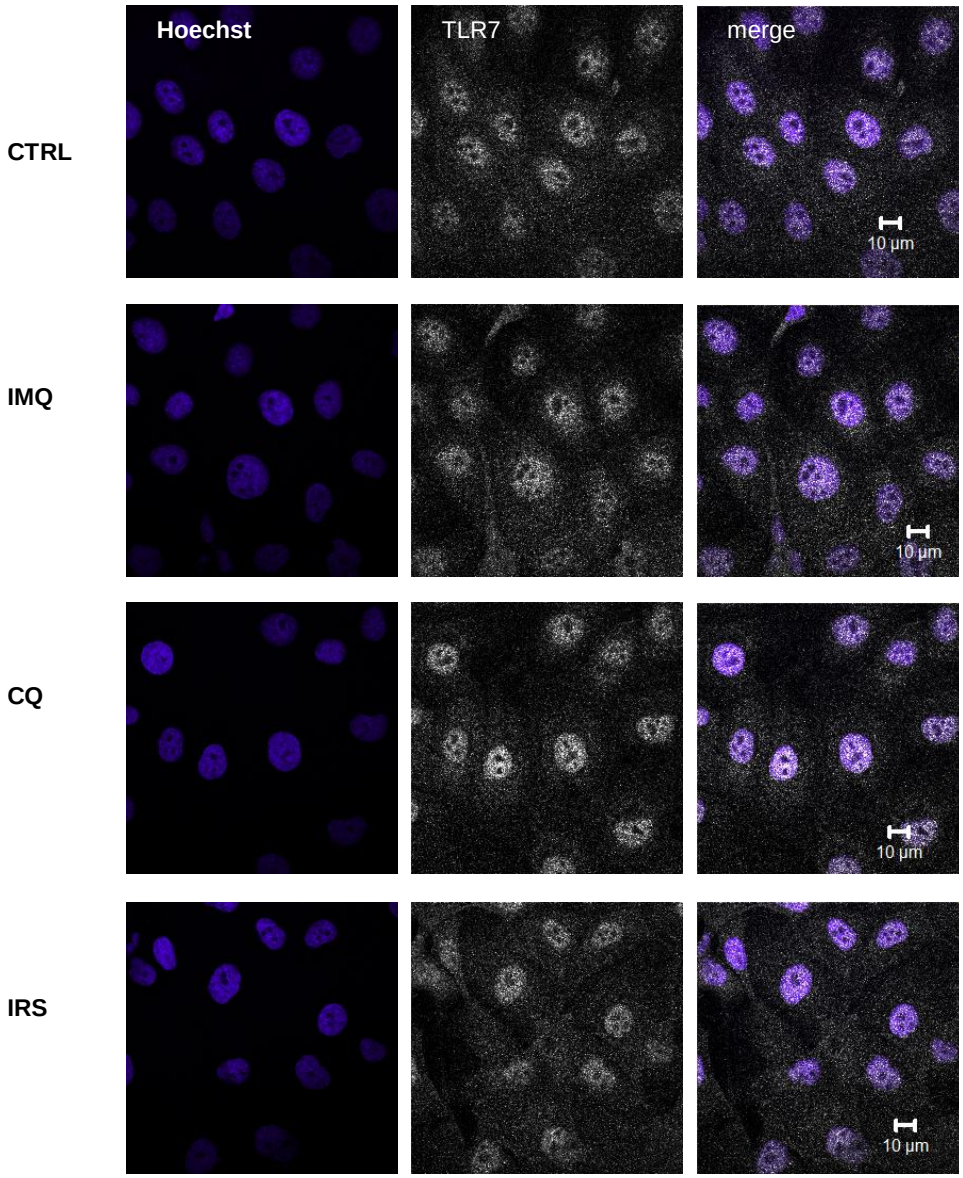

Figure 74: TLR7 expressed in HuCCT1 mainly in the nucleus with residual expression in the cytoplasm. Immunofluorescence staining of methanol fixed HuCCT1 showed that TLR7 distribution and localisation did not change with IMQ, chloroquine or IRS treatment TLR7 (white colour) and nuclear staining Hoechst 33342 (blue) (scale bar =10µm).

4.6.5 TLR9 expression shifts towards the nucleus in HuCCT1 treated with CpG or chloroquine

HuCCT1 cells stained with TLR9 showed diffuse localisation in the cell membrane, cytoplasm and the nucleus. CpG-ODN treatment resulted in TLR9 crowding around and inside the nucleus. The perinuclear accumulation was observed also with chloroquine treatment. IRS treatment did not induce any change TLR9 localisation compared to control (Fig. 75).

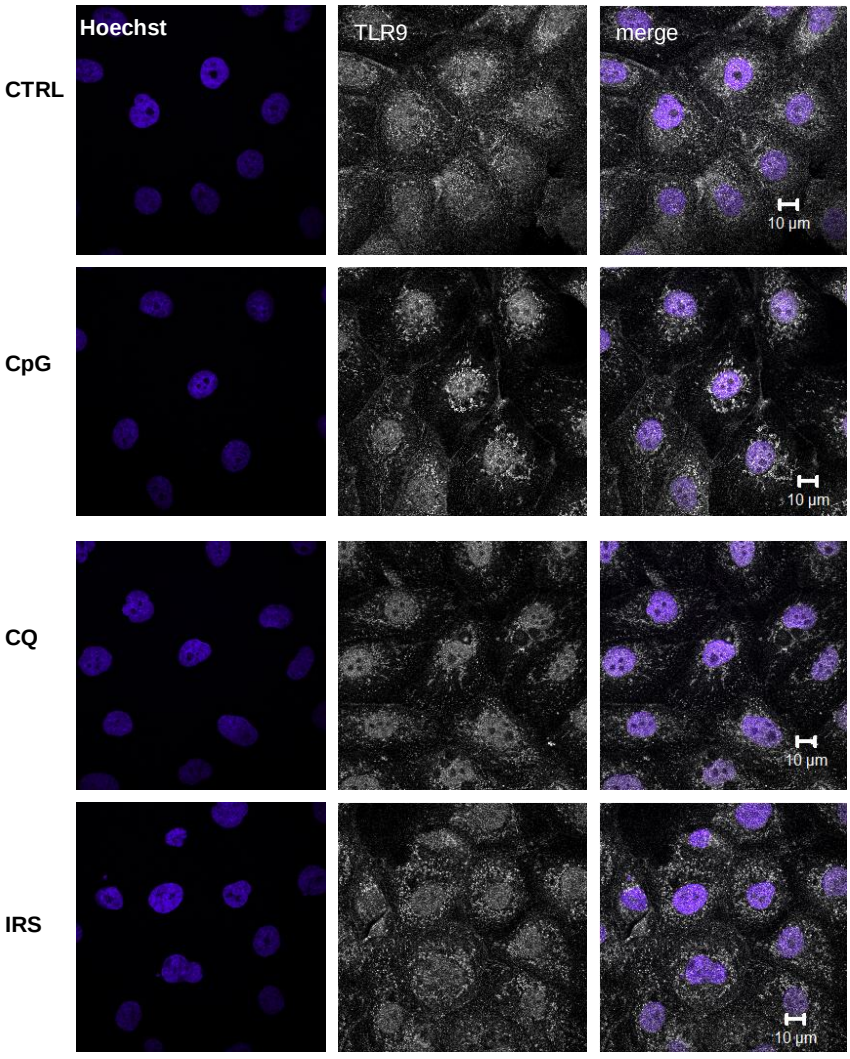

Figure 75: Immunofluorescence staining of TLR9 in HuCCT1 showing the localisation difference upon stimulation and inhibition. In control untreated cells, TLR9 was found in the cell membrane, cytoplasm and nucleus. With CpG stimulation there was more nuclear TLR9. With chloroquine, TLR9 was perinuclear while with IRS the staining was the same as the control TLR9 (white) and nuclear staining Hoechst 33342 (blue) (scale bar =10µm).

4.6.6 Increased co-localisation of TLR9 with the endoplasmic reticulum marker calnexin in response to chloroquine & IRS treatment

The subcellular distribution TLR9 was changed with CpG and with chloroquine treatment. Co-staining of HuCCT1 cells with TLR9 and cell organelle markers was performed using immunofluorescence staining. Confocal microscopy analysis revealed that there were limited co-localisation between TLR9 and endoplasmic reticulum marker calnexin in untreated HuCCT1. With CpG-ODN treatment, this limited co-localisation was not detected. However with chloroquine and IRS treatment this localisation was clearly detected (Fig. 76).

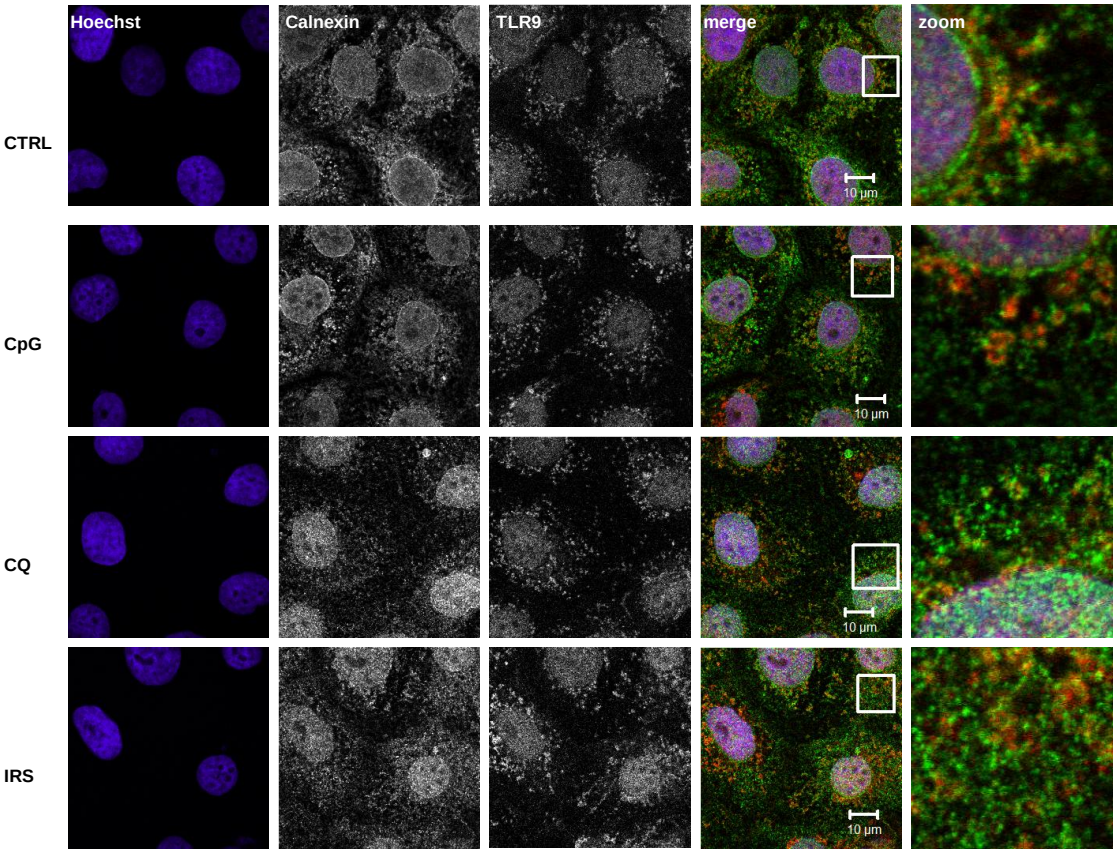

Figure 76: Co-localisation between TLR9 and calnexin with chloroquine and IRS treatment. Co-immunofluoresence staining of endoplasmic reticulum marker calnexin and TLR9 in methanol fixed HuCCT1. There was focal co-localisation between TLR9 and calnexin in untreated HuCCT1. With CpG treatment no co-localisation was observed. With chloroquine and IRS treatment, co-localisation was detected. The merge channel showing the calnexin (green color), TLR9 (red color) and Hoechst 33342 (blue). Zooming box showing the individual green and red granules. No yellow staining detected with CpG treatment. With chloroquine and IRS treatment there were yellow granules showing the co-localisation between TLR9 and calnexin.

4.6.7 Swelling of lysosomes in response to chloroquine treatment of HuCCT1 cells

With CpG-ODN and IMQ treatment of HuCCT1 there was no change in the morphology of lysosome labeled with lamp-1 compared to the untreated cells. Alongwith what was previously demonstrated in HuH7 cells, chloroquine treatment was associated with lysosomal swelling detected with lysosomal marker lamp-1 (Fig. 77).

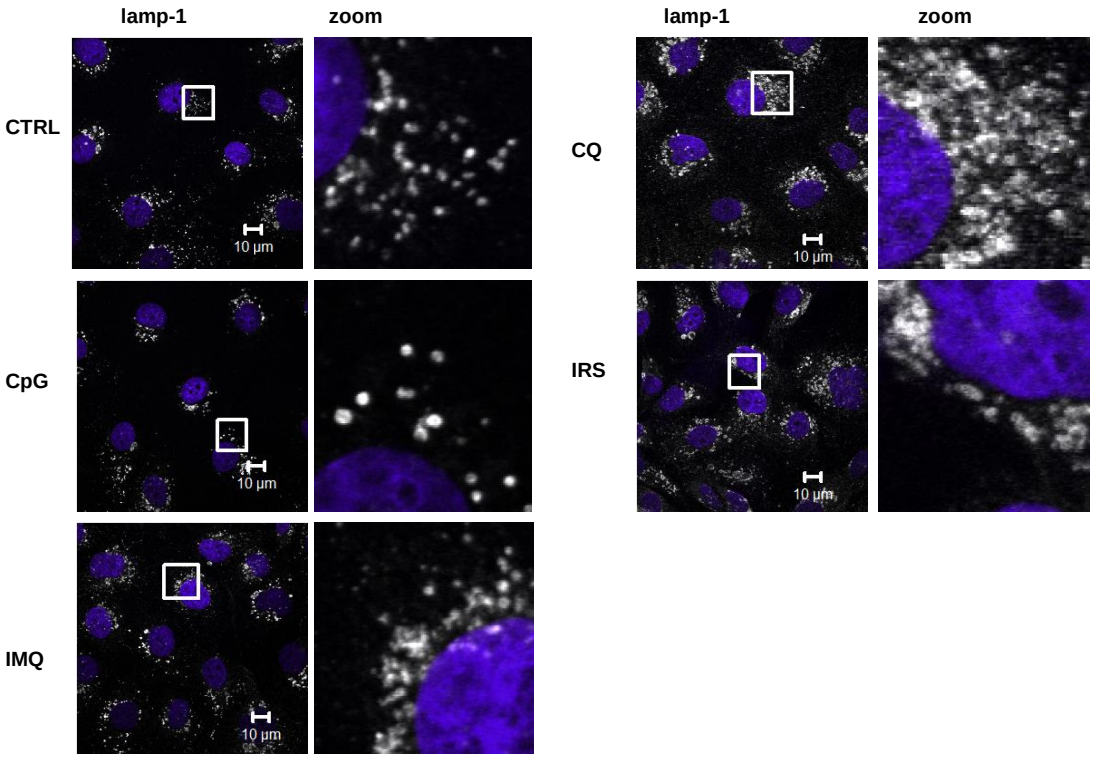

Figure 77: Immunofluorescence staining of the lysosomal marker lamp-1 in HuCCT1 cells demonstrates increased lysosomal swelling in response to chloroquine treatment. The Hoechst 33342 stained nuclei appear blue and the lamp-1 stained lysosomes appear as white granules surrounding the nuclei. No change in lysosomes was seen with CpG, IMQ or IRS treatment of the HuCCT1 cells (scale bar =10µm).

4.6.8 LC3B expression increased with chloroquine and CpG treatment of HuCCT1 cells but disappeared in response to IRS

The autophagic marker LC3B protein was detected in the cytoplasm of untreated cells or HuCCT1 cells treated with CpG-ODN as a scattered punctae mainly around the nucleus. However, LC3B protein was not detected using the same settings with IRS treatment. However, with chloroquine treatment there

were larger size granule accumulation in the juxtanulear area. This disappeared from the cytoplasm (Fig. 78).

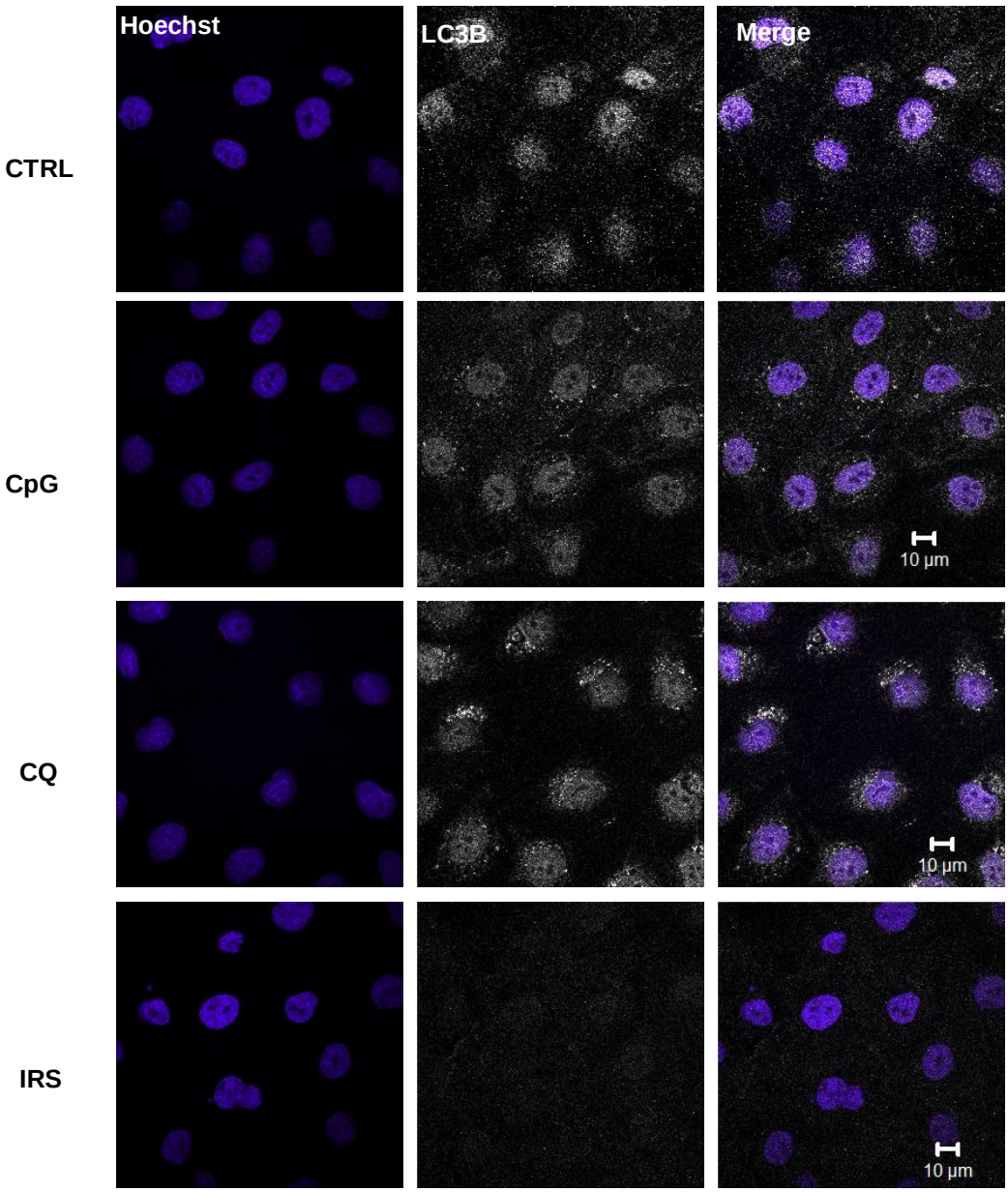

Figure 78: Immunofluorescence analysis of the autophagy marker LC3B in HuCCT1 cells. The cell nuclei are stained blue with Hoechst 33342. A slight increase in the white LC3B stained granules can be seen in response to CpG treatment of HuCCT1 cells. With chloroquine treatment there is an accumulation of LC3B around the cell nuclei and with IRS treatment the expression of LC3B disappeared completely (scale bar =10µm).

4.6.7 TLR7 & TLR9 stimulation and inhibition affect HuCCT1 cell proliferation

Cell proliferation was assessed by seeding 10,000 cells /well (96-well plate) in triplicate for each condition. Cell viability was measured by adding MTS reagent (Promega), 24h, 48h and 72h after treatment. Details for treatment and dosages are reported in materials and methods (Chapter 3).

a) IMQ treatment increased proliferation of HuCCT1 cells

Treatment of HuCCT1 cell with IMQ (TLR7 stimulant) resulted in a significant increase in cell proliferation compared to untreated controls after 48h (P <0.03).

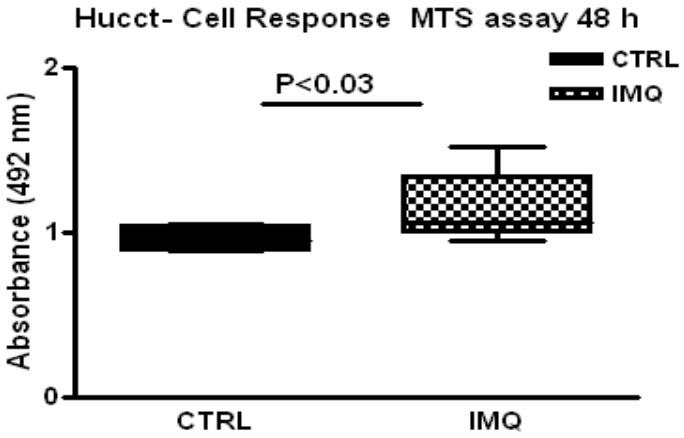

Figure 79: Increased proliferation of HuCCT1 cells in response to treatment with IMQ. HuCCT1 cells were treated with 5µg/ml of IMQ for 48 hours and their proliferation rate was then measured using the MTS assay. A significantly higher rate of cell proliferation was observed in the IMQ treated cells when compared with that of untreated HuCCT1 cells (P <0.03)

b) CpG-ODN treatment increased proliferation of HuCCT1 cells

After 48 hour stimulation of TLR9 using CpG-ODN treatment resulted in significant increase in HuCCT1 cell proliferation when compared to untreated controls (P <0.002).

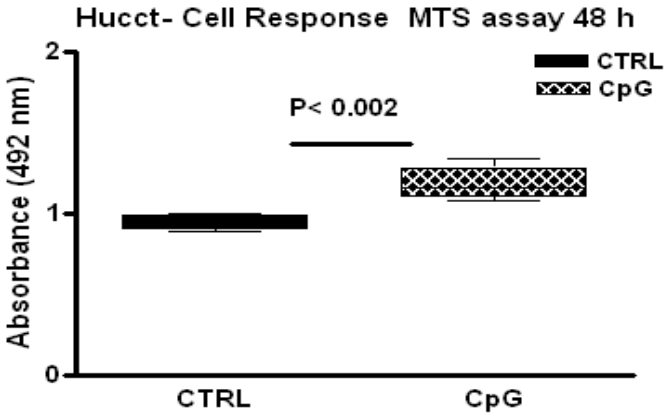

Figure 80: Increased proliferation of HuCCT1 cells in response to treatment with CpG-ODN. HuCCT1 cells were treated with 5µM of CpG-ODN for 48 hours and their proliferation rate was then measured using the MTS assay. A significantly higher rate of cell proliferation was observed in the CpG-ODN treated cells when compared with that of untreated HuCCT1 cells (P < 0.002).

c) Proliferation of HuCCT1 cells increased in response to treatment with chloroquine but not IRS

Chloroquine treatment of HuCCT1 cells for 48 hours had no effect on HuCCT1 cell proliferation. However, 72 hours of chloroquine treatment resulted in significant inhibition of HuCCT1 cell proliferation P<0.02 (t test, n=2).

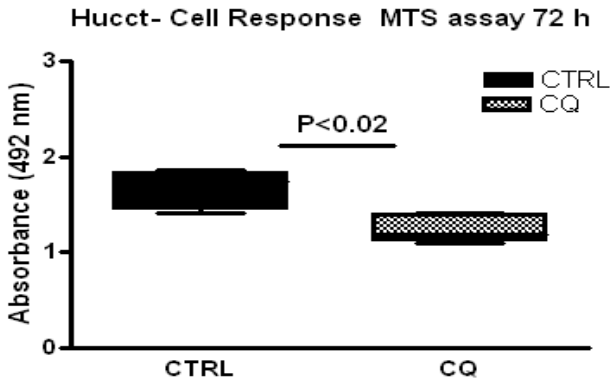

Figure 81: Inhibition of HuCCT1 cell proliferation in response to chloroquine treatment. Cells were treated with 15µM chloroquine for 72 hours and their proliferation rate was then measured using the MTS assay. A significant reduction of cell proliferation rate was observed in the chloroquine treated cells compared with that of untreated HuCCT1 cells (P <0.02).

IRS (TLR7 and TLR9 antagonist) treatment for 48 or 72 hours did not inhibit HuCCT1 cell proliferation (n=2)

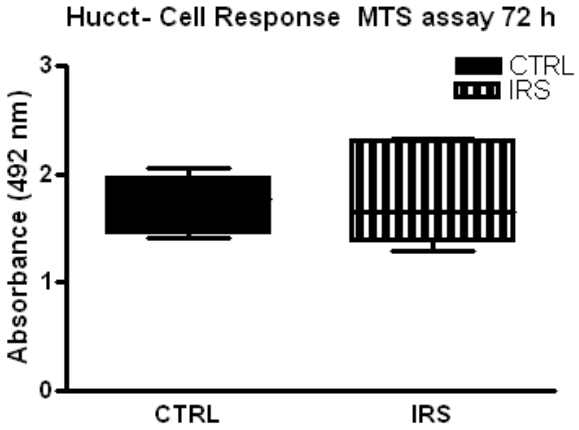

Figure 82: IRS treatment does not inhibit HuCCT1 cell proliferation. Cells were treated with 20µg/ml of IRS for 72 hours and their proliferation rates were then measured using the MTS assay. No difference in cell proliferation rate was observed between IRS treated and untreated HuCCT1 cells.

4.6.8 Effect of TLR7&TLR9 inhibition in a xenograft model of cholangiocarcinoma

A xenograft model of cholangiocarcinoma was established with injection of $5x10^6$ HuCCT1 cells into NOD-SCID mice livers details about the procedure and the tumour formation were reported in Chapter 4.1. The mice were divided into

groups and administered with either chloroquine in their drinking water (130mg/L) or injected with IRS-954 100µg (in 100µl) IP once per week a day following the implantation (control (untreated) n=7, chloroquine treated group n=4 and IRS treated group n=5).

Sixty days later after the intra-hepatic sub-capsular injection of HuCCT1 cells, tumour masses were formed. The masses were firm in consistency white in colour. The tumours were found outside the liver, and attached to the muscle of the abdominal wall. Tumour volume was calculated by measuring the three dimensions and they were multiplied. There were reduction in the tumour volume found in mice treated chloroquine and IRS. The mean tumour volume formed in control was (1.4±0.01) cm^3 whereas with chloroquine and IRS treatment this was reduced significantly to (0.5±0.03) and (0.6±0.1) cm^3 (P <0.01) and (P <0.003) respectively.

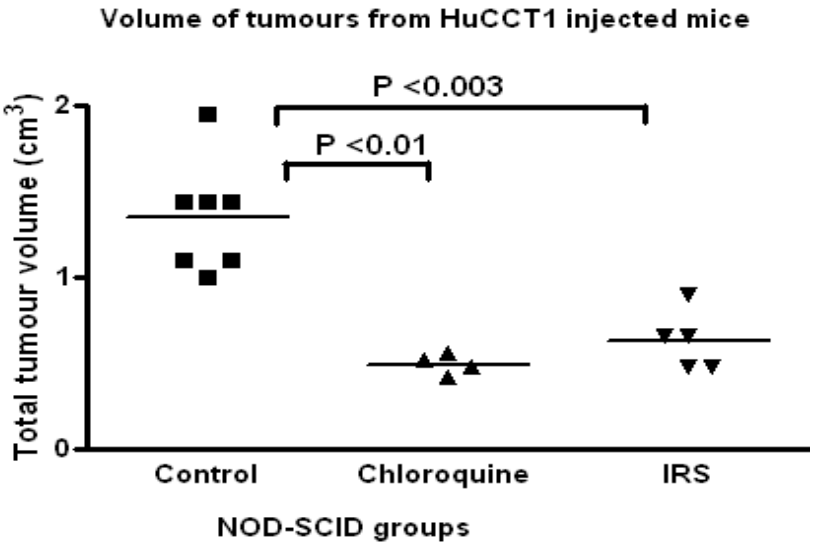

Figure 83: Chloroquine and IRS treatment reduced tumour growth in a xenograft model of cholangiocarcinoma. Tumours were measured 60 days after intra-hepatic injection of HuCCT1 cells into NOD-SCID mice. The liver tumour volume from the chloroquine and IRS treated mice was significantly smaller than from the non-treated control mice.

4.6.8 Discussion

I have previously shown in chapters 4.3, 4.4 and 4.5 that expression of TLR7 and TLR9 is up regulated in HCC and that inhibition of this expression can reduce cancer cell proliferation and growth. However, TLR4 expression was shown to be high in normal bile duct epithelium and inflammatory cells surrounding HCC but not in the malignant hepatocytes. These findings encouraged us to test whether a similar effect occurred with CC. The same experimental approach used in these studies have been now been applied examine expression of these TLRs in a small panel of cholangiocarcinoma tissue and cholangiocarcinoma cell line. The tissue microarray data revealed high expression of TLR4 (Score 2) in liver bile duct epithelium in the majority (80%) of normal liver tissue samples whilst its expression was (Score 1) in the bile ducts of the remaining cases. In contrast, TLR4 was absent from the majority (60%) of CC cases and only mildly or moderately expressed in the remainder (40%). Our results would suggest that the loss of TLR4 expression in cholangiocytes may promote tumour progression but our sample size is too small to reach any precise conclusion.

Only two studies of TLR4 in human cholangiocytes have been reported in the literature. Using RT-PCR and immunohistochemistry demonstrated TLR4 mRNA expression in 2 human intrahepatic cholangiocarcinoma (CC) cell lines, CCKSl and HuCCT1 lines and a murine biliary epithelial cell line. They speculated that TLR4 in biliary epithelial cells may play a role in the immunopathology of the intrahepatic biliary tree *in vivo* (Harada et al., 2003). Another study showed that increased TLR4 mRNA expression and activation of NF-kB could be induced in the immortalised human cholangiocyte cell line (H69 cell line) in response to stimulation by excretory/secretory products of the liver fluke *O. viverrini*. They proposed that TLR4 recognition of *O. viverrini* products could contribute to the severe inflammation associated with cholangiocarcinogenesis (Ninlawan et al., 2010).

The expression of TLR7 was found to be negative in the normal bile ducts of all normal livers examined by immunohistochemistry. TLR9 expression was also absent in the majority of cases; only one of 10 normal livers in the tissue array

demonstrated weak expression of TLR9 in the bile duct epithelial cells. In contrast, however, TLR7 or TLR9 were expressed in the majority (80%) of CC and moreover the expression of TLR7 or TLR9 was high in 50% of cases. The pattern of expression was predominantly perinuclear for TLR7 and confined to the cytoplasm in the case of TLR9, as was previously found in the HCC tissues (Chapter 4.3). A similar pattern of TLR7 and TLR9 expression was demonstrated in the HuCCT1 cholangiocarcinoma cell line i.e. peri-nuclear expression of TLR7 and cytoplasmic expression of TLR9. In addition expression of TLR9 was also seen in the membranes of HuCCT1 cells. Altogether these findings would suggest that TLR7 and TLR9 might play important roles in the progression of CC as was observed with HCC.

The intracellular distribution of TLR7 in the HuCCT1 line was not found to alter in response to treatment with IMQ (TLR7 agonist), chloroquine or IRS (both antagonists of TLR7 and TLR9). However, a shift in TLR9 distribution from the cytoplasm towards the nucleus was observed in response to chloroquine and CpG-ODN (TLR9 agonist) treatment. This same observation was previously made in the HuH7 hepatocellular carcinoma cell line in response to CpG-ODN. The findings would suggest that relationship between TLR9 activity and subcellular location is not a simple one.

In order to throw more light on the subcellular distribution localisation of TLR9, co-localisation experiments using markers of endoplasmic reticulum, lysosomes and TLR9 were conducted on the HuCCT1 cell line using immunofluorescence staining. Analysis of these markers by confocal microscopy revealed a limited co-localisation between TLR9 and the endoplasmic reticulum marker calnexin in the untreated cell line suggesting that some of the TLR9 is located within the ER. The co-localisation of TLR9 with calnexin was more obvious in the presence of the TLR9 inhibitors chloroquine or IRS but completely undetected in the presence of the TLR9 agonist CpG. These findings would suggest that the inactive form of TLR9 is located within the ER and its active form is outside of the ER. These findings are similar to those previously observed in dendritic cells and macrophages where TLR9 was reportedly located in the endoplasmic reticulum under resting condition and translocated to endolysosomal system upon stimulation (Latz et al., 2004 and Leifer et al., 2004).

The effects of stimulating or inhibiting TLR7 and TLR9 expression in the HuCCT1 cells were examined in order to assess any role these TLRs might play in cholangiocarcinogenesis. A significant increase in HuCCT1 proliferation was found after 48 hours of treatment with either IMQ ($P < 0.03$) or CpG-ODN ($P < 0.002$); TLR7 and TLR9 agonists respectively. Treatment of the cell line with chloroquine for 72 hours resulted in a highly significant reduction in cell proliferation. However, no change in the level of cell proliferation was detected with IRS treatment after 72 hours treatment. This pattern of expression is similar to what was previously seen in the HCC cell line HuH7 and would suggest that expression of TLR7 and TLR9 play an important role in the proliferation of CC as well as HCC. Autophagic pathway is important in tumourigenesis and LC3B protein was highly expressed in CC cell line (Huang and Hezel, 2012). Therefore, I studied LC3B expression using immunofluorescence staining; I found that in chloroquine treated HuCCT1 cells, LC3B protein was accumulated in one pole of the nuclei, whereas with IRS treatment there was no LC3B detection. Increased LC3B expression with chloroquine treatment was previously reported and it was associated with lysosomal swelling. This was confirmed (Yoon et al., 2010). Increased TLR7 and TLR9 expression in CC and undetectable LC3B in IRS (TLR7 and TLR9 inhibitor) treated HuCCT1 or arrest of autophagy with chloroquine treatment suggests that TLR7 and TLR9 might have role in CC carcinogensis through autophagy. Previous study reported that TLR9 is required for autophagy and CpG stimulation induced autophagy in cancer (Bertin and Pierrefite-Carle 2008). The effect of chloroquine on inhibition of lung and colon cancer was mentioned (Fan et al., 2006 and Zheng et al., 2009). Another recent study suggested that pancreatic carcinogenesis is regulated by TLR7 and its inhibition is protective against tumour progression (Ochi et al., 2012).

In order to determine whether the inhibition of TLR7 and TLR9 had the same effects on CC proliferation *in vivo* as well as *in vitro*, the mouse CC xenograft model developed in Chapter 1 was treated for 60 days with either IRS or chloroquine. A significant reduction in tumour volume was found with both chloroquine ($P < 0.01$) and IRS ($P < 0.05$) thus giving additional support to the idea that TLR7 and TLR9 signaling plays a role in the development of CC.

Our data suggest that TLR7 and TLR9 might have a pivotal role in cellular proliferation in HuCCT1 cells. Furthermore, chloroquine or IRS treatment reduced CC tumour volume in our xenograft model. These findings merit further studies to explore the possibility of exploiting it as a potential target for future therapy in CC patients

General discussion & Summary

5. General discussion

HCC is one of the commonest cancers worldwide and one which has a very low five year survival rate. Understanding the mechanisms by which this cancer arises are vital if more effective treatment strategies are to be developed.
The major risk factor for HCC is chronic liver damage caused by viral infection, excessive alcohol intake, aflatoxicosis, diabetes or metabolic syndrome. These conditions often result in liver inflammation and cirrhosis, which can persist for many years prior to development of HCC or CC. Chronic liver inflammation is therefore considered to be the main predisposing factor for initiation of hepatocarcinogenesis.

Disturbances in the gut micro flora are common feature in patients with chronic liver disease. The overgrowth of gut bacteria and increased translocation of bacteria from the intestinal lumen to the systemic circulation is believed to exacerbate the inflammatory state in patients with chronic liver disease (Weistand Garcia 2005 and Almeida et al., 2006). This has been demonstrated in animal models of chronic liver injury in which bacterial translocation has been shown to promote liver fibrosis (Seki et al., 2007). In addition, bacterial translocation has been shown to increase with progression of liver fibrosis and cirrhosis (Fukui et al., 1991, Lin et al., 1995). The mechanism of bacterial translocation is not entirely clear and probably multifactorial including gut barrier dysfunction, bacterial overgrowth and loss of systemic and local immune surveillance.

TLRs are known to play a crucial role in the induction of innate immunity against microbial pathogens. TLR4, in particular, is activated by the LPS contained within the walls of gram negative bacteria which are often elevated in the blood of patients with chronic liver disease. Much evidence has accumulated in recent years of an important role for TLR4 signaling in the pathogenesis of chronic liver disease. Mice with mutations in TLR4, for example, are found to develop less inflammation and fibrosis in their livers compared to wild type mice (Seki et al., 2007 and Aoyama et al., 2010).

A number of studies on the effects of gut bacterial translocation and TLR4 signaling on liver inflammation and cirrhosis have been reported in the literature but their effects on pathogenesis of liver cancer have not previously been examined. I therefore set out to study the effects of gut decontamination on TLR4 signaling and hepatocarcinogenesis *in vivo* using a rat model of HCC on a background of liver inflammation. The model was developed by administering rats with the carcinogens DEN&NMOR and then examining the effects of selective gut decontamination using Norfloxacin on liver inflammation, fibrosis and tumourigenesis. I found Norfloxacin treatment led to a reduction in the level of blood endotoxins and a decrease in the expression of hepatic TLR4. A concurrent reduction in liver inflammation and fibrosis was also observed. However, the Norfloxacin treatment had no visible effect on the size or frequency of tumours developing in the rat livers. Closer examination of the rat livers by immunohistochemistry revealed the malignant hepatocytes do not express TLR4 whereas it was expressed in the surrounding inflammatory cells and fibroblasts. A similar pattern of expression was found in the human HCC tissues; TLR4 was not expressed in the malignant hepatocytes but it was expressed in the inflammatory cells within or surrounding the malignant tumour. These findings suggest that TLR4 expression has some role to play in liver inflammation and fibrosis but its expression within HCCs does not appear to be necessary for their progression. However, this is does not rule out the possibility that TLR4 expression within hepatocytes could have a protective effect against malignancy, perhaps, by activating vital tumour suppressor pathways or by not allowing the malignant cells to escape immune surveillance.

Following the above findings with TLR4 I examined the possibility that other TLRs could be involved in HCC pathogenesis. A variety of TLRs have been implicated in human cancers but few studies have examined the role of TLRs in HCC. I decided to focus our attention on the expression of TLR7 and TLR9 in HCC since these have been implicated in a variety of chronic liver diseases and liver fibrosis (Gäbele et al., 2008, Stadlbauer et al., 2008, Stärkel et al., 2010, Henao-Mejia et al., 2012 and Tarantino et al., 2013). In addition, TLR7 and TLR9 have also been reported to be up regulated in a wide variety of human cancers including pancreatic cancer (Ochi et al., 2012), oesophageal cancer

(SHeyhidin et al., 2011), prostate cancer and (González-Reyes et al., 2011). Our immunohistochemistry data demonstrated a very strong association between high expression of TLR7 and TLR9, and HCC where it was shown to be expressed in the vast majority of tumours. Very little expression of these markers was found in normal, cirrhotic or hepatitis human liver. I also demonstrated a significant correlation between high Ki-67 proliferation index and high expression of TLR7 and TLR9. Overall the immunohistochemistry data suggested that the expression of TLR7 and TLR9 in HCCs may play a role in enhancing HCC proliferation and growth.

Having established a strong link between high expression of TLR7 and TLR9 and HCC in human liver tissues, *in vitro* studies were carried out on the HuH7 human HCC cell line in order to determine whether stimulation or inhibition of TLR7 or TLR9 activity has any effect on cell proliferation or whether it can influence the activity of other pathways that are known to be involved in HCC pathogenesis. I found that stimulation of TLR7 with IMQ resulted in a significant increase in HuH7 cell proliferation but this effect was not seen when the cells were treated with the TLR9 agonist CpG-ODN. The inhibition of TLR7 and TLR9 with IRS and chloroquine, respectively, however, resulted in a significant reduction in the proliferation of HuH7 cells. In addition, the data showed that the decrease in levels of proliferation were not due to cell death resulting from any cytotoxic effect of the drugs.

Our next step was to determine whether the actions of TLR7 and TLR9 on cell proliferation were being exerted via activation of the Akt pathway, which is one of the most commonly activated pathways human cancer (Chen et al., 2011, Zhou et al., 2011 and Xu et al., 2013). The expression of pAkt protein, which is the active form of Akt, was found to disappear almost completely in HuH7 cells in response to treatment with the TLR7 and TLR9 inhibitors chloroquine and IRS, respectively. In addition, a slight increase in pAkt protein expression was detected in response the TLR7 agonist IMQ. The inferences I drew from these findings was that the proliferation of human HCC cells were under the control of TLR7 and TLR9 and that these may be exerting their actions by influencing the Akt pathway.

As well as acting as an inhibitor of TLR7 and TLR9 chloroquine is also known to interfere with the autophagic pathway which is often used by cancer cells as a cyto-protective mechanism at times of stress. I therefore examined the HuH7 cells for expression of LC3B which is a marker of autophagy but found no evidence that this pathway was activated in this cell line. Furthermore, it could not be induced in response to activation of TLR7 or TLR9 by IMQ and CpG-ODN, respectively. These findings were further evidence that proliferation of HuH7 cells was under the control of TLR7 and TLR9 and was not being influenced by the autophagic pathway.

Following the *in vitro* work on TLR7 and TLR9 in the human liver tissues and HuH7 cell line I wanted to see if the results obtained from these studies could be confirmed *in vivo u*sing a mouse xenograft model of human HCC and a DEN & NMOR-induced rat model of human HCC with cirrhosis. The administration of TLR7 and TLR9 inhibitors led to a significant reduction in liver tumour growth in both models of HCC. In addition, chloroquine treatment was found to have a significantly beneficial effect on liver inflammation and fibrosis as well as a beneficial effect on liver function in the rat model. Furthermore, the expression of TLR7, TLR9 and NF-kB, Akt and pAkt were found to be reduced in response to chloroquine treatment in the livers of the rat HCC model. These findings were concordant with the *in vitro* data and provided further support for a role for TLR7 and TLR9 in HCC pathogenesis.

My studies in CC revealed a similar pattern of TLR expression to the one found in the HCCs. TLR4 was not expressed in the majority of CC but highly expressed in the bile duct epithelial cells. TLR7 and TLR9 were also found to be expressed in the majority of cholangiocarcinoma. Stimulation of TLR7 and TLR9 with IMQ or CpG, respectively, resulted in increased proliferation of the HuCCT1 cells and inhibition of these TLRs with chloroquine led to a reduction in cell proliferation. Furthermore, inhibition of TLR7 or TLR9 with chloroquine and IRS, inhibited tumour growth in a mouse xenograft model of CC. However, unlike the HCC HuH7 cells, the autophagy pathway was also found to be activated in the HuCCT1 cell line and treatment of these cultures with the TLR9

agonist CpG resulted in elevated expression of the autophagy marker LC3B in addition to increasing cell proliferation.

In summary, TLR7 and TLR9 are highly up regulated in human HCC tissues and cultures as well as animal models of HCC but their expression is low in normal, cirrhotic or hepatitis human livers. Inhibition of TLR7 and TLR9 is associated with a marked reduction in proliferation of human HCC cell cultures and xenograft models of human HCC. It was also associated with a reduction in liver inflammation, fibrosis and tumour growth, as well as decreased expression of Akt and NF-κB in the animal models of HCC. Stimulation of TLR7 resulted in increased proliferation of human HCC cultures. TLR4 is not expressed in human HCC or animal models of HCC. However, gut decontamination led to a decrease of TLR4 and NF-κB expression and a reduction in liver inflammation and fibrosis in the animal models. The pattern of TLR4, TLR7 and TLR9 expression and the effects of up regulating or down regulating TLR7 or TLR9 in the cholangiocarcinoma were also similar those in the HCCs.

Our findings would suggest that the inhibition of TLR7 and TLR9 using chloroquine or other antagonists of these TLRs may serve as novel approaches for the treatment of HCC and CC. However, before translation into the clinical arena, a more thorough investigation of the precise role(s) played by these TLRs in HCC and CC pathogenesis is essential since any therapeutic intervention involving the immune system can sometimes lead to unpredictable and harmful consequences. Also, since a large proportion of HCCs and CCs arise as within the context of HBV or HCV infection in humans, the effects of TLR7 or TLR9 inhibition on viral propagation is another important factor that needs to be taken into consideration in any future therapies that may target these TLRs.

Future research

The focus of any future studies should include an examination of the following:

- The pattern of TLR4, TLR7 and TLR9 expression in a much larger group of human HCCs and CCs from a variety of aetiologies in order to identify more precisely the liver cells involved and examine any correlation between tumour grade, stage or metastasis and expression of these TLRs.
- Studies to understand the ligands for TLR7 and TLR9 that may drive their stimulation in chronic hepatic inflammation.
- The effects of TLR4, TLR7 and TLR9 stimulation or inhibition in a much larger group of animals and over a longer period of time to look for any unforeseeable side effects.
- The optimum dose of chloroquine which can give a maximum therapeutic result without any harmful side effects in animal models.
- HCC and CC development within TLR4, TLR7 and TLR9 knockout animals in order to understand the relationship between the tumour and its environment with respect to expression of these TLRs.
- The links between TLR7 and TLR9 expression and the PIk3/Akt/mTOR pathway in order identify the exact targets within these pathways that can elicit tumour inhibition

Conclusion

The results presented in this thesis suggest that modulation of TLR7 and TLR9 may provide a safe and effective approach to the treatment of HCC and CC. Appropriate clinical trials should be planned after consideration of the pending issues.

Works were presented from this study

1) Mohamed F, Dhar D, Shah N, Winstanley A, Behbodi S, Mookergee R, Olde Damink S, Davis N and Jalan R. **Cytoplasmic expression of Toll-like receptor-9 is associated with increased cellular proliferation in Hepatocellular carcinoma** (Poster): Gut 2010;59:A23. The British Association for the Study of the Liver (BASL) and the American Association for the Study of Liver Diseases (AASLD).

2) Mohamed F, Dhar D, Shah N, Davies N, Habtesion A, Luong T, Winstanley A, Dhillon A P, Mookerjee R and Jalan R. **TLR7 expression is increased in hepatocellular cancer (HCC) and its modulation is associated with alterations in tumour growth: A novel therapeutic target** (Poster): Gut 2012;61:A110-A111. The Digestive Disorders Federation Meeting (DDF).

3) Mohamed F, Dhar D, Shah N, Davies N, Habtesion A, Luong T, Winstanley A, Dhillon A P, Mookerjee R and Jalan R. **Selective Gut decontamination reduces hepatic expression of toll-like receptor (TLR) 4 and development of cirrhosis but does not prevent development of Hepatocellular carcinoma (HCC)** (Poster): Gut 2012;61:A196**.** The European Association for the Study of Liver (EASL) and (DDF).

4) Mohamed F, Minogue S Dhar D, Shah N, Davies N, Habtesion A, Luong T, Winstanley A, Dhillon A P, Mookerjee R and Jalan R. TLR 9 inhibition: **A novel target of therapy for Primary Liver Cancer (Poster):** J Hepatol. 2012;56: S121**.** The European Association for the Study of Liver (EASL).

5) Mohamed F, Minogue S, Winstanley A, Luong T, Habtesion A, Davies N and Jalan R. **Chloroquine: A novel strategy for the prevention of Hepatocellularcarcinoma** (Poster): Hepatology 2012; 612A - 613A. The American Association for the Study of Liver Diseases (AASLD).

6) Mohamed F, Minouge M, Dhar D, Andreola F, Davies N, Olde Damink S, Winstanley A, Loung T, Mookerjee R and Jalan R**. Targeting TLR7 and 9: A Novel strategy for treatment of cholangiocarcinoma (**Poster): J Hepatol. 2013;58,S436-S437. The European Association for the Study of Liver (EASL).

7) Mohamed F, Minogue S , Andreola F, Winstanley A, Olde Damink S, Malagó M, Al-Jehani R, Davies N, Loung T, Dhillon P, Mookerjee R, Dhar D and Jalan R. **Effect of Toll-Like Receptor 7 and 9 Targeted Therapy to Prevent Development of Hepatocellular Carcinoma.** 2013 (in the process of submission)

References

6. References

- Adams S, O'Neill DW, Nonaka D, Hardin E, Chiriboga L, Siu K, et al. Immunization of malignant melanoma patients with full-length NY-ESO-1 protein using TLR7 agonist imiquimod as vaccine adjuvant. *J Immunol* 2008;181(1):776-84.
- Akira S, Uematsu S, Takeuchi O. Pathogen recognition and innate immunity. *Cell* 2006;124(4):783-801.
- Akira S. Toll receptor families: structure and function. *Semin Immunol* 2004;16(1):1-2.
- Alexopoulou L, Holt AC, Medzhitov R, Flavell RA. Recognition of double-stranded RNA and activation of NF-kappaB by Toll-like receptor 3. *Nature* 2001;413(6857):732-8.
- Almeida J, Galhenage S, Yu J, Kurtovic J, Riordan SM. Gut flora and bacterial translocation in chronic liver disease. *World J Gastroenterol* 2006;12(10):1493-502.
- Anderson KV, Bokla L, Nusslein-Volhard C. Establishment of dorsal-ventral polarity in the Drosophila embryo: the induction of polarity by the Toll gene product. *Cell* 1985;42(3):791-8.
- Aoyama T, Paik YH, Seki E. Toll-like receptor signaling and liver fibrosis. *Gastroenterol Res Pract*;2010.
- Armstrong GL, Alter MJ, McQuillan GM, Margolis HS. The past incidence of hepatitis C virus infection: implications for the future burden of chronic liver disease in the United States. *Hepatology* 2000;31(3):777-82.
- Arslan F, de Kleijn DP, Timmers L, Doevendans PA, Pasterkamp G. Bridging innate immunity and myocardial ischemia/reperfusion injury: the search for therapeutic targets. *Curr Pharm Des* 2008;14(12):1205-16.
- Baek KH, Park HY, Kang CM, Kim SJ, Jeong SJ, Hong EK, et al. Overexpression of hepatitis C virus NS5A protein induces chromosome instability via mitotic cell cycle dysregulation. *J Mol Biol* 2006;359(1):22-34.
- Balkwill F, Mantovani A. Inflammation and cancer: back to Virchow? *Lancet* 2001;357(9255):539-45.
- Barrat FJ, Meeker T, Gregorio J, Chan JH, Uematsu S, Akira S, et al. Nucleic acids of mammalian origin can act as endogenous ligands for Toll-like receptors and may promote systemic lupus erythematosus. *J Exp Med*

2005;202(8):1131-9.

- Basith S, Manavalan B, Yoo TH, Kim SG, Choi S. Roles of toll-like receptors in cancer: a double-edged sword for defense and offense. *Arch Pharm Res* 2012;35(8):1297-316.
- Bauer TM, Schwacha H, Steinbruckner B, Brinkmann FE, Ditzen AK, Aponte JJ, et al. Small intestinal bacterial overgrowth in human cirrhosis is associated with systemic endotoxemia. *Am J Gastroenterol* 2002;97(9):2364-70.
- Bauer TM, Schwacha H, Steinbruckner B, Brinkmann FE, Ditzen AK, Aponte JJ, et al. Small intestinal bacterial overgrowth in human cirrhosis is associated with systemic endotoxemia. *Am J Gastroenterol* 2002;97(9):2364-70.
- Benias PC, Gopal K, Bodenheimer H, Jr., Theise ND. Hepatic expression of toll-like receptors 3, 4, and 9 in primary biliary cirrhosis and chronic hepatitis C. Clin Res Hepatol Gastroenterol 2012;36(5):448-54.
- Bertin S, Pierrefite-Carle V. Autophagy and toll-like receptors: a new link in cancer cells. *Autophagy* 2008;4(8):1086-9.
- Bhaskar PT, Hay N. The two TORCs and Akt. *Dev Cell* 2007;12(4):487-502.
- Boya P, Gonzalez-Polo RA, Casares N, Perfettini JL, Dessen P, Larochette N, et al. Inhibition of macroautophagy triggers apoptosis. *Mol Cell Biol* 2005;25(3):1025-40.
- Brenner DA. Molecular pathogenesis of liver fibrosis. *Trans Am Clin Climatol Assoc* 2009;120:361-8.
- Broadley SA, Hartl FU. The role of molecular chaperones in human misfolding diseases. *FEBS Lett* 2009;583(16):2647-53.
- Calle EE, Rodriguez C, Walker-Thurmond K, Thun MJ. Overweight, obesity, and mortality from cancer in a prospectively studied cohort of U.S. adults. *N Engl J Med* 2003;348(17):1625-38.
- Cao Z, Ren D, Ha T, Liu L, Wang X, Kalbfleisch J, et al. CpG-ODN, the TLR9 agonist, attenuates myocardial ischemia/reperfusion injury: involving activation of PI3K/Akt signaling. *Biochim Biophys Acta* 2013;1832(1):96-104.
- Caramalho I, Lopes-Carvalho T, Ostler D, Zelenay S, Haury M, Demengeot J. Regulatory T cells selectively express toll-like receptors and are

activated by lipopolysaccharide. *J Exp Med* 2003;197(4):403-11.

- Chadwick R, Galizzi J, Heathcote J, Lyssiotis T, Cohen B, Scheuer P, Sherlock S. Chronic persistent hepatitis: hepatitis B virus markers and histological follow-up. *Gut 1979;*20: 372-377
- Chan CC, Hwang SJ, Lee FY, Wang SS, Chang FY, Li CP, et al. Prognostic value of plasma endotoxin levels in patients with cirrhosis. *Scand J Gastroenterol* 1997;32(9):942-6.
- Chang YJ, Wu MS, Lin JT, Chen CC. Helicobacter pylori-Induced invasion and angiogenesis of gastric cells is mediated by cyclooxygenase-2 induction through TLR2/TLR9 and promoter regulation. *J Immunol* 2005;175(12):8242-52.
- Chantajitr S, Wilasrusmee C, Lertsitichai P, Phromsopha N. Combined hepatocellular and cholangiocarcinoma: clinical features and prognostic study in a Thai population. *J Hepatobiliary Pancreat Surg* 2006;13(6):537-42.
- Charbel H, Al-Kawas FH. Cholangiocarcinoma: epidemiology, risk factors, pathogenesis, and diagnosis. *Curr Gastroenterol Rep* 2011;13(2):182-7.
- Chen KF, Yu HC, Liu CY, Chen HJ, Chen YC, Hou DR, et al. Bortezomib sensitizes HCC cells to CS-1008, an antihuman death receptor 5 antibody, through the inhibition of CIP2A. *Mol Cancer Ther* 2011;10(5):892-901.
- Chen R, Alvero AB, Silasi DA, Steffensen KD, Mor G. Cancers take their Toll--the function and regulation of Toll-like receptors in cancer cells. *Oncogene* 2008;27(2):225-33.
- Cherfils-Vicini J, Platonova S, Gillard M, Laurans L, Validire P, Caliandro R, et al. Triggering of TLR7 and TLR8 expressed by human lung cancer cells induces cell survival and chemoresistance. *J Clin Invest* 2010;120(4):1285-97.
- Cherry S, Silverman N. Host-pathogen interactions in drosophila: new tricks from an old friend. *Nat Immunol* 2006;7(9):911-7.
- Chochi K, Ichikura T, Kinoshita M, Majima T, Shinomiya N, Tsujimoto H, et al. Helicobacter pylori augments growth of gastric cancers via the lipopolysaccharide-toll-like receptor 4 pathway whereas its lipopolysaccharide attenuates antitumour activities of human mononuclear cells. *Clin Cancer Res* 2008;14(10):2909-17.

- Choi JH, Yang YR, Lee SK, Kim SH, Kim YH, Cha JY, et al. Potential inhibition of PDK1/Akt signaling by phenothiazines suppresses cancer cell proliferation and survival. *Ann N Y Acad Sci* 2008;1138:393-403.
- Corradi F, Brusasco C, Fernandez J, Vila J, Ramirez MJ, Seva-Pereira T, et al. Effects of pentoxifylline on intestinal bacterial overgrowth, bacterial translocation and spontaneous bacterial peritonitis in cirrhotic rats with ascites. *Dig Liver Dis* 2012;44(3):239-44.
- Coussens LM, Werb Z. Inflammation and cancer. *Nature* 2002;420(6917):860-7.
- Dalby KN, Tekedereli I, Lopez-Berestein G, Ozpolat B. Targeting the prodeath and prosurvival functions of autophagy as novel therapeutic strategies in cancer. *Autophagy* 2010;6(3):322-9.
- Damiano V, Caputo R, Bianco R, D'Armiento FP, Leonardi A, De Placido S, et al. Novel toll-like receptor 9 agonist induces epidermal growth factor receptor (EGFR) inhibition and synergistic antitumour activity with EGFR inhibitors. *Clin Cancer Res* 2006;12(2):577-83.
- Dapito DH, Mencin A, Gwak GY, Pradere JP, Jang MK, Mederacke I, et al. Promotion of hepatocellular carcinoma by the intestinal microbiota and TLR4. *Cancer Cell* 2012;21(4):504-16.
- de Jong SD, Basha G, Wilson KD, Kazem M, Cullis P, Jefferies W, et al. The immunostimulatory activity of unmethylated and methylated CpG oligodeoxynucleotide is dependent on their ability to colocalise with TLR9 in late endosomes. *J Immunol* 2010;184(11):6092-102.
- Delgado MA, Elmaoued RA, Davis AS, Kyei G, Deretic V. Toll-like receptors control autophagy. *EMBO J* 2008;27(7):1110-21.

- Dengjel J, Nastke MD, Gouttefangeas C, Gitsioudis G, Schoor O, Altenberend F, et al. Unexpected abundance of HLA class II presented peptides in primary renal cell carcinomas. *Clin Cancer Res* 2006;12(14 Pt 1):4163-70.
- Dengjel J, Schoor O, Fischer R, Reich M, Kraus M, Muller M, et al. Autophagy promotes MHC class II presentation of peptides from intracellular source proteins. *Proc Natl Acad Sci U S A* 2005;102(22):7922-7.
- Ding ZB, Hui B, Shi YH, Zhou J, Peng YF, Gu CY, et al. Autophagy activation in hepatocellular carcinoma contributes to the tolerance of oxaliplatin via reactive oxygen species modulation. *Clin Cancer Res* 2011;17(19):6229-38.
- Dolganiuc A, Chang S, Kodys K, Mandrekar P, Bakis G, Cormier M, et al. Hepatitis C virus (HCV) core protein-induced, monocyte-mediated mechanisms of reduced IFN-alpha and plasmacytoid dendritic cell loss in chronic HCV infection. *J Immunol* 2006;177(10):6758-68.
- Dragani TA. Risk of HCC: genetic heterogeneity and complex genetics. *J Hepatol* 2010;52(2):252-7.
- Drebber U, Dienes HP. [Diagnosis and differential diagnosis of hepatocellular carcinoma]. *Pathologe* 2006;27(4):294-9.
- Droemann D, Albrecht D, Gerdes J, Ulmer AJ, Branscheid D, Vollmer E, et al. Human lung cancer cells express functionally active Toll-like receptor 9. *Respir Res* 2005;6:1.
- Efe C, Purnak T, Ozaslan E, Ozbalkan Z, Karaaslan Y, Altiparmak E, et al. Autoimmune liver disease in patients with systemic lupus erythematosus: a retrospective analysis of 147 cases. *Scand J Gastroenterol* 2011;46(6):732-7.
- el Sader MH, Doyl E, Kay E, et al. Proliferation indexes--a comparison between cutaneous basal and squamous cell carcinomas. *J Clin Pathol.* 1996;49:549-51
- El-Serag HB, Rudolph KL. Hepatocellular carcinoma: epidemiology and molecular carcinogenesis. *Gastroenterology* 2007;132(7):2557-76.
- El-Serag HB. Hepatocellular carcinoma. *N Engl J Med* 2011;365(12):1118-27.
- Elsharkawy AM, Mann DA. Nuclear factor-kappaB and the hepatic inflammation-fibrosis-cancer axis. *Hepatology* 2007;46(2):590-7.

- Ewald SE, Lee BL, Lau L, Wickliffe KE, Shi GP, Chapman HA, et al. The ectodomain of Toll-like receptor 9 is cleaved to generate a functional receptor. *Nature* 2008;456(7222):658-62.
- Fairbanks KD, Tavill AS. Liver disease in alpha 1-antitrypsin deficiency: a review. *Am J Gastroenterol* 2008;103(8):2136-41; quiz 42.
- Fan C, Wang W, Zhao B, Zhang S, Miao J. Chloroquine inhibits cell growth and induces cell death in A549 lung cancer cells. *Bioorg Med Chem* 2006;14(9):3218-22.
- Farazi PA, DePinho RA. Hepatocellular carcinoma pathogenesis: from genes to environment. *Nat Rev Cancer* 2006;6(9):674-87.
- Fava G, Demorrow S, Gaudio E, Franchitto A, Onori P, Carpino G, et al. Endothelin inhibits cholangiocarcinoma growth by a decrease in the vascular endothelial growth factor expression. *Liver Int* 2009;29(7):1031-42.
- Feo F, Frau M, Tomasi ML, Brozzetti S, Pascale RM. Genetic and epigenetic control of molecular alterations in hepatocellular carcinoma. *Exp Biol Med (Maywood)* 2009;234(7):726-36.
- Firat E, Gaedicke S, Tsurumi C, Esser N, Weyerbrock A, Niedermann G. Delayed cell death associated with mitotic catastrophe in gamma-irradiated stem-like glioma cells. *Radiat Oncol* 2011;6:71.
- Fisson S, Darrasse-Jeze G, Litvinova E, Septier F, Klatzmann D, Liblau R, et al. Continuous activation of autoreactive CD4+ CD25+ regulatory T cells in the steady state. *J Exp Med* 2003;198(5):737-46.
- Fitzgerald KA, Rowe DC, Barnes BJ, Caffrey DR, Visintin A, Latz E, et al. LPS-TLR4 signaling to IRF-3/7 and NF-kappaB involves the toll adapters TRAM and TRIF. *J Exp Med* 2003;198(7):1043-55.
- Frances R, Zapater P, Gonzalez-Navajas JM, Munoz C, Cano R, Moreu R, et al. Bacterial DNA in patients with cirrhosis and noninfected ascites mimics the soluble immune response established in patients with spontaneous bacterial peritonitis. *Hepatology* 2008;47(3):978-85.
- Franco LM, Krishnamurthy V, Bali D, Weinstein DA, Arn P, Clary B, et al. Hepatocellular carcinoma in glycogen storage disease type Ia: a case series. *J Inherit Metab Dis* 2005;28(2):153-62.
- Frasinariu OE, Ceccarelli S, Alisi A, Moraru E, Nobili V. Gut-liver axis

and fibrosis in nonalcoholic fatty liver disease: An input for novel therapies. *Dig Liver Dis*. 2012;(12)00430-6.

- Fukata M, Chen A, Klepper A, Krishnareddy S, Vamadevan AS, Thomas LS, et al. Cox-2 is regulated by Toll-like receptor-4 (TLR4) signaling: Role in proliferation and apoptosis in the intestine. *Gastroenterology* 2006;131(3):862-77.
- Fukui H, Brauner B, Bode JC, Bode C. Plasma endotoxin concentrations in patients with alcoholic and non-alcoholic liver disease: reevaluation with an improved chromogenic assay. *J Hepatol* 1991;12(2):162-9.
- Fung J, Lai CL, Yuen MF. Hepatitis B and C virus-related carcinogenesis. *Clin Microbiol Infect* 2009;15(11):964-70.
- Gabele E, Muhlbauer M, Dorn C, Weiss TS, Froh M, Schnabl B, et al. Role of TLR9 in hepatic stellate cells and experimental liver fibrosis. *Biochem Biophys Res Commun* 2008;376(2):271-6.
- Gao M, Ha T, Zhang X, Wang X, Liu L, Kalbfleisch J, et al. The Toll-like Receptor 9 Ligand, CpG Oligodeoxynucleotide, Attenuates Cardiac Dysfunction in Polymicrobial Sepsis, Involving Activation of Both Phosphoinositide 3 Kinase/Akt and Extracellular-Signal-Related Kinase Signaling. *J Infect Dis* 2013;207(9):1471-9.
- Gong G, Waris G, Tanveer R, Siddiqui A. Human hepatitis C virus NS5A protein alters intracellular calcium levels, induces oxidative stress, and activates STAT-3 and NF-kappa B. *Proc Natl Acad Sci U S A* 2001;98(17):9599-604.
- Gonzalez-Reyes S, Fernandez JM, Gonzalez LO, Aguirre A, Suarez A, Gonzalez JM, et al. Study of TLR3, TLR4, and TLR9 in prostate carcinomas and their association with biochemical recurrence. *Cancer Immunol Immunother* 2011;60(2):217-26.
- Gozuacik D, Kimchi A. Autophagy as a cell death and tumour suppressor mechanism. *Oncogene* 2004;23(16):2891-906.
- Grimm M, Kim M, Rosenwald A, Heemann U, Germer CT, Waaga-Gasser AM, et al. Toll-like receptor (TLR) 7 and TLR8 expression on CD133+ cells in colorectal cancer points to a specific role for inflammation-induced TLRs in tumourigenesis and tumour progression. *Eur J Cancer* 2010;46(15):2849-57.
- Guarner C, Gonzalez-Navajas JM, Sanchez E, Soriando G, Frances R,

Chiva M, et al. The detection of bacterial DNA in blood of rats with CCl4-induced cirrhosis with ascites represents episodes of bacterial translocation. *Hepatology* 2006;44(3):633-9.

Guiducci C, Ghirelli C, Marloie-Provost MA, Matray T, Coffman RL, Liu YJ, et al. PI3K is critical for the nuclear translocation of IRF-7 and type I IFN production by human plasmacytoid predendritic cells in response to TLR activation. *J Exp Med* 2008;205(2):315-22.

- Guiducci C, Gong M, Xu Z, Gill M, Chaussabel D, Meeker T, et al. TLR recognition of self nucleic acids hampers glucocorticoid activity in lupus. *Nature* 2010;465(7300):937-41.
- Hacker H, Mischak H, Miethke T, Liptay S, Schmid R, Sparwasser T, et al. CpG-DNA-specific activation of antigen-presenting cells requires stress kinase activity and is preceded by non-specific endocytosis and endosomal maturation. *EMBO J* 1998;17(21):6230-40.
- Hanahan D, Weinberg RA. Hallmarks of cancer: the next generation. *Cell* 2011;144(5):646-74.
- Hanahan D, Weinberg RA. The hallmarks of cancer. *Cell* 2000;100(1):57-70.
- Harada K, Ohira S, Isse K, Ozaki S, Zen Y, Sato Y, et al. Lipopolysaccharide activates nuclear factor-kappaB through toll-like receptors and related molecules in cultured biliary epithelial cells. *Lab Invest* 2003;83(11):1657-67.
- Harmey JH, Bucana CD, Lu W, Byrne AM, McDonnell S, Lynch C, et al. Lipopolysaccharide-induced metastatic growth is associated with increased angiogenesis, vascular permeability and tumour cell invasion. *Int J Cancer* 2002;101(5):415-22.
- Harmey JH, Bucana CD, Lu W, Byrne AM, McDonnell S, Lynch C, et al. Lipopolysaccharide-induced metastatic growth is associated with increased angiogenesis, vascular permeability and tumour cell invasion. *Int J Cancer* 2002;101(5):415-22.
- Hasimu A, Ge L, Li QZ, Zhang RP, Guo X. Expressions of Toll-like receptors 3, 4, 7, and 9 in cervical lesions and their correlation with HPV16 infection in Uighur women. *Chin J Cancer* 2011;30(5):344-50.

- Hayashi F, Smith KD, Ozinsky A, Hawn TR, Yi EC, Goodlett DR, et al. The innate immune response to bacterial flagellin is mediated by Toll-like receptor 5. *Nature* 2001;410(6832):1099-103.
- He W, Liu Q, Wang L, Chen W, Li N, Cao X. TLR4 signaling promotes immune escape of human lung cancer cells by inducing immunosuppressive cytokines and apoptosis resistance. *Mol Immunol* 2007;44(11):2850-9.
- Heil F, Hemmi H, Hochrein H, Ampenberger F, Kirschning C, Akira S, et al. Species-specific recognition of single-stranded RNA via toll-like receptor 7 and 8. *Science* 2004;303(5663):1526-9.
- Heindryckx F, Colle I, Van Vlierberghe H. Experimental mouse models for hepatocellular carcinoma research. *Int J Exp Pathol* 2009;90(4):367-86.
- Hemmi H, Takeuchi O, Kawai T, Kaisho T, Sato S, Sanjo H, et al. A Toll-like receptor recognizes bacterial DNA. *Nature* 2000;408(6813):740-5.
- Henao-Mejia J, Elinav E, Jin C, Hao L, Mehal WZ, Strowig T, et al. Inflammasome-mediated dysbiosis regulates progression of NAFLD and obesity. *Nature* 2012;482(7384):179-85.
- Hines IN, Wheeler MD. Recent advances in alcoholic liver disease III. Role of the innate immune response in alcoholic hepatitis. *Am J Physiol Gastrointest Liver Physiol* 2004;287(2):G310-4.
- Homann N, Stickel F, Konig IR, Jacobs A, Junghanns K, Benesova M, et al. Alcohol dehydrogenase 1C*1 allele is a genetic marker for alcohol-associated cancer in heavy drinkers. *Int J Cancer* 2006;118(8):1998-2002.
- Huang B, Zhao J, Shen S, Li H, He KL, Shen GX, et al. Listeria monocytogenes promotes tumour growth via tumour cell toll-like receptor 2 signaling. *Cancer Res* 2007;67(9):4346-52.
- Huang H, Shiffman ML, Friedman S, Venkatesh R, Bzowej N, Abar OT, et al. A 7 gene signature identifies the risk of developing cirrhosis in patients with chronic hepatitis C. *Hepatology* 2007;46(2):297-306.
- Huang JL, Hezel AF. Autophagy in intra-hepatic cholangiocarcinoma. *Autophagy* 2012;8(7):1148-9.
- Huang WT, Weng SW, Huang CC, Lin HC, Tsai PC, Chuang JH. Expression of Toll-like receptor9 in diffuse large B-cell lymphoma: further exploring CpG oligodeoxynucleotide in NFkappaB pathway. *APMIS*

2012;120(11):872-81.

- Huleatt JW, Nakaar V, Desai P, Huang Y, Hewitt D, Jacobs A, et al. Potent immunogenicity and efficacy of a universal influenza vaccine candidate comprising a recombinant fusion protein linking influenza M2e to the TLR5 ligand flagellin. *Vaccine* 2008;26(2):201-14.
- Hussain SP, Schwank J, Staib F, Wang XW, Harris CC. TP53 mutations and hepatocellular carcinoma: insights into the etiology and pathogenesis of liver cancer. *Oncogene* 2007;26(15):2166-76.
- Igney FH, Krammer PH. Immune escape of tumours: apoptosis resistance and tumour counterattack. *J Leukoc Biol* 2002;71(6):907-20.
- Ilvesaro JM, Merrell MA, Li L, Wakchoure S, Graves D, Brooks S, et al. Toll-like receptor 9 mediates CpG oligonucleotide-induced cellular invasion. *Mol Cancer Res* 2008;6(10):1534-43.
- Ilvesaro JM, Merrell MA, Swain TM, Davidson J, Zayzafoon M, Harris KW, et al. Toll like receptor-9 agonists stimulate prostate cancer invasion in vitro. *Prostate* 2007;67(7):774-81.
- Inoue S. [Analyses of cell cycle and DNA]. *Rinsho Byori* 2001;49(9):835-41.
- Ishak K, Baptista A, Bianchi L, Callea F, De Groote J, Gudat F, et al. Histological grading and staging of chronic hepatitis. *J Hepatol* 1995;22(6):696-9.
- Jahrsdorfer B, Jox R, Muhlenhoff L, Tschoep K, Krug A, Rothenfusser S, et al. Modulation of malignant B cell activation and apoptosis by bcl-2 antisense ODN and immunostimulatory CpG ODN. *J Leukoc Biol* 2002;72(1):83-92.
- Jahrsdorfer B, Wooldridge JE, Blackwell SE, Taylor CM, Griffith TS, Link BK, et al. Immunostimulatory oligodeoxynucleotides induce apoptosis of B cell chronic lymphocytic leukemia cells. *J Leukoc Biol* 2005;77(3):378-87.
- Janecke AR, Mayatepek E, Utermann G. Molecular genetics of type 1 glycogen storage disease. *Mol Genet Metab* 2001;73(2):117-25.
- Janeway CA, Jr., Medzhitov R. Innate immune recognition. *Annu Rev Immunol* 2002;20:197-216.
- Janku F, McConkey DJ, Hong DS, Kurzrock R. Autophagy as a target for anticancer therapy. *Nat Rev Clin Oncol* 2011;8(9):528-39.

- Janssens S, Beyaert R. Role of Toll-like receptors in pathogen recognition. *Clin Microbiol Rev* 2003;16(4):637-46.
- Jego G, Bataille R, Geffroy-Luseau A, Descamps G, Pellat-Deceunynck C. Pathogen-associated molecular patterns are growth and survival factors for human myeloma cells through Toll-like receptors. *Leukemia* 2006;20(6):1130-7.
- Jing YY, Han ZP, Sun K, Zhang SS, Hou J, Liu Y, et al. Toll-like receptor 4 signaling promotes epithelial-mesenchymal transition in human hepatocellular carcinoma induced by lipopolysaccharide. *BMC Med* 2012;10:98.
- Kalinski T, Roessner A. Hepatocellular carcinoma: pathology and liver biopsy. *Dig Dis* 2009;27(2):102-8.
- Kauppila JH, Takala H, Selander KS, Lehenkari PP, Saarnio J, Karttunen TJ. Increased Toll-like receptor 9 expression indicates adverse prognosis in oesophageal adenocarcinoma. *Histopathology* 2011;59(4):643-9.
- Kawai T, Akira S. TLR signaling. *Cell Death Differ* 2006;13(5):816-25.
- Kelly MG, Alvero AB, Chen R, Silasi DA, Abrahams VM, Chan S, et al. TLR-4 signaling promotes tumour growth and paclitaxel chemoresistance in ovarian cancer. *Cancer Res* 2006;66(7):3859-68.
- Kew MC. Hepatic iron overload and hepatocellular carcinoma. *Cancer Lett* 2009;286(1):38-43.
- Kim KM, Kwon SN, Kang JI, Lee SH, Jang SK, Ahn BY, et al. Hepatitis C virus NS2 protein activates cellular cyclic AMP-dependent pathways. *Biochem Biophys Res Commun* 2007;356(4):948-54.
- Kouroumalis EA, Koskinas J. Treatment of chronic active hepatitis B (CAH B) with chloroquine: a preliminary report. *Ann Acad Med Singapore* 1986;15(2):149-52.
- Kowdley KV. Iron, hemochromatosis, and hepatocellular carcinoma. *Gastroenterology* 2004;127(5 Suppl 1):S79-86.
- Krawitt EL. Autoimmune hepatitis. *N Engl J Med* 1996;334(14):897-903.
- Krieg AM. TLR9 and DNA 'feel' RAGE. *Nat Immunol* 2007;8(5):475-7.
- Krieg AM. Toll-like receptor 9 (TLR9) agonists in the treatment of cancer. *Oncogene* 2008;27(2):161-7.
- Kundu SD, Lee C, Billips BK, Habermacher GM, Zhang Q, Liu V, et al.

The toll-like receptor pathway: a novel mechanism of infection-induced carcinogenesis of prostate epithelial cells. *Prostate* 2008;68(2):223-9.

- Kuznik A, Bencina M, Svajger U, Jeras M, Rozman B, Jerala R. Mechanism of endosomal TLR inhibition by antimalarial drugs and imidazoquinolines. *J Immunol* 2011;186(8):4794-804.
- Latz E, Schoenemeyer A, Visintin A, Fitzgerald KA, Monks BG, Knetter CF, et al. TLR9 signals after translocating from the ER to CpG DNA in the lysosome. *Nat Immunol* 2004;5(2):190-8.
- Lee J, Chuang TH, Redecke V, She L, Pitha PM, Carson DA, et al. Molecular basis for the immunostimulatory activity of guanine nucleoside analogs: activation of Toll-like receptor 7. *Proc Natl Acad Sci U S A* 2003;100(11):6646-51.
- Lehner M, Morhart P, Stilper A, Petermann D, Weller P, Stachel D, et al. Efficient chemokine-dependent migration and primary and secondary IL-12 secretion by human dendritic cells stimulated through Toll-like receptors. *J Immunother* 2007;30(3):312-22.
- Leifer CA, Kennedy MN, Mazzoni A, Lee C, Kruhlak MJ, Segal DM. TLR9 is localised in the endoplasmic reticulum prior to stimulation. *J Immunol* 2004;173(2):1179-83.
- Lemaitre B, Nicolas E, Michaut L, Reichhart JM, Hoffmann JA. The dorsoventral regulatory gene cassette spatzle/Toll/cactus controls the potent antifungal response in Drosophila adults. *Cell* 1996;86(6):973-83.
- Leong TY, Leong AS. Epidemiology and carcinogenesis of hepatocellular carcinoma. *HPB (Oxford)* 2005;7(1):5-15.
- Levine B, Mizushima N, Virgin HW. Autophagy in immunity and inflammation. *Nature* 2011;469(7330):323-35.

- Li N, Fan XG, Tang SE, Zhu C. [Toll-like receptor 9 in cpG oligodeoxynucleotides-induced species-specific immune responses]. *Zhong Nan Da Xue Xue Bao Yi Xue Ban* 2005;30(5):533-5.
- Lim EJ, Park DW, Lee JG, Lee CH, Bae YS, Hwang YC, et al. Toll-like receptor 9-mediated inhibition of apoptosis occurs through suppression of FoxO3a activity and induction of FLIP expression. *Exp Mol Med* 2010;42(10):712-20.
- Lin KJ, Lin TM, Wang CH, Liu HC, Lin YL, Eng HL. Down-regulation of Toll-like receptor 7 expression in hepatitis-virus-related human hepatocellular carcinoma. *Hum Pathol* 2013;44(4):534-41.
- Lin RS, Lee FY, Lee SD, Tsai YT, Lin HC, Lu RH, et al. Endotoxemia in patients with chronic liver diseases: relationship to severity of liver diseases, presence of esophageal varices, and hyperdynamic circulation. *J Hepatol* 1995;22(2):165-72.
- Llovet JM, Bartoli R, Planas R, Vinado B, Perez J, Cabre E, et al. Selective intestinal decontamination with Norfloxacin reduces bacterial translocation in ascitic cirrhotic rats exposed to hemorrhagic shock. *Hepatology* 1996;23(4):781-7.
- Loehberg CR, Strissel PL, Dittrich R, Strick R, Dittmer J, Dittmer A, et al. Akt and p53 are potential mediators of reduced mammary tumour growth by cloroquine and the mTOR inhibitor RAD001. *Biochem Pharmacol* 2012;83(4):480-8.
- Lu YC, Yeh WC, Ohashi PS. LPS/TLR4 signal transduction pathway. *Cytokine* 2008;42(2):145-51.
- Luedde T, Schwabe RF. NF-kappaB in the liver--linking injury, fibrosis and hepatocellular carcinoma. *Nat Rev Gastroenterol Hepatol* 2011;8(2):108-18.

- Luo JL, Maeda S, Hsu LC, Yagita H, Karin M. Inhibition of NF-kappaB in cancer cells converts inflammation- induced tumour growth mediated by TNFalpha to TRAIL-mediated tumour regression. *Cancer Cell* 2004;6(3):297-305.
- Macfarlane DE, Manzel L. Antagonism of immunostimulatory CpG-oligodeoxynucleotides by quinacrine, chloroquine, and structurally related compounds. *J Immunol* 1998;160(3):1122-31.
- Majewski S, Marczak M, Mlynarczyk B, Benninghoff B, Jablonska S. Imiquimod is a strong inhibitor of tumour cell-induced angiogenesis. *Int J Dermatol* 2005;44(1):14-9.
- Mammucari C, Schiaffino S, Sandri M. Downstream of Akt: FoxO3 and mTOR in the regulation of autophagy in skeletal muscle. *Autophagy* 2008;4(4):524-6.
- Mandrekar P, Szabo G. Signalling pathways in alcohol-induced liver inflammation. *J Hepatol* 2009;50(6):1258-66.
- Martin M, Rehani K, Jope RS, Michalek SM. Toll-like receptor-mediated cytokine production is differentially regulated by glycogen synthase kinase 3. *Nat Immunol* 2005;6(8):777-84.
- Matsukura S, Kokubu F, Kurokawa M, Kawaguchi M, Ieki K, Kuga H, et al. Synthetic double-stranded RNA induces multiple genes related to inflammation through Toll-like receptor 3 depending on NF-kappaB and/or IRF-3 in airway epithelial cells. *Clin Exp Allergy* 2006;36(8):1049-62.
- McKillop IH, Moran DM, Jin X, Koniaris LG. Molecular pathogenesis of hepatocellular carcinoma. *J Surg Res* 2006;136(1):125-35.
- McKillop IH, Schrum LW. Alcohol and liver cancer. *Alcohol* 2005;35(3):195-203.
- Mencin A, Kluwe J, Schwabe RF. Toll-like receptors as targets in chronic liver diseases. *Gut* 2009;58(5):704-20.
- Mencin A, Kluwe J, Schwabe RF. Toll-like receptors as targets in chronic liver diseases. *Gut* 2009;58(5):704-20.
- Merino I, Thompson JD, Millard CB, Schmidt JJ, Pang YP. Bis-imidazoles as molecular probes for peripheral sites of the zinc endopeptidase of botulinum neurotoxin serotype A. *Bioorg Med Chem* 2006;14(10):3583-91.

- Merrell MA, Ilvesaro JM, Lehtonen N, Sorsa T, Gehrs B, Rosenthal E, et al. Toll-like receptor 9 agonists promote cellular invasion by increasing matrix metalloproteinase activity. *Mol Cancer Res* 2006;4(7):437-47.
- Min R, Zun Z, Siyi L, Wenjun Y, Lizheng W, Chenping Z. Increased expression of Toll-like receptor-9 has close relation with tumour cell proliferation in oral squamous cell carcinoma. *Arch Oral Biol* 2011;56(9):877-84.
- Monick MM, Mallampalli RK, Carter AB, Flaherty DM, McCoy D, Robeff PK, et al. Ceramide regulates lipopolysaccharide-induced phosphatidylinositol 3-kinase and Akt activity in human alveolar macrophages. *J Immunol* 2001;167(10):5977-85.
- Morisato D, Anderson KV. Signaling pathways that establish the dorsal-ventral pattern of the Drosophila embryo. *Annu Rev Genet* 1995;29:371-99.
- Mozer-Lisewska I, Sluzewski W, Kaczmarek M, Jenek R, Szczepanski M, Figlerowicz M, et al. Tissue localization of Toll-like receptors in biopsy specimens of liver from children infected with hepatitis C virus. *Scand J Immunol* 2005;62(4):407-12.
- Muccioli M, Sprague L, Nandigam H, Pate M, Benencia F. Toll-Like Receptors as Novel Therapeutic Targets for Ovarian Cancer. *ISRN Oncol.* 2012;2012: 642141
- Munz C. Enhancing immunity through autophagy. *Annu Rev Immunol* 2009;27:423-49.
- Nakanishi C, Toi M. Nuclear factor-kappaB inhibitors as sensitizers to anticancer drugs. *Nat Rev Cancer* 2005;5(4):297-309.
- Ninlawan K, O'Hara SP, Splinter PL, Yongvanit P, Kaewkes S, Surapaitoon A, et al. Opisthorchis viverrini excretory/secretory products induce toll-like receptor 4 up regulation and production of interleukin 6 and 8 in cholangiocyte. *Parasitol Int* 2010;59(4):616-21.
- Oblak A, Jerala R. Toll-like receptor 4 activation in cancer progression and therapy. *Clin Dev Immunol* 2011;2011:609579.
- Ochi A, Graffeo CS, Zambirinis CP, Rehman A, Hackman M, Fallon N, et al. Toll-like receptor 7 regulates pancreatic carcinogenesis in mice and humans. *J Clin Invest* 2012;122(11):4118-29.
- Palapattu GS, Wu C, Silvers CR, Martin HB, Williams K, Salamone L, et al. Selective expression of CD44, a putative prostate cancer stem cell marker,

in neuroendocrine tumour cells of human prostate cancer. *Prostate* 2009;69(7):787-98.

- Palmer WC, Patel T. Are common factors involved in the pathogenesis of primary liver cancers? A meta-analysis of risk factors for intrahepatic cholangiocarcinoma. *J Hepatol* 2012;57(1):69-76.
- Pang R, Tse E, Poon RT. Molecular pathways in hepatocellular carcinoma. *Cancer Lett* 2006;240(2):157-69.
- Paone A, Starace D, Galli R, Padula F, De Cesaris P, Filippini A, et al. Toll-like receptor 3 triggers apoptosis of human prostate cancer cells through a PKC-alpha-dependent mechanism. *Carcinogenesis* 2008;29(7):1334-42.
- Park SJ, Song HY, Youn HS. Suppression of the TRIF-dependent signaling pathway of toll-like receptors by isoliquiritigenin in RAW264.7 macrophages. *Mol Cells* 2009;28(4):365-8.
- Parkin DM, Bray F, Ferlay J, Pisani P. Estimating the world cancer burden: Globocan 2000. *Int J Cancer* 2001;94(2):153-6.
- Parkin DM, Bray F, Ferlay J, Pisani P. Global cancer statistics, 2002. *CA Cancer J Clin* 2005;55(2):74-108.
- Parola M and Pinzani M. Hepatic wound repair Fibrogenesis Tissue Repair 2009;2:4
- Pawar RD, Ramanjaneyulu A, Kulkarni OP, Lech M, Segerer S, Anders HJ. Inhibition of Toll-like receptor-7 (TLR-7) or TLR-7 plus TLR-9 attenuates glomerulonephritis and lung injury in experimental lupus. *J Am Soc Nephrol* 2007;18(6):1721-31.
- Pevsner-Fischer M, Morad V, Cohen-Sfady M, Rousso-Noori L, Zanin-Zhorov A, Cohen S, et al. Toll-like receptors and their ligands control mesenchymal stem cell functions. *Blood* 2007;109(4):1422-32.
- Pikarsky E, Porat RM, Stein I, Abramovitch R, Amit S, Kasem S, et al. NF-kappaB functions as a tumour promoter in inflammation-associated cancer. *Nature* 2004;431(7007):461-6.
- Pineau P, Marchio A, Battiston C, Cordina E, Russo A, Terris B, et al. Chromosome instability in human hepatocellular carcinoma depends on p53 status and aflatoxin exposure. *Mutat Res* 2008;653(1-2):6-13.
- Pinlaor S, Sripa B, Ma N, Hiraku Y, Yongvanit P, Wongkham S, et al.

Nitrative and oxidative DNA damage in intrahepatic cholangiocarcinoma patients in relation to tumour invasion. *World J Gastroenterol* 2005;11(30):4644-9.

Pinzone MR, Celesia BM, Di Rosa M, Cacopardo B, Nunnari G. Microbial translocation in chronic liver diseases. *Int J Microbiol* 2012;2012:694629.

- Pivtoraiko VN, Stone SL, Roth KA, Shacka JJ. Oxidative stress and autophagy in the regulation of lysosome-dependent neuron death. *Antioxid Redox Signal* 2009;11(3):481-96.
- Platta HW, Stenmark H. Endocytosis and signaling. *Curr Opin Cell Biol* 2011;23(4):393-403.
- Polesel J, Zucchetto A, Montella M, Dal Maso L, Crispo A, La Vecchia C, et al. The impact of obesity and diabetes mellitus on the risk of hepatocellular carcinoma. *Ann Oncol* 2009;20(2):353-7.
- Pradere JP, Troeger JS, Dapito DH, Mencin AA, Schwabe RF. Toll-like receptor 4 and hepatic fibrogenesis. *Semin Liver Dis* 2010;30(3):232-44.
- Pries R, Hogrefe L, Xie L, Frenzel H, Brocks C, Ditz C, et al. Induction of c-Myc-dependent cell proliferation through toll-like receptor 3 in head and neck cancer. *Int J Mol Med* 2008;21(2):209-15.
- Pull SL, Doherty JM, Mills JC, Gordon JI, Stappenbeck TS. Activated macrophages are an adaptive element of the colonic epithelial progenitor niche necessary for regenerative responses to injury. *Proc Natl Acad Sci U S A* 2005;102(1):99-104.
- Rabiller A, Nunes H, Lebrec D, Tazi KA, Wartski M, Dulmet E, et al. Prevention of gram-negative translocation reduces the severity of hepatopulmonary syndrome. *Am J Respir Crit Care Med* 2002;166(4):514-7.
- Rakoff-Nahoum S, Medzhitov R. Role of toll-like receptors in tissue repair and tumourigenesis. *Biochemistry (Mosc)* 2008;73(5):555-61.
- Rakoff-Nahoum S, Paglino J, Eslami-Varzaneh F, Edberg S, Medzhitov R. Recognition of commensal microflora by toll-like receptors is required for intestinal homeostasis. *Cell* 2004;118(2):229-41.
- Rallabhandi P, Bell J, Boukhvalova MS, Medvedev A, Lorenz E, Arditi M, et al. Analysis of TLR4 polymorphic variants: new insights into TLR4/MD-2/CD14 stoichiometry, structure, and signaling. *J Immunol* 2006;177(1):322-32.

- Ramser B, Kokot A, Metze D, Weiss N, Luger TA, Bohm M. Hydroxychloroquine modulates metabolic activity and proliferation and induces autophagic cell death of human dermal fibroblasts. *J Invest Dermatol* 2009;129(10):2419-26.
- Ramadori G, Moriconi F, Malik I, Dudas J. Physiology and pathophysiology of liver inflammation, damage and repair. J Physiol Pharmacol .2008;59(1):107-17
- Ratziu V, Giral P, Charlotte F, Bruckert E, Thibault V, Theodorou I, et al. Liver fibrosis in overweight patients. *Gastroenterology* 2000;118(6):1117-23.
- Ratziu V, Trabut JB, Poynard T. Fat, diabetes, and liver injury in chronic hepatitis C. *Curr Gastroenterol Rep* 2004;6(1):22-9.
- Razack AH. Bacillus Calmette-Guerin and bladder cancer. *Asian J Surg* 2007;30(4):302-9.
- Ren T, Wen ZK, Liu ZM, Qian C, Liang YJ, Jin ML, et al. Targeting toll-like receptor 9 with CpG oligodeoxynucleotides enhances anti-tumour responses of peripheral blood mononuclear cells from human lung cancer patients. *Cancer Invest* 2008;26(5):448-55.
- Repetto G, del Peso A, Zurita JL. Neutral red uptake assay for the estimation of cell viability/cytotoxicity. *Nat Protoc* 2008;3(7):1125-31.
- Roach JC, Glusman G, Rowen L, Kaur A, Purcell MK, Smith KD, et al. The evolution of vertebrate Toll-like receptors. *Proc Natl Acad Sci U S A* 2005;102(27):9577-82.
- Rocken C, Carl-McGrath S. Pathology and pathogenesis of hepatocellular carcinoma. *Dig Dis* 2001;19(4):269-78.
- Roda JM, Parihar R, Carson WE, 3rd. CpG-containing oligodeoxynucleotides act through TLR9 to enhance the NK cell cytokine response to antibody-coated tumour cells. *J Immunol* 2005;175(3):1619-27.
- Rudnick DA, Perlmutter DH. Alpha-1-antitrypsin deficiency: a new paradigm for hepatocellular carcinoma in genetic liver disease. *Hepatology* 2005;42(3):514-21.
- Rutz M, Metzger J, Gellert T, Luppa P, Lipford GB, Wagner H, et al. Toll-like receptor 9 binds single-stranded CpG-DNA in a sequence- and pH-dependent manner. *Eur J Immunol* 2004;34(9):2541-50.

- Sakaguchi S. Naturally arising CD4+ regulatory t cells for immunologic self-tolerance and negative control of immune responses. *Annu Rev Immunol* 2004;22:531-62.
- Salaun B, Coste I, Rissoan MC, Lebecque SJ, Renno T. TLR3 can directly trigger apoptosis in human cancer cells. *J Immunol* 2006;176(8):4894-901.
- Salaun B, Coste I, Rissoan MC, Lebecque SJ, Renno T. TLR3 can directly trigger apoptosis in human cancer cells. *J Immunol* 2006;176(8):4894-901.
- Sanjuan M, Dillon C, Tait S, Moshiach S, Dorsey F, Connell S, et al. Toll-like receptor signalling in macrophages links the autophagy pathway to phagocytosis. *Nature*. 2007; 450(7173):1253-7
- Sato Y, Goto Y, Narita N, Hoon DS. Cancer Cells Expressing Toll-like Receptors and the Tumour Microenvironment. *Cancer Microenviron* 2009; 1:205-14
- Scatton O, Chiappini F, Liu XH, Riou P, Marconi A, Debuire B, et al. Generation and modulation of hepatocellular carcinoma circulating cells: a new experimental model. *J Surg Res* 2008;150(2):183-9.
- Schmausser B, Andrulis M, Endrich S, Muller-Hermelink HK, Eck M. Toll-like receptors TLR4, TLR5 and TLR9 on gastric carcinoma cells: an implication for interaction with Helicobacter pylori. *Int J Med Microbiol* 2005;295(3):179-85.
- Schmid D, Munz C. Innate and adaptive immunity through autophagy. *Immunity* 2007;27(1):11-21.
- Schneberger D, Caldwell S, Suri SS, Singh B. Expression of toll-like receptor 9 in horse lungs. *Anat Rec (Hoboken)* 2009;292(7):1068-77.
- Schon MP, Schon M. TLR7 and TLR8 as targets in cancer therapy. *Oncogene* 2008;27(2):190-9.
- Schutte K, Bornschein J, Malfertheiner P. Hepatocellular carcinoma--epidemiological trends and risk factors. *Dig Dis* 2009;27(2):80-92.
- Seki E, Brenner DA. Toll-like receptors and adaptor molecules in liver disease: update. *Hepatology* 2008;48(1):322-35.
- Seki E, De Minicis S, Osterreicher CH, Kluwe J, Osawa Y, Brenner DA,

et al. TLR4 enhances TGF-beta signaling and hepatic fibrosis. *Nat Med* 2007;13(11):1324-32.

- Seki E, Schnabl B. Role of innate immunity and the microbiota in liver fibrosis: crosstalk between the liver and gut. *J Physiol*;590(Pt 3):447-58.
- Seki E, Schnabl B. Role of innate immunity and the microbiota in liver fibrosis: crosstalk between the liver and gut. *J Physiol* 2012;590(Pt 3):447-58.
- Sester DP, Brion K, Trieu A, Goodridge HS, Roberts TL, Dunn J, et al. CpG DNA activates survival in murine macrophages through TLR9 and the phosphatidylinositol 3-kinase-Akt pathway. *J Immunol* 2006;177(7):4473-80.
- Sfondrini L, Rossini A, Besusso D, Merlo A, Tagliabue E, Menard S, et al. Antitumour activity of the TLR-5 ligand flagellin in mouse models of cancer. *J Immunol* 2006;176(11):6624-30.
- Shah N, Dhar D, El Zahraa Mohammed F, Habtesion A, Davies NA, Jover-Cobos M, et al. Prevention of acute kidney injury in a rodent model of cirrhosis following selective gut decontamination is associated with reduced renal TLR4 expression. *J Hepatol* 2012;56(5):1047-53.
- Sherman M. Surveillance of hepatocellular carcinoma: we must do better. *Am J Med* 2008;121(2):89-90.
- Sheyhidin I, Nabi G, Hasim A, Zhang RP, Ainiwaer J, Ma H, et al. Overexpression of TLR3, TLR4, TLR7 and TLR9 in esophageal squamous cell carcinoma. *World J Gastroenterol* 2011;17(32):3745-51.
- Shi YH, Ding ZB, Zhou J, Hui B, Shi GM, Ke AW, et al. Targeting autophagy enhances sorafenib lethality for hepatocellular carcinoma via ER stress-related apoptosis. *Autophagy* 2011;7(10):1159-72.
- Shimizu S, Takehara T, Hikita H, Kodama T, Tsunematsu H, Miyagi T, et al. Inhibition of autophagy potentiates the antitumour effect of the multikinase inhibitor sorafenib in hepatocellular carcinoma. *Int J Cancer* 2012;131(3):548-57.
- Shishodia S, Aggarwal BB. Nuclear factor-kappaB activation: a question of life or death. *J Biochem Mol Biol* 2002;35(1):28-40.
- Simons M, O'Donnell M, *Griffith T. Role of neutrophils in BCG immunotherapy for bladder cancer. Urol Oncol.* 2008;26(4):341-5
- Smits EL, Ponsaerts P, Van de Velde AL, Van Driessche A, Cools N,

Lenjou M, et al. Proinflammatory response of human leukemic cells to dsRNA transfection linked to activation of dendritic cells. *Leukemia* 2007;21(8):1691-9.

- Soares JB, Pimentel-Nunes P, Roncon-Albuquerque R, Leite-Moreira A. The role of lipopolysaccharide/toll-like receptor 4 signaling in chronic liver diseases. *Hepatol Int* 2010;4(4):659-72.
- Stadlbauer V, Mookerjee RP, Wright GA, Davies NA, Jurgens G, Hallstrom S, et al. Role of Toll-like receptors 2, 4, and 9 in mediating neutrophil dysfunction in alcoholic hepatitis. *Am J Physiol Gastrointest Liver Physiol* 2009;296(1):G15-22.
- Standish RA, Cholongitas E, Dhillon A, Burroughs AK, Dhillon AP. An appraisal of the histopathological assessment of liver fibrosis. *Gut* 2006;55(4):569-78.
- Starkel P, De Saeger C, Strain AJ, Leclercq I, Horsmans Y. NFkappaB, cytokines, TLR 3 and 7 expression in human end-stage HCV and alcoholic liver disease. *Eur J Clin Invest* 2010;40(7):575-84.
- Sun S, Rao NL, Venable J, Thurmond R, Karlsson L. TLR7/9 antagonists as therapeutics for immune-mediated inflammatory disorders. *Inflamm Allergy Drug Targets* 2007;6(4):223-35.
- Tada M, Omata M. Another key molecule for pathogenesis of hepatocellular carcinoma. *J Gastroenterol Hepatol* 2009;24(12):1803-4.
- Takala H, Kauppila JH, Soini Y, Selander KS, Vuopala KS, Lehenkari PP, et al. Toll-like receptor 9 is a novel biomarker for esophageal squamous cell dysplasia and squamous cell carcinoma progression. *J Innate Immun* 2011;3(6):631-8.
- Takeda K, Akira S. Microbial recognition by Toll-like receptors. *J Dermatol Sci* 2004;34(2):73-82.
- Takeuchi O, Akira S. Pattern recognition receptors and inflammation. *Cell* 2010;140(6):805-20.
- Takeuchi O, Akira S. Toll-like receptors; their physiological role and signal transduction system. *Int Immunopharmacol* 2001;1(4):625-35.
- Takeuchi O, Sato S, Horiuchi T, Hoshino K, Takeda K, Dong Z, et al. Cutting edge: role of Toll-like receptor 1 in mediating immune response to microbial lipoproteins. *J Immunol* 2002;169(1):10-4.

- Tanaka J, Sugimoto K, Shiraki K, Tameda M, Kusagawa S, Nojiri K, et al. Functional cell surface expression of toll-like receptor 9 promotes cell proliferation and survival in human hepatocellular carcinomas. *Int J Oncol* 2010;37(4):805-14.
- Tandon Y, Brodell RT. Local reactions to imiquimod in the treatment of basal cell carcinoma. *Dermatol Online J* 2012;18(9):1.
- Tarantino G, Di Cristina A, Pipitone R, Almasio PL, Di Vita G, Craxi A, et al. In vivo liver expression of TLR2, TLR3 and TLR7 in chronic hepatitis C. *J Biol Regul Homeost Agents* 2013;27(1):233-9.
- Teoh NC. Proliferative drive and liver carcinogenesis: too much of a good thing? *J Gastroenterol Hepatol* 2009;24(12):1817-25.
- Testro AG, Gow PJ, Angus PW, Wongseelashote S, Skinner N, Markovska V, et al. Effects of antibiotics on expression and function of Toll-like receptors 2 and 4 on mononuclear cells in patients with advanced cirrhosis. *J Hepatol* 2010;52(2):199-205.
- Thiele A, Wasner M, Muller C, Engeland K, Hauschildt S. Regulation and possible function of beta-catenin in human monocytes. *J Immunol* 2001;167(12):6786-93.
- Vanags D, Williams B, Johnson B, Hall S, Nash P, Taylor A, et al. Therapeutic efficacy and safety of chaperonin 10 in patients with rheumatoid arthritis: a double-blind randomised trial. *Lancet* 2006;368(9538):855-63.
- Vespasiani-Gentilucci U, Carotti S, Onetti-Muda A, Perrone G, Ginanni-Corradini S, Latasa MU, et al. Toll-like receptor-4 expression by hepatic progenitor cells and biliary epithelial cells in HCV-related chronic liver disease. *Mod Pathol* 2012;25(4):576-89.
- Wang C, Fei G, Liu Z, Li Q, Xu Z, Ren T. HMGB1 was a pivotal synergistic effecor for CpG oligonucleotide to enhance the progression of human lung cancer cells. *Cancer Biol Ther* 2012;13(9):727-36.
- Wang JS, Groopman JD. DNA damage by mycotoxins. *Mutat Res* 1999;424(1-2):167-81.
- Wei XQ, Guo YW, Liu JJ, Wen ZF, Yang SJ, Yao JL. The significance of Toll-like receptor 4 (TLR4) expression in patients with chronic hepatitis B. *Clin Invest Med* 2008;31(3):E123-30.

- Wolska A, Lech-Maranda E, Robak T. Toll-like receptors and their role in carcinogenesis and anti-tumour treatment. *Cell Mol Biol Lett* 2009;14(2):248-72.
- Wong CM, Ng IO. Molecular pathogenesis of hepatocellular carcinoma. *Liver Int* 2008;28(2):160-74.
- Woo HG, Lee JH, Yoon JH, Kim CY, Lee HS, Jang JJ, et al. Identification of a cholangiocarcinoma-like gene expression trait in hepatocellular carcinoma. *Cancer Res* 2010;70(8):3034-41.
- Wu GP, Li SH, Li DP, Yang ZH, He XC, Liao Y, et al. [Establishment of animal model for electroporation-mediated gene therapy in distraction osteogenesis of rabbit mandible]. *Zhonghua Zheng Xing Wai Ke Za Zhi* 2009;25(4):280-3.
- Wu W, Pang Y, Shen GA, Lu J, Lin J, Wang J, et al. Molecular cloning, characterization and expression of a novel trehalose-6-phosphate synthase homologue from Ginkgo biloba. *J Biochem Mol Biol* 2006;39(2):158-66.
- Wysocka M, Benoit BM, Newton S, Azzoni L, Montaner LJ, Rook AH. Enhancement of the host immune responses in cutaneous T-cell lymphoma by CpG oligodeoxynucleotides and IL-15. *Blood* 2004;104(13):4142-9.
- Xu L, Wen Z, Zhou Y, Liu Z, Li Q, Fei G, et al. MicroRNA-7-regulated TLR9 signaling-enhanced growth and metastatic potential of human lung cancer cells by altering the phosphoinositide-3-kinase, regulatory subunit 3/Akt pathway. *Mol Biol Cell* 2013;24(1):42-55.
- Xu N, Yao HP, Lv GC, Chen Z. Downregulation of TLR7/9 leads to deficient production of IFN-alpha from plasmacytoid dendritic cells in chronic hepatitis B. *Inflamm Res* 2012;61(9):997-1004.
- Xu Y, Jagannath C, Liu XD, Sharafkhaneh A, Kolodziejska KE, Eissa NT. Toll-like receptor 4 is a sensor for autophagy associated with innate immunity. *Immunity* 2007;27(1):135-44.
- Yamamoto M, Takeda K. Current views of toll-like receptor signaling pathways. *Gastroenterol Res Pract* 2010;2010:240365.
- Yang L, Seki E. Toll-like receptors in liver fibrosis: cellular crosstalk and mechanisms. *Front Physiol* 2012;3:138.
- Yang Q, Zhu P, Wang Z, Jiang Jn J. Toll-like receptor 4, a novel signal

transducer for lipopolysaccharide. *Chin J Traumatol* 2002;5(1):55-8.

- Yang ZZ, Novak AJ, Ziesmer SC, Witzig TE, Ansell SM. Malignant B cells skew the balance of regulatory T cells and TH17 cells in B-cell non-Hodgkin's lymphoma. *Cancer Res* 2009;69(13):5522-30.
- Yano Y, Yamamoto J, Kosuge T, Sakamoto Y, Yamasaki S, Shimada K, et al. Combined hepatocellular and cholangiocarcinoma: a clinicopathologic study of 26 resected cases. *Jpn J Clin Oncol* 2003;33(6):283-7.
- Yasuda H, Leelahavanichkul A, Tsunoda S, Dear JW, Takahashi Y, Ito S, et al. Chloroquine and inhibition of Toll-like receptor 9 protect from sepsis-induced acute kidney injury. *Am J Physiol Renal Physiol* 2008;294(5):F1050-8.
- Yeoman AD, Al-Chalabi T, Karani JB, Quaglia A, Devlin J, Mieli-Vergani G, et al. Evaluation of risk factors in the development of hepatocellular carcinoma in autoimmune hepatitis: Implications for follow-up and screening. *Hepatology* 2008;48(3):863-70.
- Yi AK, Krieg AM. Rapid induction of mitogen-activated protein kinases by immune stimulatory CpG DNA. *J Immunol* 1998;161(9):4493-7.
- Yi AK, Tuetken R, Redford T, Waldschmidt M, Kirsch J, Krieg AM. CpG motifs in bacterial DNA activate leukocytes through the pH-dependent generation of reactive oxygen species. *J Immunol* 1998;160(10):4755-61.
- Yoon YH, Cho KS, Hwang JJ, Lee SJ, Choi JA, Koh JY. Induction of lysosomal dilatation, arrested autophagy, and cell death by chloroquine in cultured ARPE-19 cells. *Invest Ophthalmol Vis Sci* 2010;51(11):6030-7.
- Yoshino H, Futakuchi M, Cho YM, Ogawa K, Takeshita F, Imai N, et al. Modification of an in vivo lung metastasis model of hepatocellular carcinoma by low dose N-nitrosomorpholine and diethylnitrosamine. *Clin Exp Metastasis* 2005;22(5):441-7.
- Zhang W, Gu Y, Chen Y, Deng H, Chen L, Chen S, et al. Intestinal flora imbalance results in altered bacterial translocation and liver function in rats with experimental cirrhosis. *Eur J Gastroenterol Hepatol* 2010;22(12):1481-6.
- Zhang YH, Wang C, Pang BS, Zhai ZG, Weng XZ. [The effect of VEGF antisense oligonucleotides combined with low molecular weight heparin on the growth and metastasis of mice Lewis lung cancer]. *Zhonghua Yi Xue Za Zhi* 2006;86(11):749-52.

- Zheng Y, Zhao YL, Deng X, Yang S, Mao Y, Li Z, et al. Chloroquine inhibits colon cancer cell growth in vitro and tumour growth in vivo via induction of apoptosis. *Cancer Invest* 2009;27(3):286-92.
- Zhou Q, Lui VW, Yeo W. Targeting the PI3K/Akt/mTOR pathway in hepatocellular carcinoma. *Future Oncol* 2011;7(10):1149-67.

7. Appendix

1. Reticulin stain reagents

- Acidified potassium permanganate 5% potassium permanganate 5ml, 2% hydrochloric acid 3ml, Distilled water 42 ml.
- 1%aqueous oxalic.
- 2.5% ferric ammonium sulphate.
- Ammonical silver nitrate: in fume hood 10% silver nitrate 5ml then concentrate cold ammonium hydroxide was added drop by drop until the formed precipitate just redissolve (clear colour). 3%aqueous sodium hydroxide 5ml then added to the sliver and ammonium hydroxide and a dark precipitate was formed. Redissolve the precipitate by adding ammonium hydroxide but stop adding the ammonium hydroxide with few precipitate granules remaining. Dilute to 50 ml with distilled water.
- 10% formalin in tap water.

2. Picro-Sirius Red staining reagents

To prepare Sirius red stain: 1% aqueous Sirius RedF3B 10ml was added to aqueous picric acid (90ml). The two solutions were mixed together and allowed to stand for 24 hours before use. The collagen and reticulin were stained red with this stain.

3. Endotoxin kinetic LAL assay measurement reagents and material

- Endotoxin free tips were used for this experiment,
- LAL Reagent Water, Lyofilized Limulus Amebocyte Lysate LAL reagent
- Standard Endotoxin (Endosafe Endochrome-K).
- Flat bottomed 96 well plate.
- Endotoxin free basin.

4. Tissue Lysis Buffer

- 0.3gm of Trizma base in 45ml deionised H2O PH:7.4
- 2.1 ml of 1 molar HCL
- 1 mM EDTA (Sigma) = 19 mg
- 20 µl/ml Protease Inhibitor Cocktail (Sigma)* Added just before use.
- 100 mM Phenylmethanesulfonyl fluoride (PMSF)

(10µl / ml stock solution prepared by dissolving 0.172 in 10 ml Ethanol).

5. Preparation of Biuret solution reagents

- 0.75gm of Copper (II) sulfate ($CuSO_4$),
- 3gm of NaK tartarate,
- 25gm of NaOH and
- 500ml deionised water
- Copper II sulphate ($CuSO_{4)}$ and potassium sodium tartarate (NaK tartarate) were added together in 400ml of de-ionised water in a flask and placed on hot plate. Then sodium hydroxide (NaOH) was added slowly with constant stirring. When this was dissolved de-ionised water was added to make up 500ml of solution.

6. Tris-Buffered Saline and Tween 20 (TBST) buffer

- 20 ml of 1M Tris-HCl pH 7.5
- 29g of NaCl
- 1 ml of Tween 20
- De-ionised H2O to 1 litre

7. TNF- α ELISA reagents

1- Coating Buffer: 0.1M Sodium Carbonate = 7.13g NaHCO3, 3.56g Na2CO3 in 1L of deionised H_2O pH 9.5

2- Phosphate Buffer Solution (PBS) : 8g NaCl, 0.2g KCl, 1.15g Na2HPO4, 0.2g KH2PO4 (for 10x) in 1L of dioniesed H_2O then 1X was prepared by dilution 1:10 H_2O PH 7.4

3- Wash Buffer: 0.05% Tween 20 in PBS, pH 7.4.

4- Assay Diluent: 1% Bovine serum albumin (BSA) in PBS, pH 7.2 – 7.4 (1g/100ml)

5- Substrate Solution : O-Phenylenediamine dihydrochloride. (Dissolve 1 tablet in 0.05M phosphate citrate buffer, add 1 tablet, at final moment add 40uL of 30% hydrogen peroxide)(1 tablet dissolved phosphate citrate buffer dissolved in 100ml of distilled water).

6- Stop Solution: 1M H2SO4 (2ml H2SO4 added to 34ml water).

8. Immunohistochemistry antibodies

Human tissue antibodies

Rabbit polyclonal anti TLR4 (1:100) was purchased from Lifespam, UK. Rabbit polyclonal anti TLR7 (1:100), mouse monoclonal anti TLR9 (1:200), rabbit polyclonal anti ki-67 (1:100) and rabbit polyclonal anti VEGF (1:100) were purchased from Abcam, UK.

Animal tissue antibodies

Antibody for animal tissue; Rabbit polyclonal anti TLR4 Lifespam, UK, TLR7, TLR9 and smooth muscle actin (SMA) (1:100) (Abcam, UK).

9. Micro BCA Kit Reagents (Pierce, thermoscientific, UK)

Reagent A

NaOH solution. containing:

- Na carbonate
- Na bicarbonate
- BCA
- Na tartrate

Reagent B

4% cupric sulphate